

STUDY OF THE ORIENTATION OF AXIAL AMINO-LIGANDS IN SOME Co(III) DIOXIMATES

Andrei Rija*, Eduard Coropceanu

Institute of Chemistry, Academy of Sciences of Moldova, 3, Academiei str., Chisinau MD-2028, Republic of Moldova
*e-mail: andreirija@yahoo.com

Abstract. A comparative study of the orientation of the axial ligands relative to the equatorial plane in Co(III) α -dioximates was performed. Co(III) α -dioximates obtained by us and those founded in Cambridge data base have been selected for this study. As a result of this study it was observed that anions from the external sphere and the solvent molecules contribute to the orientation of the axial ligands, such as thiocarbamide and selenourea. For the ligands such as aniline and sulfanilamide it is more advantageous the almost parallel orientation, when π - π interactions between the aromatic rings of the ligand and metalocycle of the equatorial plane are formed. Solvent molecules such as water can be found in the crystal structure in the vicinity of thiocarbamide and selenourea ligands, which are oriented parallel to the equatorial plane. In the case when diphenylglyoxime is located in the equatorial plane, water can be found in the vicinity of parallel and perpendicularly oriented ligands. The molecules within the crystal are arranged so closely that there are no gaps in the crystal lattice of these compounds.

Keywords: Co(III) dioximates, fluorine containing anions, ligands orientation, H-bonds, biostimulation properties.

Introduction

The use of ligands containing oxime functionalities creates prerequisites for assembling of coordination compounds with diverse composition and architecture: monooxime ligands are widely used for clusters synthesis [1,2] and compounds with polymeric structure [2,3]; dioxime ligands are often used for the synthesis of mononuclear compounds [4]. However, due to their ability to coordinate both through the nitrogen and the oxygen atoms of the oxime group, it is possible to obtain heteronuclear complexes as well [5]; by combining IIB group metals with some dioxime molecules coordination polymers have been obtained [6]; polyoxime ligands are used for the synthesis of poly- and heteronuclear compounds [7].

Transition metal compounds with chelate ligands have an important place in coordination chemistry. Dioximates of transition metals also belong to this class. The coordination ability of α -dioximes to *d*-metals have received considerable attention not only from the perspective of synthesis of B₁₂ vitamin models or hemoglobin [8], but as well as substances that feature a broad spectrum of synthetic, analytical and structural possibilities. Dioximes can be used as catalysts in industrial processes [9], stimulators of erythropoetic functions [10], antihypoxanth drugs [11], antidote properties [12], as basis for the obtaining of new semiconductors [13], for the separation and purification of metal generating complexes, etc. It has been found that some dioximes play the role of a bridging ligand in the systems of iron complexes [14]. It should be mentioned that in this role, the dimethylglyoxime molecule has a *trans* configuration, as in the free crystalline dimethylglyoxime.

The diversity of transition metal dioximates is represented by the mono- and polynuclear, heteronuclear compounds with di- and polymeric structures etc. Mononuclear dioximates are well known compounds with a high stability, on the strength of pseudo-metalocycles formed by coordination of monoanionic dioximes in the equatorial plane stabilized by intramolecular hydrogen bonds between oxime groups. The synthesis of different types of heteronuclear dioximates has been performed subsequently [15,16], and showed a various capacity of transition metals to coordinate to oxime group (through nitrogen or oxygen atoms). A particular interest in the field of molecular design and obtaining of complexes with various compositions has clathrochelated *tris*-dioximates of some transition metals [17]. The dioximates of transition metals have a highly stable M(DioxH)₂ moiety and only 1,6 positions of octahedron give the possibility of manipulation of diverse apical ligands of various nature. Depending on the specific ligands functional groups, there might appear diverse interactions which are able to influence their apical orientation. The utilization of bridging ligands gives de possibility to assemble the complexes with di- and polymeric structures [18]. The interactions that may influence the orientation of axial ligands could arise due to equatorial ligands either, which are endowed with various functional groups. The synthesis of new dioximes with diverse functional groups, which gives new possibilities for molecular composition and structural architectures, is one of the perspective directions in this field [19].

Nowadays the researches are focused on the relationship between the composition, structure of complexes and their biological activity. The factors that influence the architecture of molecular design are studied, and a series of stability of the complexes as a function of atom donor features of the apical ligand of cation complex are trying to

be found. The thermal stability and the decomposition process of Co(III) dioximates which contain thiocarbamide (Thio) and selenourea (Seu) have been studied by Ablov A.V. et al. [20]. It has been established that the decomposition of these compounds is followed by a series of exothermic effects. The comparison of thermal stability showed that dioximates which contain thiocarbamide in the apical position are more stable, as example for $[\text{Co}(\text{DH})_2(\text{Thio})_2]\text{NO}_3$, where DH is the monoanion of dimethylglyoxime, thermal decomposition starts at a temperature of $\sim 50^\circ\text{C}$ higher than for $[\text{Co}(\text{DH})_2(\text{Seu})_2]\text{NO}_3$.

The inclusion of fluorine ions or its anion complexes in cobalt dioximates allowed the highlighting of the possibilities of unusual packing comparing with other halogenated complexes. The study of Co(III) dioximates with polyfluorine anions showed that the last ones influence the orientation of some apical ligands of the complex cations, and the large number of fluorine atoms able to form a hydrogen bonds network increase the stability of these complexes due to their supramolecular systems formed on the basis of these bonds. The inclusion of organic molecules as ligands in metal complexes can essentially modify their activity, assigning them effective biological properties. As a result of the biological tests, in which fluorine containing Co(III) dioximates was added to the nutrient medium of microorganisms, it was established that they act as biostimulators in the biosynthesis of vitamin B₁₂ by *Spirulina platensis* cyanobacteria [21]. These studies created prerequisites to initiate the synthesis of producing synthetic analogues of natural systems, simulating the biological functions and achievement the processes which occur in these systems. Recent investigations have demonstrated that in Co(III) dioximates, the anions from the external sphere play an important role regarding the chemical and biological properties, and represent an important factor in packing of the crystal components in the complexes [22-24]. Due to the high electronegativity of the fluorine atom, strong hydrogen bonds with crystallization water molecules and NH₂ groups [the case of complex cations which possess apical ligands, which contain such groups as Thio, Seu, sulfanilamide (Sam)] are formed, leading to assembly of supramolecular assemblies, which influence directly the stability of these complexes. The anion from the external sphere may influence, as well, the orientation of apical molecules.

Results

Schrauzer et al. [25] have observed that benzyl cobalamines undergo a more rapid decomposition than neopentyl fragment in solution and this fact is not exclusively due to steric reasons; there are other forces which make the Co–benzyl bond weaker. A study of compounds design has shown that benzyl cobaloximes behave differently in comparison with alkyl cobaloximes. The difference in reactivity is due to some interactions between benzyl group and dioxime, and these interactions are missing in alkyl groups [26]. Many recent studies were concentrated on the structural and spectral properties, intensively using the NMR method for this purpose [27,28]. In the majority of cobaloxime complexes, the signal for the DH methyl groups appears as a singlet at ~ 2.0 ppm in the ¹H NMR spectra, which indicates the chemical equivalence of all four methyl groups. However, a non-equivalence has been observed in a few cases, when any of the axial ligand is chiral: $\text{Me}(\text{CN})\text{CHCo}(\text{DH})_2\text{Py}$ and $\text{MeCo}(\text{DH})_2\text{NH}(\text{Me})\text{-CH}_2\text{Ph}$ [29]. A fast rotation of the Co–C bond produces two sets of diastereomers, to show the DH methyl groups at a 1:1 ratio. Recently, there were found some complexes that have nonequivalent DH(Me) protons; for example nonequivalence results in a hindered rotation of axial 2-aminopyridine ligand in $\text{CF}_3\text{CH}_2\text{Co}(\text{DH})_2(2\text{-NH}_2\text{Py})$, caused by H-bonding of the NH₂ group to O–H \cdots O bridges of the DH ligand [30]. In a similar way, a hindered rotation of 2-fluorocyclohexyl around Co–C in 2-fluorocycloalkylcobaloxime causes nonequivalence and DH methyl groups appear as two signals in a 1:1 ratio [31].

Mandal et al. [32] have studied a few important questions regarding the orientation of the axial ligands in cobaloximes: what is the origin of hindered rotation of the Co–C or C–Ph bond? Is there any conclusive evidence to show that the hindered rotation is partly due to an interaction of aromatic ring π -electrons with the dioxime ring current? What is the role of the 2-substituent; does it have any direct interaction with the dioxime or CH₂ protons or does it simply affect the electron density in the aromatic ring? In order to rationalize the above questions and to understand the role of the 2-substituent, they have undertaken ¹H NMR studies for 2-X-C₆H₄CH₂Co(dioxime)₂Py. In this case, the substituent X has been chosen such that it varies in steric size and in electron donation/withdrawal capacity. Results have shown that the 2-Ph group affects the chemical shift. The 2-substituent contributes to the total electron density in the benzyl group that interacts with the dioxime protons, and the chemical shift of dioxime protons follows the electronic effect of the 2-substituent. The nature of the substituent at the 2-position as well the electron density in the dioxime affects the extent of nonequivalence.

Anions from the external sphere of the studied compounds are rich in electronegative atoms which participate to the formation of hydrogen bonds N–H \cdots F, O–H \cdots F and even C–H \cdots F, therefore, they represent a great interest for the research of their influence on the orientation of the axial ligands. In this study we have been examined fluorine-containing anions with different charges as well as complexes which do not contain fluoride anions.

Table 1.

Structural parameters of some Co(III) dioximates with thiocarbamide or aniline and different inorganic anions

Complexes	Cations		Co-S (Thio) or Co-N (Aniline) d, (Å)		Deviation Co(III) from the plane d, (Å)	Orientation of ligands with respect to the equatorial plane N ₄ degrees		Hydrogen bond d, (Å)			Interactions π-π d, (Å)			References			
			Lig. A	Lig. B		A	B	Inter cations	Inter with the anion		Inter with water molecules or other solvent*		num		val.		
									A	B	A	B					
1	2	3	2.292	2.292	5	6	7	8	9	10	11	12	13	14	15	16	17
[Co(DH) ₂ (Thio) ₂]NO ₃			2.292	2.292	0.000	70.00	70.00	3.042	3.042	2.983	2.863, 2.869	2.863, 2.869	-	-	-	-	[33]
[Co(DH) ₂ (Thio) ₂]CF ₃ SO ₃			2.298	2.279	0.018	22.28	87.61	-	3.048, 3.180 bifurc.	2.845, 2.955	2.820, 2.896	2.814, 2.920	-	-	1	2.999	[34]
[Co(DH) ₂ (Thio) ₂]BeF ₄ C ₂ H ₅ OH			2.307	2.280	0.019	20.43	83.69	-	3.119, 3.125 bifurc.	2.836 A, 3.039 A	2.628-2.979	2.735-2.828	3.112*	3.289*	1	2.955	[35]
[Co(DH) ₂ (Thio) ₂] ₂ [SiF ₆] ₂ ·2H ₂ O·C ₂ H ₅ OH	a		2.299	2.289	0.009	87.21	75.98	2.971	2.996	2.868, 3.051	2.856, 3.000, 3.046	3.055 (3.080) bifurc.	-	2.887*	-	-	[36]
	b		2.293	2.315	0.012	84.15	19.28	2.773	-	-	2.920, 3.032	2.903	-	2.896, 2.917	1	2.978	
[Co(DH) ₂ (Thio) ₂] ₂ [ZrF ₆] ₂ ·2H ₂ O			2.290	2.303	0.016	84.93	25.01	2.855	-	2.897	2.889, 2.904, 2.907	-	-	2.843	1	2.998	[37]
[Co(D)(DH) ₂ (Thio) ₂] ₂ [TiF ₆] ₂ ·2DMF			2.317	2.286	0.021	14.10	86.60	-	2.890	2.887, 2.934	2.794, 2.849	2.844, 2.994	-	3.065*, 3.129*	1	2.927	[38]
[Co(DH) ₂ (Thio) ₂] ₂ [AlF ₆] ₂ ·2H ₂ O	a		2.292	2.292	0.000	85.11	85.11	3.015	3.015	2.805	2.728, 2.809	2.728, 2.809	-	-	-	-	[39]
	b		2.329	2.297	0.005	19.69	78.84	-	2.876	-	2.701, 2.884	2.710, 2.884	2.805	-	1	2.986	
[Co(NioxH) ₂ (Thio) ₂] ₂ SO ₄ ·2H ₂ O	a		2.296	2.298	0.003	33.67	22.06	3.072	-	2.966b, 2.825b	2.795, 2.846	2.843, 3.050	-	2.965	2	3.199, 2.920	[40]
	b		2.280	2.300	0.007	71.66	22.84	2.926	-	2.867b, 2.794b	2.858, 2.907	2.831, 2.907	-	2.885	1	2.985	
[Co(NioxH) ₂ (Thio) ₂] ₂ [SiF ₆]	a		2.306	2.306	0.000	47.58	47.58	3.002 bifurc.	2.965, 3.002 bifurc.	3.039	2.852, 2.900, 2.904	2.852, 2.900, 2.904	-	-	-	-	[41]
	b		2.292	2.292	0.000	81.60	81.60	2.854	2.854	2.941	2.788, 2.879	2.788, 2.879	-	-	-	-	

[Co(NioxH) ₂ (Thio) ₂] ₂ [SiF ₆] ₃ ·3H ₂ O	a	2.318	2.300	0.015	23.49	62.07	–	2.982	2.826, 2.826	2.859, 2.876, 2.921	2.841	2.898	–	1	3.049	[42]
	b	2.302	2.336	0.003	53.96	31.05	3.018	–	3.090, 3.225	2.832, 2.887	2.866, 2.866	–	2.913	1	2.994	
[Co(NioxH) ₂ (Thio) ₂] ₂ [TiF ₆] ₃ ·3H ₂ O	a	2.292	2.308	0.015	61.87	22.85	2.930	–	2.826, 2.840	2.812	2.811, 2.856, 2.862	–	2.886	1	3.040	[38]
	b	2.321	2.292	0.007	21.86	65.07	–	3.206	3.207	2.844, 2.918	2.824, 2.868	2.862	–	1	2.970	
[Co(NioxH) ₂ (Thio) ₂] ₂ [ZrF ₆] ₃ ·3H ₂ O	a	2.293	2.278	0.018	22.35	62.81	–	2.912	2.818 a, 2.839 a	2.774, 2.858	2.756	2.902	–	1	3.042	[37]
	b	2.279	2.310	0.010	77.19	21.40	2.848	–	–	2.851, 2.898	2.829, 2.908	–	2.908	1	2.990	
[Co(DH) ₂ (Thio) ₂] ₂ [BF ₄] ₄ ·0.5H ₂ O	a	2.288	2.300	0.001	82.69	72.45	2.997	2.925	2.867, 2.913	2.964	3.011	2.964	–	–	–	[35]
	b	2.281	2.281	0.000	40.10	40.10	2.987	2.987	2.918, 2.948	2.952	2.952	–	–	–	–	
[Co(DH) ₂ (Thio) ₂] ₂ [TiF ₆] ₄ ·4DMF·1.5H ₂ O	a	2.288	2.302	0.004	41.12	40.91	3.027	2.981	–	2.775, 2.860	2.844, 2.873	2.824 DMF	2.811	–	–	[38]
	b	2.286	2.282	0.017	78.36	69.17	2.807	2.925	–	2.768, 2.922	2.762	2.609, 2.733*	2.797*, 2.862*	–	–	
[Co(Hafdo) ₂ (Thio) ₂] ₂ [NO ₃]	a	2.296	2.296	0.000	55.86	55.86	2.969 3.070	2.969 3.070	2.941	2.922, 2.943	2.922, 2.943	–	–	–	–	
	b	2.302	2.302	0.000	38.48	38.48	–	–	–	2.873, 2.876, 2.893, 2.978	2.873, 2.876, 2.893, 2.978	–	–	1	3.131	[43]
[Co(DH) ₂ (An) ₂] ₂ [ZrF ₆] ₂ ·2H ₂ O	a	2.004	2.004	0.000	32.92	32.92	–	–	2.966	–	–	2.923	–	2	3.752	[44]
	b	2.014	2.014	0.000	28.83	28.83	–	–	–	2.809	2.809	–	–	2	3.644	
[Co(NioxH) ₂ (An) ₂] ₂ [ZrF ₆] ₆ ·6H ₂ O		2.012	2.013	0.011	30.17	32.81	–	–	2.892, 2.893	2.857	–	–	2.870	2	3.992, 3.996	[44]
		2.001	2.001	0.000	31.97	31.97	–	–	2.916	3.192	3.192	–	–	2	4.078	[45]
[Co(DH) ₂ (An) ₂] ₂ [BF ₄]		2.003	2.004	0.002	35.02	28.64	–	–	–	2.905	2.963	–	–	2	4.022, 3.533	[46]
		2.011	2.011	0.000	32.10	32.10	–	–	–	3.192	3.192	2.916	2.916	2	3.630	[47]

As axial ligands, the molecules of thiocarbamide (containing NH_2 group which are able to build H-bonds network) and aniline molecule (whose NH_2 group involved in H-bonds network cannot influence molecule orientation), have been selected. For comparison, we used compounds synthesized by us and compounds selected from the Cambridge Crystallographic Data Centre. The emphasis in this study was made on the analysis of Co–S bonds lengths, the deviation of the central atom from the N_4 plane, the orientation of axial ligands with respect to the equatorial plane in the complex cation, hydrogen bonds formed by axial ligands and π - π interactions of the complex, the number of solvent molecules incorporated in the crystal lattice, the volume and nature of the anion of the external sphere.

In the literature, there are known enough Co(III) dioximates which contain on the axial coordinate molecules of thiocarbamide with different orientations with respect to equatorial plane. The authors of these works explain the position of the respective molecules as being due to the formation of multiple hydrogen bonds of axial ligands with the external anions and solvent molecules. Hydrogen bonds are very important for crystal packing, especially considering that in some cases, as it was observed in $[\text{Co}(\text{NioxH})_2(\text{An})_2][\text{ZrF}_6] \cdot 6\text{H}_2\text{O}$ (where NioxH is monoanion of 1,2-cyclohexanedionedioxime and An - aniline) [44], the crystallization water molecules and external anions form a supramolecular H-bonds system. All anions used in this study are able to form hydrogen bonds because of the high electronegativity of atoms, which they contain.

In this study, we were taking into account both the surroundings of the axial ligands and the position of the anion from the external sphere with respect to these ligands. All necessary parameters for discussion regarding the influence of the external factors to orientation of axial ligands have been summarized in table 1.

Studying the dioximate $[\text{Co}(\text{DH})_2(\text{Thio})_2]\text{NO}_3$ [33] which contains the axially coordinated thiocarbamide molecules, and the NO_3^- anion in the external sphere, it was observed that the cation is centrosymmetric with the same arrangement of thiocarbamide molecules. The orientation of the molecules is performed by intermolecular hydrogen bonds with the anion from the external sphere (two of these), oxygen of the oxime group from the neighboring complex cation and an intramolecular hydrogen bond with oxygen of the equatorial oxime group. All donor-acceptor atoms involved in these hydrogen bonds are practically in the same plane. Therefore, we considered that these are responsible for the orientation of thiocarbamide molecules with an angle of 70° . The length of Co–S bonds in this compound is of 2.292 Å. This value was found in the case of three dioximates with different inorganic anions where the complex cation is centrosymmetric, and the orientation of thiocarbamide molecules is almost perpendicular to the equatorial plane N_4 (in the studied dioximates the Co–S bond varies in the range of 2.278 – 2.329 Å). The almost perpendicular orientation excludes the possibility of π -interactions of thiocarbamide fragment with the dioxime ring current. The absence of solvent molecules in the crystal lattice is attributed to the compact arrangement of ions within the crystal so as the free space which may hold the solvent molecules are missing. In the case of $[\text{Co}(\text{DH})_2(\text{Thio})_2]\text{CF}_3\text{SO}_3$ [34] complex, even if the composition of molecules are similar to the previous one, major changes are observed in the axial ligands position. It is necessary to mention that in the fluorine-containing anion CF_3SO_3^- , the CF_3 group behaves as a CH_3 group and it is not H-bonded. For this compound, the complex cation isn't anymore symmetric and the thiocarbamide molecules are oriented differently with respect to the equatorial plan N_4 . In the case of parallel orientation, the thiocarbamide molecule is "held" in this position through four intermolecular hydrogen bonds, two with anions from external sphere (2.820, 2.896 Å) and two with the oxygen atoms of oxime groups of the neighboring complex cations (2.845, 2.955 Å). This type of orientation involves also the π -interaction between the fragment of thiocarbamide and dioxime ring current (2.999 Å). In the case of perpendicular orientation, the thiocarbamide fragment is H-bonded with the anions from the external sphere and a bifurcated intramolecular hydrogen bond with the oxime group oxygens also has been observed. Even though the CF_3SO_3^- anion is bigger than NO_3^- , a reason that should increase the possibility of the incorporation of solvent molecules in the crystal lattice, in this complex they are also missing.

The crystalline structure of $[\text{Co}(\text{DH})_2(\text{Thio})_2][\text{BeF}_4] \cdot \text{C}_2\text{H}_5\text{OH}$ [35] complex differs from the previous one, due to the fact that a molecule of ethanol participates at packing, which create a disordering for $[\text{BeF}_4]^{2-}$ anion. However, the orientation of thiocarbamide molecules with respect to the equatorial plane is similar with the former one, including the number of hydrogen bonds that the thiocarbamide molecules form: the molecule of parallel thiocarbamide with respect to N_4 equatorial plane forms 4 hydrogen bonds, two with oxygen atoms from the oxime groups of the neighboring complex cations and two with anions from external sphere or with the anion and the molecule of ethanol; the perpendicular oriented molecule - a bifurcated intermolecular hydrogen bond with the oxime groups oxygens and two hydrogen bonds with the anions from the external sphere or with the anion and the ethanol molecule. The crystal of $[\text{Co}(\text{DH})_2(\text{Thio})_2][\text{SiF}_6] \cdot 2\text{H}_2\text{O} \cdot \text{C}_2\text{H}_5\text{OH}$ [36] compound contains two crystallographically independent complex cations. In the complex cation **a**, both thiocarbamide molecules are oriented almost perpendicularly with respect to the equatorial plane N_4 . The dihedral angle is 87.21° and this thiocarbamide forms an intramolecular hydrogen bond with the oxygen atom from the oxime groups and three hydrogen bonds with the fluorine atoms. The thiocarbamide with the dihedral angle 75.98° forms a bifurcated intra- and intermolecular hydrogen bond with the oxime group oxygens, a hydrogen bond with the oxygen from the

neighboring cation, a bifurcated hydrogen bond with fluorine atoms and a hydrogen bond with the oxygen atom of the ethanol molecule.

In both cases, the possibility of π -interaction between the thiocarbamide fragment and dioximic ring current is excluded. Atoms, donors and acceptors, which participate to these hydrogen bonds, are practically planar excluding the oxygen atom of the ethanol molecule and one of the fluorine atoms which participates to a bifurcated hydrogen bond.

These atoms are within a distance of 1.5 Å with respect to the average plan of other donor-acceptor atoms. In the complex cation **b** the thiocarbamide molecules are oriented differently (parallel and perpendicular) with respect to the equatorial plane N_4 . In the case of perpendicular orientation, the position of thiocarbamide molecule is fixed by an intramolecular H-bond and two hydrogen bonds with fluorine atoms of the anion, and in the case of parallel orientation, thiocarbamide forms two hydrogen bonds with crystallization water molecules and one with the fluorine atom. In addition, parallel orientation allows the formation of π -interaction between the thiocarbamide fragment and metalocycle.

The $[\text{Co}(\text{DH})_2(\text{Thio})_2]_2[\text{ZrF}_6] \cdot 2\text{H}_2\text{O}$ [37] compound consists of two complex cations $[\text{Co}(\text{DH})_2(\text{Thio})_2]^+$, the centro-symmetric anion $[\text{ZrF}_6]^{2-}$ and two crystallographically independent crystallization water molecules. In the complex cation, one thiocarbamide molecule is oriented parallel and the other perpendicularly with respect to the same plane N_4 . The dihedral angles between the equatorial plane N_4 and thiocarbamide molecules planes formed by atoms Co1-S1-C9 and Co2-S2-C10 are of 25.01 and 84.93°, respectively (Fig. 1).

As in the case of other dioximates used in the study, for this compound it was also observed that the thiocarbamide molecule parallel to the equatorial plane is oriented over metalocycle. This fact leads to a π -interaction between the thiocarbamide fragment and the centre of metalocycle. In the case of the perpendicular thiocarbamide molecule, this is located along the pseudo-heterocycles of six atoms which are formed due to intramolecular hydrogen bonds of the oxime fragments. This orientation allows the formation of intramolecular hydrogen bonds between the NH_2 group of thiocarbamide and the oxygen atom of the oxime group. It was also observed for this complex that the hydrogen bonds, in which perpendicular thiocarbamide molecules are involved, are practically in the same plane (Fig. 2).

This fact may contribute essentially to the explanation of the molecules orientation with respect to the equatorial plane N_4 .

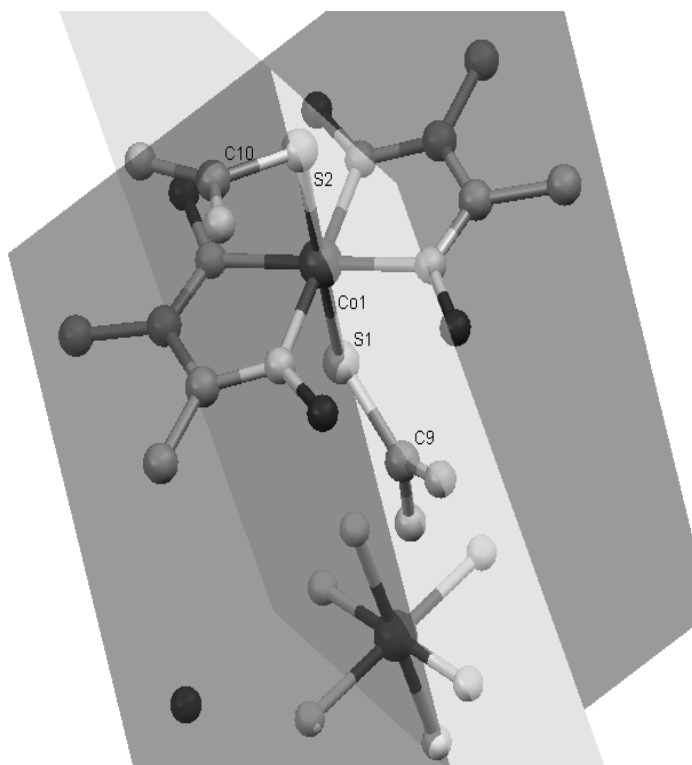


Figure 1. Orientation of the CoSC planes of thiocarbamide molecules with respect to the metalocycle from the equatorial plane in $[\text{Co}(\text{DH})_2(\text{Thio})_2]_2[\text{ZrF}_6] \cdot 2\text{H}_2\text{O}$.

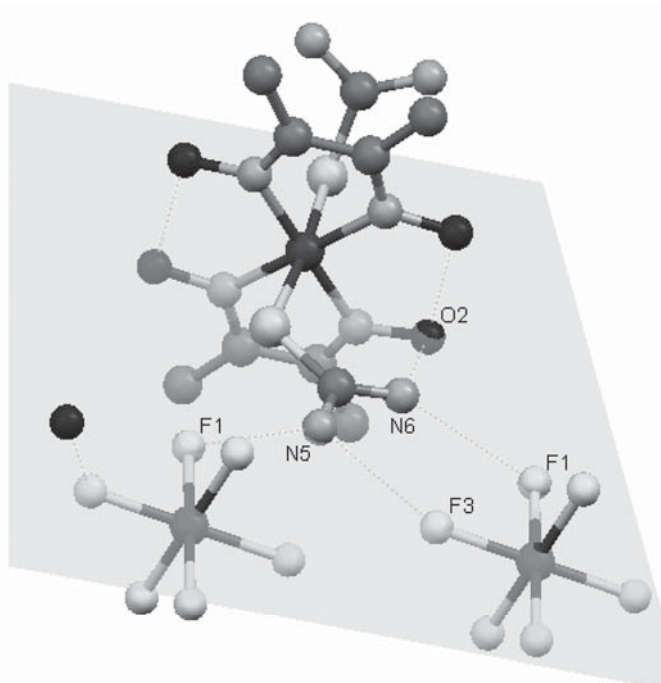


Figure 2. The planarity of hydrogen bonds which contribute to the orientation of thiocarbamide molecules oriented perpendicularly with respect to the equatorial plane N_4 $[\text{Co}(\text{DH})_2(\text{Thio})_2]_2[\text{ZrF}_6] \cdot 2\text{H}_2\text{O}$.

In the case of parallel orientation the electronegative atoms which are H-bonded aren't located in the same plane but vary from the average plane formed by all these electronegative atoms in the limits of 0.083–1.366 Å. The oxygen atom of the water molecule is the most out of this plane. However, the parallel orientation is mostly supported by the π - π interaction, which in this case is equal to approximately 3 Å, and hydrogen bonds are just reinforcing this position. Also, it worth to note that the thiocarbamide molecule oriented perpendicularly is not H-bonded to the crystallization water molecules. These water molecules are located in the vicinity of the parallel oriented thiocarbamide.

The complex compound $[\text{Co}(\text{D})(\text{DH}_2)(\text{Thio})_2][\text{TiF}_6] \cdot 2\text{DMF}$ [38] (where D is bideprotonated dimethylglyoxime) consists of a single crystallographically independent complex cation. Comparing to previous compounds, in this case the dimethylglyoxime molecules are coordinated in the equatorial plane, one in bideprotonated form and the other - unprotonated. The axial thiocarbamide ligands are also oriented differently with respect to the equatorial plane. One thiocarbamide molecule lies at the angle of 14.10° to the equatorial plane N_4 , and the other molecule – at the angle of 86.60° . The parallel oriented thiocarbamide molecule is H-bonded with the neighboring electronegative atoms and all H-bonds are practically in the same plane (Fig. 3) as in the case of the perpendicularly oriented thiocarbamide molecule analyzed in the previously complex (Fig. 2).

Hydrogen bonds which are formed by the perpendicularly oriented thiocarbamide molecule slightly differ from the planarity due to DMF molecules which are disordered in the crystal lattice. In this complex, the cations form chains along the b axis based on NH_2 groups of the thiocarbamide H-bonded to oxygen of the oxime groups. These chains are linked through $[\text{TiF}_6]^{2-}$ anions which form hydrogen bonds with parallel and perpendicularly oriented thiocarbamide molecules. Therefore, the oriented along the b axis $[\text{TiF}_6]^{2-}$ anions, link around them four similar chains. Molecules of the disordered dimethylformamide are located in the vicinity of the perpendicularly oriented thiocarbamide molecules and are H-bonded to them.

In the crystal structure of $[\text{Co}(\text{DH})_2(\text{Thio})_2][\text{AlF}_6] \cdot 2\text{H}_2\text{O}$ [39], two crystallographically independent complex cations are present and one of them is centrosymmetric. In the centrosymmetric cation a thiocarbamide molecules lies at the angle of 85.11° to the equatorial plane N_4 being fixed through 4 hydrogen bonds (one intramolecular, two with the anion and one with the neighboring cation). In the complex cation **b** thiocarbamide molecules are oriented both perpendicularly and parallel. In the case of perpendicular orientation, the thiocarbamide molecule is fixed through three hydrogen bonds (one intramolecular with the oxygen atom of the oxime group and two intermolecular with fluorine atoms of the anion).

The almost parallel orientation of the molecule B is caused by the formation of two hydrogen bonds (one with the crystallization water molecule and one with the fluorine atom of the anion) and a π - π interaction with the metallocycle of the equatorial plane.

As a result, it was established that when thiocarbamide molecules are oriented parallel and perpendicularly with respect to the equatorial plane N_4 , the crystallization water molecules are in the vicinity of parallel oriented thiocarbamide molecules and in principle this orientation causes gaps in the crystal lattice suitable for solvent molecules incorporation.

Also, in the majority of these cases, donor and acceptor atoms which participate in the formation of hydrogen bonds and influence the orientation of thiocarbamide molecules are arranged practically in the same plane, and π - π interactions which appear between the parallel oriented thiocarbamide fragment and the metallocycle of the equatorial plane fix the respective position of the ligand. There have not been encountered so far the cases, where in the symmetric cation the thiocarbamide molecules are oriented almost parallel.

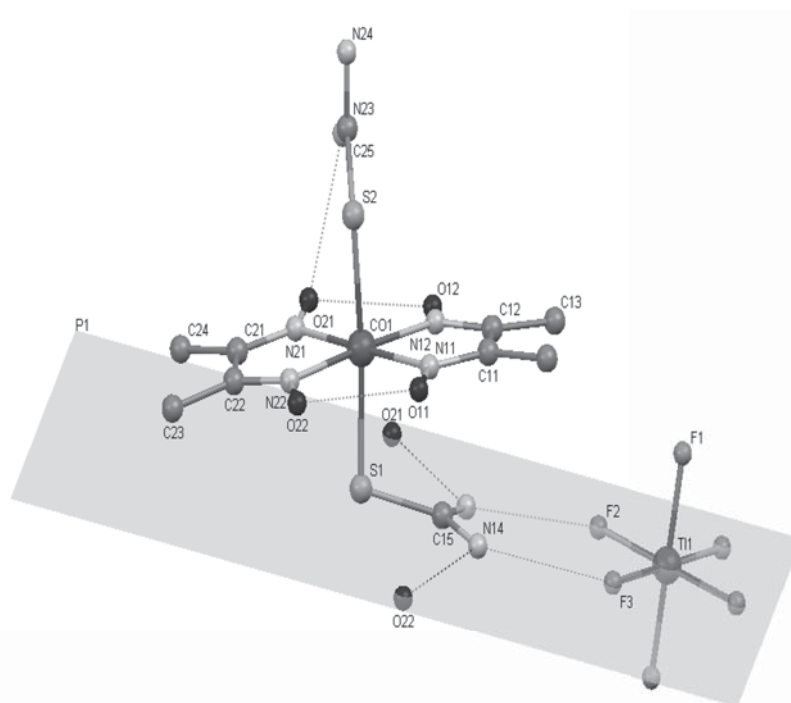


Figure 3. The planarity of hydrogen bonds which contribute to the orientation of thiocarbamide molecules oriented parallel with respect to the equatorial plane N_4 $[\text{Co}(\text{D})(\text{DH}_2)(\text{Thio})_2][\text{TiF}_6] \cdot 2\text{DMF}$. For clarity, hydrogen atoms are omitted.

Mostly, they are oriented almost perpendicularly or in some cases – intermediary, such as $[\text{Co}(\text{DfH})_2(\text{Thio})_2][\text{BF}_4] \cdot 0.5\text{H}_2\text{O}$ (where DfH is monoanion of diphenylglyoxime) [35] and $[\text{Co}(\text{NioxH})_2(\text{Thio})_2][\text{SiF}_6]$ [41] complexes (Table 1). Besides the fact that the parallel orientation of thiocarbamide molecules in the cation and the presence of crystallization water molecules are interdependent, it was established that in the case of complexes $[\text{Co}(\text{NioxH})_2(\text{Thio})_2]\text{SO}_4 \cdot 2\text{H}_2\text{O}$ [40], $[\text{Co}(\text{NioxH})_2(\text{Thio})_2][\text{SiF}_6] \cdot 3\text{H}_2\text{O}$ [42] and $[\text{Co}(\text{NioxH})_2(\text{Thio})_2][\text{SiF}_6]$, the orientation of thiocarbamide molecules is different, all compounds contain pairs of crystallographically independent complex cations. In the first compound, thiocarbamide molecules are oriented almost parallel in the cation **a** and mixed (perpendicular and parallel) in cation **b**. In cation **a** of the second compound, molecules are almost parallel and perpendicular, in cation **b** – intermediate and parallel, and in the third compound, where a crystallization water molecule is missing, thiocarbamide molecules in the cation **a** are oriented intermediate (47.58°), and in cation **b** – perpendicularly (81.60°).

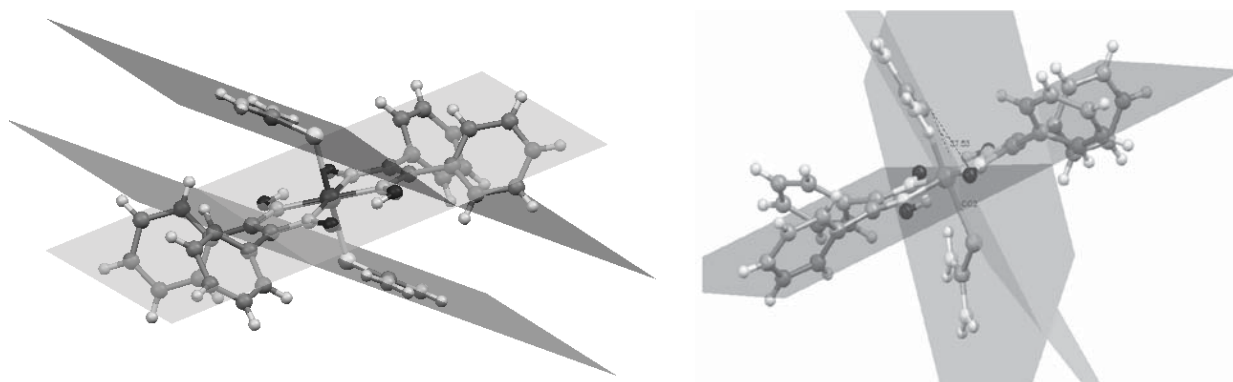


Figure 4. Orientation of thiocarbamide molecules in the complex cation A (left) and B (right) of $[\text{Co}(\text{DfH})_2(\text{Thio})_2][\text{TiF}_6] \cdot 3.5\text{DMF} \cdot 1.5\text{H}_2\text{O}$.

In these compounds it wasn't observed for water molecules to form hydrogen bonds with the thiocarbamide oriented perpendicularly with respect to the equatorial plane N_4 . Even though some crystallization water molecules do not participate directly in the formation of hydrogen bonds with thiocarbamide molecules, however, they are located in the space created by the parallel oriented thiocarbamide.

In table 1 are presented two compounds which contain in the equatorial plane of the complex cation diphenylglyoxime and thiocarbamide as the axial ligand. From this table it can be observed that thiocarbamide molecules are oriented intermediary and almost perpendicular to the equatorial plane and a parallel orientation of these ligands were not observed. The parallel orientation of the thiocarbamide molecules probably is not aleatory, but is conditioned by its

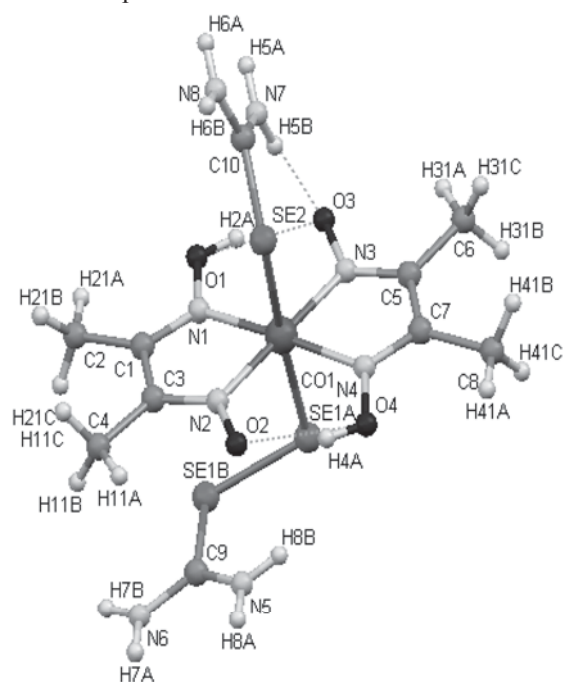


Figure 5. Complex cation in $[\text{Co}(\text{DH})_2(\text{Seu})(\text{Se-Seu})][\text{ZrF}_6] \cdot 3\text{H}_2\text{O}$.

intermolecular H-bonds. In both cases there is a pair of complex cations crystallographically independent where, in the complex cation thiocarbamide molecules are oriented parallel to each other and in the other the dihedral angle between the plains of these molecules is equal to approximately 38° (Fig. 4). Also, in these compounds, solvent molecules from the crystal lattice may form hydrogen bonds with molecules which are located in the perpendicular position with respect to equatorial plane N_4 . This can be explained by the fact that dioxime fragments in this case being more voluminously create greater possibilities of crystallization of solvent molecules even in the vicinity of thiocarbamide molecules perpendicularly oriented.

The study of Co(III) dioximates which contain in the axial plane molecules of selenourea, allowed to obtain the crystalline structure of two compounds of this type [48]. The X-ray investigations showed that synthesis triggered some chemical transformations forming a new unusual ligand Se-Seu. In this case, molecules of selenourea and Se-Seu are located in the axial plane. In both cases, molecules of Se-Seu are oriented parallel to the metallocycle of the

equatorial plane forming π - π interactions between the uncoordinated atom of selenium and the π -delocalized system of the metallocycle of the equatorial plane. Selenourea molecules are oriented approximately perpendicular with respect to the equatorial plane with the formation of an intramolecular hydrogen bond with the oxygen from the oxime group (Fig. 5). Atoms which participate in the formation of hydrogen bonds both with Seu and Se-Seu are located approximately in the same plane as in the case of Co(III) dioximates which contain in the equatorial plane thiocarbamide molecules.

Three new compounds, with the molecular formulae $[\text{Co}(\text{DH})_2(\text{Thio})_2][\text{Rh}(\text{Thio})_6][\text{BF}_4]_4$ (Fig. 6), $[\text{Co}(\text{DH})_2(\text{Thio})_2][\text{Rh}(\text{Thio})_6][\text{TiF}_6]_2 \cdot \text{H}_2\text{O}$ and $[\text{Co}(\text{NioxH})_2(\text{Thio})_2][\text{Rh}(\text{Thio})_5\text{Cl}][\text{TiF}_6]_2 \cdot 4\text{H}_2\text{O}$ were synthesized and studied by using different physical methods of analysis [49]. They represent new ionic structures, each of them having in their composition two types of complex cations based on octahedrally coordinated Co(III) and Rh(III). In all these three compounds, the coordination of α -dioximes to Co(III) and of thiocarbamide to Rh(III) with the formation of distinct complex cations was observed.

In the case of these compounds thiocarbamide molecules from complex cations $[\text{Co}(\text{DH})_2(\text{Thio})_2]^+$ are oriented from intermediary to perpendicular position with respect to the equatorial plane (the angle between the fragment of thiocarbamide and equatorial plane is in the range of 62 - 65°) forming intramolecular hydrogen bonds with the oxygen atom of the oxime group. In the $[\text{Co}(\text{NioxH})_2(\text{Thio})_2][\text{Rh}(\text{Thio})_5\text{Cl}][\text{TiF}_6]_2 \cdot 4\text{H}_2\text{O}$ compound two crystallographically independent complex cations $[\text{Co}(\text{NioxH})_2(\text{Thio})_2]^+$ are present.

In the cation B the thiocarbamide molecules are oriented with respect to the equatorial plane N_4 in the same way to that of the similar dioximes, with dihedral angles of $\sim 56^\circ$. Therefore, intramolecular hydrogen bonds between NH_2 group and oxygen atom from the oxime group are formed. In the case of cation A, the orientation of thiocarbamide molecules differs as compared to previous cations, dihedral angles between those planes are equal to 30.53 and 35.17° , respectively.

In the complex cations $[\text{Rh}(\text{Thio})_6]^{3+}$ it was observed that each pair of *trans* thiocarbamide molecules are oriented differently to the plane S_4 which belong to the sulfur atoms of the other thiocarbamide molecules, angles varying in the range 70 - 85° . In the case of these cations, a NH_2 group of thiocarbamide molecule forms an intramolecular hydrogen bond with the sulfur atom of the neighboring molecule (Fig. 6). The cations are linked between them through external fluor-containing anions which form a complicated hydrogen bonds network.

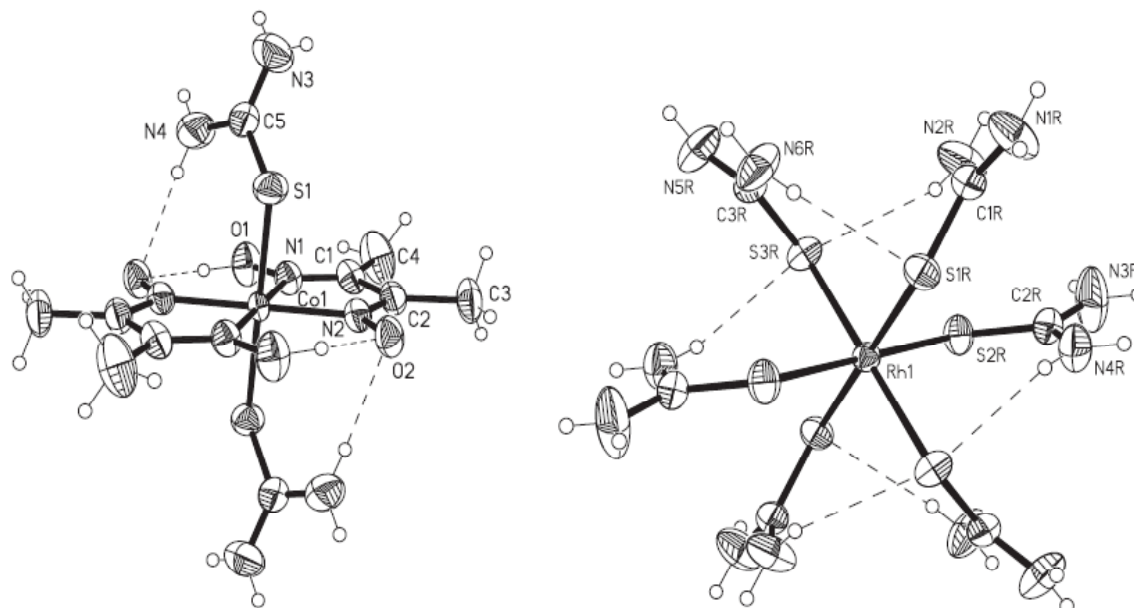


Figure 6. ORTEP drawing of the complex cations Co(III) and Rh(III) of $[\text{Co}(\text{DH})_2(\text{Thio})_2][\text{Rh}(\text{Thio})_6][\text{BF}_4]_4$ with the numbering scheme.

In the case of these complex cations, a tendency of planar arrangement of hydrogen bonds formed between NH_2 groups of the thiocarbamide molecules and surrounding electronegative atoms was observed. It was also established that anions from the external sphere contribute essentially to the stability of crystalline structure through numerous hydrogen bonds in which these anions participate.

An analysis of complexes which contain aniline molecules in apical position established that these are oriented almost parallel to the equatorial plane N_4 forming π - π interactions between the centers of metallocycles and phenyl rings. Aniline molecules do not contain functional groups which could cause a different orientation of these ligands through the formation of hydrogen bonds (NH_2 group of the aniline molecule is coordinated to the central atom and does not

influence in any case the steric factor of the benzene ring, and for this reason it was excluded from the study). However, besides π - π interactions which are formed between the benzene ring and the metallocycle of the equatorial plane, in some cases weak hydrogen bonds such as C-H \cdots F or C-H \cdots O were observed [44].

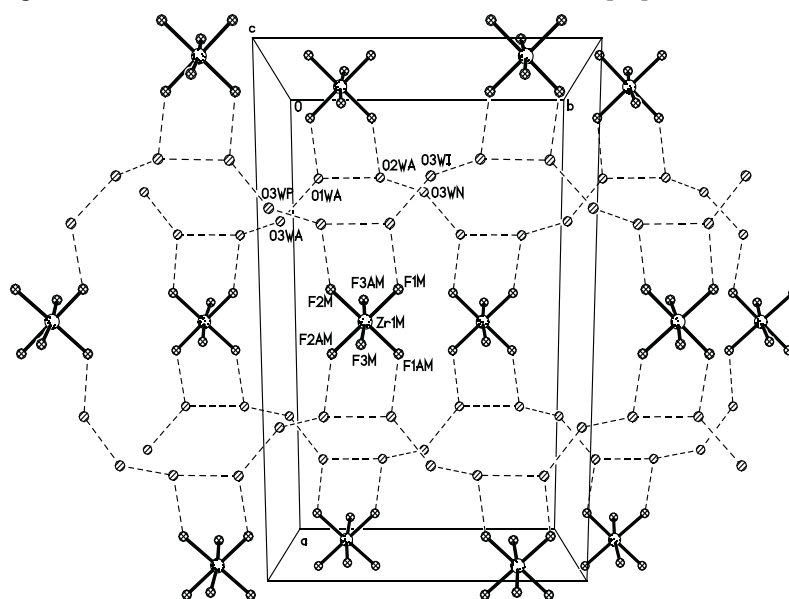


Figure 7. Supramolecular system formed by external fluor-containing anions and crystallization water molecules viewed along the [001] direction in $[\text{Co}(\text{NioxH})_2(\text{An})_2]_2[\text{ZrF}_6] \cdot 6\text{H}_2\text{O}$.

For some compounds as $[\text{Co}(\text{NioxH})_2(\text{An})_2]_2[\text{ZrF}_6] \cdot 6\text{H}_2\text{O}$ [44] it was observed that anions and water molecules form their own supramolecular system under a complicated system of hydrogen bonds (Fig. 7).

In the case of dioximates which contain aniline molecules the length of Co-N bonds doesn't vary as much as in the case of dioximates with thiocarbamide. Interdependence between the orientation of molecules from apical position and the deviation of cobalt atom from the plane N_4 hasn't been found yet. As consequence, the anion from the external sphere and solvent molecules influence the orientation of aniline molecules with respect to the equatorial plane N_4 in a lesser extent than thiocarbamide molecules in Co(III) dioximes. The same is observed in the case of Co(III) dioximates which contain in the axial positions molecules of sulfanilamide. The latter are oriented approximately parallel to the metallocycle of the equatorial plane (angles formed by the respective planes are in the range of 25–28°) also forming π - π interactions between the aromatic ring of sulfanilamide and the π -delocalized system of metallocycle.

Although sulfanilamide contains a NH_2 group, it does not contribute to the orientation of the respective molecule. However, it participates in the formation of intermolecular hydrogen bonds contributing to the stability of the crystalline structure [50].

The ability of crystal packing is confirmed by the presence of voids in the crystal lattice. For this class of compounds the formation of voids in the crystal lattice is not usual. Almost all the combinations of the studied complexes in this article don't contain cavities. Only for three complexes voids were identified, the largest being in the $[\text{Co}(\text{DH})_2(\text{Thio})_2]\text{NO}_3$ complex [33] (Fig. 8), cavities forming 124.3 Å³ (5,7%) of the crystal volume. Usually, more voluminous ligands are required. Sulfanilamide could contribute to the formation of these cavities. The distance between NH_2 groups in sulfanilamide is

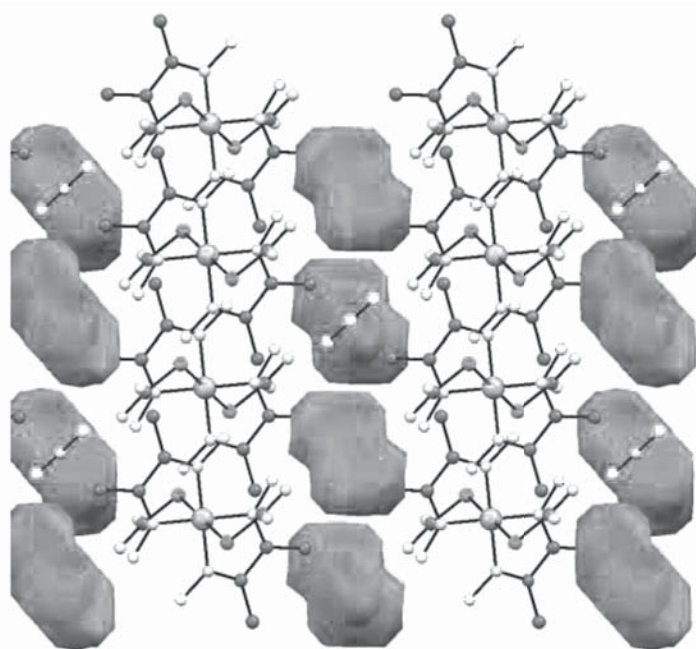


Figure 8. Packing in the crystal lattice of the complex $[\text{Co}(\text{DH})_2(\text{Thio})_2]\text{NO}_3$.

equal to $\sim 7,6$ Å. However, even in the case of coordination compounds which contain sulfanilamide as axial ligands these cavities are not formed. In the case of compounds with sulfanilamide, as it was mentioned, the planes of aromatic rings of the respective ligand are oriented under an angle smaller than 28° with respect to the metallocycle of the equatorial plane giving the possibility to form π -interactions with the dioxime ring current.

The cations are arranged tightly (Fig. 9) and linked by hydrogen bonds forming a pseudo-polymer chains that excludes any possibility to form cavities in the crystal lattice. Even in the case when solvent molecules are removed from the crystal lattice, the volume of obtained cavities does not exceed 10%.

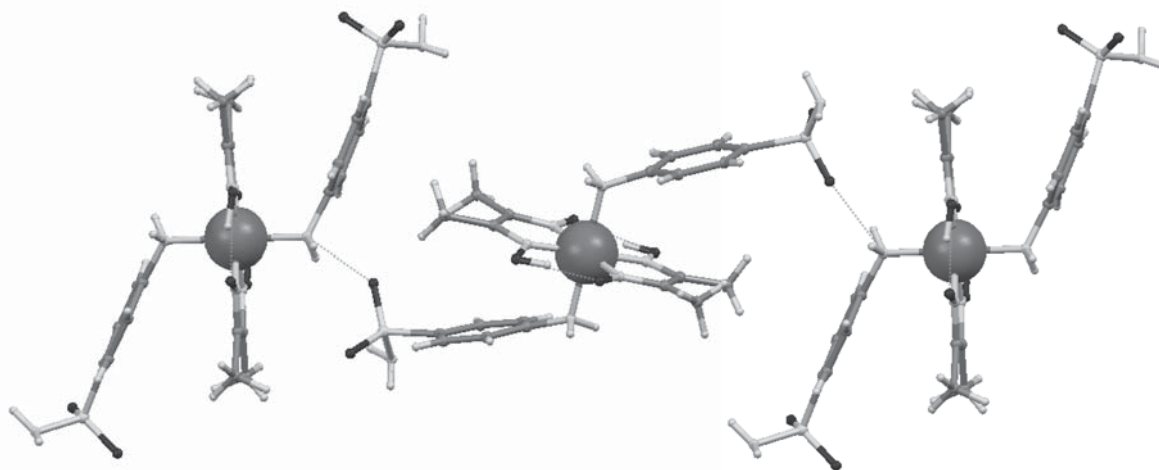


Figure 9. Arrangement of cations within the crystal of $[\text{Co}(\text{DH})_2(\text{Sam})_2]_2[\text{ZrF}_6] \cdot 5\text{H}_2\text{O}$.

Therefore, it can be assumed that these complexes cannot be treated as porous substances. Instead, as a general result of our research it was found that these complexes can be successfully used as biostimulators of some enzymogenetic processes in some strains of fungi as *Aspergillus niger* 33 CNMN FD 06A, *Aspergillus niger* 33-19 CNMN FD 02A, *Rhizopus arrhizus* F67 and *Rhizopus arrhizus Fischer* CNMN FD 03L etc. Also it was found that for some fungi the complexes that contain sulfanilamide as axial ligands reduce the technologic cycle to 48 hours which represent about 33% of total period.

Conclusions

In the case of complexes which contain thiocarbamide and selenourea, the orientation of these molecules in the axial plane is conditioned by hydrogen bonds formed with the external sphere anions, vicinal complex cations, solvent molecules, intramolecular hydrogen bonds with oxygen from the oxime group and π - π interactions with the metallocycle from the equatorial plane.

The hydrogen bonds which contribute to the orientation of thiocarbamide and selenourea molecules in most of the cases are located in the same plane, being responsible for the steric factor of these molecules. Thiocarbamide and selenourea molecules oriented approximately parallel are influenced by π - π interactions between the respective fragment and the metallocycle of the equatorial plane as well.

The parallel thiocarbamide and selenourea molecules are oriented along the metallocycle of the equatorial plane, while molecules oriented perpendicularly are located in the direction of intramolecular hydrogen bond formed by oxime fragments.

In some coordination compound the fluor-containing anions and solvent molecules, can form their own supramolecular system of hydrogen bonds, which essentially contributes to stability of these compounds. This is one more evidence that external fluorine-containing anions play an important role at the crystal packing.

The solvent molecules incorporated in the crystal lattice, are located in the vicinity of thiocarbamide or selenourea molecules oriented parallel, some of them forming hydrogen bonds directly with the NH_2 group. In the case of oxime radicals, which are more voluminous as diphenylglyoxime, solvent molecules can be located in the vicinity of thiocarbamide and selenourea molecules perpendicularly oriented as well.

In the case of axial ligands such as aniline, sulfanilamide, etc., the approximately parallel orientation is more convenient, with the formation of π - π interactions between the phenyl ring and the π -delocalized system of the equatorial plane metallocycle. These types of ligands in the majority of the cases are oriented in the direction of the equatorial plane metallocycle.

The molecules within the crystal are arranged in a manner that the cavities from the crystal lattice are practically

missing due to compact packing. The formation of cavities in the crystal lattice is observed only in a few cases but they do not exceed 6% of the crystal volume. Therefore, bis-dioximates of Co(III) from this series cannot be used as porous materials.

References:

- [1] Stamatatos, T.C.; Christou, G. *Inorganic Chemistry*. 2009, 48, pp. 3308-3322.
- [2] Miliotis, C.J.; Stamatatos, T.C.; Perlepes, S.P. *Polyhedron*. 2006, 25, pp. 134-194.
- [3] Croitor, L.; Coropceanu, E.; Siminel, A.; Fonari, M. *Polyhedron*. 2013, 60, pp. 140-150.
- [4] Follett, A.; McNabb, K.A.; Peterson, A.A. *Inorganic Chemistry*. 2007, 46, pp. 1645-1654.
- [5] Chaudhuri, Ph. *Coord. Chem. Rev.* 2003, 243, pp. 143-190.
- [6] Croitor, L.; Coropceanu, E.B.; Siminel, A.V. et al. *CrystEngComm*. 2012, 14, pp. 3750-3758.
- [7] Akine, S.; Taniguchi, T.; Saiki, T.; Nabeshima, T.J. *Am. Chem. Soc.* 2005, 127, 2, pp. 540-541.
- [8] Bresciani-Pahor, N.; Farcolin, M.; Marzilli, L.G. et al. *Coord. Chem. Rev.* 1985, 63, pp. 1-125.
- [9] Rogaciov, B.G.; Hindekel, M.L. *Russ. Chem. Bull.* 1969, 1, pp. 141-142. (in russian)
- [10] Matcovschii, C.L.; Balan, N.A.; Batyr, D.G. et al. *Journ. A.S.M. Life sciences*. 1969, 4, pp. 3-5. (in russian)
- [11] Matcovschii, C.L. *Journ. A.S.M. Life sciences*. 1971, 5, pp. 88-89. (in russian)
- [12] Matcovschii, C.L.; Bologa, O.A. *Globe of Science*. 2006, 6, 34-36. (in russian)
- [13] Thomas, T.W.; Underhill, A.E. *Chem. Commun.* 1969, 13, 725a.
- [14] Bulhac, I. *Sinteza, proprietățile fizico-chimice și structura compușilor coordinațivi de fier, cobalt, nichel și cupru cu α -dioxime*. Teza de doctor habilitat. Chișinău. 2000.
- [15] Samus', N.M.; Yushchenko, S.P.; Horoshun, I.V. et al. *Russ. Journ. Inorg. Chem.* 1989, 34, 4, pp. 892-897. (in russian)
- [16] Burdinski, D.; Birkelbach, F.; Weyhermuller, T. et al. *Inorg. Chem.* 1998, 37, pp. 1009-1020.
- [17] Voloshin, Y.Z.; Kostromina, N.A.; Kramer, R. *Clathrochelates: synthesis, structure and properties*. 2002. Amsterdam: Elsevier. 419 p.
- [18] Croitor, L.; Coropceanu, E.; Jeanneau, E. et al. *Crystal Growth & Design*. 2009, 9, pp. 5233-5243.
- [19] Gok, Y.; Yildiz, S.Z. *Synthesis and Reactivity in Inorganic and Metal-Organic Chemistry*. 1992, 22, pp. 1327-1341.
- [20] Proskina, N.N.; Shafransky, V.N.; Ablov, A.V. *Journ. A.S.M. Life sciences*. 1968, 6, pp. 7-11. (in russian)
- [21] Gulya, A.P.; Rudic, V.F.; Gerbelev, N.V. et al. *Patent №1616111 (USSR)*.
- [22] Bourosh, P.N.; Gerbelev, N.V.; Gdaniec, M. et al. *Russ. Journ. Inorg. Chem.* 2006, 51, 2, pp. 309-315. (in russian)
- [23] Gărbălău, N.; Simonov, Yu.; Bouroș, P. et al. *Patent MD 2833*.
- [24] Gărbălău, N.; Simonov, Yu.; Deseatnic, A. et al. *Patent MD 1203*.
- [25] Schrauzer, G.N.; Grate, J.H. *J. Am. Chem. Soc.* 1981, 103, pp. 541-546.
- [26] (a) Toscano, P.J.; Brand, H.; Liu, S.; Zubieta, J. *Inorg. Chem.* 1990, 29, 2101. (b) Ng, F.T.T.; Rempel, G.L.; Mancuso, C.; Halpern, J. *Organometallics*. 1990, 9, 2762. (c) Brown, T.M.; Cooksey, C.J.; Dronsfield, A.T.; Fowler, J.H. *Inorg. Chim. Acta*. 1999, 288, 112. (d) Brown, T.M.; Dronsfield, A.T.; Wilkinson, A.S. *Inorg. Chim. Acta*. 1997, 262, 97. (e) Daikh, B.E.; Finke, R.G. *J. Am. Chem. Soc.* 1992, 114, 2938.
- [27] Bresciani-Pahor, N.; Geremia, S.; Lopez, C. et al. *Inorg. Chem.* 1990, 29, 1043. (b) Toscano, P.J.; Marzilli, L.G. *Prog. Inorg. Chem.* 1985, 31, 105. (c) Gilaberte, J.M.; Lo'pez, C.; Alvarez, S. et al. *New J. Chem.* 1993, 17, 193. (d) Lo'pez, C.; Alvarez, S.; Solans, X.; Font-Altaba, M. *Inorg. Chim. Acta*. 1986, 111, L19.
- [28] Mandal, D.; Gupta, B. D. *Organometallics*. 2005, 24, pp. 1501-1510.
- [29] (a) Clifford, B.; Cullen, W. R. *J. Chem. Educ.* 1983, 60, 555. (b) Naumberg, M.; Duong, K.N.V.; Gaudemer, F.; Gaudemer, A. *C. R. Acad. Sci., Ser. C* 1970, 270, 1301. (c) Cabaret, D.; Maigrot, N.; Welvart, Z.; Duong, K. N. V.; Gaudemer, A. *J. Am. Chem. Soc.* 1984, 106, 2870.
- [30] Marzilli, L.G.; Summers, M.F.; Zangrando, E. et al. *J. Am. Chem. Soc.* 1986, 108, pp. 4830-4838.
- [31] Galinkina, J.; Rusanov, E.; Wagner, C. et al. *Organometallics*. 2003, 22, pp. 4873-4884.
- [32] Mandal, D.; Gupta, B.D. *Organometallics*. 2007, 26, 3, pp. 658-670.
- [33] Rusanovskii, M.E.; Samus', I.D.; Proskina, N.N. *Izvestiya Akademii Nauk Moldavskoi SSR. Seria Fiziko-Tekhnicheskikh i Matematicheskikh Nauk*. 1984, 2, pp. 55-57. (in russian)
- [34] Gradinaru, J.; Malinovskii, S.; Gdaniec, M.; Zecchin, S. *Polyhedron* 2006, 25, 17, pp. 3417-3426.
- [35] Malinovsky, S.T.; Bologa, O.A.; Coropceanu E.B. et al. *Journ. Struct. Chem.* 2007, 48, 4, pp. 740-746. (in russian)
- [36] Bourosh, P.N.; Coropceanu, E.B.; Simonov, Yu.A. et al. *Russ. Journ. Coord. Chem.* 2002, 28, 9, pp. 689-697. (in russian)
- [37] Malinovsky, S.T.; Coropceanu, E.B.; Bologa, O.A. et al. *Journ. Struct. Chem.* 2007, 48, 3, pp. 532-538. (in russian)

- [38] Rija, A.; Coropceanu, E.; Bologa, O. et al. Russ. Journ. Inorg. Chem. 2013, 58, 4, pp. 506-516. (in russian)
- [39] Bourosh, P.N.; Coropceanu, E.B.; Simonov, Yu.A. et al. Russ. Journ. Inorg. Chem. 2002, 47, 10, pp. 1604-1609. (in russian)
- [40] Bourosh, P.N.; Bologa, O.A.; Gdaniec M. et al. Journ. Struct. Chem. 2005, 46, 3, 488-493. (in russian)
- [41] Bourosh, P.N.; Coropceanu, E.B.; Bologa, O.A. et al. Russ. Journ. Coord. Chem. 2004, 30, 6, pp. 403-409. (in russian)
- [42] Simonov, Yu.A.; Gerbeleu, N.V.; Gdaniec, M. et al. Russ. Journ. Coord. Chem. 2001, 27, 5, pp. 368-379. (in russian)
- [43] Sakhawat Hussain, M.; Al-Mohdhar, H.M.; Schlemper, E.O. Journal of Crystallographic and Spectroscopic Research. 1989, 19, 1, pp. 77-91.
- [44] Rija, A.; Coropceanu, E.; Bologa, O. et al. Journ. Struct. Chem. 2007, 48, 6, pp. 1197-1202. (in russian)
- [45] Battaglia, L.P.; Corradi, A.M.; Palmieri, C.G. et al. Acta Cryst. B30, 1974, pp. 1114-1116.
- [46] Malinovsky, S.T.; Coropceanu, E.B.; Bologa, O.A.; Bel'sky, V.K. Russ. Journ. Coord. Chem. 2002, 28, 5, pp. 370-376. (in russian)
- [47] Coropceanu, E.B.; Rija, A.P.; Lozan, V.I. et al. Russ. Journ. Coord. Chem. 2012, 38, 8, pp. 575-581. (in russian)
- [48] Rija, A.P.; Nicolescu, A.; Soran, A. et al. Russ. Journ. Coord. Chem. 2011, 37, 10, pp. 759-767. (in russian)
- [49] Bourosh, P.; Coropceanu, E.; Rija, A. et al. Journ. Molec. Struct. 2011, 998, pp. 198-205.
- [50] Coropceanu, E.B.; Rija, A.P.; Shafransky, V.N. et al. Journ. Struct. Chem. 2007, 48, 6, pp. 1175-1182.

MOLECULAR REARRANGEMENTS OF HIGHLY FUNCTIONALIZED TERPENES. AN UNIQUE REACTIVITY OF BICYCLIC FRAMEWORK AND POLIENIC CHAIN INHIBITION UNDER SUPERACIDIC TREATMENT

Marina Grinco, Veaceslav Kulcički, Pavel F. Vlad, Alic Barba,
Elena Gorincioi, Nicon Ungur*

Institutul de Chimie al Academiei de Științe a Moldovei, 3, Academiei str., Chisinau MD-2028, Republic of Moldova
**e-mail: nicon.ungur@gmail.com, phone / fax: (+373 22) 73 97 75*

Abstract. Synthesis of polyfunctional triterpene derivative [8(27),13*E*,17*E*,21*E*]-15-phenylsulfonyl-16-oxo-bicyclofarnesylfarnesol benzyl ether (**8**) from commercially available monoterpene geraniol and diterpene manool has been accomplished in 73% yield and its chemical transformation in superacid medium has been investigated. An unexpected rearrangement of **8** occurred, which involved methyl migration in the bicyclic fragment and total inhibition of the lateral polienic chain. A new bicyclic triterpene product [5(10),13*E*,17*E*,21*E*]-15-phenylsulfonyl-16-oxo-30(10→9)-abeo-bicyclofarnesylfarnesol benzyl ether (**9**), with rearranged new carbon skeleton has been obtained. Its bicyclic moiety is analogous to this of a natural triterpene neopolypodatetraene.

Keywords: triterpenes, synthesis, superacid, isomerization.

Introduction

Triterpenes is a group of terpenes with a high structural diversity, which includes natural products with more than 100 types of skeleton [1–3]. Reviews related to biological activities of triterpenes appear regularly and are focused on their anti-inflammatory [4], antitumor [5], anti-HIV [6,7] and insecticidal [8] activities, and also their use in treatment of metabolic and vascular diseases [9].

Results and discussions

The aim of the present work is development of the method for synthesis of bicyclic polyfunctional triterpenes with a new carbon skeletons and study of their conversion in superacid medium.

Synthesis of the bicyclic triterpenoids containing two structural blocks, fragment A (monoterpene - aliphatic) and fragment B (diterpene - bicyclic) has been drawn, in order to achieve the proposed goal.

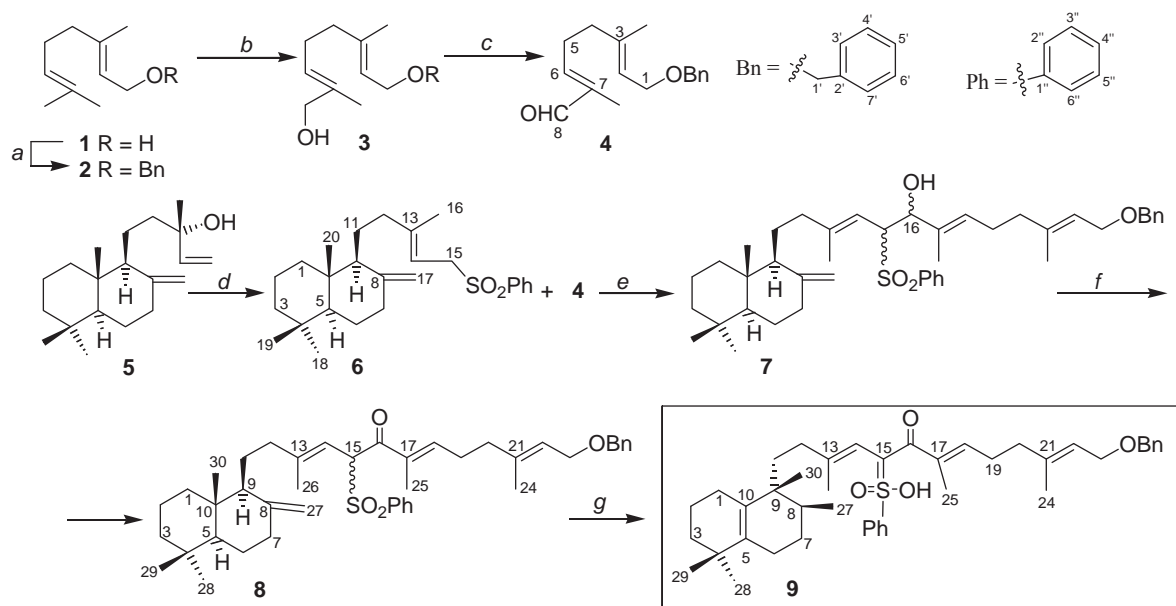
Fragment A has been obtained from commercially available monoterpene – geraniol (**1**) in three steps (Scheme 1). Treatment of geraniol (**1**) with benzyl chloride in dichloromethane and sodium hydride led to the corresponding benzyl ether. Its spectral data and physico-chemical constants are in accordance with the reported ones [10]. Compound **2** has been subjected to oxidation with selenium dioxide in ethanol furnishing the α,ω -bifunctionalized derivative **3** in a modest 45% yield. Finally, the monoterpene alcohol **3** has been oxidized with pyridinium chlorochromate (PCC) into the corresponding aldehyde **4** [11] (fragment A) in a 72% yield, its overall yield is ~32%.

Synthesis of fragment B has been achieved starting from commercially available manool (**5**). It was transformed into new diterpenic phenylsulfone **6** in a two-step sequence, according to the reported method [12]. It should be mentioned that from reaction product by column chromatography also the 13*Z*- isomer of diterpenyl-phenylsulfone **6** was obtained in ~20% yield.

The *n*-BuLi-assisted coupling reaction of aldehyde **4** (fragment A) and diterpenylphenylsulfone **6** (fragment B) in tetrahydrofuran gave bicyclic triterpene compound **7** in a 62% yield. Compound **7** was subjected to Swern oxidation giving the [8(27),13*E*,17*E*,21*E*]-15-phenylsulfonyl-16-oxo-bicyclofarnesylfarnesol benzyl ether (**8**) in acceptable yield (73%). It should be mentioned that an alternative oxidation of compound **7** with PCC in dichloromethane, led to a complex mixture of compounds where the content of target compound **8** does not exceed ~30%.

The structures of coupling reaction **7** and oxidation reaction **8** products have been established on the basis of their spectral data (see Experimental part).

Since the molecule of bicyclic triterpene derivative **8** is characterized by more than one double bond that is prone to chemical transformation in acid medium, the behavior of compound **8** in superacid medium at low temperature has been further explored [13-16]. Thus, following a previous elaboration, [8(27),13*E*,17*E*,21*E*]-15-phenylsulfonyl-16-oxo-bicyclofarnesylfarnesol benzyl ether (**8**) has been treated with fluorosulfonic acid in 2-nitropropane at -78°C [12,17].



Scheme 1

Reagents and conditions. (a) NaH, BnCl, TBAI, CH₂Cl₂, r.t., 12 h, 92%; (b) SeO₂, EtOH, reflux, 3h, 45%; (c) PCC, CH₂Cl₂, r.t., 1.5h, 70%; (d) 1) PBr₃/Et₂O; 2) NaSO₂Ph/DMF, overall for two steps 74%; (e) *n*-BuLi/THF, 66%; (f) (COCl)₂/DMSO, CH₂Cl₂, -60°C, Et₃N, 73%; (g) FSO₃H, *i*-PrNO₂, -78°C, 20 min, 62%.

The product [5(10),13*E*,17*E*,21*E*]-15-phenylsulfonyl-16-oxo-30(10→9)-abeo-bicyclopentacyclononane benzyl ether (**9**) has been isolated in a 62% yield, its structure being assigned by IR and NMR spectroscopic data. The IR spectrum exhibited absorption bands at 1145, 1385, 1451, 1668, 1793, 2286, 2993 and 3362 cm⁻¹, suggesting the presence of carbonyl-, phenylsulfonyl- and olefinic groups. NMR characteristics of compound **9** have been obtained on the basis of its 1D (¹H, ¹³C, DEPT-13°) and 2D homo- (¹H/¹H COSY-45°) and heteronuclear (¹H/¹³C HSQC and ¹H/¹³C HMBIC) correlation spectra (Fig. 1). The ¹H NMR spectrum (Table 1) displayed singlets of geminal dimethyl at δ_H 0.99, 1.01, (each 3H, H-28, H-29), signal of one tertiary and one secondary methyl groups at δ_H 0.86 (6H, H-30, H-27) that appears as a multiplet due to overlapping, low-field singlets of three methyls attached to double bonds at δ_H 1.49, 1.66, 1.80 (each 3H, H-26, H-24, H-25), downfield signals of ether methylenes at δ_H 4.00 (*d*, *J* = 6.6 Hz, H-23) and δ_H 4.50 (*s*, H-1') and deshielded signals of three sp² methines: δ_H 5.44 (*tg*, *J* = 6.6; 1.1 Hz, H-22), 5.74 (*br. s.*, H-14), 6.96 (*tg*, *J* = 7.2; 1.2 Hz, H-18).

The ¹H NMR spectrum of compound **9** also contains the signals of two phenyl groups: one belonging to benzyl moiety, for which strong signal overlapping has been noted, at δ_H 7.26-7.35 (*m*, 4H, H-3'-7') and another one, identifying phenylsulfone fragment at δ_H 7.50 (*bt*, *J* = 8.0 Hz, H-3'', 5'' and 8.09 (*dm*, *J* = 8.0 Hz, H-2'', 6''). The clear substructures H-18 - H-19 - H-20; H-14 - H-26; H-22 - H-23 - H-24 - H-20 and, in contrast to the precursor **8** - H-2'' - H-3'', H-4'', H-5'' - are evident in ¹H/¹H COSY spectrum, the accurate description of all methylene protons being difficult because of severe signal overlapping (see: Table 1). The ¹³C NMR data exhibited thirty nine carbon signals, which were assigned by a DEPT experiment as seven methyls, eleven sp³ methylenes, one sp³ and nine sp² methines, two sp³ and ten sp² quaternary carbons. The presence of α,β-unsaturated carbonyl moiety has been corroborated in the molecules of precursor **8**, by the ¹H and ¹³C NMR data [δ_C 190.3 (C-16), 132.4 (C-17), 147.0 (C-18); δ_H 1.80 (*s*, 3H, H-25)]. The rearranged carbon framework of **9** becomes obvious while examining its HMBIC spectrum. Thus, the observed correlations from both H-6 and H-1 to two sp² hybridized (C-5, δ_C 137.8 and C-10, δ_C 131.7) instead of two sp³ (C-5, δ_C 51.9 and C-10, δ_C 40.4) in the former compound **8** were indicative on Δ^{5,10} localization, which was supported also by the correlations of H₃-29/C-5, H₃-28/C-5. The logical migration of methyl H₃-30 from C-10 to C-9 position has been ascertained by H₃-30/C-10, H₃-30/C-9 and H₃-30/C-11 cross-peaks in the HMBIC spectrum, while the evident substitution of two olefinic carbons (C-8, δ_C 148.5 and C-27, δ_C 106.2) in the precursor **8** by the corresponding sp³ atoms in **9** (C-8, δ_C 33.6 and C-27, δ_C 16.1) has been proved by long-range correlations H₃-27/C-6, H₃-27/C-7 and H₃-27/C-9.

Table 1.

¹H (400.13 MHz) and ¹³C NMR (100.61 MHz) data of compound 9 in CDCl₃ (δ in ppm).

Position	Compound 9		
	δ ¹ H	m, J (Hz)	δ ¹³ C ^{a,b}
1	1.73, 1.98	m ^c	25.9 CH ₂
2	1.49-1.65	m ^c	20.0 CH ₂
3	1.37, 1.48	m ^c	40.0 CH ₂
4	--	--	34.6 qC
5	--	--	137.8 qC
6	1.96	m ^c	25.2 CH ₂
7	1.43	m ^c	34.2 CH ₂
8	1.60	m ^c	33.6 qC
9	--	--	40.6 qC
10	--	--	131.7 qC
11	1.34, 1.48	m ^c	27.2 CH ₂
12	1.70, 2.00	m ^c	35.9 CH ₂
13	--	--	150.8 qC
14	5.74	br. s.	119.4 qC
15	--	--	not detected
16	--	--	190.3 qC
17	--	--	132.4 qC
18	6.96	tq (7.2; 1.2)	147.0 CH
19	2.40	m	27.7 CH ₂
20	2.10	m	37.8 CH ₂
21	--	--	138.5 qC
22	5.44	tq (6.6; 1.1)	122.0 CH
23	4.00	d (6.6)	66.5CH ₂
24	1.66	s	16.5 CH ₃
25	1.80	s	12.4 CH ₃
26	1.49	s	18.4 CH ₃
27	0.86	m ^c	16.1 CH ₃
28	0.99	s	29.2 CH ₃
29	1.01	s	27.7 CH ₃
30	0.86	m ^c	21.2 CH ₃
1'	4.50	s	72.3 CH ₂
2'	--	--	138.4 qC
4', 6'	7.30	m ^c	127.8 CH
3', 7'	7.30	m ^c	128.4 CH
5'	7.30	m ^c	128.4 CH
1''	--	--	136.5 qC
2'', 6''	8.09	dm (8.0)	132.5 CH
3'', 5''	7.50	br.t. (8.0)	128.2 CH
4''	7.64	dm (7.5)	134.0 CH

^a – degree of protonation found by DEPT sequence,^b –HMBC experiments (*J* = 8 Hz),^c – signal overlapping.

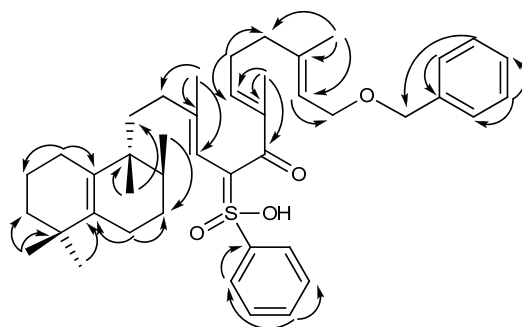
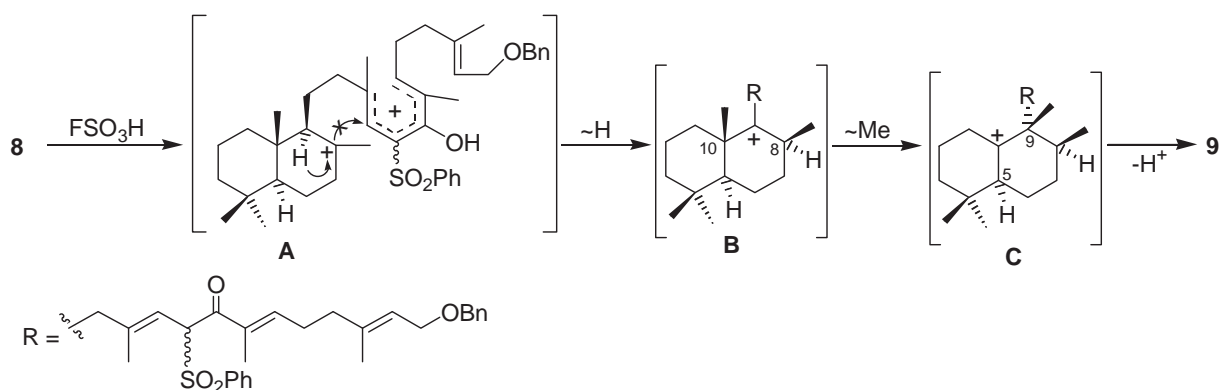


Figure 1. Selected HMBC correlations for compound 9.

The rearranged triterpene derivative **9** has been thereby obtained as a result of selective reactivity of the bicyclic part under superacidic treatment. Its plausible formation from compound **8** is depicted in Scheme 2. Due to the presence of oxygenated groups in side chain at C-16 and C-17 that can be easily protonated the bication A, which blocks the carbocyclisation in acid medium, is formed. In such a manner only the migration of proton from C-9 to C-8 takes place, producing the carbocation B. The latter is subjected to ulterior conversion into the carbocation C, as a result of methyl group migration from C-10 to C-9. While „quenching” the carbocation C the separation of proton at C-5 occurs and the final product **9** is obtained.



Scheme 2. Superacid-promoted molecular isomerization of compound 8.

It should be noted that the polyfunctional triterpene derivative **9** can be considered a congener of natural triterpenoid neopolypodatetraene (**10**), especially on considering the similarity in the bicyclic fragment (Figure 2). The latter has been isolated from a squalene hopene cyclase mutant of the prokaryotic bacterium *Alicyclobacillus acidocaldarius* F365A [18].

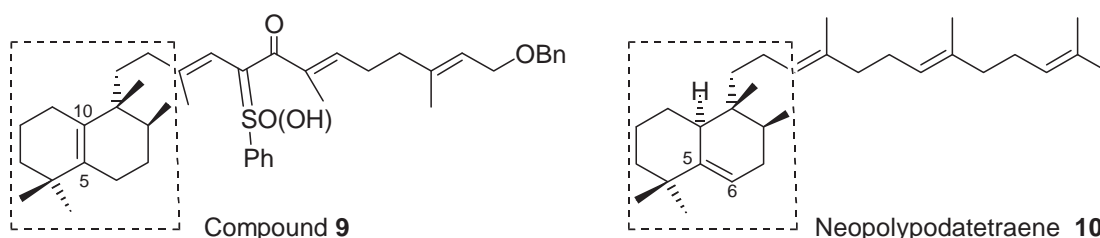


Figure 2.

Conclusions

Synthesis of polyfunctional triterpene derivative [8(27),13*E*,17*E*,21*E*]-15-phenylsulfonyl-16-oxo-bicyclopentacyclotetraene has been achieved and its chemical transformation in superacid medium has been

studied. Mentioned bicyclic triterpene product with rearranged carbon framework, which is a structural analogous of the natural triterpene neopolypodatetraene, has been obtained for the first time.

Experimental

General. Melting points (mp) were determined on a Boetius hot stage. IR Spectra were recorded on a Spectrum-100 FT-IR spectrophotometer (Perkin-Elmer), with the universal ATR sampling accessory (ν in cm^{-1}). ^1H - and ^{13}C -NMR spectra were recorded in CDCl_3 on Bruker 400 Avance III spectrometer (400.13 and 100.61 MHz); chemical shift are given in ppm and are referenced to measured in chloroform (CHCl_3) as internal standard ($\delta = 7.26$ ppm for proton and $\delta = 77.0$ for carbon). Optical rotations were measured in chloroform on a Jasco DIP 370 polarimeter, using 5 cm cell. Commercial Merck Si gel 60 (70–230 mesh ASTM) was used for flash chromatography, and Merck pre-coated SiO_2 plates were used for TLC. The chromatograms were sprayed with 0.1% solution of cerium (IV) sulfate in 2N sulfuric acid and heated at 80°C for 5 min to detect the spots. GC/MS analysis were recorded on Agilent 7890A chromatograph, equipped with quadrupole MS detector MSD 5975C and HP-5 ms capillary column (30 m/0.25 mm). Treatment of reaction mixtures in organic solvents included the extraction by Et_2O , washing of the extract with H_2O up to neutral reaction, drying over anhydrous Na_2SO_4 , and solvent removal *in vacuo*.

Geraniol benzyl ether (2). Geraniol (**1**) (12 g, 77.9 mmol) in dry THF (103 mL) was treated with 60% NaH (3.68 g), benzyl chloride (10.61 mL, 92.2 mmol) and tetrabutylammonium iodide (2.88 g, 7.79 mmol). The reaction mixture was stirred for 12 h at room temperature. Then, 10% aqueous solution of H_2SO_4 (20 mL) was added. Usual work up gave a crude reaction product (25 g), which was purified by flash chromatography using 1% ethyl acetate/light petroleum ether mixture to yield 17.52 g (92%) of the geraniol benzyl ether (**2**), as a pale yellow oil. IR liquid film (ν , cm^{-1}): 735, 1069, 1101, 1270, 1377, 1453, 1496, 1670, 1726, 2924. ^1H NMR (400 MHz, δ_{H}): 1.62 (s, 3H, H-9), 1.66 (s, 3H, H-10), 1.69 (d, $J = 0.9$ Hz, 3H, H-8), 2.06 (m, 2H, H-4), 2.12 (m, 2H, H-5), 4.04 (dd, $J = 6.8, 0.3$ Hz, 2H, H-1), 4.51 (s, 2H, H-1'), 5.12 (m, 1H, H-6), 5.42 (m, 1H, H-2), 7.34 (m, 5H, Ar-H). ^{13}C NMR (100 MHz, δ_{C}): 16.4 (q, C-10), 17.6 (q, C-9), 25.6 (q, C-8), 26.4 (t, C-5), 39.6 (t, C-4), 66.6 (t, C-1), 71.9 (t, C-1'), 138.6 (d, C-2), 124.0 (d, C-6), 127.5 (d, C-5'), 127.8 (d, C-3', 7'), 128.3 (d, C-4', 6'), 131.6 (s, C-7), 138.6 (s, C-2'), 140.3 (s, C-3). All physical properties and spectroscopic data were identical with those reported in literature [10].

8-Hydroxygeraniol benzyl ether (3). A suspension of selenium dioxide (1.45 g, 13.08 mmol) in ethanol (9 mL) was added to a solution of geranylbenzyl ether (**2**) (6.38 g, 26.15 mmol) in ethanol (89 mL). The mixture was refluxed for 3 h, cooled to 0°C, treated with NaBH_4 (500 mg, 13.08 mmol) and stirred at the same temperature for 2 h. After, the reaction was quenched with a 10% soln. of H_2SO_4 (10 mL), and the mixture was worked up as usual. The crude product (7.5 g) was submitted to flash chromatography on silica gel (200 g) with increasing gradient of ethyl acetate in light petroleum ether to give starting ether (**2**) (3.14 g, 49%) and 8-hydroxygeraniol benzyl ether (**3**) (3.05 g, 45%), as colorless viscous oil. IR liquid film (ν , cm^{-1}): 697, 736, 1067, 1453, 1639, 3429. ^1H NMR (400 MHz, δ_{H}): 1.65 (s, 3H, H-10), 1.66 (s, 3H, H-9), 2.08 (t, $J = 7.3$ Hz, 2H, H-4), 2.17 (q, $J = 7.3$ Hz, 2H, H-5), 3.97 (s, 2H, H-8), 4.02 (d, $J = 6.8$ Hz, 2H, H-1), 4.50 (s, 2H, H-1'), 5.39 (m, 2H, H-2 and H-6), 7.31 (m, 5H, Ar-H). ^{13}C NMR (100 MHz, δ_{C}): 13.6 (q, C-9), 16.4 (q, C-10), 25.8 (t, C-5), 39.1 (t, C-4), 66.5 (t, C-1), 68.9 (t, C-8), 72.1 (t, C-1'), 121.1 (d, C-2), 125.5 (d, C-6), 127.5 (d, C-5'), 127.8 (d, C-3', 7'), 128.3 (d, C-4', 6'), 135.1 (s, C-3), 139.9 (s, C-7). All physical properties and spectroscopic data were identical with those reported in literature [10].

8-Oxo-geraniol benzyl ether (4). Hydroxyether (**3**) (1.41 g, 5.42 mmol) was dissolved in dry CH_2Cl_2 (83 mL) and PCC (1.75 g, 8.13 mmol) was added. After stirring the reaction mixture at room temperature for 1.5 h, it was diluted with diethyl ether (60 mL) and passed through a short silica gel pad. The crude product (1.9 g) was subjected to flash chromatography. Elution with 4% ethyl acetate/light petroleum ether mixture gave 980 mg (70%) of unsaturated aldehyde (**4**), as a pale yellow oil. IR liquid film (ν , cm^{-1}): 697, 736, 1069, 1116, 1381, 1453, 1686, 2857, 2975. ^1H NMR (400 MHz, δ_{H}): 1.69 (s, 3H, H-10), 1.76 (d, $J = 0.8$ Hz, 3H, H-9), 2.23 (t, $J = 7.6$ Hz, 2H, H-4), 2.5 (q, $J = 7.6$ Hz, 2H, H-5), 4.06 (d, $J = 6.7$ Hz, 2H, H-1), 4.51 (s, 2H, H-1'), 5.46 (apparent tq, $J = 6.7, 1.2$ Hz, 1 H, H-2), 6.47 (td, $J = 7.6, 1.3$ Hz, 1H, H-6), 7.31 (m, 5H, Ar-H), 9.39 (s, 1H, H-8). ^{13}C NMR (100 MHz, δ_{C}): 9.0 (q, C-9), 16.2 (q, C-10), 26.9 (t, C-5), 37.6 (t, C-4), 66.3 (t, C-1), 72.0 (t, C-1'), 121.9 (d, C-2), 127.4 (d, C-5'), 127.5 (d, C-3', 7'), 128.2 (d, C-4', 6'), 138.2 (s, C-2'), 138.3 (s, C-3), 139.3 (s, C-7), 153.5 (d, C-6), 194.8 (d, C-8). All physical properties and spectroscopic data were identical with those reported in literature [11].

Synthesis of 8(17),13E-bicyclogeranylgeranylphenylsulfone (6). A solution of phosphorus tribromide (1.54 g, 5.69 mmol) in dry ether (5.0 mL) was added dropwise to a stirred solution of manool (**5**) (1.20 g, 4.14 mmol) in dry ether (10 mL) with cooling on an ice bath. The mixture was stirred for 2 h at room temperature and treated with saturated NaHCO_3 solution. The ether layer was separated, washed with brine, dried, and concentrated *in vacuo*. The resulting

bromide (1.25 g, 86%) was added to a solution of the sodium salt of benzenesulfonic acid (0.90 g, 5.45 mmol) in dry DMF (10 mL). The mixture was stirred at room temperature under argon in the dark for 3 h, treated with NaCl solution, and extracted with ether. The extract was worked up as usual to afford a liquid product that was chromatographed on silica gel (42 g) with gradient elution by petroleum ether: AcOEt to elute 13*E*-bicyclogeranylgeranylphenylsulfone (**6**) (1.09 g, overall for two steps ~74%), as colorless crystals, m.p. 87-88°C (from hexane), $[\alpha]_D^{25} +32.2^\circ$ (*c* 1.45, CHCl₃). IR liquid film (ν , cm⁻¹): 730, 1149, 1306, 1447, 1587, 1642, 2927. ¹H NMR (400 MHz, δ_H): 0.65 (*s*, 3H, H-20), 0.79 (*s*, 3H, H-19), 0.86 (*s*, 3H, H-18), 1.29 (*s*, 3H, H-16), 3.80 (*d*, *J* = 8 Hz, 2H, H-15), 4.42 (*d*, *J* = 1.2 Hz, 1H, H_b-17), 4.80 (*d*, *J* = 1.4 Hz, 1H, H_a-17), 5.14 (*td*, *J* = 8.0, 1.3 Hz, 1H, H-14), 7.68 (*m*, 5H, Ph-H). ¹³C NMR (100 MHz, δ_C): 14.5 (*q*, C-20), 16.2 (*q*, C-16), 19.4 (*t*, C-2), 21.7 (*q*, C-19), 21.8 (*t*, C-11), 24.4 (*t*, C-6), 33.6 (*s*, C-4), 33.6 (*q*, C-18), 38.3 (*t*, C-7), 38.6 (*t*, C-12), 39.1 (*t*, C-1), 39.7 (*s*, C-10), 42.1 (*t*, C-3), 55.5 (*d*, C-5), 56.1 (*t*, C-15), 56.3 (*d*, C-9), 106.2 (*t*, C-17), 110.0 (*d*, C-14), 128.6 (*d*, C-3'', 5''), 128.9 (*d*, C-2'', 6''), 133.4 (*d*, C-4''), 138.8 (*s*, C-1'') 147.2 (*s*, C-13), 148.5 (*s*, C-8). Found (%): C, 75.42; H, 9.31. C₂₆H₃₈SO₂. Calculated (%): C, 75.31; H, 9.24.

[8(27),13E,17E,21E]-15-phenylsulfonyl-16-hydroxy-bicyclofarnesylfarnesol benzyl ether (7). Compound **6** (529 mg, 1.28 mmol, 1.2 eq.) was co-evaporated with benzene, dried under high vacuum, and then dissolved in anhydrous THF (4.6 mL) and cooled to -78 °C. Then *n*-BuLi (1.7 M, 0.75 mL, 1.28 mmol, 1.2 equiv) was added drop-wise to the 8(17),13*E*-bicyclogeranylgeranylphenylsulfone (**6**) solution over 2 min. under argon atmosphere. The resulting bright yellow solution was stirred at -78°C for 30 min and gradually warmed to -40°C over 1 h and then cooled to -78°C. Aldehyde **4** (279 mg, 1.07 mmol, 1 equiv) was dried under high vacuum, dissolved in THF (4.6 mL), cooled to -78 °C, and added drop-wise to the sulfone anion solution using a syringe. After 30 min of stirring at -78°C, the reaction mixture was gradually heated to -40°C and sat. aq. NH₄Cl (4 mL) was added followed by usual workup. The residue (900 mg) was purified by silica gel flash column chromatography (10% ethyl acetate/light petroleum ether mixture) affording compound **7** (472 mg, 66%), as a clear yellow oil. IR liquid film (ν , cm⁻¹): 730, 1144, 1230, 1446, 2191, 2290, 2947. ¹H NMR (400 MHz, δ_H): 0.64 (*s*, 3H, H-30), 0.79 (*s*, 3H, H-29), 0.86 (*s*, 3H, H-28), 1.11 (*s*, 3H, H-26), 1.49 (*s*, 3H, H-25), 1.61 (*s*, 3H, H-24), 3.95 (*m*, 1H, H-15), 4.00 (*d*, *J* = 6.7 Hz, 2H, H-23), 4.37 (*d*, *J* = 0.8 Hz, 1H, H_b-27), 4.49 (*s*, 2H, H-1'), 4.61 (*d*, *J* = 9.7 Hz, 1H, H-16), 4.67 (*m*, 1H, H-14), 4.80 (*d*, *J* = 0.9 Hz, 1H, H_a-27), 5.37 (*t*, *J* = 6.7 Hz, 1H, H-22), 5.42 (*t*, *J* = 6.8 Hz, 1H, H-18), 7.31 (*m*, 5H, Ar-H), 7.68 (*m*, 5H, Ph-H). ¹³C NMR (100 MHz, δ_C): 10.6 (*q*, C-25), 14.5 (*q*, C-30), 16.1 (*q*, C-26), 16.5 (*q*, C-24), 19.4 (*t*, C-2), 21.7 (*q*, C-29), 24.4 (*t*, C-6), 26.0 (*t*, C-11), 29.7 (*t*, C-19), 33.3 (*s*, C-4), 33.6 (*q*, C-28), 38.3 (*t*, C-7), 38.8 (*t*, C-12), 38.9 (*t*, C-20), 39.2 (*t*, C-1), 39.8(*s*, C-10), 42.2 (*t*, C-3), 55.6 (*d*, C-5), 56.5 (*d*, C-9), 66.6 (*t*, C-23), 68.6 (*d*, C-15), 72.1 (*t*, C-1'), 76.5 (*d*, C-16), 106.2 (*t*, C-27), 114.0 (*d*, C-14), 121.3 (*d*, C-22), 127.5 (*d*, C-5'), 127. 8 (*d*, C-3', 7'), 128.3 (*d*, C-4', 6'), 128.8 (*d*, C-3'', 5''), 129.4 (*d*, C-2'', 6''), 130.2 (*d*, C-18), 133.4 (*s*, C-17), 133.8 (*d*, C- 4''), 137.7 (*s*, C-1''), 138.6 (*s*, C-2'), 139.6 (*s*, C-21), 145.3 (*d*, C-13), 148.5 (*s*, C-8). Found (%): C, 76.53; H, 8.89. C₄₃H₆₀SO₄. Calculated (%): C, 76.74; H, 8.99.

[8(27),13E,17E,21E]-15-phenylsulfonyl-16-oxo-bicyclofarnesylfarnesol benzyl ether (8). A solution of DMSO (0.085 mL, 1.21 mmol) in CH₂Cl₂ (1.8 mL) was added dropwise to a stirred solution of oxalyl chloride (0.07 mL, 0.61 mmol) in CH₂Cl₂ (1.8 mL) cooled to -60 °C. After 5 min of stirring at this temperature, a solution of compound (**7**) (185 mg, 0.275 mmol) in CH₂Cl₂ (1.8 mL) was added dropwise. After 30 min of stirring (-60°C) triethylamine (0.5 mL, 3.03 mmol) was added to the reaction mixture, and after another 15 min the cooling bath was removed and water (3 mL) was added at room temperature. After separation of the phases, the aqueous phase was extracted with CH₂Cl₂ (3×10 mL) and the combined organic phase was subsequently washed with a 20% H₂SO₄, a sat. NaHCO₃ solution, brine to neutral pH. Drying with Na₂SO₄ and subsequent evaporation of the solvent gave a crude reaction product, which was submitted to flash chromatography (8% ethyl acetate/light petroleum ether) to give polar ketone **8** (134 mg, 0.2 mmol, 73%), as a pale yellow oil. IR liquid film (ν , cm⁻¹): 745, 1144, 1309, 1394, 1449, 1665, 1791, 2289, 2986, 3365. ¹H NMR (400 MHz, δ_H): 0.82 (*s*, 3H, H-29), 0.87 (*s*, 3H, H-28), 0.92 (*s*, 3H, H-30), 1.65 (*s*, 3H, H-26), 1.68 (*s*, 3H, H-24), 1.82 (*s*, 3H, H-25), 4.04 (*d*, *J* = 6.6 Hz, 2H, H-23), 4.42 (*d*, *J* = 0.9 Hz, 1H, H_b-27), 4.51 (*s*, 2H, H-1'), 4.82 (*d*, *J* = 1.0 Hz, 1H, H_a-27), 5.15 (*d*, *J* = 3.0 Hz, 1H, H-14), 5.46 (*t*, *J* = 6.6 Hz, 1H, H-22), 5.63 (*d*, *J* = 3.0 Hz, 1H, H-15), 6.69 (*m*, 1H, H-18), 7.31 (*m*, 5H, Ar-H), 7.65 (*m*, 5H, Ph-H). ¹³C NMR (100 MHz, δ_C): 11.8 (*q*, C-25), 16.4 (*q*, C-24), 17.1 (*q*, C-26), 26.3 (*t*, C-11), 19.3 (*t*, C-2), 20.1 (*q*, C-30), 21.7 (*q*, C-29), 24.4 (*t*, C-6), 27.6 (*t*, C-19), 33.25 (*s*, C-4), 33.28 (*q*, C-28), 37.9 (*t*, C-20), 38.3 (*t*, C-7), 39.0 (*t*, C-1), 40.39 (*t*, C-12), 40.41 (*s*, C-10), 41.8 (*t*, C-3), 51.9 (*d*, C-5), 56.3 (*d*, C-9), 66.5 (*t*, C-23), 68.7 (*d*, C-15), 72.3 (*t*, C-1'), 106.2 (*t*, C-27), 113.5 (*d*, C-14), 122.2 (*d*, C-22), 127.5 (*d*, C-5'), 127.8 (*d*, C-3', 7'), 128.3 (*d*, C-4', 6'), 128.5 (*d*, C-3'', 5''), 130.0 (*d*, C-2'', 6''), 133.7 (*d*, C- 4''), 137.4 (*s*, C-1''), 137.8 (*s*, C-17), 138.4 (*s*, C-2'), 138.6 (*s*, C-21), 145.0 (*d*, C-18), 147.1 (*s*, C-13), 148.5 (*s*, C-8), 192.2 (*s*, C-16). Found (%): C, 76.83; H, 8.82. C₄₃H₅₈SO₄. Calculated (%): C, 76.97; H, 8.71.

[5(10),13E,17E,21E]-15-phenylsulfonyl-16-oxo-30(10→9)-abeo-bicyclofarnesylfarnesol benzyl ether (9). Compound **8** (40 mg, 0.06 mmol) was dissolved in 2-nitropropane (0.7 mL) and a solution of FSO₃H (0.017 mL, 0.3 mmol, 5 equiv.) in 2-nitropropane (0.2 mL) was added under argon to the resulting solution at -78°C. After 20 min of stirring,

the reaction mixture was quenched with a solution of triethylamine (0.5 mL) in light petroleum ether (0.5 mL), then reaction mixture was warmed to room temperature, diluted with brine (10 mL). After usual work-up the crude reaction product (42 mg), was submitted to flash chromatography (1% ethyl acetate/benzene) to give compound **9** (25 mg, 62%). IR liquid film (ν , cm^{-1}): 740, 1145, 1312, 1385, 1451, 1668, 1793, 2286, 2993, 3362. ^1H NMR (see: Table 1). ^{13}C NMR (see: Table 1). Found (%): C, 77.12; H, 8.91. $\text{C}_{43}\text{H}_{58}\text{SO}_4$. Calculated (%): C, 76.97; H, 8.71.

References

- [1] Hill, R. A.; Connolly, J. D. *Nat. Prod. Rep.*, 2013, 30 (7), pp. 1028-1065, and previous reviews.
- [2] Domingo, V.; Arteaga, J. F.; del Moral, J. F. Q.; Barrero, A. F. *Nat. Prod. Rep.*, 2009, 26 (1), pp. 115-134.
- [3] Xu, R.; Fazio, G. C.; Matsuda, S. P. *Phytochemistry*, 2004, 65 (3), pp. 261-291.
- [4] Sporn, M. B.; Liby, K. T.; Yore, M. M.; Fu, L.; Lopchuk, J. M.; Gribble, G. W. *J. Nat. Prod.*, 2011, 74, pp. 537-545.
- [5] Bishayee, A.; Ahmed, S.; Brankov, N. Perloff, M. *Front. Biosci.*, 2011, 16, pp. 980-996.
- [6] Cassels, B. K.; Asencio, M. *Phytochem. Rev.*, 2011, 10, pp. 545-564.
- [7] Kuo, R.-Y.; Qian, K.; Morris-Natschke, S. L.; Lee, K.-H. *Nat. Prod. Rep.*, 2009, 26 (10), pp. 1321-1344.
- [8] Gonzalez-Coloma, A.; Lopez-Balboa, C.; Santana, O.; Reina, M. and Fraga, B. M.; *Phytochem. Rev.*, 2011, 10, pp. 245-260.
- [9] Sheng, H.; Sun, H. *Nat. Prod. Rep.*, 2011, 28, pp. 543-593.
- [10] Altman, L. J.; Ash, L.; Stuart Marson, S. *Synthesis*, 1974; (2), pp. 129-131.
- [11] Masaki, Y.; Hashimoto, K.; Kaji, K. *Tetrahedron Lett.*, 1978, 19 (46), pp. 4539-4542.
- [12] Kulcički, V.; Ungur, N.; Vlad, P. F. *Tetrahedron*, 1998, 54 (39), pp. 11925-11934.
- [13] Ungur, N.; Nguen, V. T.; Popa, N. P.; Vlad, P. F. *Chem. Nat. Comp.*, 1993, 28 (6), pp. 561-568.
- [14] Korchagina, D. V.; Gavrilyuk, O. A.; Barkhash, V. A.; Vlad, P. F.; Ungur, N. D.; Popa, N. P. *Zh. Org. Khim.*, 1993, 29 (2), pp. 323-325.
- [15] Ungur, N. ; Popa, N. P.; Kulcički, V. N.; Vlad, P. F. *Chem. Nat. Comp.*, 1993, 29 (5), pp. 618-621.
- [16] Ungur, N.; Popa, N. P.; Vlad, P. F. *Chem. Nat. Comp.*, 1993, 29 (5), pp. 613-617.
- [17] Kulcički, V.; Grinco, M.; Barba, A.; Ungur, N.; Vlad, P. F. *Chem. Nat. Comp.* 2007, 43 (3), pp. 268-273.
- [18] Sato, T; Hoshino, T. *Biosci., Biotechnol., Biochem.*, 2001, 65 (10), pp. 2233-2242.

A REVIEW OF THE BIOGENESIS OF IRON NANOPARTICLES USING MICROORGANISMS AND THEIR APPLICATIONS

Lilia Anghel^{a*}, Gheorghe Duca^b

^a*Institute of Chemistry of the Academy of Science of Moldova, 3, Academiei str., Chisinau MD-2028, Republic of Moldova*

^b*Academy of Science of Moldova, 1, Stefan cel Mare Blvd., Chisinau MD-2001, Republic of Moldova*

**e-mail: anghel.lilia@gmail.com*

Abstract. Iron-based nanoparticles have gained a lot of attention due to their properties which offer a broad range of biomedical and industrial applications. Traditional methods of synthesis of iron nanoparticles strongly influence their properties and limit their applicability. Recently, there has been a growing interest in the development of biological routes of syntheses of iron nanoparticles as the resulting particles have structural characteristics required by biomedical field. The mechanism for the synthesis of iron-based nanoparticles by microorganisms and its current limitation are presented.

Keywords: nanoparticles, iron, microorganisms, biological synthesis, biomedical applications.

Introduction

Iron is one of the most abundant metals of the Earth's crust. It is found mostly in different forms of iron oxide widespread in nature and readily synthesized in the laboratory [1]. Iron based nanoparticles have been studied extensively because of their wide range of applications including magnetic recording media, environmental remediation, and biomedicines [2-7]. The physical and chemical properties of iron nanoparticles are mainly determined by their size, shape, composition, crystallinity and structure [8-10]. Therefore, in almost all applications the preparation method of the nanoparticles is one of the most important factors that will influence their properties and potential applicability. Various methods of synthesis have been reported including chemical reduction, thermal decomposition, hydrothermal synthesis, microemulsion, and decomposition by ultrasonic treatment, electrochemical generation [11-18]. Nonetheless, development of pathways for nanoparticles production with a better control over the particle size, monodispersity, morphology, purity, quantity and quality by employing economical process is still of a great challenge [19]. One of the options to overcome this challenge is to use microorganisms to synthesize nanoparticles.

Biological routes of synthesis are preferred mainly due to their overcoming advantages over other methods. Advantages such as reaction conditions benign for environment, adequate range of material sources present and good nature of reduction takes place to form nanoparticles. The time for completion of the reaction, which is an obvious advantage of the biosynthetic procedures compared to the chemical methods [20]. The biogenic approach is also sustained by the fact that most of the microorganisms inhabit ambient conditions of varying temperature, pH, and pressure [21]. It was found that biosynthesized nanoparticles due to their specific properties excel those obtained by means of physical or chemical methods [22]. Biogenic nanoparticles have a higher catalytic reactivity, greater specific surface area, and an improved contact between the enzyme and metal salt in question due to the bacterial cell wall network [21, 23, 24].

Various methods have been developed for the biosynthesis of iron nanoparticles [25]. According to the location where nanoparticles are formed, these processes are classified into intracellular [26] and extracellular [27,28] synthesis. Biogenic processes are important in the formation of these nanoparticles, in general terms they are known as biomineralization. The mechanism of nanoparticles formation in microorganisms is complicated because of implication of different metabolic systems, but generally it can be described as a two-step process. The first step is the uptake of the organic or inorganic metal species, both soluble and insoluble, by physic-chemical mechanism such as adsorption. Metal ions are adsorbed onto the surface of cells by interactions between metals and functional groups displayed on the surface of cells. The second step is a redox-mediated mechanism which involves the participation of membrane proteins responsible for acquisition of a specific metal ion. These processes end with transportation of ions through cell's membrane, their deposition and intracellular nanoparticles formation.

Hereby, we attempt to present the current perspectives in the research field focused on biological synthesis of iron-based nanoparticles. This is followed by concise discussions of the nanoparticles properties arising from the size/shape and monodispersity of particles. Next, current applications of iron nanoparticles in the technological and biomedical fields are presented.

Biological synthesis of iron-based nanoparticles

Iron is used by microorganism to build enzymes that catalyze biochemical reactions within the cell [29]. Yet, when the cellular concentration of iron becomes greater it causes oxygen to react destructively with many

biomolecules. As a result, microorganisms have evolved mechanism for buffering high concentrations. When a microorganism takes in more metal than it needs, it stores the excess in either protein storages or simple nanoparticles extracellularly or intracellularly. These storages are accessed by microorganisms when there is not enough iron in their environment.

The exact mechanism for the biosynthesis of metal nanoparticles using microorganisms has not been established yet. One of the reasons is that microorganisms react differently with metal ions and also the existence of different metabolic processes which contribute to the synthesis of nanoparticles. In addition, the mechanism for intracellular and extracellular synthesis of nanoparticles is different for various microorganisms. A major factor which influences the intracellular synthesis of nanoparticles is the chemical composition of the cell wall of the microorganism [30]. The negatively charged cell wall will interact electrostatically with the positively charged metal ions. The proteins present within the cell wall reduce the metal ions to nanoparticles, and finally the smaller sized nanoparticles get diffused through the cell wall. As mentioned earlier, biological synthesis of metal nanoparticles is a two-step process, wherein biosorption of metal ions is followed by bio-reduction to metal nanoparticles extracellularly or intracellularly.

Biosorption processes

Biosorption has been defined as a multitude of metabolically independent processes based on passive uptake of ions, which occur in non-living biomass. It has been attested that biosorption processes comprise different mechanisms and not just one, depending on the ionic species used, the type of biomass and how it is pretreated [31-33]. Furthermore, there are other factors affecting the biosorption of metal species by biomass that should be considered, such as:

- cell size and morphology;
- pH of the external media;
- cation and anion concentration in the external media;
- metal speciation;
- temperature;
- physiology of the biomass [34].

It has been established that metal sequestration is achieved through the following processes: physical sorption, ion exchange, chelation; and ion fixation in inter- and intrafibrillar capillaries and spaces of the structural polysaccharide matrix as a result of the concentration gradient and diffusion through cell walls [35-37]. Cells biomass has a very complicated chemical composition being composed of various active groups which participate in the binding of chemical substances or ions, contributing to their entrapment in the biomass solid substance [38]. According to Volesky [39-41], there are several chemical groups that could contribute to the metals acquisition by biomass: acetamido groups of chitin, structural polysaccharides of fungi, amino and phosphate groups in nucleic acids, amino, amido, sulfhydryl, and carboxyl groups in proteins, hydroxyls in polysaccharides, and mainly carboxyls and sulfates in the polysaccharides of marine algae. However, the presence of some functional group is not the main factor which contributes to the biosorption processes [42].

Biomineralization

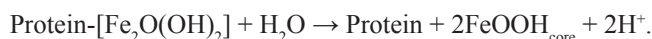
The second step in nanoparticles formulation consists of processes of metabolically mediated reduction, transport and deposition of chemical specie. The initial stages of iron nucleation require the participation of the protein / enzyme which is also responsible for iron transport within the cell of the microorganism [43,44]. At this stage, depending on the microorganism metabolic pathways there are several proteins able to participate: transferrin, lactoferrin, iron transport multicopper oxidase (Fet3p). Graphical representations of these proteins are presented in Figure 1. The high-resolution crystallographic structures had Protein Data Bank [45] codes of 1ZPU (iron transport multicopper oxidase structure file) [46], 3QYT (transferrin structure file) [47], 1B0L (lactoferrin structure file) [48].

It was shown that the inner surface of the protein shell is a source of ligands which are responsible for partial coordination of iron and with a coordination degree available for mineral phase anions withal. This specific coordination gives start to the biomineralization process resulting in the formation of ferrihydrite core which serves as precursor for iron nanoparticles [49].

The overall reaction of the iron interaction with ferrioxidase protein confirmed by Chasteen 1999 [50] is postulated as follows:



According to Chasteen 1999 [50] iron is transferred from the ferrioxidase complex to the core nucleation sites through the following reaction:



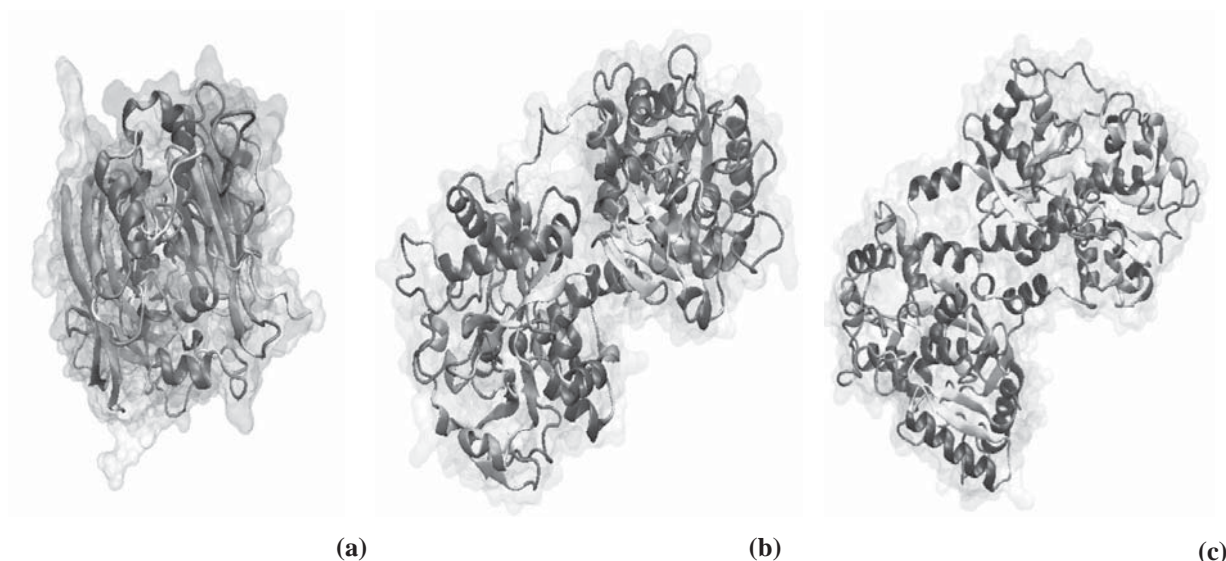


Figure 1. Ribbon representation of iron transport multicopper oxidase (a), transferrin protein (b) and lactoferrin protein (c) based on the coordinates from Protein Data Bank. The images were obtained using graphical interface software Visual Molecular Dynamics [51].

A hypothetical mechanism of iron uptake by Gram-negative bacteria and yeast cell is presented in Figure 2. According to the literature sources [49], in case of Gram-negative bacteria, bounded iron is transported to specific membrane receptors which are responsible for unloading Fe^{3+} ions from lactoferrin, transferrin, haem or haem containing molecules, or Fe^{3+} –siderophores synthesized by bacteria and fungi. It is also mentioned that there are three proteins inserted in the cytoplasmic membrane and coupled to the receptors are TonB, ExbB and ExbD. The last ones being responsible for forwarding the energy delivered by the proton-motive force of the cytoplasmic membrane for active transport across the outer membrane. Thus, periplasmic binding proteins deliver Fe^{3+} and Fe^{3+} siderophores to one or two integral cytoplasmic membrane proteins, which translocate them into the cytoplasm at the expense of ATP provided by ATPases associated with the inside of the cytoplasmic membrane. A similar mechanism of the transport system is attributed to Gram-positive bacteria with the exception consisting in the lack of protein receptors and of TonB, ExbB and ExbD proteins. Fe^{2+} transport system differs from the one of Fe^{3+} , it is accomplished under anaerobic conditions and through the Feo system. Yeast cells have a much simpler mechanism for iron acquisition. This mechanism involves the participation of a protein, Fet3p, which is responsible for mediation of iron oxidation, resulting in plasma membrane iron transport through the permease Ftr1p, leading to iron deposition and formulation of nanocrystals.

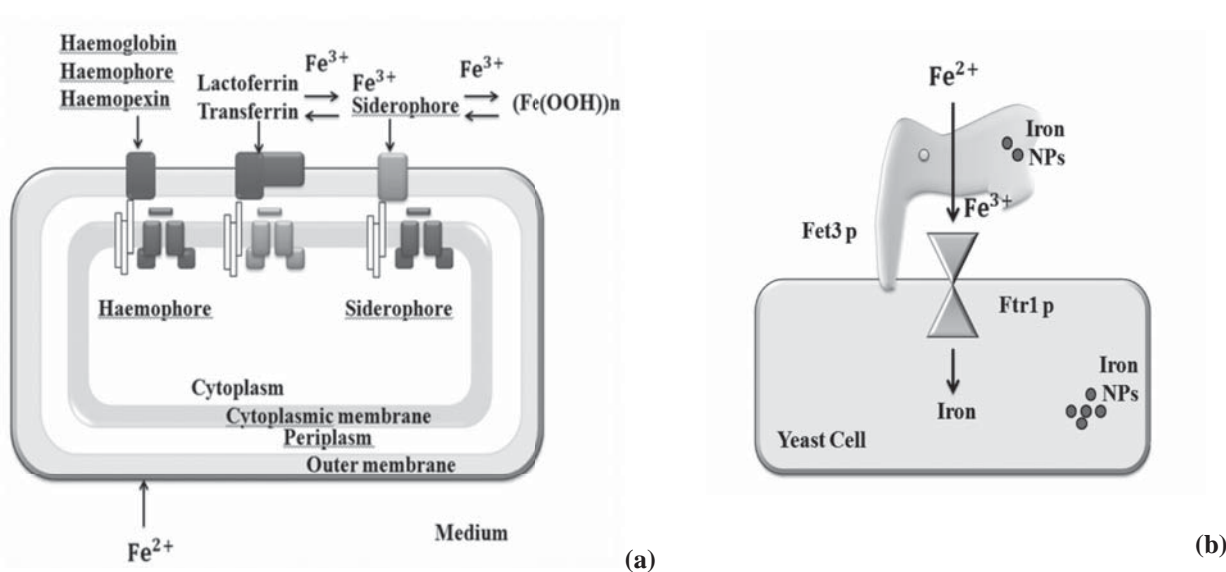


Figure 2. Comparison iron uptake mechanism and nanoparticles formulation within the cell of Gram-negative bacteria (a) and yeast (b), as stated by Crichton 2001 [49].

Table 1.

Biosynthesis of iron nanoparticles by different microorganisms.					
Microorganisms	Product	Size	Shape	Location	References
Recombinant AMB-1	magnetite	20nm	Octahedral, cubo-octahedral	intracellular	[52]
Magnetotactic bacteria	Magnetite (Fe_3O_4) and Greigite Fe_3S_4	32–43nm	Cubic	intracellular	[53]
Yeast cells	Iron phosphate (FePO_4)	50-200nm	Spherical aggregations	extracellular	[54]
HSMV-1	magnetite	< 45nm	Bullet or flat-top shaped	intracellular	[55]
<i>Sargassum muticum</i>	magnetite	18±4 nm	Cubic	extracellular	[56]
BoFeN1 <i>Acidovorax</i> sp.	Iron phosphate	100±25nm 40nm	Globular, flat-shaped	extracellular/ intracellular	[57]
<i>Shewanella oneidensis</i>	magnetite	40-50nm	Cubic, rhombic	extracellular	[58]
<i>Desulfovibrio magneticus</i>	Magnetite, hematite	40nm 5-10nm	Elongated	intracellular/ extracellular	[59]
QH-2	Magnetite	58±20nm	not available	intracellular	[60]
<i>Aspergellius fumigates</i>	Magnetite	42.40nm	powder	not available	[61]
<i>Chaetomium globusum</i>	magnetite	25.30nm	powder	not available	[61]
<i>Curvularia lunata</i>	magnetite	20.80nm	powder	not available	[61]
<i>Aspergillius wentii</i>	magnetite	46.50nm	powder	not available	[61]
<i>Alcaligenes faecalis</i>	Ferrous sulfate (FeSO_4), magnetite	43.60nm, 12.30nm	powder	not available	[61]
<i>Bacillus coagulans</i>	Ferrous sulfate (FeSO_4)	Not detected	powder	not available	[61]
<i>Fussarium oxysporum</i>	Magnetite	20-50nm	Quasi-spherical	extracellular	[62]
<i>Verticillium</i> sp.	Magnetite	10-40nm	Cubic	extracellular	[62]
<i>Klebsiella oxytoca</i>	Ferrihydrite, magnetite	Not detected	Not available	extracellular	[63]

Nonetheless, not all the microorganisms are found to be competent for the synthesis of iron-based nanoparticles. Some of the iron-based nanoparticles biologically synthesized using microorganisms are summarized in Table 1.

Properties of iron-based nanoparticles

It was established that iron-based nanoparticles with appropriate surface chemistry are an effective tool for numerous *in vivo* applications such as magnetic resonance imaging contrast enhancement, tissue repair, immunoassay, detoxification of biological fluids, hyperthermia and drug delivery, etc [64-66]. The unique properties of nanoparticles are strongly determined by their size and shape [66]. For example, magnetite Fe_3O_4 has attracted attention because bulk Fe_3O_4 has a high Curie temperature ($T_c \sim 850 \text{ K}$) and nearly a full spin polarization at room temperature, both properties of great potential for applications in giant magneto-electronic and spin-valve devices based on magnetic films [68].

Nanoparticles of iron oxide such as maghemite, $\gamma\text{-Fe}_2\text{O}_3$, magnetite, Fe_3O_4 and haematite, $\alpha\text{-Fe}_2\text{O}_3$, have been thoroughly investigated for their potential applications in the field of biomedical engineering. Among afore mentioned iron oxides, magnetite has proven to be the most promising for this particular field of applications [69,70]. Biomedical applications require particles of a nanometric scale [70]. This requirement is explained by the fact that the size of nanoparticles is similar to that of most biological molecules and structures making them good candidates for application in both *in vivo* and *in vitro* biomedical research [71].

In addition to the specific structural characteristics, biomedical applications require non-toxic and biocompatible iron nanoparticles. Several studies [72] conducted on the cytotoxicity of iron nanoparticles have not indicated any membrane permeability alterations and low cytotoxicity of nanoparticles *in vitro* and *in vivo*. The cytotoxicity was due to the material chemistry. Therefore an important factor which may influence their possible applications is the chosen route for their synthesis. At this point, production of nanoparticles using microorganism seems to be the most suitable route of synthesis.

Applications

Industrial applications

Iron nanoparticles are successfully implemented in a broad spectrum of applications from magnetic recording to biomedical applications. Each potential application of these nanoparticles requires different properties and different coating agents. For example in data storage applications, the ferromagnetic and antiferromagnetic properties of nanostructured components influence the recording medium capacity. The exchange coupling can supply the extra anisotropy which is needed for magnetization stabilization, thus generating magnetically stable particles [73,74]. Other industrial application of iron-based nanoparticles includes their use as Fenton-like catalyst for the degradation of aqueous organic solutes [75-77].

Iron based catalyst such as magnetite and hematite have been widely used in various industrial productions, including the synthesis of NH_3 (the Haber process), the desulfurization of natural gas, dehydrogenation of ethylbenzene to styrene, the Fischer-Tropsch synthesis for hydrocarbons, the oxidation of alcohols, and the large scale manufacture of butadiene [78]

Biomedical applications

Iron containing nanoparticles offer some attractive possibilities in biomedicine and biological research. Their applications include targeted cancer therapy, hyperthermia, drug carrier, DNA analysis, antibacterial agent, biosensor, cells separation, magnetic resonance imaging (MRI) [79].

Hyperthermia

Targeted therapy for cancer has attracted great attention from researchers. The concept of hyperthermia consists of cancer treatment by heating the tumor. For this purpose iron oxide nanoparticles are used, as they are efficient heat mediators and at the same time they are drug carriers [80,81]. Heating effect is induced by magnetic nanoparticles (localized within a tumor) under the influence of an oscillating magnetic field. Using this effect once the temperature at the localized region reaches 40-50°C, cancerous cells will be destroyed without causing extensive damage to healthy tissue (cancerous cells are more sensitive to heat than normal cells) [82-84].

Drug delivery

Drug delivery systems are developed to enable drugs to reach targeted organs allowing a fast preconcentration of drugs in target area and diminish their side effects. Targeted nano-carriers must navigate through blood-tissue barriers to reach targeted cells. They must have a small size so that these particles bypass the blood-brain barrier and the tight epithelial junction of the skin that normally impede delivery of drugs to the desired targeted site. Magnetic drug delivery system uses magnetic carriers that can be loaded with the drugs and directed toward a desired zone, such as tumor cells or blood clots by means of a magnetic field gradient [85]. Even though this method seems to be ideal for specific diseases treatment, there are few requirements which must be fulfilled. It should be taken into account the fluid flow rate, strength

of the applied magnetic field, the content of magnetic nanoparticles, distribution of the magnetic nanoparticles and concentration of the injected drug [86-88].

MRI imaging

Functionalized iron nanoparticles have been successfully implemented in the diagnostics due to the possibility to guide them using an external magnetic field [89,90]. Magnetic resonance imaging (MRI) is one of the best imaging technique which is used to visualize detailed internal structure in the body and is safe to patients. The basic principle of MRI technique is based on the counterbalance between the small magnetic moment on a proton and the large number of protons present in biological tissue. Resulting effect is measured in the presence of large magnetic field [91]. MRI requires magnetic resonance agents to provide the contrast between the targeted cells and the healthy cells in the body [91-93]. Currently, MRI technique is limited by the properties of iron nanoparticles, improving their properties would help to improve this technique.

Conclusions

Iron nanoparticles can be produced using microorganisms. These methods offer promising alternatives to the traditional techniques which are commonly used to produce these particles. The development of biogenic methods for iron nanoparticles synthesis is of considerable importance to expand their biotechnological applications, as these methods provide clean, nontoxic nanoscaled particles. However, in order to improve efficiency of the nanoparticles synthesis using microorganisms it is necessary to gather a complete knowledge of the molecular mechanism involved in this procedure. With further studies it may be possible to produce the material at large scales for commercial availability using environmentally benign routes.

References

- [1] Cornell, M. and Schwertmann, U. The Iron Oxides: Structure, Properties, Reactions, Occurrences and Uses. Wiley-VCH GmbH & Co. KGaA, Weinheim, 2003.
- [2] Farrell, D.; Cheng, Y.; McCallum, R.W.; Sachan, M. and Majetich, S.A. Magnetic interactions of iron nanoparticles in arrays and dilute dispersions. *Journal of Physical Chemistry B.*, 2005, 109(28), pp. 13409-13419.
- [3] Jain, T.P.; Richey, J.; Strand, M.; Leslie-Pelecky, D.L.; Flask, C. and Labhasetwar, V. Magnetic Nanoparticles with Dual Functional Properties: Drug Delivery and Magnetic Resonance Imaging. *Biomaterials*, 2008, 29(29), pp. 4012-4021.
- [4] Maeda, M.; Kuroda, C.S.; Shimura, T.; Tada, M.; Abe, M.; Yamamuro, S.; Sumiyama, K. and Handa, H. Magnetic carriers of iron nanoparticles coated with a functional polymer for high throughput bioscreening. *Journal of Applied Physics*, 2006, 99, 08H103.
- [5] Khurshid, H.; Tzitzios, V.; Colak, L.; Fang, F. and Hadjipanayis, G.C. Metallic Iron-Based Nanoparticles for Biomedical Applications. *Journal of Physics: Conference Series*, 2010, 200, 072049.
- [6] Bendrea, A.-D.; Catargiu, A.-M.; Grigoras, M.; Hybrid organic-inorganic composite materials for application in chemical sensors. *Chemistry Journal of Moldova. General, Industrial and Ecological Chemistry*, 2009, 4(2), pp.100-104.
- [7] Akhmedov, F.I.; Asadova, A.Z.; Guseynova, M.E.; Kuliyeu, A.D. The study of conductivity of the macrosystem dielectric polypropylene (PP) - semiconductor α -(Fe_2O_3). *Surface Engineering and Applied Electrochemistry. Electrical Precision Treatment of Materials*, 2011, 47(5), pp. 15-17, (Rus.).
- [8] Lacroix, L.-M.; Lachaize, S.; Falqui, A.; Blon, T.; Carrey, J. and Respaud, M. Ultrasmall iron nanoparticles: Effect of size reduction on anisotropy and magnetization. *Journal of Applied Physics*, 2008, 103, 07D521.
- [9] Anghel, L.; Balasoiu, M.; Ishchenko, L.A.; Stolyar, S.V.; Rogachev, A.V.; Kurkin, T.S.; Kuklin, A.I.; Raikher, Yu.L.; Iskhakov, R.S.; Arzumanian, G.M. SAXS studies of ultrasonicated dispersions of biomineral particles produced by *Klebsiella oxytoca*. *Solid State Phenomena*, 2012, Vol. 190, pp. 621-624.
- [10] Anghel, L.; Balasoiu, M.; Ishchenko, L.A.; Stolyar, S.V.; Kurkin, T.S.; Rogachev A.V.; Kuklin, A.I.; Kovalev, Yu.S.; Raikher, Yu.L.; Iskhakov, R.S.; Duca, Gh. Characterization of bio-synthesized nanoparticles produced by *Klebsiella oxytoca*. *Journal of Physics: Conference Series*, 2012, 351, 012005, pp. 1-7.
- [11] Huang, K.-C.; Chou, K.-S. Microstructure changes to iron nanoparticles during discharge/charge cycles. *Electrochemistry Communications*, 2007, 9, pp. 1907-1912.
- [12] Wu, W.; He, Q. and Jinag, C. Magnetic Iron Oxide Nanoparticles: Synthesis and Surface Functionalization Strategies. *Nanoscale Research Letters*, 2008, 3, pp. 397-415.
- [13] Gubin, S.P.; Kosharov, Yu.A.; Khomutov, G.B. and Yurkov, G.Yu. Magnetic nanoparticles: preparation, structure and properties. *Russian Chemical Reviews*, 2005, 74(6), pp. 489-520.
- [14] Schmidt, H.; Nanoparticles by chemical synthesis, processing to materials and innovative applications. *Applied Organometallic Chemistry*, 2001, 15, pp. 331-343.
- [15] Kura, H.; Takahashi, M. and Ogawa, T. Synthesis of Monodisperse Iron Nanoparticles with a High Saturation

- Magnetization Using an Fe(CO)_x Oleylamine Reacted Precursor. Journal of Physical Chemistry C, 2010, 114, pp. 5835-5838.
- [16] Liu, J.; Sun, Z.; Deng, Y.; Zou, Y.; Li, C.; Guo, X.; Xiong, L.; Gao, Y.; Li, F. and Zhao, D. Highly Water-Dispersible Biocompatible Magnetite Particles with Low Cytotoxicity Stabilized by Citrate Groups. Angewandte Chemie International Edition, 2009, 48, pp. 5875-5879.
- [17] Sipavičius, Č.; Mažeika, K.; Padgurskas, J.; Vaitiekūnas, P.; Žunda, A. Generation of ferromagnetic micro- and nanoparticles by laser and mechanical milling methods. Surface Engineering and Applied Electrochemistry. Electrical Precision Treatment of Materials, 2011, 47(3), pp. 10-14.
- [18] Jankauskas, V.; Padgurskas, J.; Žunda, A.; Prosyčevs, I. Research into nanoparticles obtained by electric explosion of conductive materials. Surface Engineering and Applied Electrochemistry. Electrical Processes in Engineering and Chemistry, 2011, 47(2), pp. 79-85.
- [19] Mohapatra, M. and Anand, S. Synthesis and applications of nano-structured iron oxides/hydroxides – a review. International Journal of Engineering, Science and Technology, 2010, 2(8), pp. 127-146
- [20] Kannan, N. and Subbalaxmi, S. Biogenesis of nanoparticles – A current perspective. Reviews on Advanced Material Science, 2011, 27, pp. 99-114.
- [21] Li, X.; Xu, H.; Chen, Z.-S. and Chen, G. Biosynthesis of Nanoparticles by Microorganisms and Their Applications. Journal of Nanomaterials, 2011, Article ID 270974.
- [22] Carvallo, C.; Sainctavit, P.; Arriero, M.-A.; Menguy, N.; Wang, Y., Ona-Nguema, G. and Brice-Profeta, S. Biogenic vs. abiogenic magnetite nanoparticles: A XMCD study. American Mineralogist, 2008, 93, pp. 880-885.
- [23] Battacharya, R. and Mekherjee, P. Biological properties of “naked” metal nanoparticles. Advanced Drug Delivery Review, 2008, 60(11), pp. 1289-1306.
- [24] Albrecht, M.; Janke, V.; Sievers, S.; Siegner, U.; Schüler, D. and Heyen, U. Scanning force microscopy study of biogenic nanoparticles for medical applications. Journal of Magnetism and Magnetic Materials, 2005, pp. 290-291.
- [25] Abhilash, K.R. and Pandey, B.D. Microbial synthesis of iron-based nanomaterials - A review. Bulletin of Materials Science, 2011, 34(2), pp. 191-198.
- [26] Faivre, D. and Schüler, D. Magnetotactic Bacteria and Magnetosomes. Chemical Reviews, 2008, 108, pp. 4875-4898.
- [27] Roh, Y.; Vali, H.; Phelps, T.J. and Moon, J.-W. Extracellular Synthesis of Magnetite and Metal-Substituted Magnetite Nanoparticles. Journal of Nanoscience and Nanotechnology, 2006, 6, pp. 3517-3520.
- [28] Sundaram, P.A.; Augustine, R. and Kannan, M. Extracellular Biosynthesis of Iron Oxide Nanoparticles by *Bacillus subtilis* Strains Isolated from Rhizosphere Soil. Biotechnology and Bioprocess Engineering, 2012, 17, pp. 835-840.
- [29] Duca, Gh. Homogeneous Catalysis with Metal Complexes: Fundamentals and Applications. Springer Series in Chemical Physics: Berlin; Heidelberg, 2012, XII, 478 p.
- [30] Yeoung-Sang, Y. Characterization of Functional Groups of Protonated *Sargassum polycystum* Biomass Capable of Binding Protons and Metal Ions. Journal of Microbiology and Biotechnology, 2004, 14(1), pp. 29-34.
- [31] Wilke, A.; Buchholz, R. and Bunke, G. Selective biosorption of heavy metals by algae. Environmental Biotechnology, 2006, 2(2), pp. 47-56
- [32] Das, K. and Thiagarajan, P. Mycobiosynthesis of Metal Nanoparticles. International Journal of Nanotechnology and Nanoscience, 2012, 1, pp. 1-10.
- [33] Zinicovscaia, I.; Duca, Gh.; Rudic, V.; Cepoi, L.; Chiriac, T.; Frontasyeva, M.V.; Pavlov, S.S.; Gundorina, S.F. *Spirulina platensis* as biosorbent of zinc in water. Environmental Engineering and Management Journal, 2013, 12(5), pp. 1079-1084.
- [34] Wase, J. and Forster, C. Biosorbents for Metal Ions. Taylor and Francis Ltd, Gunpowder Square, London, England, 1997.
- [35] Ahalya, N.; Ramachandra, T.V. and Kanamadi, R.D. Biosorption of Heavy Metals. Research Journal of Chemistry and Environment, 2003, 7(4), pp. 71-79.
- [36] Benderliev, K. Algae and Cyanobacteria Release Organic Chelators in the Presence of Inorganic Fe(III) thus Keeping Iron Dissolved. Bulgarian Journal of Plant Physiology, 1999, 25(1-2), pp. 65-75.
- [37] Singh, C.; Sharma, V.; Naik, Kr. P.; Khandelwal, V.; Singh, H. A Green Biogenic Approach for Synthesis of Gold and Silver Nanoparticles Using *Zingiber Officinale*. Digest Journal of Nanomaterials and Biostructures, 2011, 6(2), pp. 535-542.
- [38] Sag, Y. and Kutsal, T. Recent Trends in the Biosorption of Heavy Metals: A Review. Biotechnology and Bioprocess Engineering, 2001, 6, pp. 376-385.
- [39] Volesky, B. and Holan, Z.R. Biosorption of Heavy Metals, Biotechnology Progress, 1995, 11, pp. 235-250.
- [40] Kratochvil, D.; Pimentel, P. and Volesky, B. Removal of Trivalent and Hexavalent Chromium by Seaweed Biosorbent. Environmental Science and Technology, 1998, 32, pp. 2693-2698.

- [41] Yang, J. and Volesky, B. Modeling Uranium – Proton Ion Exchange in Biosorption. Environmental Science and Technology, 1999, 33, pp. 4079-4085.
- [42] Schiewer, S. and Wong, M.H. Ionic Strength Effects in Biosorption of Metals by Marine Algae. Chemosphere, 2001, 41, pp. 271-282.
- [43] Waldron, K.J.; Rutherford, J.C.; Ford, D.; Robinson, N.J. Metalloproteins and metal sensing. Nature, 2009, 460, pp. 823-830.
- [44] Paz, Y.; Katz, A.; Pick, U. A Multicopper Ferroxidase Involved in Iron Binding to Transferrins in *Dunaliella salina* Plasma Membranes. The Journal of Biological Chemistry, 2007, 282(12), pp. 8658-8666.
- [45] Protein Data Bank – an information portal to biological macromolecules
<http://www.rcsb.org/pdb/home/home.do>
- [46] Taylor, A.B.; Stoj, C.S.; Ziegler, L.; Kosman, D.J.; Hart, P.J. Crystal Structure of Fet3p, a Multicopper Oxidase that Functions in Iron Import. Proceedings of the National Academy of Science USA, 2005, 106, pp. 15459-15464.
- [47] Yang, N.; Zhang, H.; Wang, M.; Hao, Q.; Sun, H. Iron and bismuth bound human serum transferrin reveals a partially-opened conformation in the N-lobe. Scientific Reports, 2012, 2, doi:10.1038/srep00999.
- [48] Sun, X.L.; Baker, H.M.; Shewry, S.C.; Jameson, G.B.; Baker, E.N. Structure of recombinant human lactoferrin expressed in *Aspergillus awamori*. Acta Crystallographica Section D, 1999, 55, pp. 403-407.
- [49] Crichton, R. Inorganic Biochemistry of Iron Metabolism: From Molecular Mechanisms to Clinical Consequences. 2nd ed, John Wiley&Sons, Chichester, England, 2001.
- [50] Chasteen, D.N. and Harrison, P. Mineralization in Ferritin: An Efficient Means of Iron Storage. Journal of Structural Biology, 1999, 126, pp. 182-194.
- [51] Humphrey, W.; Dalke, A. and Schülten, K. VMD - Visual Molecular Dynamics, Journal of Molecular Graphics, 1996, 14, pp. 33-38.
- [52] Amemiya, Y.; Arakaki, A.; Staniland, S.S.; Tanaka, T.; Matsunaga, T. Controlled formation of magnetite crystal by partial oxidation of ferrous hydroxide in the presence of recombinant magnetotactic bacterial protein Mms6. Biomaterials, 2007, 28, pp. 5381-5389.
- [53] Bazylinski, D.A.; Frankel, R.B.; Heywood, B.R.; Mann, S.; King, J.W.; Donaghay, P.L.; Hanson, A.K. Controlled Biomineralization of Magnetite (Fe₃O₄) and Greigite (Fe₃S₄) in a *Magnetotactic Bacterium*. Applied and Environmental Microbiology, 1995, 61(9), pp. 3232-3239.
- [54] He, W.; Zhou, W.; Wang, Y.; Zhang, X.; Zhao, H.; Zhao, H.; Li, Z.; Yan, S. Biomineralization of iron phosphate nanoparticles in yeast cells. Material Science and Engineering C, 2009, 29, pp. 1348-1350
- [55] Lefevre, Ch.T.; Abreu, F.; Lins, U.; Bazylinski, D.A. Nonmagnetotactic Multicellular Prokaryotes from Low-Saline, Nonmarine Aquatic Environments and Their Unusual Negative Phototactic Behavior. Applied and Environmental Microbiology, 2010, 76(10), pp.3220-3227.
- [56] Mahdavi, M.; Namvar, F.; Bin Ahmad, M.; Mohamad, R. Green Biosynthesis and Characterization of Magnetic Iron Oxide (Fe₃O₄) Nanoparticles Using Seaweed (*Sargassum muticum*) Aqueous Extract. Molecules, 2013, 18, pp. 5954-5964.
- [57] Miot, J.; Benzerar, K.; Morin, G.; Andreas, K.; Bernard, S.; Obst, M.; Ferard, C.; Skouri-Panet, F.; Guigner, J.M.; Posth, N.; Galvez, M.; Brown Jr., G.E.; Guyot, F. Iron biomineralization by anaerobic neutrophilic iron-oxidizing bacteria. Geochimica et Cosmochimica Acta, 2009, 73, pp. 696-711.
- [58] Perez-Gonzales, T.; Jimenez-Lopez, C.; Neal, A.L.; Rull-Perez, F.; Rodriguez-Navarro, A.; Fernandez-Vivas, A.; Ianez-Pareja, E. Magnetite biomineralization induced by *Shewanella oneidensis*. Geochimica et Cosmochimica Acta, 2010, 74, pp. 967-979.
- [59] Posfai, M.; Moskowitz, B.M.; Arato, B.; Schüller, D.; Flies, Ch.; Bazylinski, D.A.; Frankel, R.B. Properties of intracellular magnetite crystals produced by *Desulfovibrio magneticus* strain RS-1. Earth and Planetary Science Letters, 2006, 249, pp. 444-455.
- [60] Zhu, K.; Pan, H.; Li, J.; Yu-Zhang, K.; Zhang, S.D.; Zhang, W.Y.; Zhou, K.; Yue, H.; Pan, Y.; Xiao, T.; Wu, L.F. Isolation and characterization of a marine magnetotactic spirillum axenic culture QH-2 from an intertidal zone of the China Sea. Research in Microbiology, 2010, 161, pp. 276-283.
- [61] Kaul, R.K.; Kumar, P.; Burman, U.; Joshi, P.; Agrawal, A.; Raliya, R.; Tarafdar, J.C. Magnesium and iron nanoparticles production using microorganisms and various salts. Material Science-Poland, 2012, 30(3), pp. 254-258.
- [62] Bharde, A.; Rautaray, D.; Bansal, V.; Ahmad, A.; Sarkar, I.; Yusuf, M.S.; Sanyal M.; Sastry, M. Extracellular Biosynthesis of Magnetite using Fungi. Small, Wiley InterScience, 2006, 2(1), pp. 135-141.
- [63] Arçon, I.; Piccolo, O.; Pagnelli, S.; Baldi, F. XAS analysis of a nanostructured iron polysaccharide produced anaerobically by a strain of *Klebsiella oxytoca*. Biometals, 2012, DOI 10.1007/s10534-012-9554-6.
- [64] Boisseau, P. and Loubaton, B. Nanomedicine, Nanotechnology in medicine. Comptes Rendus de L'Academie des Science, 2011, hal-00598930.

- [65] Frankel, B.R. Biological Permanent Magnets. *Hyperfine Interactions*, 2003, 151/152, pp. 145-153
- [66] Gupta, A.K. and Gupta, M. Cytotoxicity Suppression and Cellular Uptake Enhancement of Surface Modified Magnetic Nanoparticles, *Biomaterials*, 2004, doi:10.1016/j.biomaterials.2004.05.022.
- [67] Rai, M. and Duran, N. *Metal Nanoparticles in Microbiology*. Springer-Verlag, Berlin, Heidelberg, 2011
- [68] Goya, G.F.; Bersquo, T.S.; Fonseca, F.C. and Morales, M.P. Static and Magnetic Properties of Spherical Magnetite Nanoparticles. *Journal of Applied Physics*, 2003, 94(5), pp. 3520-3528.
- [69] Lodhia, J.; Mandarano, G.; Ferris, N.J., Eu, P.; Cowell, S.F. Development and use of iron oxide nanoparticles (Part 1): Synthesis of iron oxide nanoparticles for MRI. *Biomedical Imaging and Intervention Journal*, 2010, 6(2), doi: 10.2349/bij.6.2.e12.
- [70] Gupta, A.K. and Gupta, M. Synthesis and Surface Engineering of Iron Oxide Nanoparticles for Biomedical Applications. *Biomaterials*, 2005, 26(18), pp. 3995-4021.
- [71] Mendez-Vilas, A. *Science against Microbial Pathogens: Communicating current research and technological advances*. Volume 1, Formatex Research Center, 2011.
- [72] Yang, Z., Liu, Z.W.; Allaker, R.P.; Reip, P.; Oxford, J.; Ahmad, Z. and Ren, G. Review of Nanoparticles Functionality and Toxicity on the Central Nervous System. *Journal of the Royal Society Interface*, 2010, doi:10.1098/rsif.2010.0158.focus.
- [73] Lu, A.-H.; Salabas, E.L. and Schüth, F. Magnetic Nanoparticles: Synthesis, Protection, Functionalization, and Application. *Angewandte Chemie*, 2007, 46, pp. 1222-1244.
- [74] Zhang, X.X.; Wen, G.H.; Huang, S.; Dai, L.; Gao, R.; Wang, Z.L. Magnetic Properties of Fe Nanoparticles Trapped at the Tips of the Aligned Carbon nanotubes. *Journal of Magnetism and Magnetic Materials*, 2001, 231, L9-L12.
- [75] Shahwan, T.; Abu Sirriah, S.; Nairat, M.; Boyaci, E.; Eroglu, A.E.; Scott, T.B.; Hallam, K.R. Green synthesis of iron nanoparticles and their application as a Fenton-like catalyst for the degradation of aqueous cationic and anionic dyes. *Chemical Engineering Journal*, 2011, 172, pp. 258-266.
- [76] Shin, S.; Yoon, H.; Jang, J. Polymer-encapsulated iron oxide nanoparticles as highly efficient Fenton catalysts. *Catalysis Communications*, 2008, 10, pp. 178-182.
- [77] Xu, L.; Wang, J. A heterogeneous Fenton-like system with nanoparticulate zero-valent iron for removal of 4-chloro-3-methyl phenol, *Journal of Hazardous Materials*, 2011, 186, pp. 256-264.
- [78] Faraji, M.; Yamini, Y.; Rezaee, M. Magnetic Nanoparticles: Synthesis, Stabilization, Functionalization, Characterization, and Applications. *Journal of the Iranian Chemical Society*, 7(1), 2010, pp. 1-37.
- [79] Berry, C.C.; Curtis, A.S.G. Functionalisation of Magnetic Nanoparticles for Applications in Biomedicine. *Journal of Physics D: Applied Physics*, 2003, 36, pp. R198-R206.
- [80] Yang, C.; Rait, A.; Pirollo, K.F.; Dagata, J.A.; Farkas, N.; Chang, E.H. Nanoimmunoliposome Delivery of Superparamagnetic Iron Oxide Markedly Enhances Targeting and Uptake in Human Cancer Cells *In Vitro* and *In Vivo*. *Nanomedicine*, 2008, 4(4), pp. 318-329.
- [81] Byrne, J.M.; Coker, V.S.; Moiser, S.; Wincott, P.L.; Vaughan, D.J.; Tuna, F.; Arenholz, E.; van der Laan, G.; Patrick, R.A.D.; Lloyd, J.R.; Telling, N.D. Controlled Cobalt Doping in Biogenic Magnetite Nanoparticles. *Journal of the Royal Society: Interface*, 2013, 10, 20130134.
- [82] Miaskowski, A. and Krawczyk, A. Magnetic Fluid Hyperthermia for Cancer Therapy. *Przegląd Elektrotechniczny (Electrical Review)*, 2011, ISSN 0033-2097, R. 87, NR 12b, pp. 125-127.
- [83] Cherukuri, P.; Glazer, E.S.; Curley, S.A. Targeted Hyperthermia Using Metal Nanoparticles. *Advanced Drug Delivery Reviews*, 2010, 62, pp. 339-345.
- [84] Fortin, J.-P.; Wihlem, C.; Servais, J.; Menager, C.; Bacri, J.-P. and Gazeau, F. Size-Sorted Anionic Iron Oxide Nanomagnets as Colloidal Mediators for Magnetic Hyperthermia, *Journal of American Chemical Society*, 2007, 129, pp. 2628-2635.
- [85] Lee, J.W. and Foote, R.S. *Micro and Nano Technologys in Bioanalysis*, *Methods in Molecular Biology*, Vol. 544, Human Press, 2009.
- [86] Viroonchatapan, E.; Ueno, M.; Sato, H.; Adachi, I.; Nagae, H.; Tazawa, K. and Horikoshi, I. Preparation and Characterization of Dextran Magnetite-Incorporated Thermosensitive Liposomes: An on-line Flow System for Quantifying Magnetic Responsiveness. *Pharmaceutical Research*, 1995, 12(8), pp. 1176-1183.
- [87] Kiwada, H.; Sato, J.; Yamada, S. and Kato, Y. Feasibility of Magnetic Liposomes as a Targeting Device for Drugs. *Chemical Pharmaceutical Bulletin*, 1986, 34(10), pp. 4253-4258.
- [88] Akhtar, J.; Chaturvedi, R.; Sharma, J.; Mittal, D.; Pardhan, P. Magnetized carrier as novel drug delivery system. *International Journal of Drug Delivery Technology*, 2009, 1(1), pp. 28-35.
- [89] Shubayev, V.I.; Pisanic, T.R., Jin, S. Magnetic Nanoparticles for Theragnostics. *Advanced Drug Delivery Reviews*, 2009, 61, 467-477.
- [90] Pankhurst, Q.A.; Connolly, J.; Jones, S.K., and Dobson, J. Applications of Magnetic Nanoparticles in Biomedicine. *Journal of Physics D: Applied Physics*, 2003, 36, pp. R167-R181.

- [91] Hwang, Y. H. and Lee, D.Y. Magnetic Resonance Imaging using Heparin-Coated Superparamagnetic Iron Oxide Nanoparticles for Cell Tracking *in vivo*. *Quantitative Imaging in Medicine and Surgery*, 2012, doi: 10.3978/j.issn.2223-4292.2012.06.03.
- [92] Hadjipanayis, C.G.; Bonder, M.J.; Balakrishnan, S.; Wang, X.; Mao, H. Hadjipanayis, G.C., Metallic Iron Nanoparticles for MRI Contrast Enhancement and Local Hyperthermia. *Small*, 2008, 4(11), pp. 1925-1929.
- [93] Arbab, A.S.; Bashaw, L.A.; Miller, B.R.; Jordan, E.K.; Lewis, B.K.; Kalish, H. and Frank, J.A. Characterization of Biophysical and Metabolic Properties of Cells Labeled with Superparamagnetic Iron Oxide Nanoparticles and Transfection Agent for Cellular MR Imaging. *Radiology: MR Imaging of Superparamagnetic Iron Oxide-labeled Cells*, 2003, 229(3), pp. 838-846.

THE WATER SPRINGS - SOURCES FOR WATER SUPPLY AND IRRIGATION IN THE NISTRU RIVER BASIN

Maria Sandu^{a*}, Anatol Tarita^a, Raisa Lozan^a, Viorica Gladchi^c, Gheorghe Duca^b,
Sergiu Turcan^a, Elena Mosanu^a, Afanasie Prepelita^d

^a Institute of Ecology and Geography, 1, Academiei str., Chisinau MD-2028, Republic of Moldova

^b Academy of Science of Moldova, 1, Stefan cel Mare Blvd., Chisinau MD-2001, Republic of Moldova

^c State University of Moldova, 60, Mateevici str., Chisinau MD-2009, Republic of Moldova

^d Hydro-Geological Expedition of Moldova, Republic of Moldova

* e-mail: sandu_mr@yahoo.com, phone: (+373 22) 73 15 50; 72 17 74

In Memory of Valeriu Ropot for his scientific contributions in Waters Protection

Abstract. The present study estimates chemical composition and status of the groundwater from the Nistru (Dniester) river basin (about 360 springs and fountains). Research includes defining of springs/fountains location, evaluating physicochemical features of water, highlighting of main pollutants and pollution sources, establishing of water type and quality. It was established that springs/fountains with water that meets the criteria for drinking scope constitute 21%, sanitary acceptable for consumption is water from 129 springs/fountains, with high content of dissolved salts (mineralization >1000 mg/dm³) and hardness exceeding 10 me/dm³ (very hard water) were in 18.5% of sources and approximately 25% of the springs are water polluted with nitrates and its content is more than the MAC from 1 to 6 times.

Keywords: groundwater, chemicals state, pollution sources, correlation of components, water type and qualification.

Introduction

The groundwater plays special role in terrestrial water balance [1, 2]. It is an important component of the hydrological cycle as part of the underground water flow being the largest reservoir of freshwaters, representing more than 97% of all water available for consumption in the world. EU Framework Directive on Water, adopted in 2000, sets out the concrete objectives for groundwater related issues and namely: achieving good status (quantitative and chemical) and limiting its deterioration, "preventing or limiting" the discharge of pollutants, taking measures to reduce any significant and sustained tendencies of pollutant concentrations increase [3]. Additional conditions for chemical state and its assessment procedures, protection of groundwater against pollution and deterioration, including criteria for assessing good chemical composition are developed within Groundwater EU Directive 118/2006/EC [4].

Approximately 40% of the rural population is supplied with water from underground layers with hydrostatic pressure (6200 wells) and the first layer water (without pressure) (about 150 thousand wells and springs), which provides 1.811 million m³/day confirmed reservations [5]. From the total national administered groundwater volume only 50% can be used for drinking purposes without prior treatment.

The change of composition and physical and chemical properties of groundwater are caused by human activity. The spectrum of natural and artificial pollutants is broad (nitrogen compounds, pesticides, selenium, sulphates, etc.), the mineralization and total hardness values of groundwater is exceeding with 2-5 and more times sanitary-hygienic norms and provokes nitrate pollution [6]. Variation of NO₃⁻ content and of borehole depth is an argument for groundwater pollution by nitrates that occurs vertically from the earth's surface. In the wells up to 30-40 m are registered the highest values of nitrate [7, 8].

In Moldova, the majority of small localities haven't the centralized water supply systems. The main legal act is the Law on drinking water [9], which regulates relations in the field of drinking water supply, aspects related to water for human consumption and provisions related to non-centralized water supply systems - installation and construction (wells, springs, etc.) for potable water capture and distribution without the supply to place of consumption.

The groundwater's quality depends on the surface water status. In the areas where the ground water basis is very permeable (sand, gravel), the connection between surface water and groundwater is strong [10]. But researches show that in the Republic of Moldova inland surface waters have a high degree of pollution [11-13], as pollutants in surface waters penetrate the ground and vice versa.

A comprehensive study on the quality, type and qualification of spring's water in the country were conducted for Prut Basin (about 400 springs) [14-17]. The evaluated correlation between nitrate content and the macro components of water in several wells and springs in the country highlights the potential pollutants and their accumulation trends [18]. About 160 wells and springs from all over the country were described by Overcenco A. and co-authors [19].

In the present study was estimated chemical state of groundwater from the Nistru river basin (about 360 springs and fountains in villages and communes of the administrative districts: Rezina, Soldanesti, Telenesti, Orhei, Calarasi,

Straseni, Criuleni, Anenii Noi, Ialoveni, Causeni and Stefan Voda). Some results are published in the scientific editions [20-25]. Research includes the estimating of location in space of springs/fountains, evaluating physic-chemical features of water, highlighting pollutants and main pollution sources, establishing of water type and qualification for use.

The research was achieved within the State Program "Scientific research and water quality management" (coordinator acad. Gheorghe Duca), the project "Role of tributaries on the Nistru river water quality formation and study of springs water quality from the Nistru basin as sources for water supply and irrigation", leader Gladchi V.

Research methods

The research methods have been adopted in relation to the objectives of the study. Investigations on water sources included the following:

- **Sampling.** Water samples from springs/fountains (the Nistru river basin) were collected in accordance with regulatory requirements [26] in the type of dishware, storage conditions and performing analysis. In place of sample collection was determined smell, taste, flow, pH and water temperature.

- **Assessment of chemical composition.** Springs water content of components was determined in the laboratory by standard methods EN ISO [27, 28] and traditional [29, 30].

- **Determination of water type and qualifier for consumption.** It was evaluated water type and calculated the Stebler coefficients of irrigation [31] for researched waters. Water qualifier for consumption was established according to the provisions of the Governmental Decision of the Republic of Moldova [32].

- **Correlation between water components.** To assess the correlative links between ion concentrations was used to rank correlation index r of Spearman [33]. Spearman's rank correlation coefficient, like the Pearson r , measures the strength of relationship between two variables. While the Pearson product moment correlation coefficient requires both variables to be measured on an interval or ratio scale, the Spearman's rank correlation coefficient only requires data that are at least ordinal. When it is low of 0.05, i.e. $R < 0.05$ means lack of correlation between the concentration of ions. The correlation coefficient from empirical regression curve [34] range from very small (< 0.1) to low ($0.1 \leftrightarrow 0.3$), medium ($0.3 \leftrightarrow 0.5$), high ($0.5 \leftrightarrow 0.7$) to the very large, nearly perfect ($0.7 \leftrightarrow 0.9$ and > 0.9).

Results and discussions

According to the hydro geological characteristics in area of study, the groundwater's that feed springs/fountains are stored mainly in packages of Neogene aged rocks. The erosion processes that occurred along time, opened aquifers stratum and their water come up in the slopes of river valleys, large ravines and valleys. Over the level of rocks base erosion are spread the sub layer of rocks from inferior and medium Sarmatian. In these layers are concentrated the aquifers with stable exchange potential for spring's formation. Lower Sarmatian aquifer which has the greatest importance in the regional water supply is largely spread. The waters are concentrated in the limestone formations of shale cracked inclusions, sandstone and sand. Their thickness is ranging from 20 to 30 up to 50 m. The discharge of the springs/fountains is from 0.05 to 1.0 m³/s, but sometimes some of the water record exceeds the norm with more than 10 m³/s. The salts content parameters of the waters are sweet, with a degree of mineralization below 1.0 g/dm³ and occasionally – 1.5 g/dm³ and after ionic composition they are magnesium-sodium hydrocarbonate type that go to west in the hydrocarbonate-sulphate and sulphate – hydrocarbonate.

Medium Sarmatian aquifer is sporadic widespread, being stuck in loamy and limestone rocks, which is spread over the inferior Sarmatian formation. This aquifer has a lower capacity due to lack of border between the two aquifers in these latitudes a stable layer of impermeable rock, so the waters flow downward, thus is fuelling inferior Sarmatian aquifer and increasing its flow. The flows of the springs/fountains that form from this aquifer varies considerably from 0.01 to 1.5 m³/s for those that flow from sandy loam rocks and from 10 or more liter for the ones flowing from limestone. The water are sweet, those of hydrocarbonate type with a fixed residue between 0.4 and 0.5 g/dm³ [35].

Feeding area of aquifers practically overlaps with the limits of the target region. The presence of limestone karsts on the surface of river valleys facilitates penetration of atmospheric precipitation, which is the dominant source of supply, the same stands for the supply of the inferior Sarmatian aquifer from rivers. The Nistru river and its tributaries serve as main zone for water download, forming the hydrographical network of the territory [36].

The ionic composition occurs due to the relationship between ions accumulation in water and salts sedimentation corresponding to their solubility under the influence of physical-geographical, chemical and biological factors, but the peculiarities of water formation lead to a variety of ionic content and total mineralization. Thus the chemical composition of groundwater is not constant and supports changes both in the time and in the same aquifer values. Substances content in water increases as a result of evaporation and dissolving, the phenomenon that occurs mainly in groundwater horizons and intensifies as the temperature is increasing but the humidity decreasing, also as a result of horizontal and vertical migration, including from surface waters.

In this study, conducted during the period of 2009-2012 was determined geographical location, smell, taste, flow, pH and temperature (at sample collection), evaluated in laboratory conditions chemical composition of water from 362 springs/fountains from rural localities (about 160) of the Nistru river basin (villages and communes from

the administrative districts Rezina, Soldanesti, Telenesti, Orhei, Calarasi, Straseni, Criuleni, Anenii Noi, Ialoveni, Causeni and Stefan Voda) to identify springs/fountains, water that is contaminated with various compounds in quantities exceeding the maximum allowable concentration (MAC).

The research results denote that water from all sources is colourless, has no specific odour and taste. District average values of hardness, mineralization, nitrates and macro components content in springs/fountains water from the Nistru river basin are presented in table 1.

Table 1.

District average values of hardness, mineralization, nitrates and macro components content in springs/fountains water from the Nistru river basin.

Average values of physical-chemical indexes	Rezina	Soldanesti	Telenesti	Orhei	Calarasi	Straseni	Criuleni	Ialoveni	Anenii Noi	Causeni	Stefan Voda
Hardness, me/dm ³	10.1	7	10.9	9.5	9.6	10.4	9.8	11.4	10.6	9.96	12.9
Ca ²⁺ , mg/dm ³	123	84	134	114	92	104	82	107	145	84	44
Mg ²⁺ , mg/dm ³	49	35	54	48	63	65	68	78	43	71	129
Na ⁺ , mg/dm ³	60	95	211	91	116	127	158	136	188	240	259
Mineralization, mg/dm ³	723	636	1220	768	863	982	1042	968	1225	1008	1717
Cl ⁻ , mg/dm ³	47	42	76	56	80	120	73	85	78	126	239
HCO ₃ ⁻ , mg/dm ³	536	445	663	566	484	550	563	623	675	617	526
SO ₄ ²⁻ , mg/dm ³	101	76	354	134	219	218	256	193	271	220	407
NO ₃ ⁻ , mg/dm ³	40.8	46.4	31.8	38.4	32.4	23.1	42.0	55.2	54.8	52.2	28.6

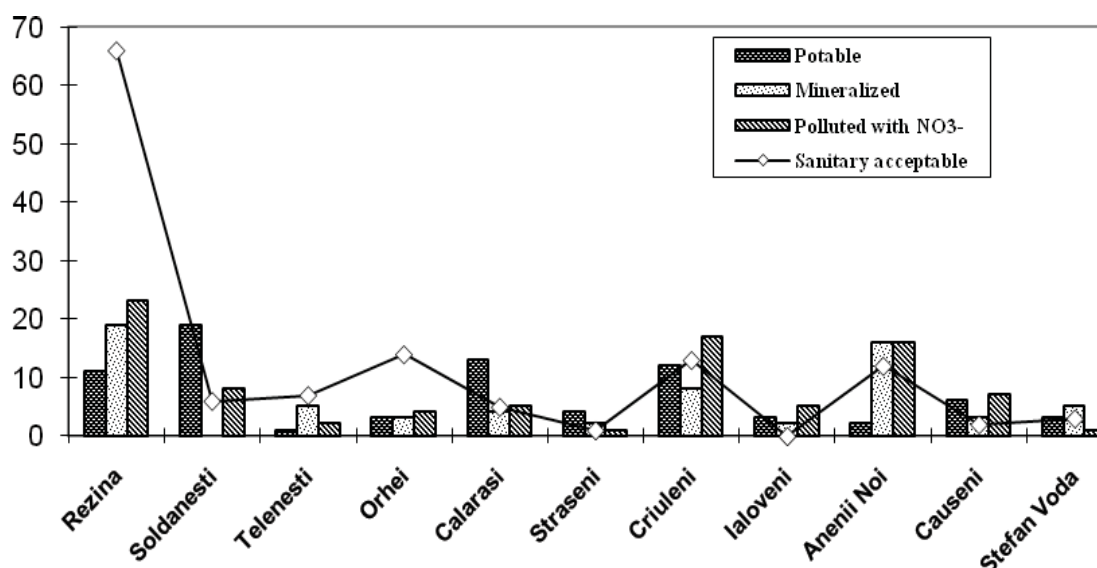


Figure 1. The qualifier of springs / fountains waters from under study localities in conformity with its chemical composition (“potable” - hardness <7 me/dm³; “acceptable sanitary” - hardness 7-10 me/dm³; “mineralized” – hardness > 10 me / dm³ and mineralization > 1000 mg/dm³).

Water springs from Stefan Voda and Ialoveni districts have the highest medium hardness, average of mineralization exceeding MAC - in villages and communes of the Stefan Voda, Anenii Noi and Telenesti districts and average nitrate content exceeding MAC - in villages and communes of the Ialoveni, Anenii Noi and Causeni districts.

The springs/fountains with water that has hardness less than 7 me/dm³ and meets the criteria for drinking scope are in total 77 (21%), most being in Soldanesti (19), Calarasi (13), Criuleni (12) and Rezina (11) districts and the least - in Ialoveni, Orhei, Telenesti, Stefan Voda and Anenii Noi. It was found that hardness does not exceed the sanitary acceptable limits for consumption (7-10 me/dm³) in water from 129 of springs/fountains, most being in Rezina, Telenesti and Orhei districts. A high content of dissolved salts (mineralization greater than 1000 mg/dm³) and hardness exceeding 10 me/dm³ (very hard water) were in 67 sources (the Rezina district there are 19 localities and Ialoveni - 16) (fig. 1).

The main concern is the fact that on average about 25% of the springs/fountains (89 out of 362) contain polluted water, the nitrate content exceed the MAC (50 mg/dm³) from 1 to 6 times, most of them being in villages/communes from Rezina (23) Criuleni (17) and Ialoveni (16) districts.

Water type

According to scientific classification the waters are defined in terms of weight cations and anions present in excess of 20% of the total chemical equivalents highlight in a litre of water.

Chemical composition of water from investigated springs/fountains shows that in 94% of cases water after anion is of bicarbonate type, with various modifications (HCO₃ - SO₄, HCO₃ - Cl, (HCO₃ - SO₄ - Cl, HCO₃ - Cl - SO₄) and only 5.8% of the waters are sulphate-bicarbonate type with variations SO₄ - HCO₃ - Cl and SO₄ - Cl - HCO₃ (fig. 2).

Along with increasing of concentration the ratio SO₄²⁻/Cl⁻ decreases, instead that due to CaCO₃ precipitation in conformity with the product solubility (PS) increases the value of ratio Mg²⁺/Ca²⁺ (PS for CaCO₃ is equal to 2.884.10⁻⁹ - 5.368.10⁻⁹). It was found also the presence of nitrate type in water of 53 springs/fountains (about 15%).

Weakly mineralized groundwater's of bicarbonate (anions) and calcium (cations) type gradually move to more mineralized waters as mixed bicarbonate (anion) and sodium or sodium-magnesium mixed (sometimes sodium) - after cations. They are also highly mineralized ground water, bicarbonate- chloride and bicarbonate-sulphate according to the anions and mixed sodium-magnesium and sodium as cations. That hydrochemical diversity is closely linked to changing of the natural conditions (precipitation, evapotranspiration intensity, depth of the groundwater etc.).

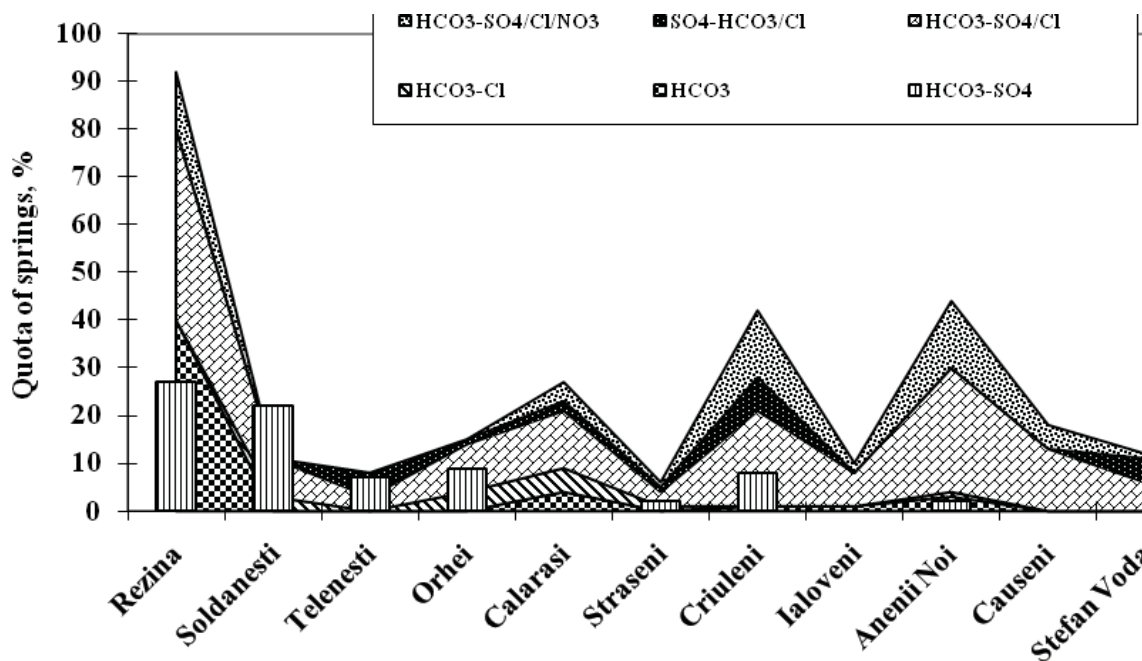


Figure 2. The quota of springs/fountains from investigated villages/communes and water type (according anions).

Depending on the cations content approx. 47% of the analyzed waters are of calcium type with different secondary cations (Ca - Mg - Na, Ca - Mg, Ca - Na - Mg, Ca - Na and Ca). Sodium ions prevail in the water composition of 41% of the springs/fountains, and the magnesium - to 12% (fig. 3).

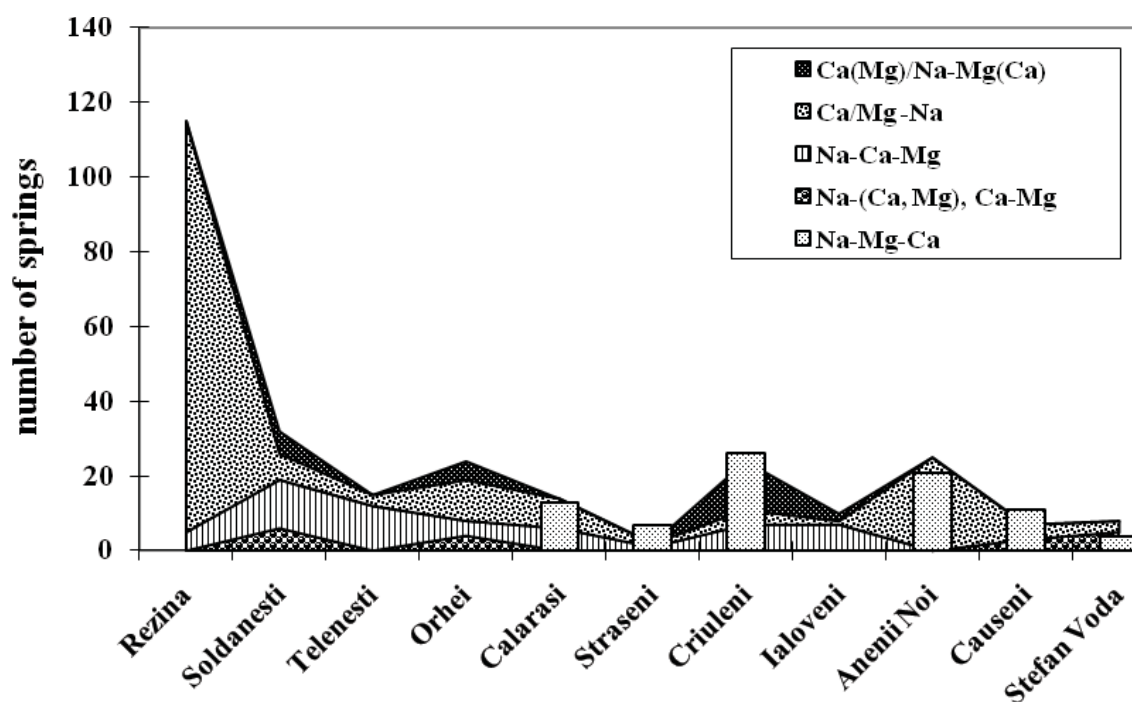


Figure 3. The quota of springs/fountains from investigated villages/communes and water type (according cations).

Correlation between components content in springs/fountains water

The correlative links between the ions concentration in springs/fountains water were assessed using rank correlation index R of Spearman with minimum value of 0.05, which lacks correlation between the content of chemical indicators. By systematizing the mineralization, hardness, content of Na^+ , Ca^{2+} , Mg^{2+} , Cl^- , SO_4^{2-} , HCO_3^- and NO_3^- ions (media per district) of springs/fountains water (basin of the Nistru river) from the centre to the south it was established a positive dynamic with high correlation of mineralization ($R^2 = 0.5171$), Na^+ ($R^2 = 0.5614$), Cl^- ($R^2 = 0.5521$) ion concentration and hardness (Ca^{2+} , Mg^{2+}) ($R^2 = 0.45$). The correlation coefficient has medium values for SO_4^{2-} -ions ($R^2 = 0.3781$) and small for HCO_3^- ($R^2 = 0.1629$). Practically the correlation for nitrate ions content is absent ($R^2 = 0.0363$) (fig. 4 a, b, c).

Thus to the Southern districts in the water increases the components concentration that arise from contact with the rock, soil solution but water springs/fountains pollution with nitrates persists regardless of studied water source location. It shows a positive correlation between the districts media content of NO_3^- ions higher than MAC and water hardness ($y = 0.72x + 9.2133$, $R^2 = 0.9959$). Thus, simultaneously with the accumulation of nitrate ions in water increases its hardness. Significantly is the correlation coefficient between the springs quota (%) water of which is polluted with nitrates, and spontaneous landfills number in districts ($R^2 = 0.7218$) (fig. 5).

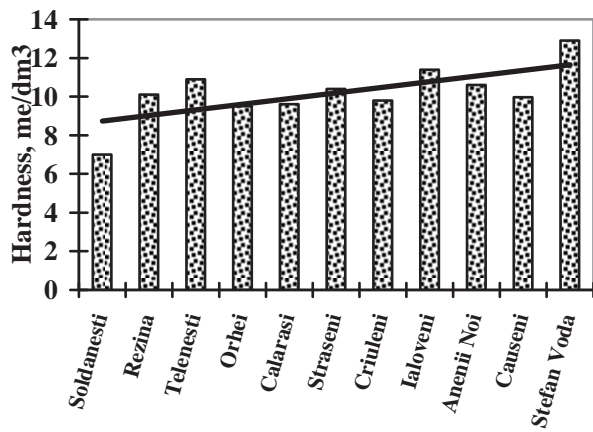
The results on nitrate in mineralization in each year of 1-2% of organic nitrogen [27] in view of the fact that their salts are very soluble in the soil solution and in the form of diffusible ions migrate into the ground water.

Qualifier of springs/fountains water for irrigation use

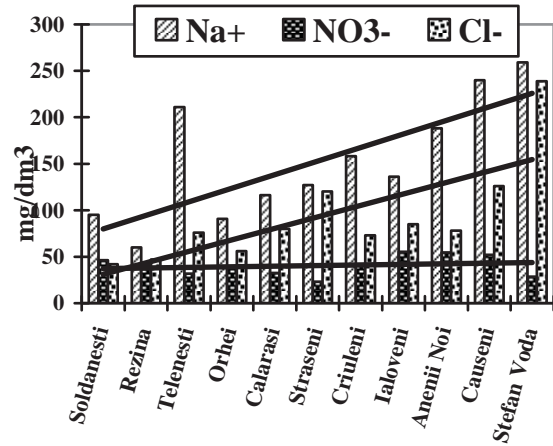
The qualification of waters for irrigation purposes was estimated by taking as a basis the coefficient Stebler. By calculating of water irrigation coefficient in the investigated zone, it was found that 213 of sources (about 59%) have water mark "good" for irrigation, 92 (25%) - "satisfactory" and 57 of springs and fountains (16%) have water mark "poor" for irrigation (fig. 6).

The results of the conducted research referred to the groundwater protection and the developed recommendations were elaborated and disseminated in the territory of district authorities and local public administration concerned.

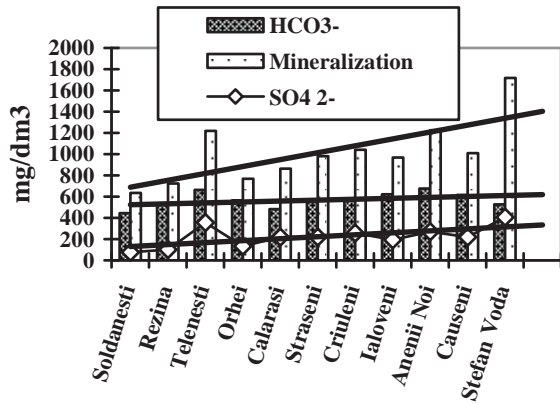
Taken into the fact that Nistru river basin (targeted by research districts) consists small number of Natural Hydrological Monuments protected by the State (14), the research conclusions will be presented to the Ministry of Environment with the scientific argumentation and ecological passports of 6-8 springs/fountains with quality water to be further included in the list of State Protected Natural Areas.



a)



b)



c)

Figure 4. The dynamics (media per district) of hardness (a), Na⁺, Cl⁻, NO₃⁻ ions (b) and mineralization, SO₄²⁻, HCO₃⁻ (c) content in springs/ fountains water (basin of the Nistru river) in direction from centre to the south.

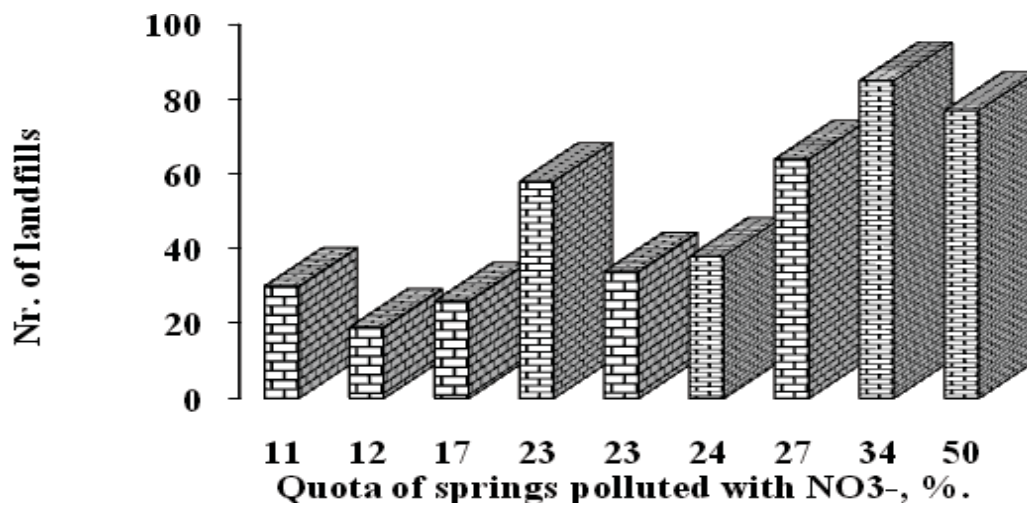


Figure 5. The correlation between the springs quota (%), water of which is polluted with nitrates, and spontaneous landfills number in districts ($R^2 = 0.7218$).

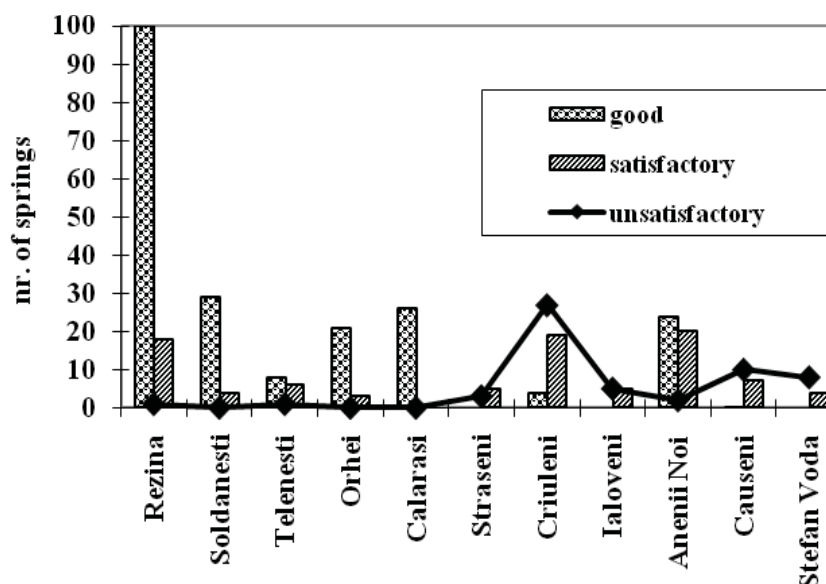


Figure 6. Qualification of waters for consumption in irrigation on districts in the study according to the chemical composition.

Conclusions

The springs/fountains with water that meets the criteria for potable purposes are in total 77 (21%); water acceptable from sanitary norms for consumption is present in 129 springs/ fountains. A high content of dissolved salts (mineralization greater than 1000 mg/dm³) and hardness exceeding 10 me/dm³ (*very hard water*) were found in 67 sources (18.5%) and approx. 25% of the springs/fountains (89) contain polluted water with nitrate content exceeding MAC with 1 to 6 times.

Chemical composition of water from investigated springs/fountains shows that in about 94% of cases water after anion is of bicarbonate type, with various modifications (HCO₃ - SO₄, HCO₃ - Cl, (HCO₃ - SO₄ - Cl, HCO₃ - Cl - SO₄) and only 6% of the waters are sulphate-bicarbonate type with variations SO₄ - HCO₃ - Cl and SO₄ - Cl - HCO₃.

Nitrate type was found in water of 53 springs/fountains (approx.15%).

Depending on the cations content approx. 47% of the analyzed waters are of calcium type with different secondary cations (Ca - Mg - Na, Ca - Mg, Ca - Na - Mg, Ca - Na and Ca). Sodium ions prevail in water composition of 41% of the springs/fountains, and the magnesium - to 12%.

The study shows that 213 of springs/fountains (about 59%) have water mark “good” for irrigation, 92 (25%) - “satisfactory” and 57 (16%) have water mark “unsatisfactory” for irrigation.

A significant coefficient correlation between the number of polluted water sources with nitrates and the spontaneous dumps in rural districts ($R^2 = 0.7218$) denote that it is necessary to conduct urgent sanitation actions to offset the pollution outbreaks.

Same recommendations for protection of water:

To prohibit in all areas of domestic and industrial waste storage (liquid and solid) in the zones of water protection, especially for drinking water supply;

To encourage scientific research and education on water protection within the target districts;

To carried out the afforestation and grassing of the area around the water sources;

To organize an ecological reconstruction of water sources, elimination of natural water pollution sources (groundwater and surface water, because the pollutant migrate from one aquifer to another).

References

- [1] Bretotean M. Groundwater, an important natural resource. Bucuresti, 1981, 128 p.
- [2] Duca, Gh.; Romanciuc, L. and Porubin, D. Groundwater Resources of Moldova and Transboundary Impact // Transboundary Aquifers in the Eastern Borders of The European Union Regional Cooperation for Effective Management of Water Resources – 2012. - Springer Science + Business Media B.V., pp. 121-127.
- [3] Directive 2000/60/EC of the European Parliament and of the Council of 23 October 2000 establishing a framework for Community action in the field of water policy.
- [4] Directive 2006/118/EC of the European Parliament and of the Council of 12.12.2006 on the protection of groundwater against pollution and deterioration.

- [5] Mustea, M.; Boian, I.; Galca, G.; Sandu, M.; Tarita, A.; Zubcov, E.; Sireteanu, D.; Gladchi, V.; Prepelita, A.; Jeleapov, V.; Serenco, L. State of Water Resources and Protection. State of the environment in the Republic of Moldova: The Second Millennium development Goals report Republic of Moldova. – Ch.: “Nova Imprim” SRL, 2011, pp. 75-80.
- [6] Ropot, V.; Stratulat, G.; Lupascu, T.; Sandu, M., et al. The problems of water resources quality, use and protection in the Republic of Moldova. Chisinau, Science, 1991, 285 p.
- [7] Dumitru, M. Analysis and evaluation of groundwater and deep groundwater resources from Crisul Repede hydrographic basin. Summary of the thesis, Oradea, 2011, 18 p.
- [8] Lacatusu, R.; Kovacsovics, B.; Plaxienco, D.; Rasnovanu, I.; Lungu, M.; Mihalache, D. Load of soils, vegetables and ground waters with fertilizer and pesticides pollutants in the south and east part of Bucharest city // The Environment protection in Agriculture, Bucuresti, 2000, Vol.1., pp. 279-293.
- [9] Law nr.272-XIV of 10.02.1999. Official Monitor of the Republic of Moldova, 1999, no. 39-41. Article 1. Basic Terms.
- [10] Zavoianu, I. Hidrology. Ed. IV, Bucharest, 2006, 256 p.
- [11] Duca, Gh.; Gladchi, V.; Goreaceva, N.; Bunduchi, E.; Borodaev, R.; Lis, A.; Anghel, L.; Surighina, O.; Romanciuc, O. Impact of right tributaries on the Dniester River water quality in the spring of 2009 year. Studia Universitatis. Ser. Science of Nature. 2010, 1, pp. 146-154.
- [12] Ropot, V.; Rusu, V.; Sandu, M.; Lozan, R.; et.al. Hydrochemistry of the Dniester river, the problems of its water quality and use. Mater. Resp. Conf. «Ecol. Problems and their solutions.» Chisinau, 1989, pp. 167-171.
- [13] Ropot, V.; Sandu, M. Water resources and their quality. National Strategic Action Program in Environment Protection, Chisinau, 1995, pp. 20-25.
- [14] Tarita, A.; Sandu, M.; Lozan, R.; Sergentu, E.; Spataru, P.; Mosanu, E.; Goreacioc, T., Jabin V. Water quality of springs and fountains in Nisporeni district// Bulletin of the ASM: Sciences of the Life, 1. pp. 164-169.
- [15] Sandu, M.; Sergentu, E.; Tarita, A.; Spataru, P.; Mosanu, E.; Lozan, R. Water quality springs and fountains in the Prut River Basin (Briceni, Edinet, Rișcani districts). The Environment, Chisinau: 2009, nr. 4(46), pp. 36-40.
- [16] Mosanu, E.; Tarita, A.; Sergentu, E.; Sandu, M.; Spataru, P.; Goreacioc, T.; Jabin, V. Water quality of springs and fountains from Glodeni and Falesti districts (the Prut River hydrographic Basin). The Environment, Chisinau: 2009, 5(47), pp. 1-4.
- [17] Lozan, R.; Tarita, A.; Sandu, M.; Mosanu, E.; Sergentu, E. Springs water - an alternative source of water supply for the rural population (Hancesti, Leova, Cahul and Cantemir districts). Bulletin of the ASM. Sciences of the Life. 2010, 1 (310), pp. 165-171.
- [18] Sandu, M. The correlation between nitrate and the natural waters macro components content//Bulletin of the ASM: Sciences of the Life. 2004, 3, pp. 116-119.
- [19] Overcenco, A.; Mihailescu, C.; Bogdevici, O.; Gilca, G. Wells and springs. Ecological Atlas.Ed. Stiinta. 2008. 208 p.
- [20] Sandu, M.; Mosanu, E.; Gladchi, V.; Tarita, A.; Duca, Gh.; Spataru, P.; Lupascu, T.; Sergentu, E.; Lozan, R.; Jabin, V.; Turcan, S. Study of springs water quality as sources of potable water and for irrigation in Rezina district. *Chem. J. Moldova*. 2010, 5 (1), pp. 84-89.
- [21] Lozan, R.; Tarita, A.; Sandu, M.; Gladchi, V.; Mosanu, E.; Procopii, D.; Spataru, P.; Jabin, V.; Turcan, S. Spring - indicator of the ecological state of the territory (Orhei, Telenesti and Soldanesti districts). The Environment, Chisinau: 2011, 2 (56), pp.15-20.
- [22] Lozan, R.; Tarita, A.; Sandu, M.; Mosanu, E.; Procopii, D.; Gladchi, V. Aspects of springs and fountains water quality parameters in Criuleni and Calarasi districts. International Scientific Conference dedicated to the 65th anniversary of USM, 21-22 September 2011. Abstracts and apers. Natural and exact Sciences, Chisinau, 2011, Vol. II. pp. 70-72.
- [23] Sandu, M.; Tarita, A.; Lozan, R.; Mosanu, E.; Spataru, P.; Procopii, D.; Turcan, S.; Jabin, V. Spring - underground aquifer indicator of pollution by nitrates (river Nistru basin). Ch.: The V Intern. Conf.-Symposium Ecological Chemistry 2012, ASM, March 2-3, 2012, pp. 60-61.
- [24] Gaidau, A.; Zlotea, A.; Tarita, A.; Lozan, R.; Sandu, M. The springs from river Nistru Basin water sources for drinking and irrigation consume (Stefan Voda district). *Ecological Chemistry and chemical risk assessment*. Ed. XII-a, 7 December 2012. Ch.: CEP USM, 2012, pp. 33-34.
- [25] Sidoren, I.; Turcan, S.; Tarita, A.; Lozan, R.; Sandu, M. The springs from river Nistru Basin –water sources for drinking and irrigation consume (Causeni district). *Ecological Chemistry and chemical risk assessment*. Ed. XII-a, 7 December 2012. Ch.: CEP USM, 2012, pp. 86-88.
- [26] SR EN 25667-2:2002. Water quality - Sampling. Part 2: Guidance on sampling techniques.
- [27] SR EN ISO 9963-1. Water quality. Determination of alkalinity. Part 1: Determination of total and permanent alkalinity.
- [28] SR ISO 7150-1. Water quality. Determination of ammonia. Part 1: Manual Spectrometric method.

- [29] Standardized methods for studying water quality. Methods for analysis of water, Nauka, Moscow, 1983, 108 p.
- [30] Novikov, I. V.; Lastocichina, S. O.; Boldina, Z. I. Methods for determining of harmful substances. Moscow: Medicine. 1981, 376 p.
- [31] Nickanorov, A.M.; Posohov, E.V. Hydrochemistry. – L., Hydrometeoizdat. 1985. 252 p.
- [32] The Government Decision of the Republic of Moldova Nr. 934 in 15.08.2007. The Official Monitor of the Republic of Moldova Nr. 131-135 in 24.08.2007. Art. nr. 970. Annex nr.2. Health norms for drinking water quality.
- [33] Anscombe, F. J. Graphs in Statistical Analysis. *American Statistician*, 1973, 27, pp. 17-21.
- [34] Hopkins, W. G. (2000). A new view of statistics. Internet Society for Sport Science: <http://www.sportsci.org/resource/stats/>.
- [35] Plotnikova N.M. Hydrogeology of USSR, T. VII. Republic of Moldova. “Nedra”, 1966, 174 p.
- [36] Prisiajniuk, A.C. Review of underground waters of the Republic of Moldova, T. I. Hydrological Report. M. 1972, 38 p.

HEAVY METALS AND PHOSPHORUS FORMS MOBILIZATION DURING THE RE-SUSPENSION OF BOTTOM SEDIMENTS OF THE PRUT RIVER

Larisa Postolachi

*Institute of Chemistry of Academy of Sciences of Moldova, 3, Academiei str., Chisinau MD-2028, Republic of Moldova
e-mail: larisapostolachi@gmail.com; phone: (+373 22) 73 97 31; fax: (+373 22) 73 99 54*

Abstract. Bottom sediments of the river are repositories for various elements, acting both as sinks and sources of supplying of elements to overlying water horizon. Re-suspension of the bottom sediments of the Prut River was performed in field conditions by „aquarium” method. The results suggest that during the re-suspension, bottom sediments can become a relevant source of heavy metals and phosphorus forms which are mobilized in the water horizon overlying the bottom sediments.

Keywords: bottom sediments, re-suspension, the Prut River.

Introduction

Metals discharged into aquatic systems are mostly adsorbed on suspended particles and fine grained sediments [1]. Bottom sediments play the essential role in the processes of phosphorus transformation and its accumulation in aquatic systems [2, 3]. Mobilization-immobilization processes on the surface of sediments occur through and/or participation of the interstitial water. During the desorption process from sediments, phosphorus compounds are accumulated in interstitial water and then can be mobilized in the water horizon overlying the bottom sediments [4]. Reverse process, the immobilization from water in sediments, also occurs through interstitial water. The direction of mobilization-immobilization processes determines pollution - self-purification processes of water bodies [5].

Sediments are not passive collectors of heavy metals. Polluted sediments are periodically subjected to re-suspension processes resulting from natural events (e.g. storms, strong waves) as well as from anthropogenic induced activities (e.g. dredging). The main part of the re-suspended material is initially in an anoxic state and will be re-oxidized more or less quickly in the oxic water column above sediments [6].

Mobilization/immobilization processes are better elucidated for marine waters (Fig. 1). The mobilization of heavy metals from sediments can be increased due to the following factors: (i) changing of redox conditions; (ii) lowering the pH and (iii) the presence of complexing agents, which can form soluble metal complexes [6, 7]. Additionally, the mechanical perturbation (erosion, dredging, bioturbation) can also affect the metals mobilization.

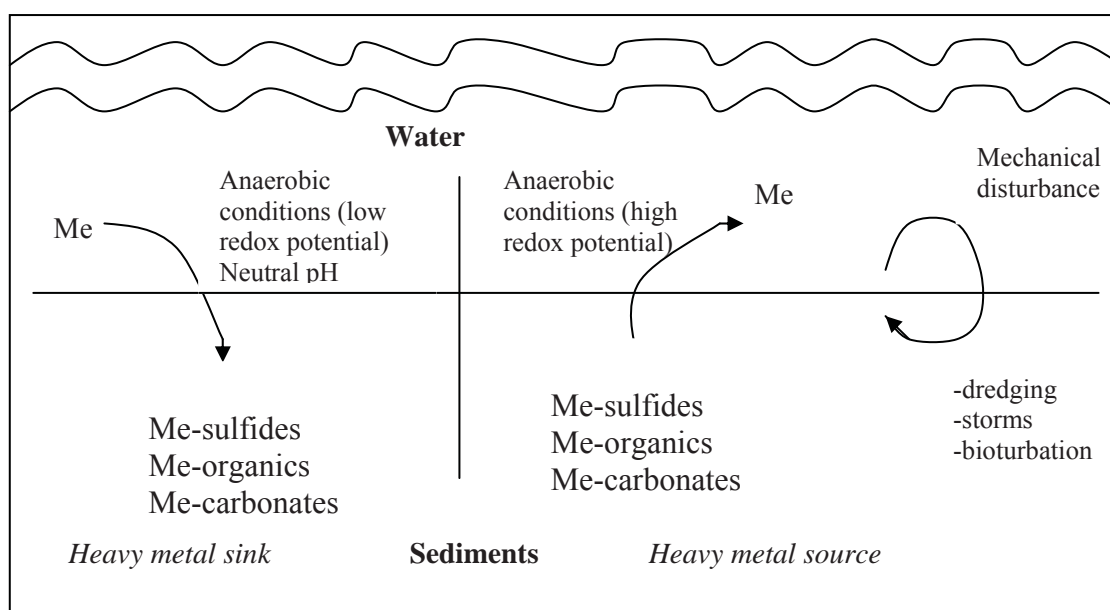


Figure 1. Sediments as a sink and a source of pollution by heavy metals (Me). Source: Stigliani W. [7].

The objectives of this paper were (i) to establish the desorbed amounts of heavy metals and phosphorus forms during the re-suspension of bottom sediments from the Prut River performed in field and laboratory conditions and (ii) to highlight the contribution of bottom sediments for surface water quality.

Material and methods

The re-suspension of bottom sediments of the Prut River was performed in field conditions by „aquarium” method - carefully mixing the sediments in a glass cylinder (without bottom, about 20 cm in diameter) implanted in the sediments at a depth of 5 cm [5]. To perform the sediments desorption, fresh (wet) samples were stirred with distilled water for 2 hours.

The content of heavy metals and phosphorus forms in the interstitial water of bottom sediments was determined after centrifugation of fresh (wet) sediments. After that interstitial water was filtered through membrane filters (0.45 μm pore diameter) and stored in the dark at 4°C until analysis. Heavy metal analyses were conducted using atomic absorption spectrometer AAS-3. The content of phosphorus forms (orthophosphates, condensed and organic phosphorus) was determined using World Health Organization recommendations [8].

Results and discussion

Heavy metals mobilization during re-suspension of bottom sediments

Mobilization/immobilization processes at the water-sediments interface is performed through direct participation of interstitial water [5]. As a rule, the content of heavy metals in the interstitial water of sediments is higher than in the water layer, which suggests that under dynamic conditions, i.e. during of re-suspension, the bottom sediments can become important sources of pollutants in the water column.

Figures 2 and 3 are presented the content of heavy metals (Cu, Zn, Fe) in the water layer, before and after the re-suspension of bottom sediments (ReS).

The obtained results indicate that the re-suspension of sediments, carried out in the field conditions, causes the increase, in the water layer, of Cu content about 1.5 times, Zn of 1.8-5.7 times and Fe of 1.1-39 times, in comparison with data recorded until the re-suspension. In such conditions, the quantities of mobilized metals in the water layer are for Cu about 19-52%, for Zn 23-100% and for Fe 7-32% of their content in the interstitial water of bottom sediments.

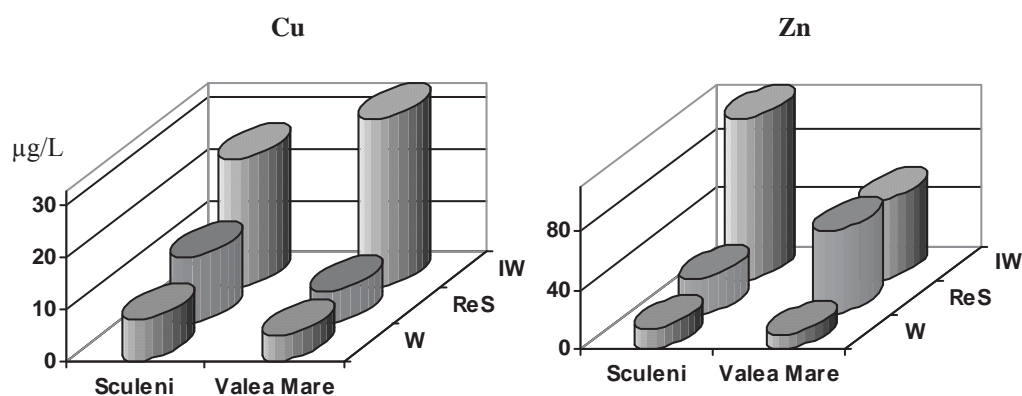


Figure 2. Dynamics of Cu and Zn in water (W) and interstitial water of sediments (IW) along the Prut River during of 2009 year. Heavy metals mobilization during of sediments re-suspension (ReS) performed in field conditions.

Taking into account the contribution of sediments in the processes of secondary pollution, it was modeled the sediments desorption, i.e. the shaking of the freshly sampled sediments in laboratory conditions (Tab. 1). The quantities of mobilized heavy metals are higher than those recorded in the water layer. The obtained results indicate that for sediments collected in summer there is characteristic a greater mobilization of heavy metals. It was found that due to the sediments desorption the content of Cu have increased in the water horizon by 2.4 times (summer), Zn – by 1.3-1.5 times (spring) and by 2.5-3 times (summer).

During spring-summer of 2009 year, the content of Mn in the Prut River water has been identified less than 5 $\mu\text{g/L}$. The obtained results indicate that during of the sediments desorption, the quantity of Mn have increased in the water layer by 1.6-6.6 times (spring) and 2-8.8 times (summer).

The intense mobility has registered for iron. The mobilized quantities of Fe, during the sediments desorption,

were by 5-15 times in the spring and by 37-101 times in summer more than data recorded in the water layer of the Prut River.

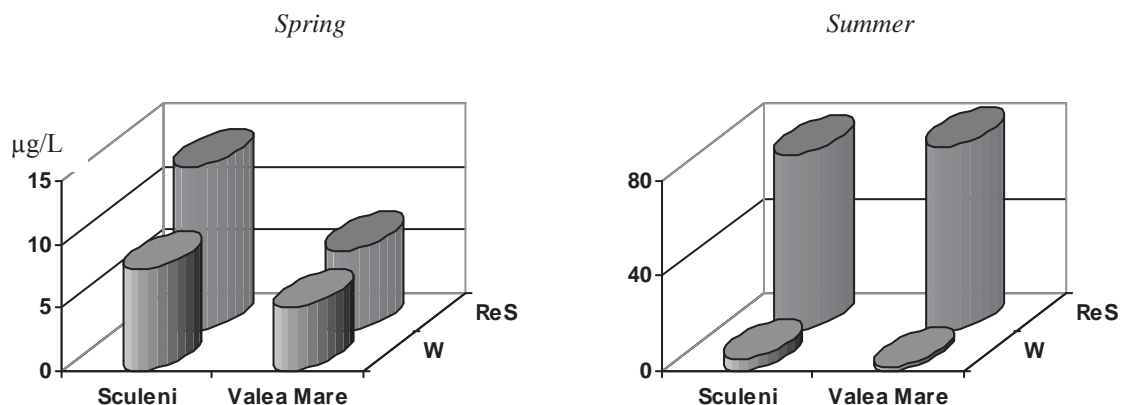


Figure 3. Iron (Fe) mobilization during of sediments re-suspension (ReS) performed in field conditions along the Prut River (2009).

Table 1.

The mobilized metals quantities during desorption from the Prut River sediments during of 2009 year, laboratory modeling

Station	Cu, µg/L	Cu, %	Zn, µg/L	Zn, %	Mn, µg/L	Mn, %	Fe, µg/L	Fe, %
Spring								
Sculeni	5	1.5	14	1.6	11	0.13	340	0.11
Valea Mare	3	1.7	13	1.0	5	0.12	650	0.44
Cahul	5.5	1.9	10	1.1	33	0.38	220	1.1
Caslita-Prut	3	1.1	15	1.7	8	0.1	450	0.17
Summer								
Sculeni	7.3	4.4	36	7	29	0.37	184	0.12
Valea Mare	12	8.7	25	4.1	16	0.48	202	0.2
Giurgiulesti	-	-	48	6.9	44	0.44	1280	0.7

Effect of bottom sediments re-suspension on phosphorus dynamics

Bottom sediments in aquatic system are repositories for various elements, acting both as sinks and sources of supplying for the elements to overlying water column. Once pollutants are discharged into rivers, these chemicals undergo interactive reactions through series of processes including dissolution/precipitation and sedimentation/re-suspension, finally settle down in bottom sediments [2].

During turbulent moments (e.g. winds), the bottom sediments are fretted and suspended in water horizon above sediments, i.e. the re-suspension phenomena takes place. Figures 4 and 5 are presenting the content of phosphorus forms (orthophosphates, poly- and pyrophosphates, organic phosphorus) in the water layer, before and after the bottom sediments re-suspension.

In such conditions the content of phosphorus-orthophosphate in the water layer of the Prut River above the sediments can increase by 1.5-3 times, compared with its quantity until the re-suspension (Fig. 4). The obtained data are the same with the information presented for other aquatic objects [9], which identified an increase of phosphorus-orthophosphate levels by 1.5-2 times due to the re-suspension of sediments. The content of condensed phosphorus forms (poly- and pyrophosphates) is also increasing by 1.6-2.6 times during the sediments re-suspension, which constitute 28-40% of its value in the interstitial water. The organic phosphorus is increasing by 1.4-2 times, in comparison with its content until the sediments re-suspension (Fig. 5).

Laboratory modeling of the bottom sediments re-suspension shows that considerable amount of phosphorus is desorbed from the bottom sediments. It was established that during of sediments desorption the content of phosphorus-

orthophosphate (P-PO₄) increased in the water horizon by 2.4-2.8 times (spring) and 1.4-2.3 times (summer) and the quantity of inorganic phosphorus (P-inorg) - by 1.1-2.7 times (Tab. 2).

The intense mobility of phosphorus were recorded during desorption of sediments sampled during of 2011 year (Tab. 3). The mobilized quantities during the sediments desorption were by ~ 4 times (P-PO₄), by 2.6-5 times (P-inorg) and by 3.2-9.5 times (P-org) higher compared to data recorded in the water layer of the Prut River.

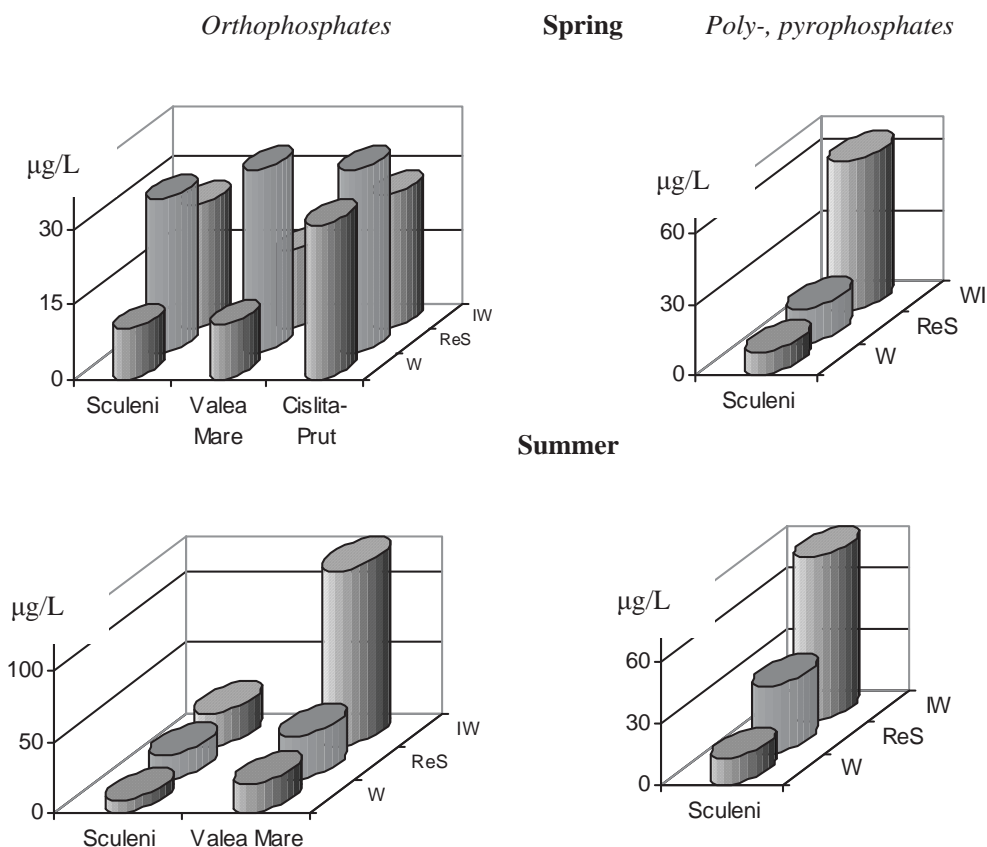


Figure 4. Dynamics of orthophosphates and poly-, pyrophosphates in water (W) and interstitial water of sediments (IW) along the Prut River during of 2009 year. Phosphorus mobilization during the sediments re-suspension (ReS) performed in field conditions.

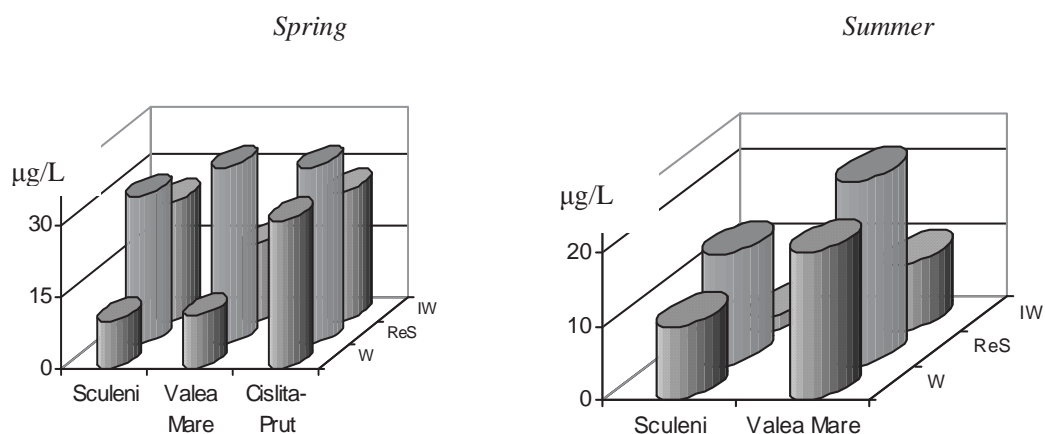


Figure 5. Dynamics of organic phosphorus in water (W) and interstitial water of sediments (IW) along the Prut River during of 2009 year. Phosphorus mobilization during the sediments re-suspension (ReS) performed in field conditions.

Results presented in the tables 2 and 3 demonstrate that under such conditions about 1.1-16% from the total quantity of inorganic phosphorus (P-inorg) and about 0.3-24% from the total quantity of organic phosphorus (P-org) can be desorbed from sediments.

Table 2.

Phosphorus amount desorbed from the bottom sediments of the Prut River during of 2009 year, laboratory modeling.

Station	P-PO ₄ , µg/L	P-inorg, µg/L	P-inorg, %	P-org, µg/L	P-org, %
Spring					
Sculeni	23	31	2.4	58	69
Valea Mare	31	62	5.8	30	24
Cahul	25	58	11	65	17
Caslita-Prut	21	116	16	4	1.6
Summer					
Cobani	13	30	3.6	7	2.7
Sculeni	13	34	4.9	3	0.8
Valea Mare	21	59	15	0.3	0.3
Giurgiulesti	18	24	2.1	20	17

Table 3.

Phosphorus amount desorbed from the bottom sediments of the Prut River during spring of 2011 year, laboratory modeling.

Station	P-PO ₄ , µg/L	P-inorg, µg/L	P-inorg, %	P-org, µg/L	P-org, %
Ungheni	38	54	1.4	21	2.8
Frasinesti	23	61	1.1	26	2.3
Leova	34	69	1.8	184	17
Branza	70	107	2.5	92	8.6

Conclusions

The results suggest that during the re-suspension, bottom sediments can become a relevant source of phosphorus forms which are mobilized in the water horizon overlying the bottom sediments.

It was established that during the re-suspension of the Prut River sediments, performed in field conditions, the content of Cu in the water layer have been increased by ~ 1.5 times, of Zn – by 1.8-5.7 times and the quantity of Fe - by 1.1-39 times, in comparison with data recorded until the re-suspension. In such conditions, the amount of Cu mobilized in the water layer is 19-52%, of Zn 23-100% and of Fe 7-32% of their content in the interstitial water, the highest migration mobility being recorded for zinc.

During the sediments re-suspension, in the water layer, the phosphorus-orthophosphate quantity have been increased by 1.5-3 times, the poly-, pyrophosphates - by 1.6-2.6 times and the content of organic phosphorus - by 1.4-2 times, in comparison with the data recorded until the re-suspension. The highest mobility was registered for organic phosphorus, establishing during the re-suspension the higher values than their content in the interstitial water.

References

- [1] Siepmann, R.; von der Kammer, F.; Calmano, W. Determination of Heavy Metal Mobility from Resuspended Sediments Using Simulated Natural Experimental Conditions, *Sediment Dynamics and Pollutant Mobility in Rivers An Interdisciplinary Approach*, Westrich B., Forstner U. (Eds.) © Springer-Verlag Berlin Heidelberg, 2007, pp. 258–268.
- [2] Lee, S.; Moon, J.; Moon, H. Heavy metals in the bed and suspended sediments of Anyang River, Korea: Implications for water quality, *Environmental Geochemistry and Health*, 2003, 25, pp. 433–452.
- [3] Krogerus, K.; Ekholm, P. Phosphorus in settling matter and bottom sediments in lakes loaded by agriculture, *Hydrobiologia*, 2003, 429, pp. 15–28.
- [4] Kowalczevska-Madura, K.; Dondajewska, R.; Goldyn, R. Changes of phosphorus concentration in bottom

- sediments and in overlying water of two strongly eutrophicated lakes in Wielkopolska Region, *Limnological Review*, 2007, 7(4), pp. 205–211.
- [5] Rusu, V.; Lupascu, T. *Chemistry of aquatic sediments. Surface properties. Physico-chemical models*. Chisinau, 2004. –272 p. (Rom).
- [6] Petersen, W.; Willer, E.; Willamowski, C. Remobilization of trace elements from polluted anoxic sediments after resuspension in oxic water, *Water, Air and Soil Pollution*, 1997, 99, pp. 515–522.
- [7] Stigliani, W. Changes in valued “capacities” of soils and sediments as indicators of nonlinear and time-delayed environmental effects, *Environmental Monitoring and Assessment*, 1988, 10, pp. 245–307.
- [8] Madera, V.; Allen, H. E.; Minear, R. A., Eds. *Examination of Water for Pollution Control*, World Health Organization. Pergamon Press: Copenhagen, Denmark, 1982; 1st Ed., vol. 2; pp. 310–319.
- [9] Martynova, M. Re-suspension effects of the bottom sediments on water body ecosystem, *Geography and natural resources*, 2007, 4, pp. 38–41 (Russ).

DISTRIBUTION OF PHOSPHORUS FORMS IN WATER-PARTICULATE MATERIALS-BOTTOM SEDIMENTS SYSTEM OF THE PRUT RIVER DURING 2009-2012 YEARS

Larisa Postolachi*, Vasile Rusu, Tudor Lupascu

Institute of Chemistry of Academy of Sciences of Moldova, 3, Academiei str., Chisinau MD-2028, Republic of Moldova
**e-mail: larisapostolachi@gmail.com; phone: (+373 22) 73 97 31; fax: (+373 22) 73 99 54*

Abstract. Phosphorus is the important nutrient which stimulates the growth of aquatic organisms in water bodies, but in excessive quantities phosphorus has a fertilizing effect that affects both the ecosystem and water quality as whole. A completed scheme for determination of phosphorus forms in water, particulate materials and bottom sediments was applied. The results obtained during of 2009-2012 years were analyzed and systematized, identifying the seasonal and spatial dynamics of phosphorus forms in water, particulate materials and bottom sediments of the Prut River.

Keywords: bottom sediments, particulate materials, phosphorus forms, the Prut River.

Introduction

Phosphorus is an essential nutrient for living organisms. In order to assess the anthropogenic impact on the chemical composition of surface water, the hydro-chemical indicators have been estimated, including either the content of phosphorus-orthophosphates [1, 2] or total phosphorus content [3], or the content of both forms [4,5]. Also, the variation of the content of some parameters that characterize the level of eutrophication, the content of nitrogen compounds, chlorophyll and total phosphorus were researched [6-9]. A few studies are focused on research of various phosphorus forms in water and particulate materials [10-12].

Phosphorus concentrations in rivers result from both external inputs and internal loading from the bottom sediments. Its chemistry in sediments is greatly influenced by the oxidation-reduction status (redox potential). Under oxidized conditions, ferric and manganese oxides and hydroxides are important adsorption sites for phosphorus; however, under reducing conditions these minerals are unstable. Mobilization-immobilization processes on the particle surface of sediments occur through interstitial water and its participation. During the desorption process from sediments, phosphorus compounds are accumulated in interstitial water, then according to environmental factors (pH, oxidation-reduction potential Eh, ionic strength, or water mineralization etc.) can be immobilized in the water horizon overlying the bottom sediments.

Phosphorus is a component of various constituents of aquatic ecosystem. But a few studies are focused on the extensive research of phosphorus compounds. Thus, it is often studied the seasonal dynamics of phosphorus compounds in the water-particulate materials system [10-12], in the particulate materials-sediments system [13], in the bottom sediments [14-17], in the interstitial water [18-20], in the water-sediments system [21-23].

The objectives of this work were (i) to evaluate peculiarities of spatial and seasonal dynamics of phosphorus forms for the entire system water - particulate materials - bottom sediments along the Prut River, (ii) to systematize the results obtained during of 2009-2012 years and (iii) to estimate the level of trophicity and quality of the Prut River.

Material and methods

During spring and summer of 2009-2012 years the samples of water, particulate materials and bottom sediments were collected along the Prut River (sampling sites: Costesti, Sculeni, Ungheni, Valea Mare, Frasinesti, Poganesti, Leova, Stoianovca, Cahul, Brinza, Caslita-Prut, Giurgiulesti). The bottom sediments with thickness of 0-5 cm were collected using all-plastic dredge sampler, fresh material being wet-sieved through 2 mm all-plastic sieve [24]. Then the samples were placed in plastic containers and stored in a portable refrigerator at 4°C during transportation to the laboratory.

The scheme for determination of phosphorus forms in water and particulate materials (Fig. 1) according to classification of World Health Organization (WHO) was applied [25]. According to WHO, phosphorus compounds occurred in natural waters are classified into 12 phosphorus forms, by chemical type – (i) orthophosphates, (ii) acid hydrolysable phosphates (poly- and pyrophosphates), (iii) organic phosphorus, (iv) total content, and by physical state – (i) dissolved (filterable), (ii) particulate, (iii) total content.

Additionally, the scheme was tested for estimation of phosphorus content in the bottom sediments [26-28]. The amount of total phosphorus was determined according to U.S. Geological Agency [24]. The content of inorganic phosphorus was determined according to WHO methods for inorganic particulate phosphorus [25].

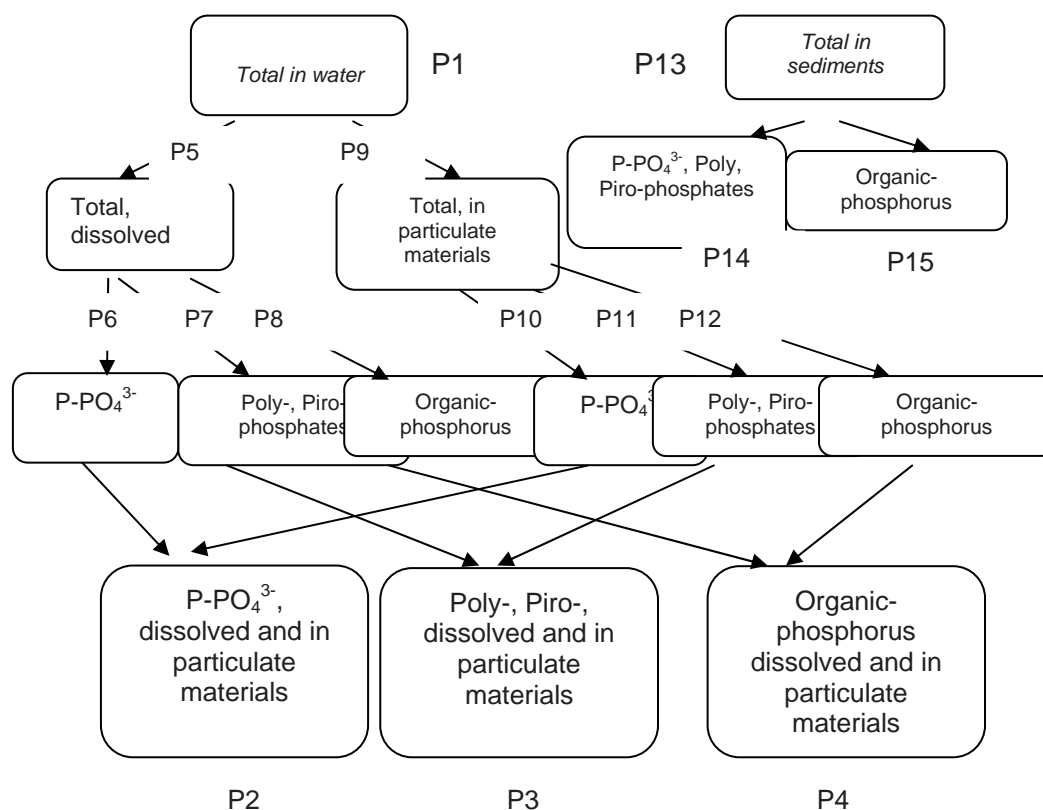


Figure 1. The scheme for analysis of the phosphorus forms in water and particulate materials according to WHO classification (forms P1-P12) [25]. Supplemented scheme for analysis of the phosphorus forms in sediments (forms P13-P15) [26-28].

The content of phosphorus forms in interstitial water was determined after centrifugation of fresh (wet) sediments. There were established amount of orthophosphates, condensed and organic phosphorus according to World Health Organization recommendations [25].

Results and discussion

Peculiarities of phosphorus content dynamics in water and particulate materials

The spatial dynamics of total phosphorus forms (namely, total P1, total dissolved P5 and total particulate P9) during of 2009-2012 years, in general, had indicated the increase of their amounts along the Prut River (Fig. 2). Seasonal dynamics of the content of phosphorus forms was the same, being established a decrease of total content of phosphorus forms from spring to summer.

The dynamics of dissolved phosphorus forms was less uniform along the Prut River (Fig. 3). During the spring of 2010 and 2011 years the spatial dynamics, in general, had the same trend, being recorded the maximal content of the orthophosphates (P6) and condensed forms (P7) at the middle sector of the river (stations Ungheni, Valea Mare).

For particulate forms of phosphorus (namely, orthophosphates P10 and organic phosphorus P12) an increase of their amounts was recorded along the river, recording the highest values at the lower sector of the river (stations Cahul, Caslita-Prut, Fig. 4). Seasonally, a decrease of particulate phosphorus from spring to summer was established during of 2009-2012 years.

Peculiarities of phosphorus dynamics in bottom sediments and their interstitial water

The spatial dynamics of phosphorus forms in the bottom sediments had, in general, the same trend during the spring of 2009 - 2011 years (Fig. 5). The higher contents of inorganic form (P14) were registered on the middle course of the Prut River. For organic phosphorus (P15) the highest contents during 2010 and 2011 years were recorded in the bottom sediments on lower course of the river. Multi-annual dynamics showed that the content of phosphorus forms in the bottom sediments was not changed significantly.

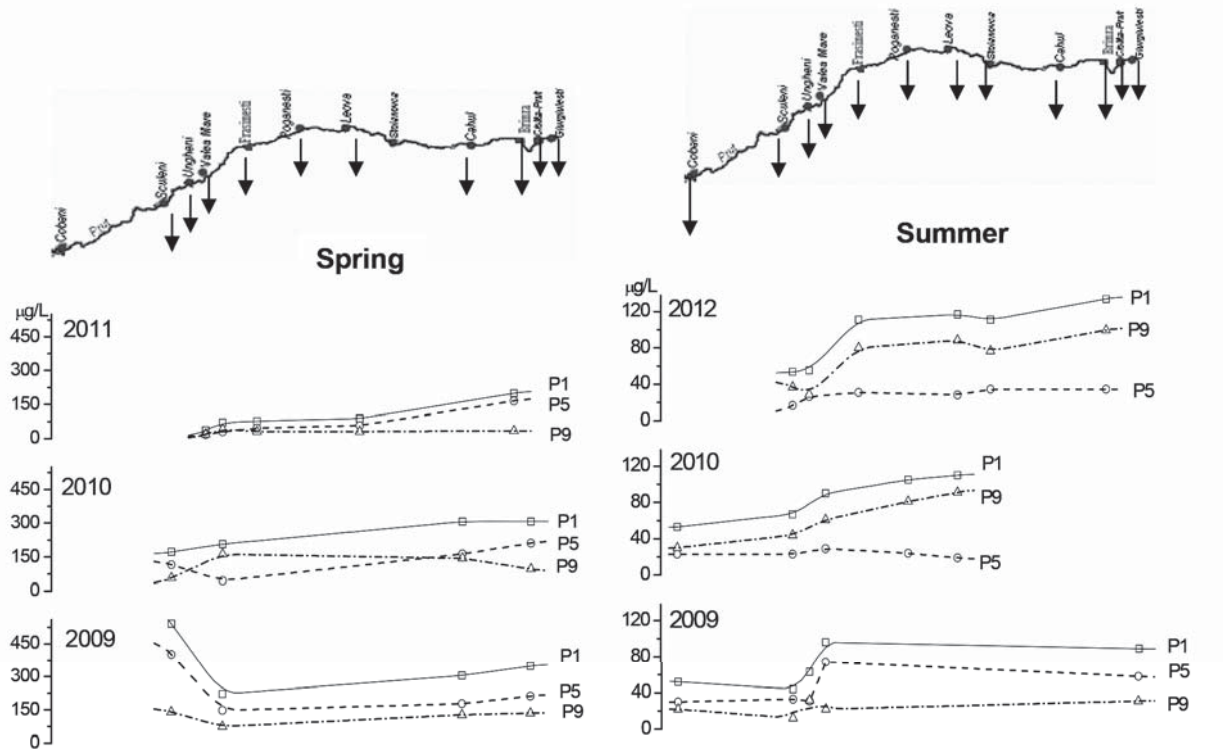


Figure 2. Dynamics of total phosphorus forms along the Prut River (P1, P9 and P5 – total phosphorus, total phosphorus in particulate materials and total dissolved phosphorus, respectively).

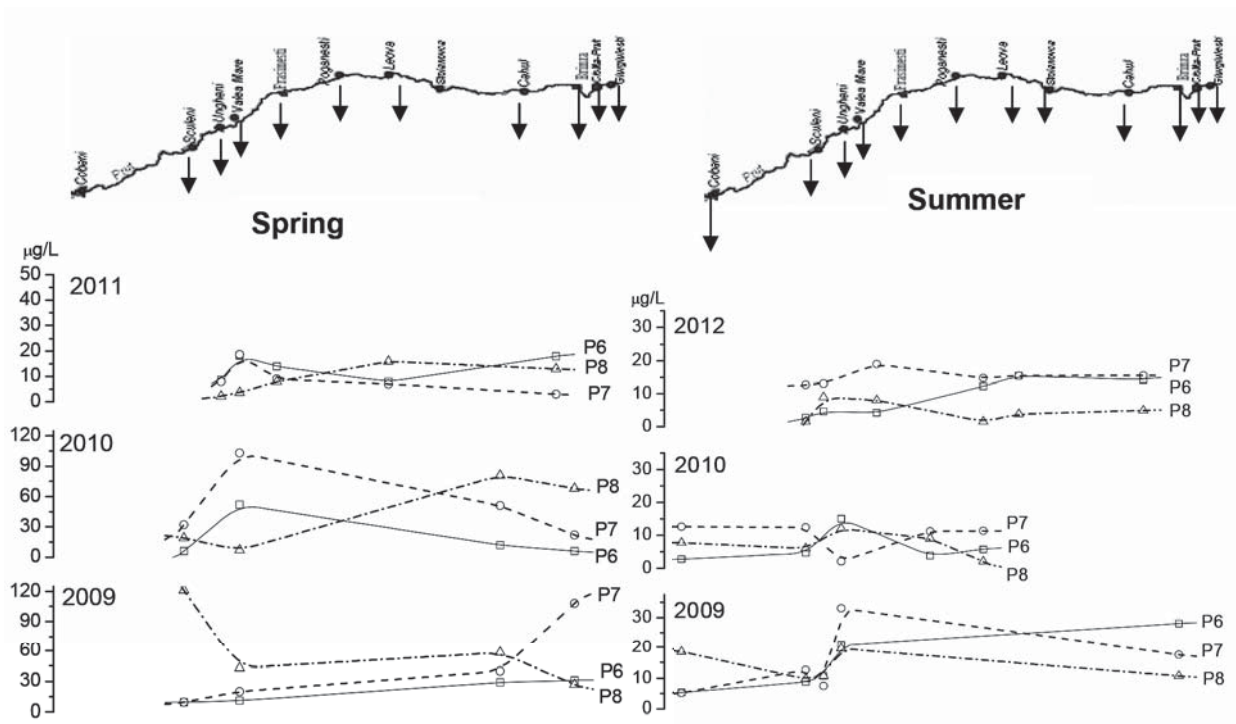


Figure 3. Dynamics of dissolved phosphorus forms along the Prut River (P6, P7 and P8—orthophosphate, condensed forms (poly- and pyrophosphates) and organic-phosphorus, respectively).

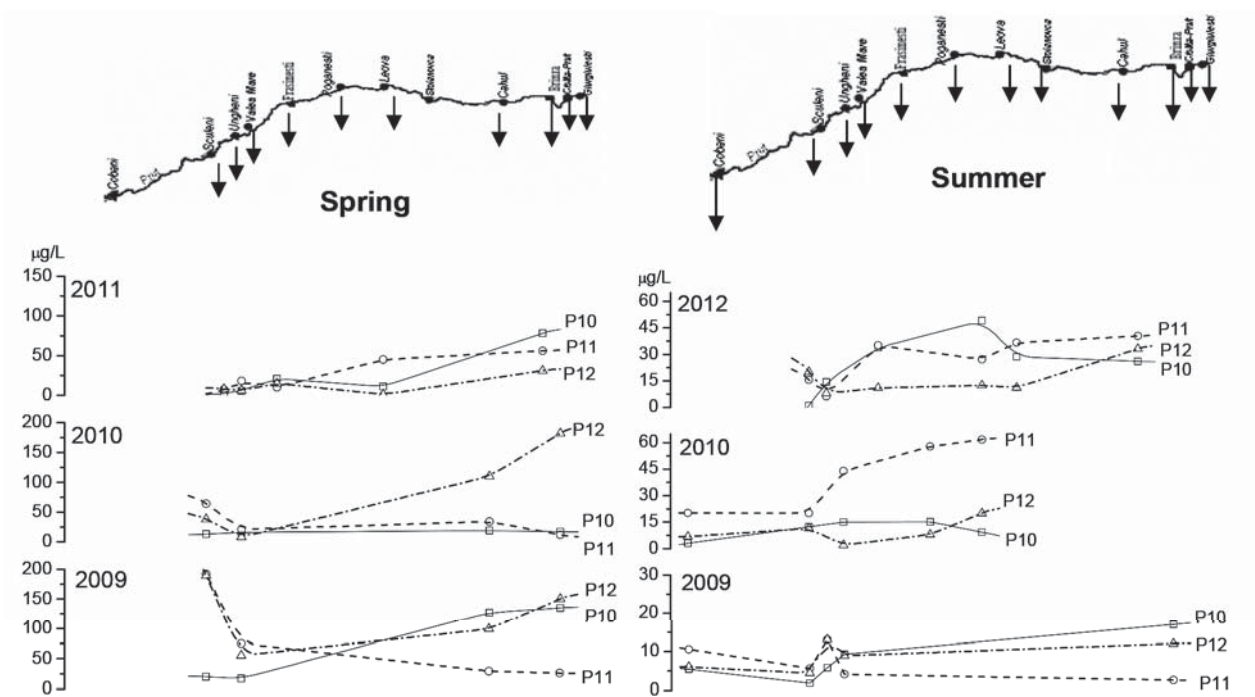


Figure 4. Dynamics of particulate phosphorus forms along the Prut River (P10, P11, P12 - orthophosphates, condensed forms and organic-phosphorus, respectively).

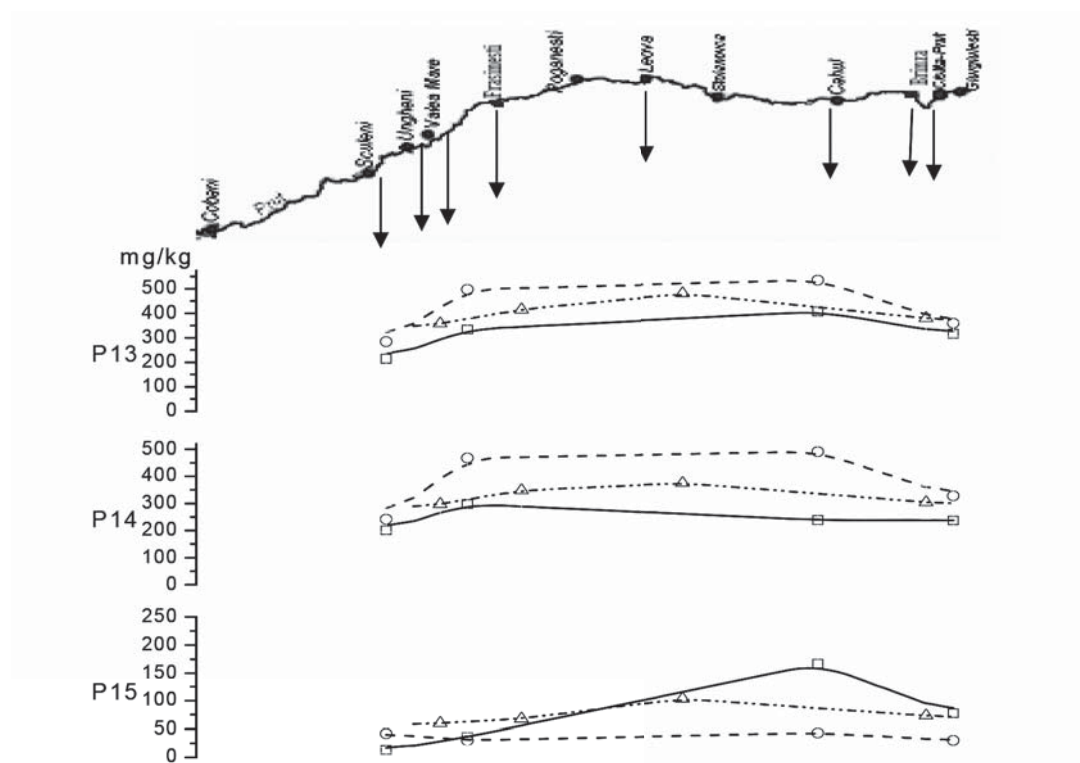


Figure 5. Dynamics of phosphorus forms in bottom sediments along the Prut River, spring (□ 2009, ○ 2010, △ 2011). Phosphorus forms in bottom sediments: P13 – total phosphorus, P14 – inorganic phosphorus, P15 – organic phosphorus.

During the summer the spatial dynamics of phosphorus forms in bottom sediments was less uniform along the Prut River (Fig. 6). Seasonal dynamics of phosphorus forms in bottom sediments was more pronounced during 2009 and 2010, being registered the tendency of decreasing of inorganic phosphorus and the tendency of increasing of organic phosphorus from spring to summer.

Ratio of inorganic: organic phosphorus (P14 : P15) in bottom sediments was similar during 2004, 2009, 2010 and 2011 years (Fig. 7), being recorded the predominance of the inorganic phosphorus which constituted about 65-95% of total amount. Also, the increasing tendency of the percentage of organic phosphorus from spring to summer was registered.

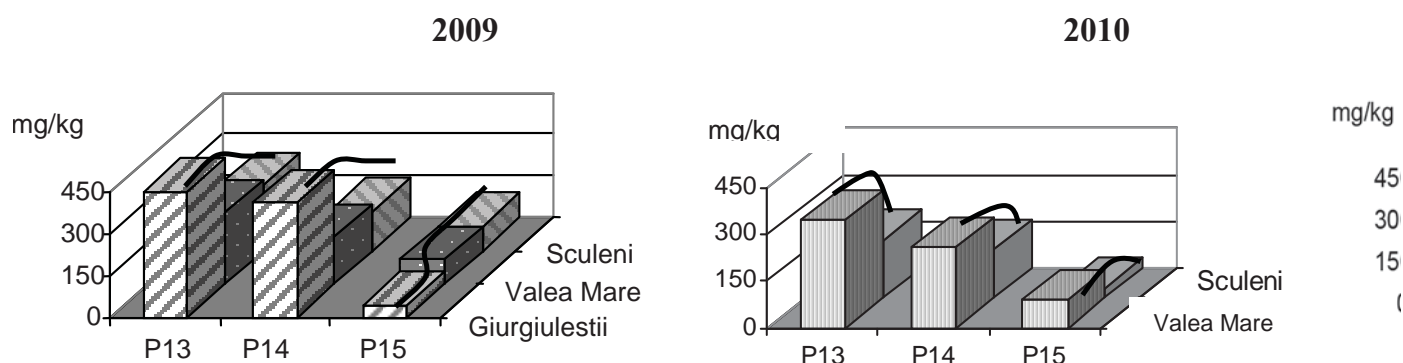


Figure 6. Dynamics of phosphorus forms in bottom sediments along the Prut River (summer).

Phosphorus forms in bottom sediments:

P13 – total phosphorus, P14 – inorganic phosphorus, P15 – organic phosphorus.

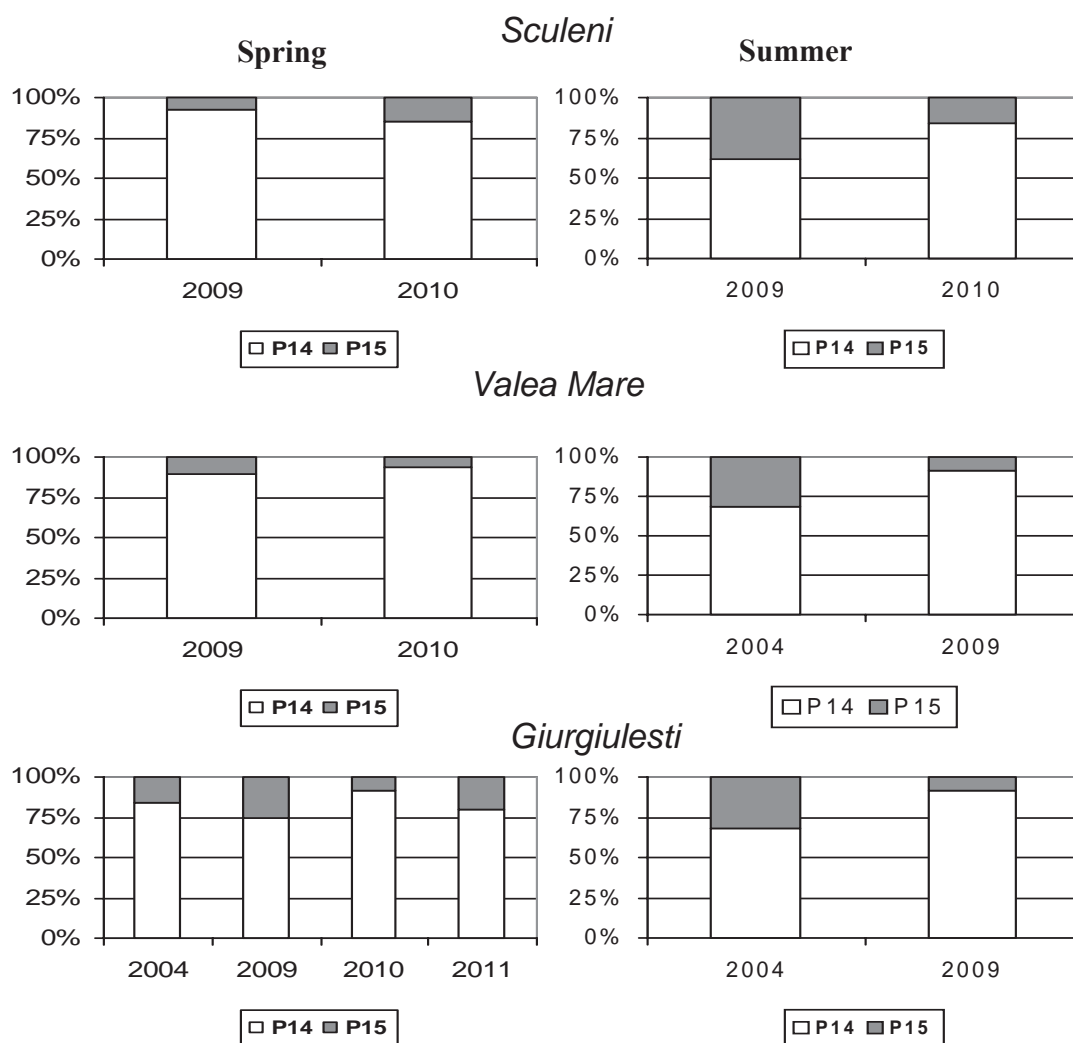


Figure 7. Proportions of inorganic (P14) and organic (P15) phosphorus in bottom sediments along the Prut River during the spring and summer of 2004, 2009, 2010 and 2011 years.

Phosphorus content in interstitial water was computed per volume of interstitial water (IW) extracted from 1 kg of bottom sediments (Fig. 8). Seasonal dynamics of phosphorus forms in interstitial water was more pronounced during 2009 and 2010, being registered the tendency of increasing of inorganic phosphorus and the tendency of decreasing of organic phosphorus from spring to summer.

During the spring of 2009 year the predominance of the organic phosphorus in interstitial water of bottom sediments was recorded which constituted about 45-78% of total phosphorus amount, while during the summer the proportion of organic phosphorus was lower (1.7-13% of total amount, Fig. 9).

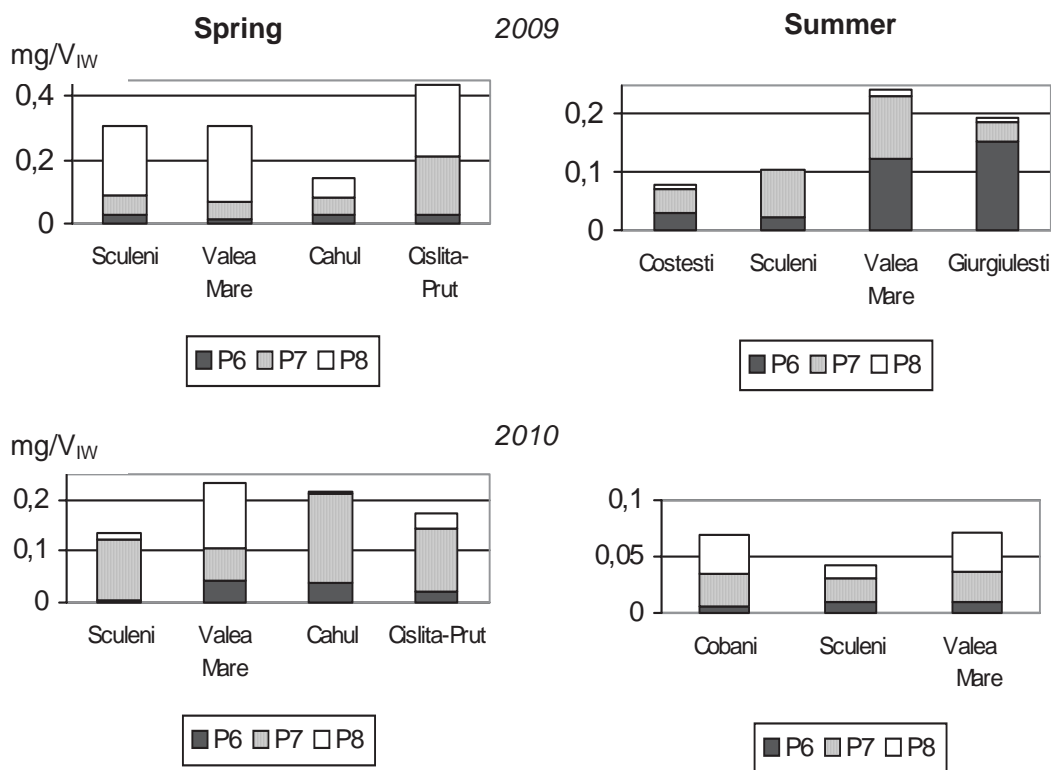


Figure 8. Dynamics of phosphorus forms (mg/V_{IW}) in interstitial water (IW) of bottom sediments along the Prut River during the spring and summer of 2009 and 2010 years. Data are computed per volume of interstitial water (IW) extracted from 1 kg of bottom sediments.

Phosphorus forms in interstitial water:

P6 – orthophosphates, P7 - condensed forms (poly- and pyrophosphates), P8 – organic phosphorus.

Level of trophicity and quality of the water

The large amounts of phosphorus compounds in aquatic ecosystems have the fertilizing effect that affects eutrophication degree. The European Community Directive 91/676/EEC recommends that the level of eutrophication in rivers should be determined on the basis of quality parameters, such as nitrate, phosphorus compounds, chlorophyll, oxygen etc. In accordance with the recommendations [29] eutrophication level is estimated according to the total phosphorus content (Tab. 1), while according to further recommendations [30] the level of eutrophication for rivers is estimated on the basis of soluble reactive phosphorus (Tab. 2).

Table 1.

Parameters used by the Member States of EC for assessment of eutrophication in rivers [29].

Parameters	Quality grade thresholds (eutrophication levels), mgP/L			
	I (Ultra-Oligotrophic)	II (Oligotrophic)	III (Mesotrophic)	IV (Eutrophic)
Total phosphorus (P1)	0 – 0.05	0.05 – 0.2	0.2 – 0.5	0.5 – 1

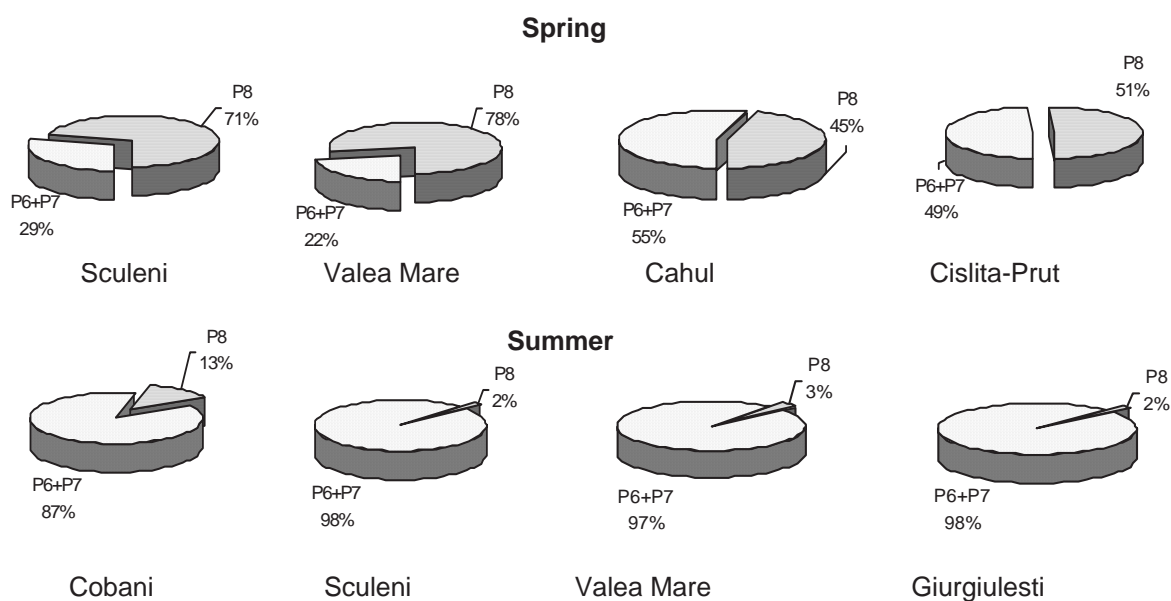


Figure 9. Proportions of inorganic (P6+P7) and organic (P8) phosphorus in interstitial water of bottom sediments along the Prut River during the spring and summer of 2009 year.

Table 2.

Directive threshold values for SRP used in Northern Ireland for assessment of eutrophication in rivers [30].

Parameters	Quality grade thresholds (eutrophication levels), mgP/L		
	I (Oligotrophic)	II (Mesotrophic)	III (Eutrophic)
Orthophosphates (SRP, P6)	0 – 0.02	0.02 – 0.10	>0.10

On the basis of the total phosphorus content (Tab. 1) and orthophosphates content (Tab. 2) the eutrophication level of the Prut River should be attributed to oligotrophic-mesotrophic level of eutrophication.

The quality of surface waters in Romania is regulated by Order 1146/2002 which includes five-quality classes [31]. The values specified for each class correspond to the maximum allowable for respective quality class (Tab. 3). On the basis of presented data in this work, the water of the Prut River should be attributed to the class I of quality according to phosphorus-orthophosphate content (P6), and to classes I-II of quality according to the content of total phosphorus (P1).

Table 3.

Quality classification of surface waters by phosphorus content (Order 1146/2002, [31]).

Limit value for classes	Class of quality, mgP/L				
	I	II	III	IV	V
Orthophosphates (P6)	0.05	0.1	0.2	0.5	>0.5
Total phosphorus (P1)	0.1	0.2	0.4	1	>1

According to the European Commission (UKTAG, 2003, [32]), the tolerated threshold (the arithmetic means calculated over a three-year period) for soluble reactive phosphorus SRP (mainly orthophosphates) is 0.20 mg/L (Tab. 4). The orthophosphate concentrations (the form P6, Fig. 3) registered for the Prut River during of 2009-2012 years didn't exceed this ecological threshold for eutrophication, the value of arithmetic mean being about 0.13 mg/L.

Table 4.

Phosphorus threshold values of SRP (mgP/L) (UKTAG, 2003, [32]).

Risk category	Not at risk	Probably at risk	At risk
Parameters			
Orthophosphates (SRP, P6)	< 0.02	0.02 – 0.04	>0.04

Actually, there aren't yet established any quality criteria for phosphorus content in the bottom sediments. Also, the criteria for phosphorus content in the interstitial water aren't standardized. In the study [33], the preliminary quality parameters of phosphorus-orthophosphates in the interstitial water of bottom sediments were proposed (Tab. 5).

According to the presented data for the content of phosphorus-orthophosphates in the interstitial water of sediments (Fig. 8), the level of eutrophication of the Prut River could be attributed to the oligotrophic level (P6 <0.1mgP/L), episodically (during the summer of 2009 year) to the mesotrophic level of eutrophication. This level of eutrophication is similar to those established on the basis of the content of phosphorus-orthophosphates in water.

Table 5.

Preliminary parameters of phosphorus-orthophosphates content (mgP/L) in the interstitial water (0-5 cm thickness of sediments) [33].

Limit value	Oligotrophic	Mesotrophic	Eutrophic	Eutrophic-hypertrophic	Hypertrophic
Orthophosphates (SRP, P6)	<0.10	0.10 – 0.25	0.25 – 1.00	1.00 – 2.50	>2.50

Conclusions

The scheme for determination of phosphorus forms in water and particulate materials according to World Health Organization classification was evaluated. Additionally, this scheme was tested for estimation of phosphorus content in bottom sediments. The supplemented scheme allows the analysis of the phosphorus forms for the entirely system "water – particulate materials – bottom sediments", extending possibilities for interpretation of phosphorus dynamics in natural waters.

The peculiarities of the spatial and seasonal dynamics of phosphorus in the water-particulate materials-sediments system during of 2009-2012 years along the Prut River were established. It was found an increasing trend of total dissolved phosphorus and in particulate materials along the Prut River. The maximum of dissolved phosphorus forms recorded on middle sector of the river (Valea Mare-Stoianovca) indicates the presence of pollution sources.

On the basis of obtained data, the water of the Prut River should be attributed to classes I-II of quality according to Romanian standards. The eutrophication level of the Prut River should be attributed to oligotrophic-mesotrophic level of eutrophication according to UE directives. According to the European Commission, the orthophosphate concentrations registered for the Prut River during of 2009-2012 years didn't exceed this ecological threshold for eutrophication. Actually, there are not yet established any quality criteria for phosphorus content in the bottom sediments.

Acknowledgements

This work has been supported by the international program SCOPES 2009-2012. Swiss National Science Foundation. Joint Research Project "Xenobiotic Input to the Prut River (XENOPRUT)".

References

- [1] Petre, J.; Vasile, G.; Cruceru, L.; Nicolau, M.; Mirita, M.; Iancu V. The evolution of water and sediments quality from the Danube delta in the period April-October of the years 2003-2004, Proc. 13th Int. Symp. on Environment and Industry, Bucharest, 2005, pp. 288–294.
- [2] Hounsou, M.; Ahamide, B.; Agbossou, E.K.; Gaiser T. Evaluation of water quality in the Oueme River (Benin), Environmentalist, 2011, 31, pp. 407–415.
- [3] Pascu, L.; Petre, J.; Vasile, G.; Vasile, I.; Dumitru, S.; Cristina, D.; Nastac, E.; Cruceru, L.; Nicolau, M.; Evaluation of physical-chemical quality characteristics of surface water and sediments from the Danube Delta in period April 2006-August 2009, Proc. 15th Int. Symp. on Environment and Industry, Bucharest, 2009, vol. 1, pp. 318–324.
- [4] Hamchevici, C.; Moldovan, C.; Popescu, V.; Constantinescu, L.; Dumitrache, F. Water quality along Romanian sector of the Danube River during of 1996-2005 years, Hidrotehnica, 2010, 55(3), pp. 26–33 (Rom).
- [5] Baborowski, M.; Buttner, O.; Einax, J. Assessment of Water Quality in the Elbe River at Low Water Conditions Based on Factor Analysis, Clean – Soil, Air, Water, 2011, 39(5), pp. 437–443.
- [6] Chmiel, S.; Głowacki, S.; Michalczyk, Z.; Sposób, J. Some issues in the assessment of eutrophication of river

- waters as a consequence of the construction of a storage reservoir (on the example of the Bystrzyca River), *Ecology & Hydrobiology*, 2009, 9, pp. 175–179.
- [7] Jung, N. C.; Popescu, I.; Price, R.K.; Solomatine, D.; Kelderman, P.; Shin, J.K. The use of the A.G.P. test for determining the phytoplankton production and distribution in the thermally stratified reservoirs: The case of the Yongdam reservoir in Korea, *Environmental Engineering and Management Journal*, 2011, 10(11), pp. 1647–1657.
- [8] Jung, N.C.; Popescu, I.; Kelderman, P.; Solomatine, D.P.; Price, R.K. Application of Model Trees and Other Machine Learning Techniques for Algal Growth Prediction in Yongdam Reservoir, Republic of Korea, *Journal of Hydroinformatics*, 2010, 12(3), pp. 262–274.
- [9] Hu, J.; Qiao, Y.; Zhou, L.; Li, S. Spatiotemporal distributions of nutrients in the downstream from Gezhouba Dam in Yangtze River, China, *Environmental Science and Pollution Research*, 2011, 19, pp. 2849–2859.
- [10] Selig, U.; Michalik, M.; Hubener, T. Assessing P status and trophic level of two lakes by speciation of particulate phosphorus forms, *Journal of Limnology*, 2006, 65(1), pp. 17–26.
- [11] Noe, G.; Harvey, J.W.; Saiers, J.E. Characterization of suspended particles in Everglades wetlands, *Limnology and Oceanography*, 2007, 52(3), pp. 1166–1178.
- [12] Yoshimura, T.; Nishioka, J.; Saito, H.; Takeda, S.; Tsuda, A.; Wells, M.L. Distributions of particulate and dissolved organic and inorganic phosphorus in North Pacific surface waters, *Marine Chemistry*, 2007, 103, pp. 112–121.
- [13] Iglesias, M.L.; Devesa-Rey, R.; Pérez-Moreira, R.; Díaz-Fierros, F.; Barral, M.T. Phosphorus transfer across boundaries: from basin soils to river bed sediments, *Journal of Soils and Sediments*, 2011, 11, pp. 1125–1134.
- [14] Wiratchapun, P.; Dharmvanij, S.; Charusiri, P. Comparison of Phosphorus Partitioning Results in Estuarine Sediments by Sedex, Modified Sedex and Agemian Extraction Schemes, *Journal of Scientific Research of Chulalongkorn University*, 2003, 28(1), pp. 23–33.
- [15] Matuszewska, K.; Białkowska, I.; Bolałek, J. Interdependence between phosphorus forms in sediments and iron in interstitial waters in the Gulf of Gdańsk, *International Journal of Oceanography and Hydrobiology*, 2003, XXXII (1), pp. 5–14.
- [16] Fang, T.; Chena, J.L.; Huhb, C.A. Sedimentary phosphorus species and sedimentation flux in the East China Sea, *Continental Shelf Research*, 2007, 27, pp. 1465–1476.
- [17] Barral, M.; Devesa-Rey, R.; Ruiz, B.; Díaz-Fierros, F. Evaluation of Phosphorus Species in the Bed Sediments of an Atlantic Basin: Bioavailability and Relation with Surface Active Components of the Sediment, *Soil and Sediment Contamination*, 2012, 21(1), pp. 1–18.
- [18] Jahnke, R.A.; Alexander, C.R.; Kostka, J.E. Advective pore water input of nutrients to the Satilla River Estuary, Georgia, USA, *Estuarine, Coastal and Shelf Science*, 2003, 56, pp. 641–653.
- [19] Jahnke, R.; Richards, M.; Nelson, J.; Robertson, C.; Rao, A.; Jahnke D. Organic matter remineralization and porewater exchange rates in permeable South Atlantic Bight continental shelf sediments, *Continental Shelf Research*, 2005, 25, pp. 1433–1452.
- [20] Adeyemo, O.; Adedokun, O.A.; Yusuf, R.K.; Adeleye, E.A. Seasonal changes in physico-chemical parameters and nutrient load of river sediments in Ibadan City, Nigeria, *Global NEST Journal*, 2008, 10(3), pp. 326–336.
- [21] Voinea, E.; Petre, J.; Lucaci, I.; Cruce, L.; Nicolau, M.; Gabriela, V.; Mitrita, M.; Rusu, G.; Ciurcanu, I.; Iancu V. The temporal and spatial dynamics of the physico-chemical quality characteristics and the biotic communities structure in the aquatic ecosystems from Danube Delta biosphere, *Proc. 12th Int. Symp. on Environment and Industry*, Bucharest, 2003, (CD).
- [22] Guangwei, Z.; Qin, B.; Zhang, L. Phosphorus forms and bioavailability of lake sediments in the middle and lower reaches of Yangtze River, *Science in China: Series D Earth Sciences*, 2006, 49, pp. 28–37.
- [23] Kowalczywska-Madura, K.; Dondajewska, R.; Gołdyn, R. Changes of phosphorus concentration in bottom sediments and in overlying water of two strongly eutrophicated lakes in Wielkopolska Region, *Limnological Review*, 2007, 7, pp. 205–211.
- [24] *Techniques of water-resources investigations of the United States Geological Survey*, Fishman M, Friedman L (Eds) Book 5, 3d edition, Washington, 1989, 545 p.
- [25] Madera, V.; Allen, H. E.; Minear, R. A., Eds. *Examination of Water for Pollution Control*, World Health Organization. Pergamon Press: Copenhagen, Denmark, 1982; 1st Ed., vol. 2; pp. 310–319.
- [26] Rusu, V.; Postolachi, L.; Lupascu, T. Phosphorus content in water, particulate materials and sediments of river Prut, *Environmental Engineering and Management Journal*, 2006, 5, pp. 591–596.
- [27] Rusu, V.; Postolachi, L. Monitoring of phosphorus content in “water-particulate materials-bottom sediments system” for river Prut, In *Air and Water components of environment*, G. Pandi and F. Moldovan (Eds), 2011, pp. 206–213.
- [28] Rusu, V.; Postolachi, L.; Povar, I.; Alder, A.; Lupascu, T. Dynamics of phosphorus forms in the bottom sediments and their interstitial water for the Prut River (Moldova), *Environmental Science and Pollution Research*, 2012, 19, pp. 3126–3131.

- [29] “Nitrates” Directive 91/676/EEC, Status and trends of aquatic environment and agricultural practice, Development guide for Member States’ reports, ISBN 92-828-9379-0.
- [30] Review of 2007-2010, Action Programme for the Nitrates Directive. Northern Ireland. Recommendations from the Scientific Working Group. On-line at: http://www.doeni.gov.uk/nap_review_final.pdf.
- [31] Order, 2002, Order of the Minister of Waters and Environmental Protection No. 1146/2002 on the approval of the Norm regarding the reference objectives for the classification of the quality of the surface waters, published in Romanian Official Monitor no 197 from 27th March 2003 (Rom).
- [32] UKTAG (2003), Guidance on selection of risk assessment criteria in relation to biological classification schemes for rivers, (Working Draft), UK Technical advisory group on the water framework directive.
- [33] Maassen, S.; Uhlmann, D.; Roske, I. Sediment and pore water composition as a basis for the trophic evaluation of standing waters, *Hydrobiologia*, 2005, 543, pp. 55–70.

BUFFER PROPERTIES OF SOIL MINERALS. PART 1. THEORETICAL ASPECTS

Igor Povar*, Oxana Spinu

Institute of Chemistry, Academy of Sciences of Moldova, 3, Academiei str., Chisinau MD 2028, Republic of Moldova
*e-mail: ipovar@yahoo.ca; phone / fax: (+373 22) 73 97 36

Abstract. The key quantitative characteristics of the theory of buffer action for polycomponent mono- and two-phase systems have been derived. It is shown, that the buffer properties in relation to the solid phase components are amplified with an increase of solubility due to protolytic or complex formation equilibria in saturated solutions. It has been established, that the buffer capacities of components are mutually proportional, whereas for heterogeneous systems these relationships depend on the stoichiometric composition of solid phases. The deduced equations can be applied to the assessment of buffer action of the systems “natural mineral – soil solution”, containing soluble and insoluble chemical species. A number of the important conclusions concerning the investigated buffer systems have been made. The obtained results are of interest for soil scientists and ecologists.

Keywords: buffer action, complex formation, soil solution, solid phase, thermodynamic stability.

Introduction

The capacity of buffer systems to oppose (resist) to the variation of their composition (usually to pH changes) by influence of external fluxes of chemical compounds of natural or anthropogenous character, that shift chemical equilibria, is called *buffer property*, and its efficiency – *buffer action*. The buffer action of soil is one of its fundamental physicochemical characteristics. The soil buffer action composes of the buffer action of a set of mineral and organic components, presented by solid, liquid and gaseous compounds. The buffer capacity of soils in relation to chemical compounds is defined by the content of chemical elements in the soil solution (the parameter of intensity) as well as by the content of mobile compounds of these elements in solid phases (the parameter of capacity). The buffer capacity of soils can be discovered by the fact that the increase of amounts of toxic metals (TM) is not accompanied by an increase of their content in plants; the different buffer action of the soils in relation to one element is manifested in unequal toxic concentrations for plants. The same soil can possess different buffer action in relation to different metals.

The chemical basis of the soil buffer capacity in relation to any chemical element is the nature of the equilibrium which is established between two groups of mobile compounds of an element. The analysis of the nature of buffer capacity of soils in relation to pollutants is essentially reduced to the analysis of laws of their absorption by soils. The more and more strongly the soil can keep pollutants, the more actively they go away from the soil solution into the composition of solid phase compounds, the better the soil resists to the increase of the concentration of polluting substances in its solution.

The problem of determination of the soil buffer capacity allows calculating the pollutant amounts which delivery does not essentially break the natural character of soil functioning, being the major one in the soil science, ecology and wildlife management. The complexity of the soil solution composition containing mineral phases and a large set of involved chemical compounds determine the possibility of simultaneous chemical reactions along with the capacity of solid phases of minerals to maintain relatively constant the aqueous solution composition. Under real conditions the buffer action of natural heterogeneous aqueous systems is expressed so as the consumption of any element from solution causes the partial dissolution of solid phases and as a result the composition of the solution is restored. Despite of an abundance of the information on buffer systems, the quantitative theory of buffer action has been developed only for mono-phase systems [1, 2]. The buffer action of mono-phase buffers is usually based on protolytic equilibria between water, a weak acid or base or ampholytic compound and their conjugate pairs. The widespread use of buffers as well as the variety of chemical processes and phenomena associated with a certain acidity of solutions explains the constant interest in designing and studying new buffer systems.

Unlike the classical mono-phase buffer systems in which the buffer components are dissolved in a unique phase, in two-phase (heterogeneous) buffers they are distributed between two phases: in aqueous phase and solid (gaseous or liquid), insoluble phase. The aqueous (buffer) phase contains all the charged particles and a restricted quantity of electro-neutral species. The solid phase contains in significant quantities only electro-neutral particles and serves as their reservoir by means of which the equilibrium is adjusted and one of parameters of buffer system is maintained constantly [2-9]. The buffer action of two-phase systems is based on the shift of complex equilibrium, both homogeneous, and heterogeneous in the aqueous phase and between phases, respectively. By increasing the acidity of solution the role of simultaneous proceeding protolytic reactions with participation of salt anions increases; with an increase of alkalinity the contribution of complex formation reactions occurring with participation of salt cations amplifies. The humic acids and especially fulvic acids, occurring in soil solutions, essentially raise the

solubility of metals and assist their moving in soils in the form of organic-mineral complexes, reducing thus the buffer action of soils in relation to heavy metal ions.

Authors [6] have proved that the buffer capacity is a special case of the sensitivity analysis, as a more general theoretical approach, which studies the answer of system to various external perturbations (as for example, the variation of the certain component concentration). We believe that it is more correct to consider, as a potential reservoir of buffer heterogeneous systems, the complex chemical heterogeneous equilibria with participation of solid phases [7]. Unfortunately, so far there are a small number of studies dedicated to the systematic investigations and the development of theoretical aspects of the buffer action for two-phase systems [1-9]. Besides, in the majority of these studies only the pH – buffer properties of heterogeneous systems were investigated. The concept of “buffer action” helps to find out which reactions control the composition of natural waters, including soil solutions [10-16]. The parameters of buffer action are integrated functions of all the soil chemical components by virtue of their capacity, by means of chemical reactions and sorption-desorption processes, to extinguish or strengthen the effect of entered pollutants [17].

Currently, extensive information on negative (harmful) transformations of soils, as a result of progressing acid and alkaline loads (in the form of mineral fertilizers, chemicals for protection of plants and industrial emissions dropping out with atmospheric precipitation) has been gathered. Thus, the quantitative assessment of the acid-base buffer action, revealing the degree of influence of the systematic use of fertilizers and technogenic pollution by substances of the acid and alkaline nature is an actual problem of the agrology. Besides, the buffer action of soils contains important information on the processes of soil formation (their orientation and intensity) which is used for the soil diagnostics and classification [17].

The aim of the present paper has been to develop the quantitative aspects of the buffer action of various components of homogeneous and heterogeneous systems and to establish their interrelation.

Theory

As a criterion for quantitative assessment of the intensity of buffer action of the studied multicomponent heterogeneous systems, one can use the value of the buffer capacity β_i^S (the superscript index “S” specifies the presence of solid phases), which can be defined as a partial derivative

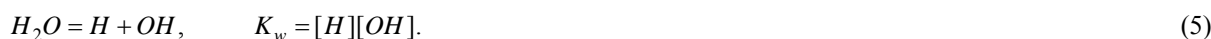
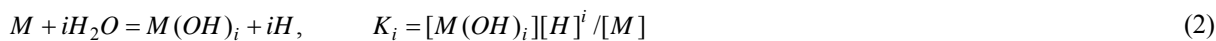
$$\beta_i^S = \left(\frac{\partial C_i^0}{\partial \ln[i]} \right)_{C_j^0 (j \neq i)},$$

where C_i^0 and $[i]$ denote the initial (analytical) concentration in mixture and equilibrium concentration of the component “i” of solid phase, correspondingly, at the same time the subscript index shows that the initial concentrations of other components of the mixture are maintained constant.

We will examine the process of formation of the sparingly soluble salt of arbitrary stoichiometric composition $M_m A_n(S)$ (M – metal ion, A – anion of salt):



The following set of possible simultaneous reactions in the saturated solution is taken into account:



For the sake of simplicity, the charges of species are omitted. Near to the reaction equations the corresponding equilibrium constants are specified. The mass balance (MB) conditions in this system can be formulated by the following equations:

$$C_M^0 = \Delta C_M + C_M^r = \Delta C_M + \sum_{i=1} \sum_{j=0} i[M_i(OH)_j] + \sum_{q=1} \sum_{r=0} [MH_r A_q] \quad (6)$$

$$C_A^0 = \Delta C_A + C_A^r = \Delta C_A + \sum_{l=0} [H_l A] + \sum_{q=1} \sum_{r=0} q[MH_r A_q] \quad (7)$$

$$C_H^0 = [H] - [OH] + \sum_{l=1} l[H_l A] - \sum_{i=1} \sum_{j=1} j[M_i(OH)_j] + \sum_{q=1} \sum_{r=1} r[MH_r A_q] \quad (8)$$

The quantity C_i^r represents the residual concentration in solution of the ion "i", e.g. the total concentration of all the species, containing a given ion, while ΔC_i is its molar quantity in the solid phase in 1 L of solution [5-8, 19, 20]. In the equations (8) C_H^0 denotes the excess of H^+ ions in relation to hydroxyl ions in two-phase mixtures ($C_H^0 = -C_{OH}^0$). The square brackets designate the equilibrium concentrations of species in solution.

From the stoichiometric composition of the solid phase, the following ratio is obtained:

$$\frac{\Delta C_M}{m} = \frac{\Delta C_A}{n} \quad \text{or} \quad \Delta C_A = \frac{n}{m} \Delta C_M \quad (9)$$

On the basis of the written equations it is possible to deduce the formulas for calculating the buffer capacity in relation to any component of the mixture. Firstly, the analysis of the deduction of the expression for the buffer capacity towards the metal ion (or the metal ion buffer capacity) will be examined. Taking the logarithm and differentiating the expression for the solubility product (1) on $\ln[M]$, one can find:

$$\left(\frac{\partial \ln K_S}{\partial \ln[M]} \right)_{C_H^0, C_A^0} = 0 = m + n \frac{\partial \ln[A]}{\partial \ln[M]}, \quad \text{and} \quad \frac{\partial \ln[A]}{\partial \ln[M]} = -\frac{m}{n}. \quad (10)$$

The subscript indices symbolize the conditions $C_H^0 = const, C_A^0 = const$, which are further omitted. Differentiating the MB equation (6) on $\ln[M]$, one can obtain the partial derivative:

$$\begin{aligned} \left(\frac{\partial C_M^0}{\partial \ln[M]} \right)_{C_H^0, C_A^0} &\equiv \beta_M^S = \frac{\partial \Delta C_M}{\partial \ln[M]} + \sum_{i=1} \sum_{j=0} i^2 [M_i(OH)_j] + \sum_{q=1} \sum_{r=0} [MH_r A_q] + \\ &+ \frac{\partial \ln[H]}{\partial \ln[M]} \left(- \sum_{i=1} \sum_{j=1} ij [M_i(OH)_j] + \sum_{q=1} \sum_{r=0} r [MH_r A_q] \right) - \frac{m}{n} \sum_{q=1} \sum_{r=0} q [MH_r A_q] \end{aligned} \quad (11)$$

The deduced equation (11) contains two unknown terms:

$$\beta_M^S = f \left(\frac{\partial \ln[H]}{\partial \ln[M]}, \frac{\partial \Delta C_M}{\partial \ln[M]} \right)$$

For their determination, the MB equations (7) and (8) are differentiated on $\ln[M]$:

$$\begin{aligned} \left(\frac{\partial C_A^0}{\partial \ln[M]} \right)_{C_M^0, C_H^0} &= 0 = \frac{n}{m} \frac{\partial \Delta C_M}{\partial \ln[M]} + \frac{\partial \ln[H]}{\partial \ln[M]} \left(\sum_{l=1} l [H_l A] + \sum_{q=1} \sum_{r=0} r q [MH_r A_q] \right) - \\ &- \frac{m}{n} \sum_{l=0} [H_l A] - \frac{m}{n} \sum_{q=1} \sum_{r=0} q^2 [MH_r A_q] + \sum_{q=1} \sum_{r=0} q [MH_r A_q], \end{aligned}$$

whence

$$\frac{\partial \Delta C_M}{\partial \ln[M]} = -\frac{m}{n} \frac{\partial \ln[H]}{\partial \ln[M]} \left(\sum_{l=1} [H_l A] + \sum_{q=1} \sum_{r=0} r q [MH_r A_q] \right) + \frac{m^2}{n^2} \sum_{l=0} [H_l A] + \frac{m^2}{n^2} \sum_{q=1} \sum_{r=0} q^2 [MH_r A_q] - \frac{m}{n} \sum_{q=1} \sum_{r=0} q [MH_r A_q]. \quad (12)$$

After that,

$$\left(\frac{\partial C_H^0}{\partial \ln[M]} \right)_{C_M^0, C_A^0} = 0 = \frac{\partial \ln[H]}{\partial \ln[M]} \left([H] + [OH] + \sum_{l=1} l^2 [H_l A] + \sum_{i=1} \sum_{j=0} j^2 [M_i(OH)_j] + \sum_{q=1} \sum_{r=1} r^2 [MH_r A_q] \right) - \sum_{i=1} \sum_{j=0} ij [M_i(OH)_j] - \frac{m}{n} \sum_{l=0} [H_l A] + \sum_{q=1} \sum_{r=1} r [MH_r A_q] - \frac{m}{n} \sum_{q=1} \sum_{r=1} r q [MH_r A_q] \quad (13)$$

From the equation (13), it follows:

$$\frac{\partial \ln[H]}{\partial \ln[M]} = \frac{\sum_{i=1} \sum_{j=0} ij [M_i(OH)_j] + \frac{m}{n} \sum_{l=1} [H_l A] - \sum_{q=1} \sum_{r=1} r [MH_r A_q] + \frac{m}{n} \sum_{q=1} \sum_{r=1} r q [MH_r A_q]}{[H] + [OH] + \sum_{l=1} l^2 [H_l A] + \sum_{i=1} \sum_{j=0} j^2 [M_i(OH)_j] + \sum_{q=1} \sum_{r=1} r^2 [MH_r A_q]} \quad (14)$$

Substituting the expression (14) in the equation (13), after some rearrangements, one can obtain:

$$\frac{\partial \Delta C_M}{\partial \ln[M]} = -\frac{m}{n} \left(\frac{\sum_{i=1} \sum_{j=0} ij [M_i(OH)_j] + \frac{m}{n} \sum_{l=1} [H_l A] - \sum_{q=1} \sum_{r=1} r [MH_r A_q] + \frac{m}{n} \sum_{q=1} \sum_{r=1} r q [MH_r A_q]}{[H] + [OH] + \sum_{l=1} l^2 [H_l A] + \sum_{i=1} \sum_{j=0} j^2 [M_i(OH)_j] + \sum_{q=1} \sum_{r=1} r^2 [MH_r A_q]} \right) \times \left(\sum_{l=1} [H_l A] + \sum_{q=1} \sum_{r=0} r q [MH_r A_q] \right) + \frac{m^2}{n^2} \sum_{l=0} [H_l A] + \sum_{q=1} \left(\frac{m^2 q^2}{n^2} - \frac{m q}{n} \right) \sum_{q=1} \sum_{r=0} [MH_r A_q] \quad (15)$$

Further, substituting the obtained expressions for $\partial \ln[H] / \partial \ln[M]$ (14) and $\partial \Delta C_M / \partial \ln[M]$ (15) into the equation (11), after a series of transformation, one can finally get:

$$\beta_M^S = -\frac{\left(\sum_{i=1} \sum_{j=0} ij [M_i(OH)_j] + \frac{m}{n} \sum_{l=1} [H_l A] - \sum_{q=1} \sum_{r=1} r [MH_r A_q] + \frac{m}{n} \sum_{q=1} \sum_{r=1} r q [MH_r A_q] \right)^2}{[H] + [OH] + \sum_{l=1} l^2 [H_l A] + \sum_{i=1} \sum_{j=0} j^2 [M_i(OH)_j] + \sum_{q=1} \sum_{r=1} r^2 [MH_r A_q]} + \frac{m^2}{n^2} \sum_{l=0} [H_l A] + \sum_{q=1} \left(\frac{m^2 q^2}{n^2} - 2 \frac{m q}{n} + 1 \right) \sum_{q=1} \sum_{r=0} [MH_r A_q] + \sum_{i=1} \sum_{j=0} i^2 [M_i(OH)_j]$$

or

$$\beta_M^S = \varphi_3 - \frac{\varphi_1^2}{\varphi_2}, \quad (17)$$

where φ_1, φ_2 and φ_3 denote the following concentration functions:

$$\varphi_1 = \sum_{i=1} \sum_{j=0} ij [M_i(OH)_j] + \frac{m}{n} \sum_{l=1} [H_l A] - \sum_{q=1} \sum_{r=1} r [MH_r A_q] + \frac{m}{n} \sum_{q=1} \sum_{r=1} r q [MH_r A_q]$$

$$\varphi_2 = [H] + [OH] + \sum_{l=1} l^2 [H_l A] + \sum_{i=1} \sum_{j=0} j^2 [M_i(OH)_j] + \sum_{q=1} \sum_{r=1} r^2 [MH_r A_q] \quad (18)$$

$$\varphi_3 = \frac{m^2}{n^2} \sum_{l=0} [H_l A] + \sum_{q=1} \left(\frac{m^2 q^2}{n^2} - 2 \frac{mq}{n} + 1 \right) \sum_{q=1} \sum_{r=0} [MH_r A_q] + \sum_{i=1} \sum_{j=0} i^2 [M_i(OH)_j]$$

Similarly, it is possible to prove that, for the buffer capacity towards proton, the following expression is valid:

$$\left(\frac{\partial C_H^0}{\partial \ln[H]} \right)_{C_M^0, C_A^0} \equiv \beta_H^S = \varphi_2 - \frac{\varphi_1^2}{\varphi_3} \quad (19)$$

For the buffer capacity towards the anion of the solid phase one can deduce:

$$\beta_A^S = \frac{n^2}{m^2} \varphi_3 - \frac{n^2}{m^2} \frac{\varphi_1^2}{\varphi_2} = \frac{n^2}{m^2} \left(\varphi_3 - \frac{\varphi_1^2}{\varphi_2} \right) = \frac{n^2}{m^2} \beta_M^S \quad (20)$$

On the basis of obtained equations (17), (19) and (20) the following remarkable conclusion follows: the buffer capacities towards different components are reciprocally proportional, while the buffer capacities in relation to the ions of the solid phase are interconnected through its stoichiometric coefficients:

$$\frac{\beta_A^S}{n^2} = \frac{\beta_M^S}{m^2} \quad (21)$$

It is worthy to mention that the obtained relations are only valid in the presence of the mineral (solid phase) $M_m A_n(S)$. The thermodynamic stability area of the latter is determined by the value of the Gibbs energy of the overall process (1)-(5) [5, 21-23]:

$$\Delta G_{S,tot} = -mRT \ln \frac{C_M^r}{C_M^0} - nRT \ln \frac{C_A^r}{C_A^0} \quad (22)$$

The solid-phase is stable if $\Delta G_{S,tot} > 0$. The condition $\Delta G_{S,tot} = 0$ corresponds to the beginning of its dissolution and (or) sedimentation.

The analysis of the derived equations shows that the buffer capacities β_i^S grow with the increase of the precipitate solubility, e.g. by rising the residual concentration of the component of minerals.

Conclusions

On the basis of the method of residual concentrations, the original mathematical expressions for the quantitative estimation of buffer capacities towards both components of the mineral phase were deduced.

The quantitative bases of the theory of buffer action for heterogeneous systems are stated. It is established, that buffer properties in relation to components of the solid phase amplify with the increase of the solubility. The buffer capacity of any component is a complex function of the equilibrium composition of multicomponent heterogeneous systems.

It is proved that the buffer capacities of components are mutually proportional and for heterogeneous systems these relations depend on the stoichiometric composition of the solid phases (minerals).

The use of results of this research allows predicting the variations of the composition and response of the soil environment at the technogenic loads increasing.

Acknowledgments

This work was supported by the Joint Operational Programme "Black Sea Basin 2007-2013".

References

- [1] Perrin, D.D.; Dempsey, B. Buffers for pH and metal ion control; Chapman and Hall: London, 1974; 175p.
- [2] Komari, N.P. Chemical metrology. Ionic heterogeneous equilibria; Vishcha Shkola: Kharkov, 1984; 208p. (Rus.)

- [3] Charykov, A.K.; Osipov, N.N. Carbonic acids and carboxylate complexes in chemical analysis; Khimia: Leningrad, 1991; pp. 204–207. (Rus.)
- [4] Pfendt, L.B. *Analyst*. 1995, 120, pp. 2129 - 2144.
- [5] Povar, I.; Rusu, V. *Can. J. Chem.* 2012, 90, pp. 395 - 402.
- [6] Fishtik, I.; Povar, I. *Can. J. Chem.* 2006, 84, pp. 1036 - 1044.
- [7] Povar, I. *Russ. J. Inorg. Chem.* 2000, 45, pp. 1632 – 1636, (Engl. Transl.).
- [8] Povar, I. *Russ. J. Inorg. Chem.* 1997, 42, pp. 607-612, (Engl. Transl.).
- [9] Povar, I.; Luca, C. *Rev. Chim.* 2003, 54, pp. 312-316, (Rom.).
- [10] Van Breemen, N.; Wielemaker, W.G. *Soil Sci. Soc. Amer. J.* 1974, 38, pp. 55-60.
- [11] Stumm, W.; Morgan, J.J. *Aquatic Chemistry*; Wiley; New York, 1981; 113 p.
- [12] Filep, D.; Radly, M. *Pochvovedenie*. 1989, 12, pp. 48 – 59, (Rus.).
- [13] Lozovik, P.A.; Potapova, I. Yu.; Bantsevich, T.V. *Geochem. Int.* 2007, 45, pp. 938 – 944, (Engl. Transl.).
- [14] Langmuir, D. *Aqueous Environmental Geochemistry*; New Jersey: Prentice Hall, 1997; 600 p.
- [15] Poznyak, S.P.; Gamkalo, M.Z. *Pochvovedenie*. 2001, 6, pp. 660 – 669, (Rus.).
- [16] Sokolova, T.A.; Motuzova, G.V.; Malinina, M.S.; Obukhovskaya T.D. *Chemical basis of soil buffer action*; MGU: M., 1991; 106 p., (Rus.).
- [17] Zaytseva, T.F. *Izv. SO AN SSSR. Ser. biol. Nauk.* 1987, 14, pp. 69-80, (Rus.).
- [18] Povar, I. *J. Anal. Chem.* 1998, 53, pp. 1113 – 1119.
- [19] Beresnev, E.N. *Method of residual concentrations*; Nauka: Moscow, 1992; 110 p., (Rus.).
- [20] Fishtik, I.; Povar, I. *Russ. J. Gen. Chem.* 1987, 57, pp. 25 – 30, (Engl. Transl.).
- [21] Povar, I. *Ukr. Khim. Zh.* 1994, 60, pp. 371 – 378, (Rus.).
- [22] Povar, I.; Rusu, V. *Can. J. Chem.* 2012, 90, pp. 326 - 332.

THE INFLUENCE OF APPLIED STABILIZATION METHOD ON THE CRYSTALLINE STABILITY OF YOUNG WHITE WINES

Ecaterina Covaci^{a*}, Gheorghe Duca^b, Rodica Sturza^c

^a Institute of Chemistry, Academy of Sciences of Moldova, 3, Academiei str., Chisinau, MD-2028, Republic of Moldova

^b Academy of Sciences of Moldova, 1, Stefan cel Mare Blvd., Chisinau, MD-2001, Republic of Moldova

^c Technical University of Moldova, 168, Stefan cel Mare Blvd., Chisinau, MD-2004, Republic of Moldova

*e-mail: covaci_ecaterina@yahoo.com

Abstract. Crystalline precipitate which occurs due to the presence of tartaric salts is frequently encountered in young wines in form of white-dirty lamellar crystals at the bottom of tank. The aim of the study was to prevent the tartaric crystal growth in young wine blend *Bianca/Sauvignon* by implementing various schemes and procedures. The recommendations of optimum regime, based on experimental results, include: the use of enzyme preparations, hot suspension of oversaturated bentonite in potassium hydrogen tartrate (KHT), cooled wine, maintained until stabilization and filtration.

Key words: young white wine, crystalline stabilization, suspension of bentonite, conductivity.

Introduction

One of the basic parameters of the quality of wines is the crystalline stability which is determined by the physical-chemical equilibrium state of tartaric acid salts present in wine. Tartaric acid, also known as dihydroxysuccinic acid can be found in wine in two forms: free and bounded [1]. The ionic species of tartaric salts which exist at physical-chemical equilibrium are unstable and more likely they will react with other compounds present in wine, such as: colored compounds, proteins, polymers, pectins, glucans, polysaccharides, etc. This interaction causes the formation of crystalline precipitate [2,3].

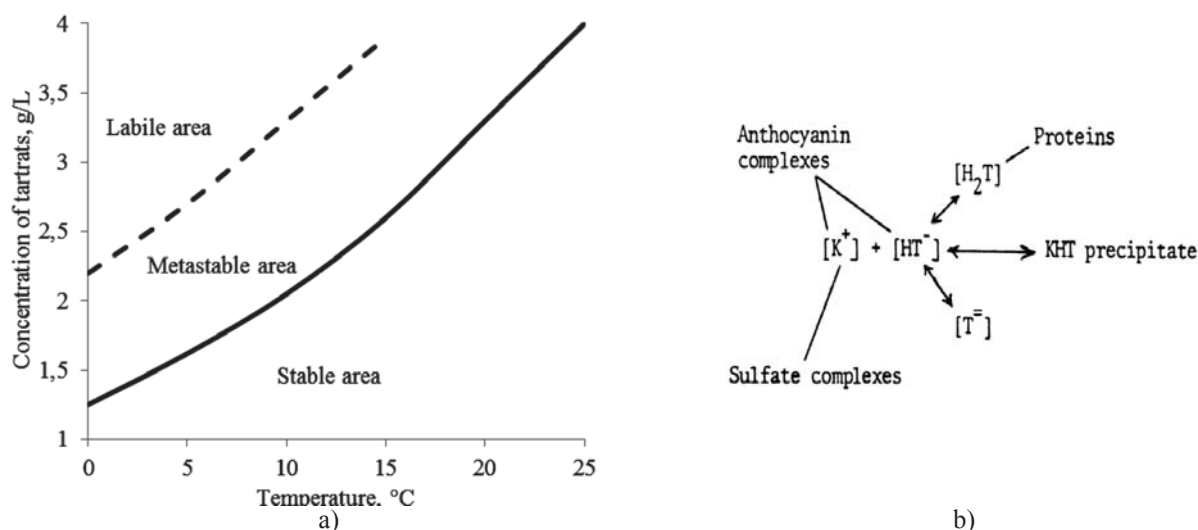


Figure 1. Overview of the process: a) changes in the steady state of tartrate as a function of temperature [2]; b) possible interactions of wine tartaric acid forms with the components of wine [4].

The interaction of tartaric species with other compounds present in wine explains the process of tartrate crystals growth, the natural precipitation and its slow stabilization.

After alcoholic fermentation, the content of tartaric salts in wine is higher than 3 g/L, as a result wine becomes an oversaturated solution of tartaric salts, which at the keeping/treating temperature are susceptible to spontaneous crystallization (instability area, Figure 1) [1,5]. During the storage of wine the content of tartaric salt diminishes slowly. The intensity of tartrate crystals precipitation and crystals size are dependent on temperature, composition (alcohol, tartaric acid, pH, potassium, calcium, etc.), the presence of nucleation and inhibition centers and the volume of storage vessels [6].

Changes of physical-chemical steady states of tartaric salts are mostly generated by temperature changes; this induces the system into a certain degree of stability or instability. The stability of young wines may be improved by implementing the cold treatment step in the winemaking process [6,7]. The process consists in reduction of the solubility of tartaric salts of wine until the formation of the oversaturated solution that initiates and/or grows tartaric crystals which

are then removed without subsequent re-solubilization (filtration at the same temperature). The difficulty of this method consists in performing of two consecutive processes: creation of micro crystals (initiation) and their subsequent growth. The creation stage (initiation) of micro crystals is slow by the formation of a new phase (solid) in the oversaturated solution which is followed by their growth, achieved by creating and maintaining the necessary conditions for their growth [7,8].

Various methods for stabilizing of young wines are discussed in the literature [6-8]. These methods include the traditional stabilization by cooling or adding of potassium salts, bentonite suspension and ethanol, followed by cooling treatment at different regimes, homogenized and stored in the cold until the stabilization.

Experimental

Samples of white wine which was stabilized through various treatment schemes, stabilization materials and thermal regimes were subjected to our study. Physical-chemical and chromatic parameters of wine samples were determined using experimental procedures described elsewhere [9,10].

The experimental wine samples no. 2, 3 and 4 were subjected to an enzymatic treatment using *Enzym'Vander* (Bordeaux, France) at a dose of 0.5 g/L, for a period of 24 hours. During all the testing period the samples were maintained at temperature of - 5°C. To prevent the re-solubilization of deposited crystals, after stabilization step, samples were filtered at the temperature of treatment.

The hot suspension of oversaturated bentonite in potassium hydrogen tartrate (THK) was prepared as follows: in the 10% *Solub* bentonite solution 75 g/L potassium hydrogen tartrate was used. This suspension was heated and maintained at the temperature of 85-95°C until the introduction of it in the cooled wine. The used hot suspension of bentonite doses in THK in the preventive cooled wine to -5 °C were 1.5 and 1.75 g/L. The crystalline stability of wines has been evaluated by methods described in the literature [6,10]. The conditions of technological procedures applied for wine stabilization are presented in Table 1.

Table 1.

Technological procedures applied for wine stabilization.

No. sample	Wine stabilization schemes
Control sample	Wine treated by the traditional method with bentonite, 2.5 g/L, filtered, cooled and kept cool throughout the stabilization.
1	Wine treated with the oversaturated hot bentonite suspension in KHT at a dose of 2 g/L and kept cold throughout the stabilization.
2	Wine treated with pectolytic enzyme product, bentonite at a dose of 1.75 g/L and kept cool throughout the stabilization.
3	Wine treated with the pectolytic enzyme product, then oversaturated hot bentonite suspension in KHT at a dose of 1.5 g/L in cooled wine and kept cool throughout the stabilization.
4	Wine treated with the pectolytic enzyme product, then oversaturated hot bentonite suspension in KHT at a dose of 1.75 g/L in cooled wine and kept cool throughout the stabilization.

The treated wine samples were tested via three tests of crystalline stability control – Mini Contact, the saturation temperature and alcohol content. The monitored parameter of the samples was conductive capacity of wine which is mainly determined by the excess of potassium hydrogen tartrate (KHT) [8]. The values of these parameters decrease with the increase of the tartaric crystal and they were determined by conductometer ECITDS - Hanna (characteristics are presented in Table 2).

The Mini Contact test consists in determination of the conductivity of wine samples, this is followed by cooling till +5°C and administration of THK; pretreated samples are kept at this temperature for 2 hours with a periodic mixing. Then the final conductivity is measured without agitation or preventive wine heating. According to the requirements of stability for stable wines the difference between the determined conductivities shall not exceed 50 µS/cm; otherwise, the wine is prone to the tartaric precipitation. Under the determination of the conductivity of wine at temperatures higher than of 18°C the saturation temperature is calculated using following mathematical expression:

$$T_{sat} = T - \frac{LF_2 - LF_1}{33}, \text{ } ^\circ\text{C}$$

where: T - temperature of the sample, °C


LF₂ – conductivity after the usage of 5g of KHT and the homogenization, µS/cm;

LF₁ – initial conductivity of the sample, µS/cm.

According to the requirements of stability of young white wines, the value of the saturation temperature should not exceed $10 \div 12^\circ\text{C}$. At higher values (ranging in the interval $12 \div 16^\circ\text{C}$), it is recommended the use of mesotartaric acid or carboxymethyl cellulose acting as inhibitors of the tartaric crystallization process.

Table 2.

Hanna conductometer parameters.

Photo overview	Specific parameters	Parameters value
	CE range	$0 \div 3999 \mu\text{S}/\text{cm} \pm 1 \mu\text{S}/\text{cm}$
	TDS range	$0 \div 2000 \text{ ppm} \pm 1 \text{ ppm}$
	Temperature range	$0 \div 60^\circ\text{C} \pm 0.1^\circ\text{C}$
	CE and TDS accuracy	$\pm 2 \% \text{ F.S.}$
	Temperature accuracy	$\pm 0.5^\circ\text{C}$
	Adjustable TDS conversion factor	$0.45 \div 1.00$
	Automatic temperature compensation	$0.0 \div 2.4 \% / ^\circ\text{C}$
	Working conditions	
	temperature range	$0 \text{ to } 50^\circ\text{C}$
	UR max	100 %
CAE	Battery type 4x1.5 V, system BEPS	
The size and the weight	$163 \times 40 \times 26 \text{ mm}$, 100 g	

Results and discussion

The physical-chemical assessment results and those of crystalline stability are dependent on applied stability process. Values obtained at the initial stage are presented in Table 3, and their evolution in dynamics was monitored. During treatment procedures, significant changes of wine parameters were registered for: sulfur dioxide (SO_2), titratable acidity, chromatic parameters, saturation temperature, content of mineral compounds (potassium, calcium, tartaric acid, etc.) and organoleptic parameters. The value of the content of sulfur dioxide was reduced by $20 \div 45\%$, the titratable acidity increased by 0.35 units of control samples and the others increased insignificantly. We have registered changes for the chromatic parameter which represents the color intensity (absorbance registered at 420nm). It has decreased to the interval $4 \div 15\%$ in dynamics being induced by the decrease of protein content in wine samples (see Figure 2).

Values of concentration and solubility product of the original wine were calculated using the established parameters: ionic strength, activity coefficient, exponents of acidity, etc (see Table 3). The value of concentration product of KHT ($P_c = 152 \cdot 10^{-6}$) was seven times higher than the solubility product of wine ($S_p = 21.8 \cdot 10^{-6}$).

Table 3.

Physical-chemical and organoleptic parameters of young wine blend „Bianca/Sauvignon”.

No. crt.	Parameters	Values
1	VAT, % vol	13.0 ± 0.1
2	Residual sugar, g/L	3.33 ± 0.11
3	Saturation temperature of $T_{\text{sat.KTH}^2}^\circ\text{C}$	17 ± 0.001
4	Saturation temperature of $T_{\text{sat.CaT}^2}^\circ\text{C}$	8 ± 0.001
5	Titratable acidity, g/L	5.82 ± 0.04
6	Volatile acidity, g/L	0.73 ± 0.04
7	pH	3.53 ± 0.01
8	Content of Iron, mg/L	0.390 ± 0.016
9	Content of sulfur dioxide (free/total), mg/L	$70/90.8 \pm 1$
10	Content of potassium, g/L	0.520 ± 0.01
11	Content of tartaric acid, g/L	2.711 ± 0.001
12	Contents of excess potassium hydrogen tartrate, mol/L	0.0062 ± 0.001
13	Type of shown instability	Crystalline and colloidal instability
14	Organoleptic characteristics	Opal wine, yellow with greenish shades. Fine flavor, clean, but dark. Stodgy taste, disharmonious and a slight acidity.

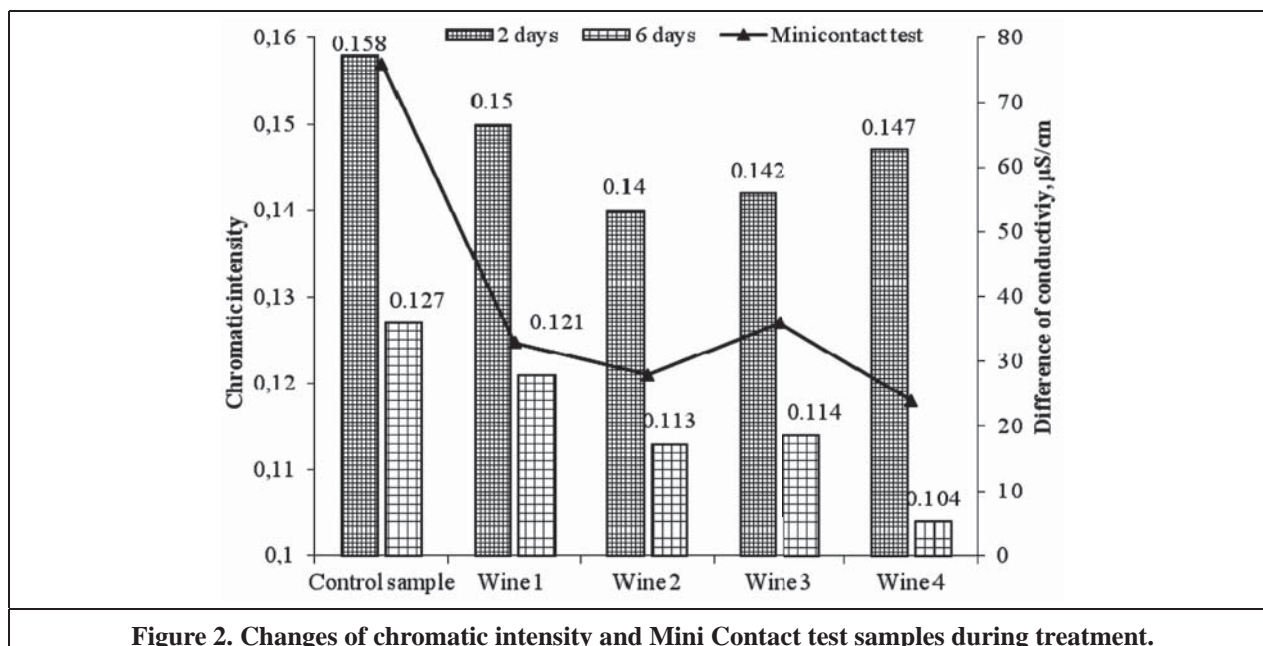


Figure 2. Changes of chromatic intensity and Mini Contact test samples during treatment.

During the treatment conditions (temperature -5°C , concentrations of tartaric acid 0.018 mol/L and of potassium 0.013 mol/L), young wine is presented to be oversaturated in potassium hydrogen tartrate. The excess quantity of potassium hydrogen tartrate is 0.0062 mol/L which causes tartaric precipitation in a short time.

The crystalline stabilization process of wine is difficult and lengthy and its effectiveness is influenced by many factors, both compositional ones as well as related to the physical-chemical properties of the wine and thermodynamic regimes applied to cooling and keeping. The effectiveness of the stabilization of samples was studied in dynamics by determination of the electro-conductivity and calculation of the saturation temperature. This parameter describes the long-term stability wine and the probability of crystalline disorders triggering in the long run. The values of these parameters decrease as tartaric crystals increase and the saturation temperature calculation was performed by the expression described in the previous section.

The maximum period of control sample has reached 10 days and a saturation temperature of 11°C , which was determined by the nucleation of slow and lasting crystallization. The experimental samples no. 3 and 4 have described a stabilization period of 4 and 6 days, illustrated in Figure 3. The stabilized wine samples were tested by the three tests of crystalline stability control and presented as stable in the calculations.

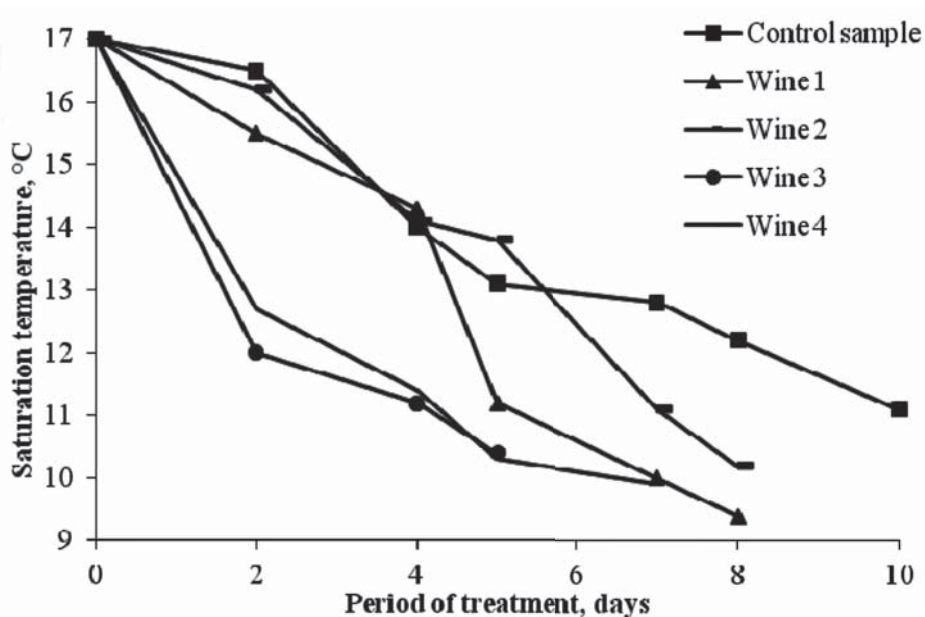


Figure 3. The dynamics of the saturation temperature.

Stabilization of wine samples has conducted to an improvement of their organoleptic characteristics, spreading the flavor, the persistence of flavor and color for this type of wine. Samples no. 3 and 4 were appreciated by the tasters with a maximum score. These changes were induced as a result of the enzymatic treatment combined with bentonite hot oversaturated suspension in KHT.

Conclusions

As a result of our study it has been established that the use of the bentonite hot oversaturated suspension in potassium hydrogen tartarate provides the best conditions for initiation and growth of tartaric crystals. The wine stability testing by determining the saturation temperature and the Mini Contact test are the important information parameters that characterize its nativity.

Summing, we recommend an optimum regime of crystalline stabilization of young white wines which includes steps such as: the use of enzymatic treatment, hot suspension of oversaturated bentonite in potassium hydrogen tartarate at a concentration of $1.5 \div 1.75$ g/L in cooled wine to -5°C , maintenance at this temperature until stabilization and filtration.

References

- [1] Cotea, V.D.; Zanoaga, C.; Cotea, V.V. *Tratat de oenochimie*. Vol. II, Bucuresti: Ed. Academiei Romane, 2009, 750 p.
- [2] Vallee, D.; Bagard, A.; Bloy, C. and Bourde, L. *Appreciation de la stabilite tartrique des vins par la temperature de saturation - Influence du facteur temps sur la stabilite (duree de stockage)*. *Rev. Fr. Oenol.*, 1990, 126, pp. 51-61.
- [3] Usseglio-Tomasset, L.; Ubigli, M. et Barbero, L. *L'etat de sursaturation des vins en tartrate acide de potassium*. *Bulletin O.I.V.*, 1992, Nr. 739, pp. 703-719.
- [4] Zoeklein, B. *A review of potassium bitartrate stabilization of wines*. Virginia Cooperative Service, 1988, Nr. 463-013, pp. 1-14.
- [5] Enache, G.; Tofan, I. *The influence of low temperature on stabilization process of wine*. *Journal of Agroalimentary Processes and Technologies*, 2007, Vol. 13, No.2, pp.319-324.
- [6] Taran, N.; Zinchenko, V. *Sovremennye tehnologii stabilizacii vin*. Chisinau: NAM, 2006, 240 p.
- [7] Prida, I.; Prida, A.; Ialovaia, A. *Procedeu de tratare a vinurilor materie prima cu frig*. B.I. MD 2010 0001, Nr. 4057 din 31.07.2010.
- [8] Prida, I.; Prida, A.; Ialovaia, A. s.a. *Procedeu de stabilizare a vinului fata de tulburarile cristaline*. B.I. MD 2012 015, Nr. 637 din 31.05.2013.
- [9] Gerzhikovej, V. *Metody tehnomiceskogo kontrolja v vinodelii*. Simferopol': Tavrida, 2009, 304 p.
- [10] *Reguli generale privind fabricarea vinurilor de struguri naturale*, RG MD 67-40582515-05:2010.

NICKEL(II) COMPLEX DERIVED FROM 2-HYDROXY-3-METHOXYBENZALDEHYDE SEMICARBAZONE AND 2,2'-BIPYRIDINE

Carolina Vomisescu^{a,b}, Paulina Bourosh^c, Victor Kravtsov^c, Diana Dragancea^{a*}

^aInstitute of Chemistry, Academy of Sciences of Moldova, 3, Academiei str., Chisinau MD-2028, Republic of Moldova

^bUniversity of Academy of Sciences of Moldova, 3/2, Academiei str., Chisinau MD-2028, Republic of Moldova

^cInstitute of Applied Physics, Academy of Sciences of Moldova, 5, Academiei str, Chisinau MD-2028, Republic of Moldova

*e-mail : ddragancea@gmail.com; phone : +(373 22) 73 96 61

Abstract. Reaction of 2-hydroxy-3-methoxybenzaldehyde semicarbazone with $\text{Ni}(\text{NO}_3)_2 \cdot 6\text{H}_2\text{O}$, in the presence of 2,2'-bipyridine, afforded a dinuclear complex (1). Crystal structure of **1** revealed the dinuclear complex, in which one nickel center is surrounded octahedrally by two monoanionic O,N,O-donor semicarbazone. The second nickel center also adopts an octahedral geometry created by two 2,2'-bipyridine ligands and the bridging phenolate oxygen of the monodeprotonated semicarbazones.

Keywords: semicarbazone, binuclear nickel(II) complex, crystal structure.

Introduction

Chemistry and pharmacological applications of semicarbazones have been extensively investigated due to their wide range of biological activities, such as antitumoral, antibacterial, antiviral and antimalarial effects [1,2]. By coordination to a metal ion, the biological properties of semicarbazones are often modified: lipophilicity, increasing of activity, decreasing of side effects, reduction of drug-resistance. Tridentate ONO Schiff base, obtained by condensation of salicylaldehyde with semicarbazide has been used for the synthesis of a large variety of synthesis of mononuclear complexes and multinuclear clusters of transition metals, such as Cu(II) [3-7], Cr(III) [8], Co(III) [9], as well as dioxovanadium(V) [10] complexes. A dinuclear zinc(II) complex with salicylaldehyde semicarbazone was prepared and structurally characterized, where the deprotonated phenol group of the ligand forms a bridge between the two zinc centers [11]. Additional coordinating groups attached to salicylaldehyde would increase both the denticity of the resulted Schiff bases, and as result the ability to generate polynuclear complexes. 2-Hydroxy-3-methoxybenzaldehyde was largely employed as carbonyl precursor for the synthesis of multimetallic assemblies due to ability of methoxy group to display a variety of bonding geometries, such as chelating, monodentate/bidentate bridging, and chelating bridging [12-14]. The Schiff base ligand, 2-hydroxy-3-methoxybenzaldehyde semicarbazone (H_2L , Figure 1) has been used to synthesize monomeric vanadium(V) and dimeric palladium complexes [15-16]. The structure of H_2L has been reported in [17].

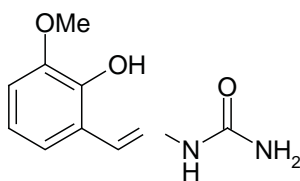


Figure 1. Structural formula of 2-hydroxy-3-methoxybenzaldehyde semicarbazone, H_2L

This variable mode of binding of 2-hydroxy-3-methoxybenzaldehyde semicarbazone has encouraged us to explore its coordination ability. We have chosen nickel as metal center due to its ability to take up different coordination environments (such as octahedral, square-planar and tetrahedral), which makes its coordination chemistry very interesting. To satisfy the remaining coordination sites on the metal center we selected 2,2'-bipyridine as additional ligand. Herein we report the synthesis and X-Ray structure characterization of a dinuclear nickel(II) complex $[\text{Ni}_2(\text{HL})_2(\text{bpy})_2](\text{NO}_3)_2$ (**1**), where H_2L - 2-hydroxy-3-methoxybenzaldehyde semicarbazone.

Results and discussion

The structure determination shows that compound **1** is a dinickel complex (Figure 2), which resides on two fold axis and thus having C_2 molecular symmetry. One Ni(II) ion is surrounded by two tridentate ONO monodeprotonated ligands HL, while the coordination sphere of the other involves two 2,2'-bipyridine ligands and two phenoxy oxygen

atoms of the HL^- . These two deprotonated oxygen atoms of two HL^- bridge the metal ions. The Ni...Ni distance and Ni-O-Ni angle are 3.163(1) Å and 99.71(9)°, respectively. These parameters corresponds to the 3.199 Å and 101.6(1) values observed in the similar dinickel complex $[\text{Ni}_2(\text{HL}')_2(2,2'\text{-bpy})_2](\text{ClO}_4)_2$ (**2**), $\text{H}_2\text{L}' = 2\text{-}[(1\text{E})\text{-N-(2-aminopropyl)ethanimidoyl}]\text{phenol}$ [18]. But in contrary to complex **2**, where the central Ni-O₂-Ni core is symmetric, with identical Ni-O bond lengths 2.063(2) Å, in **1** Ni(1)-O(1) and Ni(2)-O(1) distances differ and are 2.032(2) and 2.105(2) Å, respectively. Both Ni atoms are hexacoordinated and have distorted octahedral surrounding but differ by the set of donor atoms: O₄N₂ for Ni(1) and O₂N₄ for Ni(2) (Table 1). Comparison of conformation of neutral H₂L molecule [17] with coordinated HL^- one reveals the transformation from *trans-trans* to *cis-cis* in mutual arrangement of ONO donor atoms.

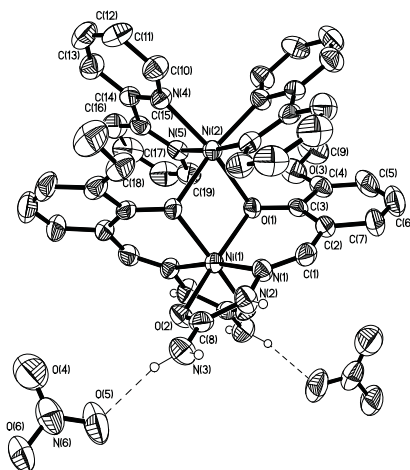


Figure 2. The molecular structure of $[(\text{Ni}_2(\text{HL})_2(\text{bpy})_2)](\text{NO}_3)_2$.

Table 1.

Bond lengths (Å) and angles (deg) in coordination polyhedra of nickel atoms.

Atom-atom	d, Å	Atom-atom-atom	ω , °
Ni(1)-O(1)	2.032(2)	O(1)-Ni(1)-N(1)	87.14(10)
Ni(1)-N(1)	2.015(3)	O(1)-Ni(1)-O(2)	162.94(9)
Ni(1)-O(2)	2.090(2)	O(1)-Ni(1)-O(1)*	82.0(1)
Ni(2)-O(1)	2.105(2)	O(1)-Ni(1)-N(1) *	100.69(10)
Ni(2)-N(4)	2.080(3)	O(1)-Ni(1)-O(2)*	92.87(9)
Ni(2)-N(5)	2.068(3)	N(1)-Ni(1)-O(2)	77.79(10)
Ni(1)-Ni(2)	3.163(1)	N(1)-Ni(1)-N(1)*	169.7(2)
		N(1)-Ni(1)-O(2)*	95.26(10)
		O(2)-Ni(1)-O(2)*	96.4(1)
		O(1)-Ni(2)-O(1)*	78.57(11)
		O(1)-Ni(2)-N(4)	168.32(9)
		O(1)-Ni(2)-N(4)*	95.53(9)
		O(1)-Ni(2)-N(5)	91.69(10)
		O(1)-Ni(2)-N(5)*	92.94(9)
		N(4)-Ni(2)-N(4)*	92.0(2)
		N(4)-Ni(2)-N(5)	78.5(1)
		N(4)-Ni(2)-N(5) *	97.3(1)
		N(5)-Ni(2)-N(5)*	174.0(2)

Symmetry transformations used to generate equivalent atoms: * $-x, y, -z+3/2$

The crystal packing of compound **1** is shown in Figure 3. The dinickel complex cations in the crystal are connected with NO_3^- anions by $\text{N-H}\cdots\text{O}$ hydrogen bonds (Table 2), in undulated layers parallel to (*ac*) crystallographic plane.

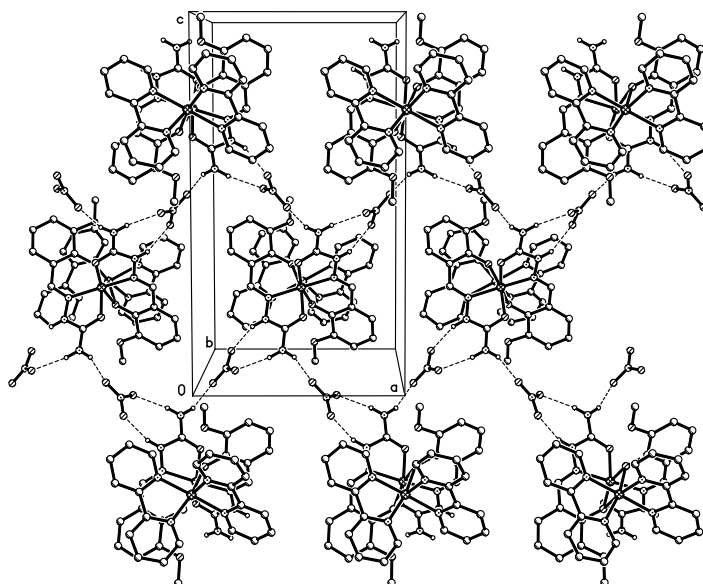


Figure 3. The crystal structure of $[(\text{Ni}_2(\text{HL})_2(\text{bpy})_2)](\text{NO}_3)_2$: undulated layers parallel to (*ac*) crystallographic plane.

Table 2.

Hydrogen bond distances for **1** (Å and deg.).

D-H \cdots A	D-H	H \cdots A	D \cdots A	< DHA	Symmetry transformations for A
N(2)–H(1) \cdots O(6)	0.86	2.04	2.816(4)	150	$x+1/2, -y+5/2, -z+1$
N(3)–H(1) \cdots O(5)	0.86	2.10	2.919(4)	158	x, y, z
N(3)–H(2) \cdots O(4)	0.86	2.11	2.966(4)	171	$x+1/2, -y+5/2, -z+1$

In concordance with the mentioned tridentate coordination mode the bands of interest which change frequency on coordination are the following: the absence of the characteristic $\nu(\text{OH})$ band in the IR spectrum of the complex, which in the ligand spectrum appears at apr. 3466 cm^{-1} , as well as the shift to lower energies (*ca.* 30 cm^{-1}) of the bands $\nu(\text{C}=\text{O})$ which in the spectrum of H_2L appears at 1670 cm^{-1} ; a sharp but weak band at 1582 cm^{-1} , assigned as $\nu(\text{C}=\text{N})$, shifts to 1568 cm^{-1} in nickel complex.

Experimental part

All reagents and solvents were obtained from commercial sources and used without further purification. Elemental analysis was performed on Vario El III elemental analyzer. The IR spectra were obtained in Vaseline on a FT IR Spectrum-100 Perkin Elmer spectrometer.

Synthesis of 2-hydroxy-3-methoxybenzaldehyde semicarbazone (HL). The ligand was prepared by a slight modification of the procedure reported previously [19]. Briefly, to a solution of semicarbazide hydrochloride (1.12 g, 10 mmol) and sodium acetate (1.36 g, 10 mmol) dissolved in a mixture of distilled water (5 mL) and ethanol (15 mL), 2-hydroxy-3-methoxybenzaldehyde (1.12 g, 10 mmol) in ethanol (15 mL) was added. The mixture was stirred at reflux for 1 h, and the resultant precipitate was filtered off, washed with ethanol, diethyl ether and dried in air. Yield: 1.65g (80%). Anal. found for $\text{C}_9\text{H}_{11}\text{N}_3\text{O}_3$ (%):C, 51.83; H, 5.41; N, 20.16. Calculated, %: C, 51.67; H, 5.30; N, 20.10.

Synthesis of $[(\text{Ni}_2(\text{HL})_2(\text{bpy})_2)](\text{NO}_3)_2$ (I). To a solution of $\text{Ni}(\text{NO}_3)_2 \cdot 6\text{H}_2\text{O}$ (0.14 g, 0.5 mmol) in methanol (20 mL) solid 2-hydroxy-3-methoxybenzaldehyde semicarbazone (0.10 g, 0.5 mmol) was added, followed by 2,2'-bipyridine (0.08 g, 0.5 mmol). The suspension was stirred until the ligand dissolved, after which the resulting greenish solution was filtered and allowed to stand overnight. The small, light green rectangular crystals which appeared were filtered off and air-dried. Yield: 0.04g (33%). Anal. found for $\text{C}_{19}\text{H}_{18}\text{NiN}_6\text{O}_6$, %: C 47,18; H 3,78; N 17.43. Calculated: C 47,04; H 3,74; N 17.33.

X-ray Crystallography. Diffraction measurement for **1** was carried out at room temperature on a CCD Xcalibur E diffractometer equipped with a graphite monochromator utilizing MoK α ($\lambda = 0.71073\text{\AA}$) radiation and ω scans. Final unit cell dimensions were obtained and refined on an entire data set. The crystal structure was solved by direct methods. All calculations to solve the structures and to refine the models were carried out with the programs SHELX97 [20]. The C- and N- bound H atoms were placed in calculated positions and were treated using a riding model approximation with Uiso(H)=1.2Ueq(C). Crystal data and details on the structure refinement are given in Table 3. Selected geometric parameters for **1** are given in Table 1. CCDC 975158 contains the supplementary crystallographic data for **1**.

Table 3.

Crystal data and structure refinement for compound (**1**).

Empirical formula	$C_{19}H_{18}N_6NiO_6$
Formula weight	485.10
Crystal system	orthorhombic
Space group	<i>Pbcn</i>
Unit cell dimensions	
<i>a</i> , \AA	11.7026(4)
<i>b</i> , \AA	17.2571(6)
<i>c</i> , \AA	20.5159(8)
<i>V</i> , \AA^3	4143.2(3)
<i>Z</i>	8
$\rho(\text{calc})$, mg/m^3	1.555
μ , mm^{-1}	0.987
<i>F</i> (000)	2000
Crystal size, mm^3	0.12x0.10x0.06
θ range for data collection, deg	2.89 - 25.50
Index ranges	$-14 \leq h \leq 11$, $-13 \leq k \leq 20$, $-24 \leq l \leq 24$
Reflections collected	17003
Independent reflections	3858 (R(int) = 0.0709)
Completeness to $\theta = 25.05^\circ$, %	99.8
Data / parameters	3858 / 290
<i>GOOF</i>	0.999
Final <i>R</i> indices ($I > 2\sigma(I)$)	$R1 = 0.0488$, $wR2 = 0.0758$
<i>R</i> indices (all data)	$R1 = 0.1055$, $wR2 = 0.0873$
Largest diff. peak and hole, $e\text{-\AA}^{-3}$	0.430 / -0.351

References

- [1] Beraldo, H.; Gambino, D. *Mini Rev. Med. Chem.*, 2003, 4, pp. 31-39.
- [2] Padhye, S.; Kauffman, G.B. *Coord. Chem. Rev.*, 1985, pp. 127-160.
- [3] Gerasimenko, A.V.; Davidovich, R.L.; Bulimestru, I.G.; Gulea, A.P. Ng, S.W. *Acta Crystallogr.*, 2005, E 61, 1816 p.
- [4] Chumakov, Yu.M.; Tsapkov, V.I.; Biyushkin, V.N.; Mazus, M.D.; Samus, N.M. *Kristallografiya*, 1996, 41, 873 p.
- [5] Patole, J.; Dutta, S.; Padhye, S.; Sinn, E. *Inorg. Chim. Acta*, 2001, 318, pp. 207-211.
- [6] W.Y. Lee, P.P.F. Lee, Y.K. Yan, M. Lau, *Metalomics*, 2010, 2, pp. 694-705.
- [7] Wang, J.-L.; Liu, B.; Yang, B.-S.; Huang, S.-P. *J. Struct. Chem.*, 2008, 49, pp. 570-574.
- [8] Yue, L.; Zhou, Y.-Zh.; Liu, J.-L.; Tu, S.-J.; Xiao, L.-M. *Chinese J. Struct. Chem.*, 2009, 7, pp. 789-796.
- [9] Bogdanović, G.A.; Leovać, V.M.; Ljiljana S. Vojinović-Ješić, L.S.; Spasojević-De Biré, A. *Serb. Chem. Soc.*, 207, 72 (1), pp. 63-71.
- [10] Noblia, P.; Baran, E.J.; Otero, L.; Draper, P.; Cerecetto, H.; Gonzalez, M.; Piro, O.E.; Castellano, E.E.; Inohara, T.; Adachi, Y.; Sakura, H.; Gambino, D. *Eur. J. Inorg. Chem.*, 2004, pp. 322-328.
- [11] Wang, J.-Lin.; Feng, J.; Xu, M.-P.; Yang, B.-S. *Spectrochimica Acta Part A*, 2011, 78, pp. 1245-1249.
- [12] Lan, Y.; Novitchi, Gh.; Clerac, R.; Tang, J.-K.; Madhu, N. T.; Hewitt, I.J.; Anson, C.E.; Brooker, S.; Powel, A.K. *Dalton Trans.*, 2009, pp. 1721-1727.
- [13] Yu, G.-M.; Zhao, L.; Guo, Y.-N.; Xu, G.-F.; Zou, L.-F.; Tang, J.; Li, Y.-H. *J. Mol. Struct.*, 2010, 982, pp. 139-144.

- [14] Tian, H.; Zhao, L.; Guo, Y.-N.; Guo, Y.; Tang, J.; Liub Z. *Chem. Commun.*, 2012, 48, pp. 708–710.
- [15] Fernández, M.; Becco, L.; Correia, I.; Benítez, J.; Piro, O.E.; Echeverria, G.A.; Medeiros, A.; Comini, M.; Lavaggi M.L.; González, M.; Cerecetto, H.; Moreno, V.; Costa Pessoa, J.; Garat, B.; Gambino, D. *J. Inorg. Biochem.*, 2013, 127, pp. 150-160.
- [16] Chellan, P.; Chibale, K.; Smith, G.S. *J. Chem. Crystallogr.*, 2011, 41, pp. 747–750.
- [17] Shu-Lan, Li; De-Xin, L.; Jian-Hua, Zh.; Fan-Qin M. *Jiegou Huaxue (Chin. J. Struct. Chem.)*, 1995, 14, pp. 88-91.
- [18] Costes, J.-P.; Maurice, R.; Vendier L. *Chem.-Eur. J.*, 2012, 18, pp. 4031-4040.
- [19] Binil, P.S.; Anoop, M.R.; Suma, S.; Sudarsanakumar, M.R. *J. Therm. Anal. Calorim.*, DOI 10.1007/s10973-012-2601-2.
- [20] Sheldrick, G.M. *Acta Cryst.* 2008, A64, pp. 112-122.

HOMOTRINUCLEAR Fe₃^{III} μ – OXO SALICYLATE CLUSTER. SYNTHESIS, STRUCTURE AND PROPERTIES

Viorina Gorinchoy^a, Sergiu Shova^a, Elena Melnic^b, Victor Kravtsov^b, Constantin Turta^{a*}

^aInstitute of Chemistry of the Academy of Sciences of Moldova, 3, Academiei str., Chisinau MD2028, Republic of Moldova

^bInstitute of Applied Physics, Academy of Sciences of Moldova, 5, Academiei str., Chisinau MD2028, Republic of Moldova

*e-mail: turtalca@gmail.com; phone: (+373 22) 73 97 22

Abstract. A reaction of iron and barium nitrate with ammonium salicylate in the mixture of solvents (MeOH, THF, DMAA) gave the new homotrimeric complex [hexa-μ-salicylato-(O,O')-μ₃-oxo(diaqua)(salicylato)triiron(III)] di(dimethylacetamide)(methanol)sesqui(tetrahydrofuran)·2.6-hydrate, [Fe₃O(SalH)₇(H₂O)₂](DMAA)₂(MeOH)(THF)_{1.5}(H₂O)_{2.6} (1). Single-crystal X-ray study has demonstrated that the titled complex {Fe₃O} belongs to the well-known group of μ₃-oxo homotrimeric carboxylates. The IR, Mössbauer spectra, thermal behaviour of the complex were studied.

Keywords: carboxy-cluster, Iron(III), salicylate, IR, Mössbauer, TG data.

Introduction

Nowadays a great scientific interest to the *nd* elements' clusters is demonstrated [1-2]. This interest is due to the architecture (design changes) of their chemical bonds, molecular and self-assembly in the crystal [3], the optical properties [4], the catalyst [5], magnetic and single molecule magnet (SMMs) [6], as well as their use as building blocks in 1D, 2D, 3D, MOFs systems [7], and precursors to obtain nanomaterials [8]. In our Laboratory of Bioinorganic Chemistry and Nanocomposites (LCBANC) the various polydentate ligands were synthesized and studied [9-13]. There are quite extensive known complexes (clusters) obtained with mono- or polycarboxylic acids in the scientific literature. However publications of clusters with salicylic acid as a ligand are scarce. In recent years we have synthesized and studied the homo- and heteronuclear complexes of copper and iron with this acid [14-16]. In continuation of our studies the synthesis and some spectral Infrared (IR), Mössbauer (MS) and thermogravimetric (TG) data of the trimeric iron (III) carboxy-cluster [Fe₃^{III}O(SalH)₇(H₂O)₂](DMAA)₂(CH₃OH)(THF)_{1.5}(H₂O)_{2.6} (1) are presented in this article.

Results and discussion

X-Ray crystallography

Single-crystal X-ray study has demonstrated that compound (1) with composition [Fe₃^{III}O(SalH)₇(H₂O)₂](DMAA)₂(CH₃OH)(THF)_{1.5}(H₂O)_{2.6}, where SalH denotes monodeprotonated salicylic acid, DMAA= dimethylacetamide, THF= tetrahydrofuran is a member of the large family of "basic carboxylates" containing a central planar [M₃(μ₃-O)]⁷⁺ core and the carboxylato ligands, which are situated above and below this plane. Three Fe³⁺ ions occupy the vertexes of isosceles triangle; Fe-Fe distances equal 3.3338(8), 3.2961(7), and 3.3019(6)Å. The structural parameters are typical of "basic carboxylates", Figure 1. Six η¹:η¹:μ₂ SalH ligands bridge the metal atoms. One terminal monodentate SalH ligand and two water molecules in the apical positions complete octahedral coordination of the iron atoms. The distances between the Fe atoms and the donor atoms of the SalH bridging ligands are in the ranges 1.999(2)–2.020(2) Å for Fe1, 1.988(3)–2.036(2) Å for Fe2, and 1.974(3)–2.026(2) Å for Fe3, the shortest Fe-O bonds in the cluster being the Fe–μ₃-O in each case, and the longest being the ones in trans respective positions (trans effect), Table 1.

The conformation of all SalH ligands is stabilized by intramolecular O-H...O hydrogen bonds, Table 2. The hydroxyl groups of the SalH ligands, which bridge Fe1 and Fe3 ions, are pointed in opposite direction, while the two other pairs of these groups stick out in the same direction. The hydroxyl groups of two bridging ligands, which are close to monodentate apical ligand, participate in bifurcated H-bonds with non-coordinated O15 atom. Since the cluster moiety in the structure is neutral no counter anions are present the 3D structure of the complex in the crystal lattice is defined by direct intercluster hydrogen-bonding as well as by H-bonds involving solvent molecules, Table 2, and by π-π stacking interactions.

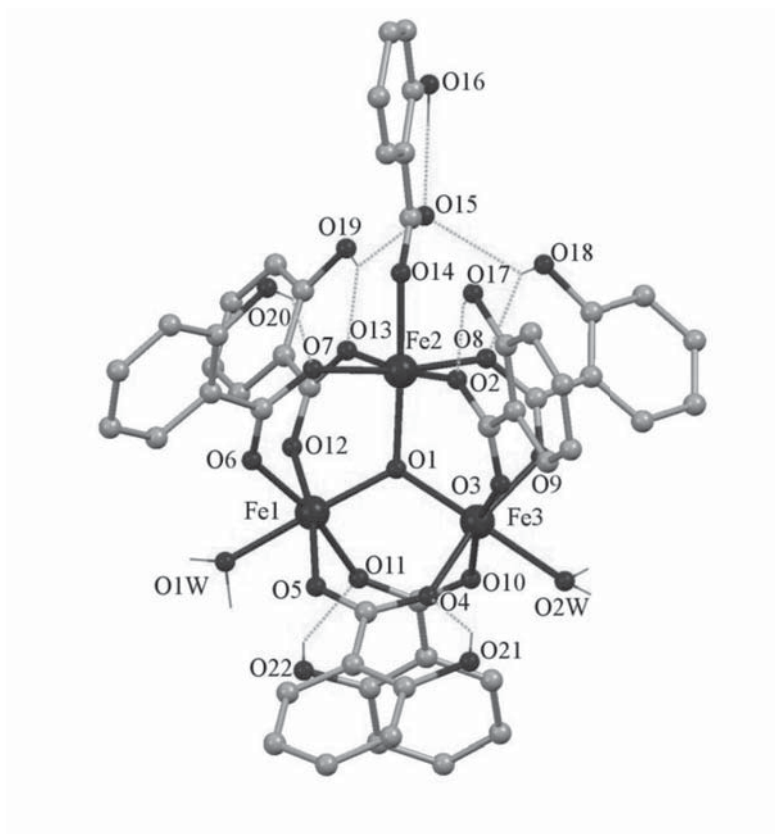


Figure 1. Molecular structure of $[\text{Fe}_3\text{O}(\text{SalH})_7(\text{H}_2\text{O})_2]$ cluster. The hydrogen atoms on carbon atoms are not presented for clarity.

Table 1.

Selected bond lengths and bond angles in coordination sphere of each metal atom.

Bond	d, Å	Bond	d, Å	Bond	d, Å
Fe1-O1	1.906(2)	Fe2-O1	1.926(2)	Fe3-O1	1.902(2)
Fe1-O6	1.999(2)	Fe2-O14	1.988(3)	Fe3-O9	1.974(3)
Fe1-O12	2.003(2)	Fe2-O8	2.021(2)	Fe3-O10	1.996(3)
Fe1-O11	2.015(3)	Fe2-O13	2.031(2)	Fe3-O3	2.009(3)
Fe1-O5	2.020(2)	Fe2-O2	2.036(2)	Fe3-O4	2.026(2)
Fe1-O1w	2.045(3)	Fe2-O7	2.037(2)	Fe3-O2w	2.076(2)
Angle	ω, deg	Angle	ω, deg	Angle	ω, deg
O1-Fe1-O6	96.28(9)	O1-Fe2-O14	170.69(10)	O1-Fe3-O9	95.98(9)
O1-Fe1-O12	93.92(9)	O1-Fe2-O8	95.21(9)	O1-Fe3-O10	97.78(10)
O6-Fe1-O12	91.32(10)	O14-Fe2-O8	91.76(10)	O9-Fe3-O10	91.82(12)
O1-Fe1-O11	93.79(9)	O1-Fe2-O13	94.32(9)	O1-Fe3-O3	96.54(10)
O6-Fe1-O11	169.31(10)	O14-Fe2-O13	92.28(10)	O9-Fe3-O3	91.74(12)
O12-Fe1-O11	91.57(11)	O8-Fe2-O13	86.28(10)	O10-Fe3-O3	164.79(10)
O1-Fe1-O5	96.48(9)	O1-Fe2-O2	92.34(9)	O1-Fe3-O4	94.14(9)
O6-Fe1-O5	87.15(11)	O14-Fe2-O2	81.26(10)	O9-Fe3-O4	169.46(10)
O12-Fe1-O5	169.60(10)	O8-Fe2-O2	91.82(10)	O10-Fe3-O4	89.69(11)
O11-Fe1-O5	88.15(11)	O13-Fe2-O2	173.22(10)	O3-Fe3-O4	84.20(11)
O1-Fe1-O1w	176.38(9)	O1-Fe2-O7	92.64(9)	O1-Fe3-O2w	178.61(9)
O6-Fe1-O1w	87.14(10)	O14-Fe2-O7	80.61(10)	O9-Fe3-O2w	85.38(10)
O12-Fe1-O1w	84.78(10)	O8-Fe2-O7	171.97(10)	O10-Fe3-O2w	82.41(10)
O11-Fe1-O1w	82.88(10)	O13-Fe2-O7	91.49(10)	O3-Fe3-O2w	83.15(10)
O5-Fe1-O1w	84.87(10)	O2-Fe2-O7	89.50(10)	O4-Fe3-O2w	84.48(10)

Table 2.

Hydrogen bond distances (Å) and angles (°).

D-H...A	d(D-H)	d(H...A)	d(D...A)	(DHA)	Symmetry transformation for acceptor
O17-H17...O2	0.84	1.87	2.590(4)	143.4	x, y, z
O19-H19A...O13	0.84	1.96	2.672(4)	142.0	x, y, z
O19-H19A...O15	0.84	2.19	2.736(5)	123.0	x, y, z
O18-H18A...O8	0.84	1.98	2.651(3)	135.7	x, y, z
O18-H18A...O15	0.84	2.30	2.862(4)	124.6	x, y, z
O22-H22...O11	0.84	1.85	2.561(4)	142.2	x, y, z
O22-H22...O1w	0.84	2.64	3.360(4)	145.0	x, y, z
O21-H21A...O4	0.84	1.81	2.546(4)	144.5	x, y, z
O20-H20A...O7	0.84	1.87	2.592(4)	143.9	x, y, z
O16-H16...O15	0.84	1.84	2.570(5)	144.5	x, y, z
O1w-H1w1...O5w1	0.91	2.06	2.647(7)	120.6	$x, y-1, z$
O1w-H2w1...O22	0.92	2.71	3.360(4)	128.8	x, y, z
O2w-H1w2...O3w	0.86	1.81	2.668(5)	175.8	$-x+1, -y+1, -z+2$

Infrared spectra

The studied compound has an IR spectrum with numerous absorption bands (Fig. 2). However there are some bands which are characteristic for specific groups: medium intensity and broad absorption band with maximum at 3238 cm^{-1} was assigned to $\nu(\text{OH})$ of water molecules and salicylate anions, including the ones forming the hydrogen bonds; 3064 and 2976 cm^{-1} – to ν_{as^s} (CH, benzene ring of salicylic ion, SalH^- , Sal^{2-}); 2879 and 2838 cm^{-1} – to ν_{as^s} (CH, methyl groups of DMAA, methanol); 1585 and 1457 cm^{-1} – to $\nu_{\text{as}^s}(\text{COO})$ for bridging bidentate fashion; 1618 cm^{-1} – to $\nu(\text{CO})$ of monodentate SalH^- anion, DMAA, $\delta(\text{H}_2\text{O})$; intensive absorption band at 1389 cm^{-1} – to bending bands, δ , of CH_3 or $\text{CH}_3\text{-CH}_3\text{-C}$ bending. The rest bands in the limits $1400\text{-}650\text{ cm}^{-1}$ may be assigned to fingerprint region of this complex [17-19].

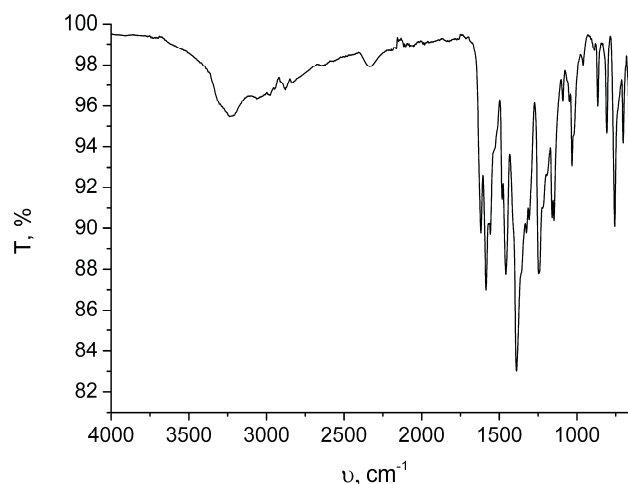


Figure 2. IR spectrum of investigated complex.

Thermogravimetric analysis

The thermo-gravimetric curves of $\{\text{Fe}_3\text{O}\}$ complex are presented in Fig. 3. They demonstrate that the complex (1) is thermo unstable. The thermolysis process is beginning at $25\text{ }^\circ\text{C}$ and involves many steps. The DTG and TG curves suggest the first process at $25\text{-}100\text{ }^\circ\text{C}$ is endothermic and corresponds to weight loss of $\sim 3\%$. It seems to be highly probable that the observed change is attributable to elimination of crystalized water molecules ($2.6\text{H}_2\text{O}$). Subsequent exothermic processes at $100\text{-}280$ (I), $280\text{-}320$ (II), $320\text{-}380$ (III) and $380\text{-}440$ (IV) $^\circ\text{C}$ are due to the elimination of all solvent molecules and destruction of remaining organic ligands (Table 3). The final thermolysis product consists of $\sim 12\%$ of the initial weight and corresponds to the iron oxide, Fe_2O_3 (calculated: 10.36%). Schematically, the decomposition of complex may be presented by the following:

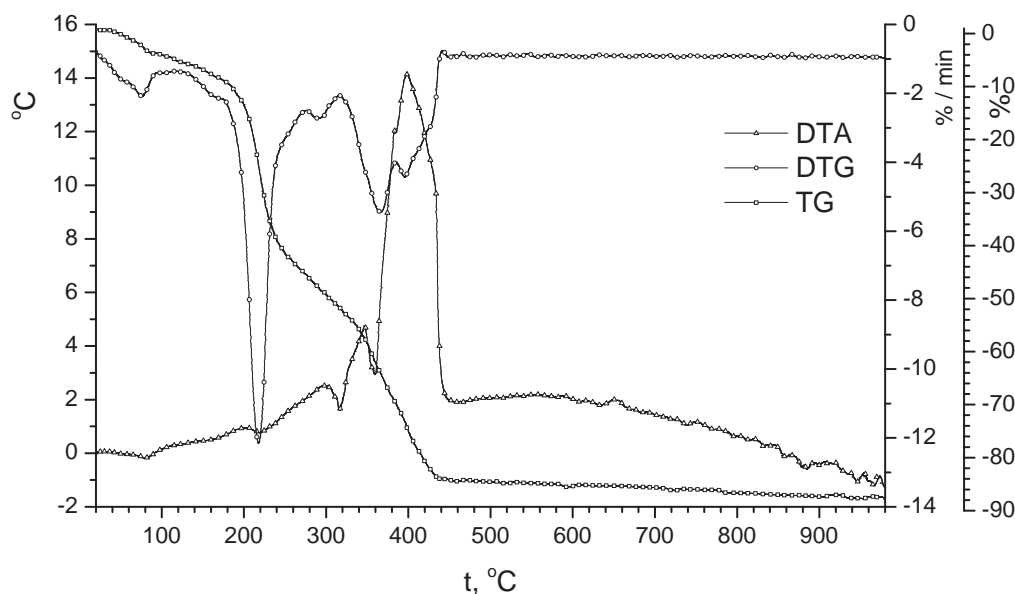
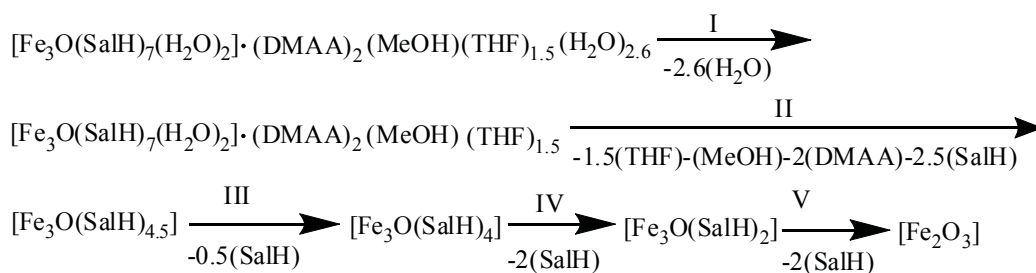


Figure 3. Thermogravimetry curves, TG, DTG, and DTA of investigated complex.

Table 3.

Thermogravimetric data for $[\text{Fe}_3\text{O}(\text{SalH})_7(\text{H}_2\text{O})_2] \cdot (\text{DMAA})_2(\text{MeOH})(\text{THF})_{1.5}(\text{H}_2\text{O})_{2.6}$ complex.

Nr. process	Effect	T, °C			Weight loss. found, %
		onset	maxim	end	
I	endo	25	70	100	3
II	exo	100	220	280	42
III	exo	280	290	320	7
IV	exo	320	360	380	17
V	exo	380	395	440	15

Mössbauer spectra

The Mössbauer spectra of the investigated complex at 300 and 80 K are presented in Fig. 4. It's clear observed that both spectra consist of more than one subspectrum. The best fit was obtained when each spectrum was approximated by 2 doublets. The parameters of subspectrums are presented in Table 4. The values of isomer shift and quadrupol splitting correspond to iron(III) in the high spin state ($S=5/2$) [20].

Taking into consideration the molecular structure of this complex it was expected that the relative area of one

subspectrum will be two times larger than another one. In reality the relative areas of these subspectrums are not so different. Only at RT the relative area of doublet I is ~ 40 % and we may suppose that doublet I corresponds to iron atom which is coordinated with monodentate SalH⁻ anion. But at the 80 K this parameter practically is the same as for doublet II. This fact may be explained if suppose that the Debye-Waller factor, f' , for iron containing Fe-H₂O or Fe-SalH bonds in {Fe₃O} fragment.

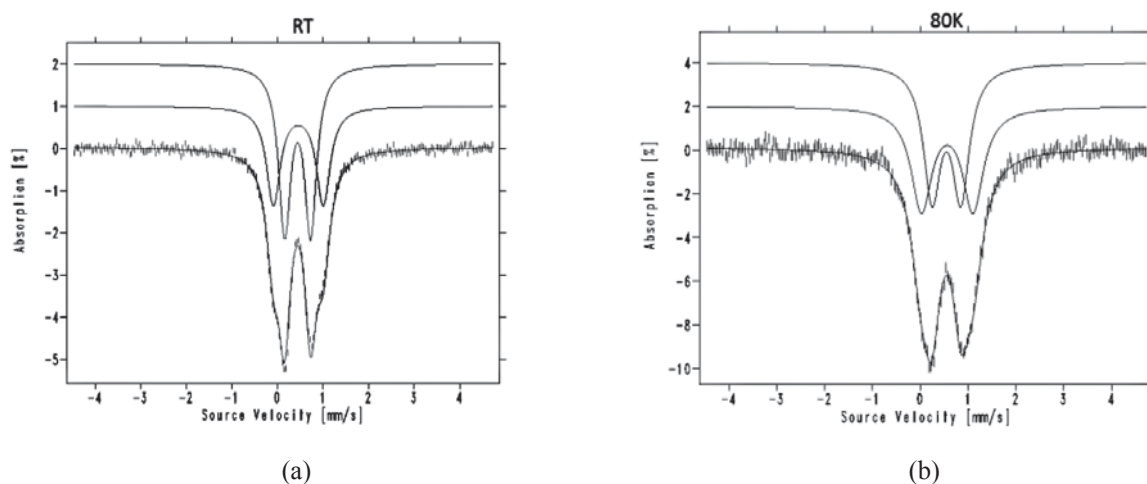


Figure 4. Mossbauer spectra of $[\text{Fe}_3\text{O}(\text{SalH})_7(\text{H}_2\text{O})_2] \cdot (\text{DMAA})_2(\text{MeOH})(\text{THF})_{1.5}(\text{H}_2\text{O})_{2.6}$ at: a-RT and b-80K.

Table 4.

Parameters of the Mössbauer spectra of $[\text{Fe}_3\text{O}(\text{SalH})_7(\text{H}_2\text{O})_2] \cdot (\text{DMAA})_2(\text{MeOH})(\text{THF})_{1.5}(\text{H}_2\text{O})_{2.6}$ cluster.

T, K	mm/s				
	δ_{Fe}	ΔE_Q	$\Gamma_L = \Gamma_R$	S_{rel}	
RT	0.459	1.094	0.363	0.42	Doublet I
	0.444	0.569	0.318	0.62	Doublet II
80	0.545	0.602	0.433	0.56	Doublet II
	0.564	1.078	0.329	0.53	Doublet I

δ_{Fe} - isomer shift relative to alpha-Fe at RT;

ΔE_Q - quadrupole splitting;

Γ_L, Γ_R - the line width;

S_{rel} - relative area of subspectrum;

RT - room temperature.

Experimental

The reaction was performed following the synthesis procedure described by us [16] but using 1.25 g Ba(NO₃)₂ instead of the CoCl₂·6H₂O. The dark red single crystals as rectangular prisms precipitated after 3 days. Yield 0.92 g (49 % relative to the iron salt). The results of elemental analysis, %: Found: C, 49.47; H, 5.53; N, 2.20. Calculated for C₆₄H_{78.2}Fe₃N₂O_{31.1}: C, 49.89; H, 5.11; N, 1.81.

IR spectrum (ν , cm⁻¹): 3238.5 sh, 3063.6 vw, 2976.1 vw, 2878.9 vw, 2878.9 vw, 1618.0 m, 1585.3 s, 1557.7 w, 1481.4 s, 1457.2 s, 1388.6 vs, 1324.8 w, 1307.2 w, 1245.7 s, 1194.4 vw, 1090.8 s, 1048.7 s, 1032.0 s, 960.35 w, 887.86 vw, 865.77 s, 807.23 s, 756.48 vs, 702.40 s, 664.15 s (vs= very strong, s= strong, m= medium, w=weak, vw= very weak and sh=shoulder).

The complex was analyzed for C, H, and N by the elemental analysis group of the Institute of Chemistry of the Academy of Sciences of Moldova.

X-ray diffraction analysis X-Ray data were collected at 200 K temperature on a *Xcalibur E* diffractometer equipped with an EOS CCD area detector and a graphite monochromator utilizing MoK α radiation. Final unit cell dimensions were obtained and refined on an entire dataset. All calculations to solve and refine the structure were carried out with the program SHELX97 [21]. Lorentz and polarization effects and absorption corrections were applied for diffracted reflections. The C-bound H atoms were placed in calculated positions and were treated using a riding model approximation with Uiso(H)=1.2Ueq(C). Crystal data and details on the structure refinement are given in Table 5. CCDC 975526 contains the supplementary crystallographic data.

Table 5.

Crystallographic parameters and the data collection statistics for complex {Fe₃O}.

Parameter	Value
Empirical formula	C ₆₄ H _{78.2} N ₂ O _{31.1} Fe ₃
Formula weight, <i>M</i>	1540.64
Temperature (K)	200
Crystal system	triclinic
Space group	<i>P</i> -1
<i>Z</i>	2
<i>a</i> (Å)	15.3001(8)
<i>b</i> (Å)	15.643(2)
<i>c</i> (Å)	18.0709(9)
α (°)	94.253(7)
β (°)	105.700(5)
γ (°)	117.134(9)
<i>V</i> , (Å ³)	3605.5(6)
<i>D</i> _{calc} (g cm ⁻³)	1.419
μ (mm ⁻¹)	0.683
<i>F</i> (000)	1606
Refinement method	Full-matrix least-squares on <i>F</i> ²
θ Range for data collection(°)	1.56 - 26.00
Limiting indices	-18 $\leq h \leq$ 17
	-19 $\leq k \leq$ 19
	-22 $\leq l \leq$ 22
Reflections collected	29738
Reflections with $I > 2\sigma(I)$	14180
Data/restraints/ parameters	14180 / 9 / 888
Goodness-of-fit on <i>F</i> ²	1.003
<i>R</i> ₁ , <i>wR</i> ₂ [$I > 2\sigma(I)$]	<i>R</i> ₁ = 0.0572, <i>wR</i> ₂ = 0.1682
<i>R</i> ₁ , <i>wR</i> ₂ (all data)	<i>R</i> ₁ = 0.0742, <i>wR</i> ₂ = 0.1809
Largest difference in peak and hole (e Å ⁻³)	1.219 and -0.556

IR spectra were recorded on a Specord M75 spectrometer in the 650–4000 cm⁻¹ range and a Perkin-Elmer 100 FT-IR spectrometer.

Integrated *thermal analysis* was carried out on a Paulik–Paulik–Erdey derivatograph in air with Al₂O₃ as a reference. The recording conditions were 1/5 (DTG), 1/10 (DTA), and 100/100 (TG), *T*_{max} = 1000 C, heating rate 5 °C/min, a sample weight 50 mg.

Mössbauer spectra were acquired using a conventional spectrometer in the constant-acceleration mode (MS4, Edina, USA) equipped with a ⁵⁷Co source (3.7 GBq) in a rhodium matrix. Isomer shifts are quoted relative to alpha-Fe at room temperature. The sample was measured at room temperature and 80 K. The spectra were fitted using the WMOSS Mössbauer Fitting Program.

Acknowledgments

We acknowledge SCSTD of Moldova for support of bilateral moldo-german research grant no.13.820.08.03/GF, application project of SCSTD no. 11.817.08.24A, also the elemental analysis group of the Institute of Chemistry of Academy of Sciences of Moldova for chemical analysis of elements.

References

- [1] Cannon, R.D.; White R.P. *Progr. Inorg.Chem.* 1988, V. 36, 195 p.
- [2] Tsuji, D. *Organic syntheses involving transition metal complexes.* Moscow: Chemistry, 1979, 256 p.
- [3] Porai-Koshits, M.A. *Itogi Nauki Tekh., Ser. Kristalokhim.,* Moscow: VINITI, 1981, V. 15, 354 p.
- [4] Carter, F.L. *Physica*, 1984, No.10D, pp.175-194.
- [5] Gonchiaruc, V.V.; Kamalov, G.L.; Kovtun, G.A.; Rudakov, E.S.; Iatsimirskii V.K. *Catalisis. Cluster approaches, mechanisms of heterogenic and homogenic catalises.* Naukova Dumka: Kiev, 2002, 541 p. (rus).
- [6] Long, J.R.; Yang, P. *Molecular Cluster Magnets.* Ed. World Scientific: Hong Kong, 2003, 291 p.
- [7] Yaghi, O.M. et all. *Science*, 2012, 336, p. 95. DOI: 10.1126/science.1220131, 1018.
- [8] Gubin, S.P.; Koksharov, Yu. A.; Homutov, G.B. *Uspehi Himii*, 2005, V. 74, Nr. 6, pp. 539-574.
- [9] Turta, C. *Sci. Hab.(Chem.) Thesis*, Chisinau, 1988.
- [10] Bobcova, S. *Cand. Sci. (Chem.) Thesis*, Chisinau, 1982.
- [11] Mereacre, V. *Cand. Sci. (Chem.) Thesis*, Chisinau, 2000.
- [12] Prodius, D.N., *Cand. Sci. (Chem.) Thesis*, Chisinau, 2007.
- [13] Melnic, S. *Cand. Sci. (Chem.) Thesis*, Chisinau, 2010.
- [14] Gorinchoi, V.V.; Turte, K.I.; Simonov, Yu.A.; Shova, S.G.; Lipkovski, Ya.; Shofranskii, V.N. *Russ. J. Coord. Chem.*, 2009, V. 35, Nr.4, pp. 279–285 (eng).
- [15] Gorinchoi, V.V.; Simonov, Yu.A.; Shova, S.G.; Shofranskii, V.N.; Turte, K.I. *Zhurnal Strukturnoi Khimii*, 2009, V. 50, Nr. 6, pp. 1196-1202.
- [16] Gorinchoy, V.V.; Zubareva, V.E.; Shova, S.G.; Shafranskii, V.N.; Lipkowski, Ya.; Stanica, N.; Simonov, Yu.A.; Turte, K.I. *Russ. J. Coord.Chem.*, 2009, V. 35, Nr.10, pp. 731–739 (eng).
- [17] *Introduction to Spectroscopy – Chemistry*, www.chemistry.msu.edu/faculty/reusch/VirtTxtJml/Spectrpy/spectro.htm
- [18] Tel'zhenskaya, P.N.; Shvarts, E.M. *Russ. Coord. Chem.*, 1977, V. 3, Nr. 9, pp. 1279-1295.
- [19] Nakomoto, K. *Infrared and Raman Spectra of Inorganic and Coordination Compounds*, New York: Wiley, 1991, 536 p.
- [20] *Chemical applications of Mössbauer spectroscopy.* Edited by V.I. Goldanskii and R.H. Herber. Academic Press, New York and London, 1968. Russian translation by B.I.Rogozeva, E.P.Stepanova, and N.K.Cherezova. Under redaction of V.I.Goldanskii, R.H.Herber and V.V.Hrapov. M.: Mir, 1970, 502 p.
- [21] Sheldrick, G.M. *SHELX-97 Manual*, Göttingen (Germany): Univ. of Göttingen, 1997, 154 p.

STUDY ON EXTRACTION PROCESS OF SUNFLOWER (*HELIANTHUS ANNUUS* L.) DRY WASTES USING DIFFERENT SOLVENTS

Olga Morarescu, Marina Grinco, Ion Dragalin, Veaceslav Kulcički, Nicon Ungur*

Institutul de Chimie al Academiei de Științe a Moldovei, 3, Academiei str., Chisinau MD-2028, Republic of Moldova
*e-mail: nicon.ungur@gmail.com, phone / fax: (+373 22) 73 97 75

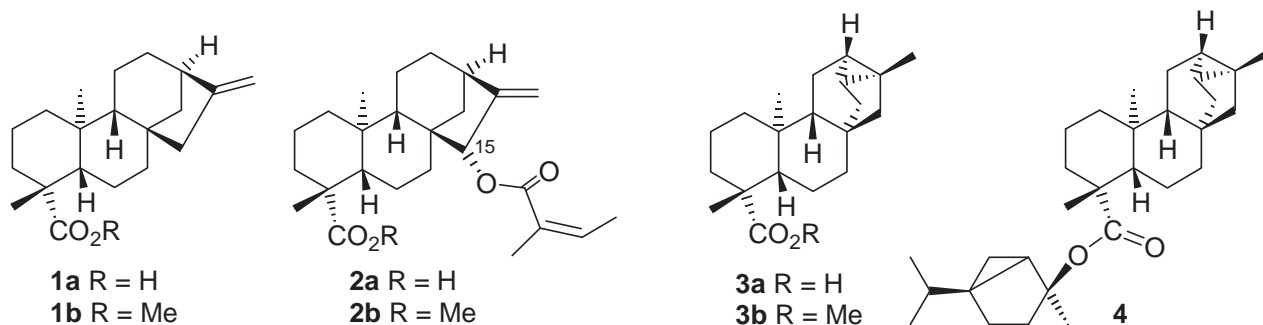
Abstract. The content of known tetra- and pentacyclic diterpenoids in extracts of sunflower (*Helianthus annuus* L.) dry wastes has been studied using different solvents for extraction. It was established that the largest extracted quantity of *ent*-kaur-16-en-19-oic acid is obtained when ethanol and diethyl ether are used for extraction of the plant material.

Keywords: *ent*-kaur-16-en-19-oic acid, 15 α -angeloyl-*ent*-kaur-16-en-19-oic acid, *ent*-trachiloban-19-oic acid, diterpene, extraction.

Introduction

The scientific interest for tetracyclic diterpenic *ent*-kaur-16-en-19-oic (**1a**) and 15-angeloyl-*ent*-kaur-16-en-19-oic (**2a**) acids, as well as for pentacyclic *ent*-trachiloban-19-oic acid (**3a**) can be explained by their broad spectrum of biological activities.

The *ent*-kaur-16-en-19-oic acid (**1a**) is an intermediate in the biogenetical scheme of gibberellic acids, which are relevant plant growth regulators [1]. Compound (**1a**) was isolated from different vegetal sources, especially from sunflower (*Helianthus* sp). [2-12]. We have achieved isolation of acids **1a–3a** from the integral sunflower (*Helianthus annuus* L.) dry wastes [13, 14].



It is noteworthy to mention, that *ent*-kaur-16-en-19-oic acid (**1a**) was reported as an inhibitor of protein tyrosine phosphatase 1B (PTP1B) and was used as remedy for treatment of type 2 diabetes and obesity [15]. It also showed selective and significant cytotoxicity for MCF-7 [16], SF-268, MCF-7 and HepG2 cell lines [9], and exhibited inhibitory activity against the enzymes prolyl endopeptidase (PEP) and thrombin [17]. Compound (**1a**) showed the antifungal activity on *Botrytis cinerea* [18] and especially against COX-2 with an IC₅₀ of 127.6 μ M [19]. *ent*-Kaur-16-en-19-oic acid (**1a**) possesses the anti-Alzheimer and antioxidant effects [20] and showed a remarkable inhibitory activity against mutans streptococci: *Streptococcus mutans* Ingbritt 1600, *S. mutans* OMZ175, *S. mutans* P20, *S. mutans* P6, *S. mutans* D1), *S. sobrinus* 6715, *S. sobrinus* P7, *S. sobrinus* S2, *S. sobrinus* S17), *S. cricetus* HS-6, *S. cricetus* P12, *S. cricetus* S2 and *S. cricetus* S38 [21]. Acid **1a** had strong inhibitory effect on the proliferation of human liver cancer (HLC) cell lines [22, 23], is genotoxic and mutagenic in human peripheral blood leukocytes (PBLs), yeast (*Saccharomyces cerevisiae*) [24], was cytotoxically active (ED₅₀ = 17.4 μ g/mL against HCT-15 COLADCAR, ED₅₀ = 15.5 μ g/mL against UIISO-SQC-1 and ED₅₀ = 19.5 μ g/mL against OVCAR-5) [25]. *ent*-Kaur-16-en-19-oic acid (**1a**) inhibited acute carrageenin- and PGE₂-induced and chronic CFA-induced inflammatory mechanical hyperalgesia [26] and possess the antimicrobial effects against *Bacillus cereus* and *Mycobacterium tuberculosis* [27].

15 α -Angeloyl-*ent*-kaur-16-en-19-oic (angeloylgrandifloric) acid (**2a**) was isolated from aerial parts of *Helianthus debilis* [11, 28], from aerial parts of *H. simulans* [11], from *H. giganteus* and from *H. angustifolius* [29]. This compound was isolated from the inflorescence of *H. annuus* L. [9], from fresh leaves of *H. annuus* cv. SH-222 [8] and from the sunflower (*H. annuus* L.) dry wastes [14].

15 α -Angeloyl-*ent*-kaur-16-en-19-oic acid (**2a**) showed weak antifeedant activity [6], also it is a spontaneous uterine contraction inhibitor (SUCI). *In vitro* bioassay proved that angeloylgrandifloric acid (**2a**) inhibited the spontaneous contractions of guinea pig uterine strips (SUCI+) at a concentration of 1.2 $\mu\text{g/mL}$ [30]. This compound showed cytotoxic activities on SF-268, MCF-7 and HepG2 cell lines [4], was cytotoxically active ($\text{ED}_{50} = 17.4 \mu\text{g/mL}$ against HCT-15 COLADCAR, $\text{ED}_{50} = 15.5 \mu\text{g/mL}$ against UISO-SQC-1 and $\text{ED}_{50} = 19.5 \mu\text{g/mL}$ against OVCAR-5) [25].

ent-Trachyloban-19-oic acid (**3a**) was isolated from sunflower (*Helianthus annuus* L.) [2, 13, 31, 32], from roots of *Iostephane heterophylla* (Asteraceae) [33], from the stem barks of *Croton robustus*. [34], and from the hexane extract of *Xylopiya sericea* [35]. The thujanol ester of *ent*-trachiloban-19-oic acid (**4**) was isolated from sunflower (*H. annuus* L.) [36, 37]. The absolute stereochemistry of *ent*-trachiloban-19-oic acid (**3a**) has been established by X-ray analysis [31], its biotransformation was studied using *Rhizopus stolonifer* [35].

Methyl trachyloban-19-oate (**3b**) exhibited weak cytotoxic activity against gastric carcinoma and colon carcinoma with ED_{50} of 9.6 and 9.1 $\mu\text{g/mL}$, respectively [34]. *ent*-Trachyloban-19-oic acid (**3a**) displayed significant *in vivo* anti-inflammatory activity [32] and it was investigated on several photosynthetic activities in spinach thylakoids. Acid (**3a**) acts as Hill reaction inhibitor. Compound **3a** did not affect photosystem I activity but inhibited uncoupled photosystem II electron flow from H_2O to DCPIP, and has not effect on electron flow from H_2O to SiMo, indicating that the site of inhibition of this compound is at the level of Q_A - Q_B [33].

Results and discussion

Because of diterpenoids **1a-3a** potential practice interest, we have investigated extracts obtained from sunflower (*Helianthus annuus* L.) dry wastes by their extraction with different organic solvents. Before we reported its extraction with diethyl ether, but here are inconveniences connected to the use of this solvent (highly flammability and volatility). For this reason we decided to consider following solvents for this purpose: petroleum ether, dichloromethane, acetone, ethanol and toluene. Diethyl ether was used as reference.

In all cases the same amounts (100 g) of dry plant material were extracted, with the same volume (750 mL) of solvents. The extractions were performed in a Soxhlet apparatus for 10 consecutive cycles. After solvent removal, all crude extracts were weighted (see Table 1) and divided into neutral and acidic part. For easier identification and quantification of the components by GC-MS analysis, each acidic part was treated with ethereal solution of diazomethane leading to diterpenic methyl esters **1b-3b** (Table 1).

Table 1.

The relative content of diterpenic esters (**1b-3b**) in extracts of sunflower (*Helianthus annuus* L.) dry wastes.

Entry	Solvent*	Extract weight (g)**	Acidic part (g)	Diterpenic acid methyl ester relative content *** (%)		
				Methyl <i>ent</i> -kaur-16-en-19- oate (1b)	Methyl 15 α -angeloil- <i>ent</i> -kaur-16-en-19-oate (2b)	Methyl <i>ent</i> -trachiloban-19-oate (3b)
1.	Petroleum ether	1.583	0.839	8.0	0	1.0
2.	Dichloromethane	2.572	1.261	12.0	0	2.0
3.	Acetone	3.138	1.568	17.0	0.5	4.0
4.	Ethanol	5.043	2.571	21.0	1.0	6.0
5.	Toluene	2.820	1.466	17.0	0.5	5.0
6.	Diethyl ether	5.082	2.592	22.0	0.5	8.0

* A volume of 750 mL of solvent was used.

** The extract weight obtained from 100 g of sunflower dry wastes.

*** Determined on the basis of GC-MS data.

GC-MS analyses have been recorded on an Agilent 7890A Gas Chromatograph with 5975C Mass Selective Detector (GC-MSD) equipped with split/splitless injector and HP-5ms capillary column (30 m/ 0.25 μm). The results of diterpenoids (**1b-3b**) chromatographic and spectral (MS) identification are presented Table 1 and were compared with those obtained before [13,14].

According to these data the predominant component of all extracts is *ent*-kaur-16-en-19-oic acid (1a). The largest quantities of this compound were found in diethyl ether and ethanol extracts, 22 and 21% respectively, and lowest in petroleum ether extract (0%). The highest content (1%) of 15 α -angeloil-*ent*-kaur-16-en-19-oic acid (**2a**) was detected in the ethanol extract, while the *ent*-trachiloban-19-oic acid (**3a**) showed the highest content (8%) in the diethyl ether extract.

In such a way, considering the results presented in Table 1, we came to the conclusion that the most recommended solvent for efficient diterpenoids **1a-3a** extraction is ethanol, which is environmentally friendly, industrial applicable and less flammable than diethyl ether.

Conclusion

The content of known tetra- and pentacyclic diterpenoids in extracts obtained from sunflower (*Helianthus annuus* L.) dry wastes using different organic solvents has been studied. It was established that the largest quantity of *ent*-kaur-16-en-19-oic acid is obtained when ethanol and diethyl ether are used for extraction.

Acknowledgment

This research was supported by the bilateral Project ASM - FCFRB № 13.820.18.03/BFof 04.04. 2013.

References

- [1] Helliwell, C. A.; Chandler, P. M.; Poole, A.; Dennis, E. S.; Peacock, W. J. Proc. Natl. Acad. Sci. U. S. A. 2001, 98, pp. 2065-2070.
- [2] Pyrek, J. St. Tetrahedron, 1970, 26, pp. 5029-5032.
- [3] Elliger, C. A.; Zinkel, D. F.; Chan, B. G.; Weiss Jr., A. C. Experientia, 1976, 32, pp. 1364-1366.
- [4] Morris, B. D.; Foster, S. P.; Grugel, S.; Charlet, L. D. J. Chem. Ecol., 2005, 31, pp. 89-102.
- [5] Mitscher, L. A.; Rao, G. S. R.; Veysoglu, T.; Drake, S.; Haas, T. J. Nat. Prod., 1983, 46, pp. 745-746.
- [6] Mullin, C. A.; Alfatafta, A. A.; Harman, J. L.; Everett, S. L. and Serino, A. A. J. Agric. Food Chem., 1991, 39, pp. 2293-2299.
- [7] Gao, Y.; Zheng, C.-D.; Li, Y.; Fan, C.; Tu, G.-H.; Gao, J.-M. Chem. Nat. Compd., 2008, 44, pp. 773-775.
- [8] Macías, F. A.; López, A.; Varela, R. M.; Torres, A.; Molinillo, J. M. G. J. Chem. Ecol., 2008, 34, pp. 65-69.
- [9] Suo, M. R.; Tian, Z.; Yang, J. S.; Lu, Y.; Wu, L.; Li, W. Acta Pharm. Sinica, 2007, 42, pp. 166-170.
- [10] Bohlmann, F.; Jakupovic, J.; King, R. M.; Robinson, H. Phytochemistry, 1980, 19, pp. 863-868.
- [11] Herz, W.; Kulanthaivel, P.; Watanabe, K. Phytochemistry, 1983, 22, pp. 2021-2025.
- [12] Herz, W.; Kulanthaivel, P. Phytochemistry, 1984, 23, pp. 1453-1459.
- [13] Ungur, N.; Grinco, M.; Kulcički, V.; Barba, A.; Bízicci, T.; Vlad, P. F. Chem. J. Mold. 2008, 4 (2), pp. 106-109.
- [14] Grinco, M.; Chetaru, O.; Kulcički, V.; Barba, A.; Boico, A.; Vlad, P. F.; Ungur, N. Chem. J. Mold. 2010, 5 (1), pp. 106-108.
- [15] Na, M. K.; Oh, W. K.; Kim, Y. H.; Cai, X. F.; Kim, S. H.; Kim, B. Y.; Ahn, J. S. Bioorg. Med. Chem. Lett., 2006, 16, pp. 3061-3064.
- [16] Fatope, M. O.; Audu, O. T.; Takeda, Y.; Zeng, L.; Shi, G.; Shimada, H.; McLaughlin, J. L. J. Nat. Prod., 1996, 59, pp. 301-303.
- [17] Diderot, N. T.; Silvere, N.; Yasin, A.; Zareen, S.; Fabien, Z.; Etienne, T.; Choudhary, M. I.; Rahman, A.-U. Biosci. Biotech. Biochem., 2005, 69, pp. 1763-1766.
- [18] Cotoras, M.; Folch, C.; Mendoza, L. J. Agric. Food Chem., 2004, 52, pp. 2821-2826.
- [19] Dang, N. H.; Zhang, X. F.; Zheng, M. S.; Son, K. H.; Chang, N. W.; Kim, H. P.; Bae, K. H.; Kang, S. S. Arch. Pharm. Res., 2005, 28, pp. 28-33.
- [20] Jung, H. A.; Lee, E. J.; Kim, J. S.; Kang, S. S.; Lee, J.-H.; Min, B.-S.; Choi, J. S. Arch. Pharm. Res., 2009, 32, pp. 1399-1408.
- [21] Yatsuda, R.; Rosalen, P. L.; Cury, J. A.; Murata, R. M.; Rehder, V. L. G.; Melo, L. V.; Koo, H. J. Ethnopharmacol., 2005, 97, pp. 183-189.
- [22] Hsieh, T. J.; Wu, Y. C.; Chen, S. C.; Huang, C. S.; Chen, C. Y. J. Chin. Chem. Soc., 2004, 51, pp. 869-876.
- [23] Zhang, Y. H.; Peng, H. Y.; Xia, G. H.; Wang, M. Y.; Han, Y. Acta Pharmacol. Sin., 2004, 25, pp. 937-942.
- [24] Cavalcanti, B. C.; Ferreira, J. R. O.; Moura, D. J.; Rosa, R. M.; Furtado, G. V.; Burbano, R. R.; Silveira, E. R.; Lima, M. A. S.; Camara, C. A. G.; Saffi, J.; Henriques, J. A. P.; Rao, V. S. N.; Costa-Lotufo, L. V.; Moraes, M. O.; Pessoa, C. Mutation Res./ Gen. Toxicol. Environm. Mutag., 2010, 70, pp. 153-63.
- [25] Rios, M. Y.; Leon, I. Chem. Nat. Compd., 2006, 42, pp. 497-498.
- [26] Mizokami, S. S.; Arakawa, N. S.; Ambrosio, S. R.; Zarpelon, A. C.; Casagrande, R.; Cunha, T. M.; Ferreira, S. H.; Cunha, F. Q.; Verri, Jr., W. A. J. Nat. Prod., 2012, 75, pp. 896-904.
- [27] Wilkens, M.; Alarcón, C.; Urzúa, A.; Mendoza, L. Planta Med., 2002, 68, pp. 452-454.
- [28] Ohno, N.; Mabry, T. J.; Zabelt, V.; Watson, W. H. Phytochemistry, 1979, 18, pp. 1687-1689.
- [29] Bohlmann, F.; Jakupovic, J.; King, R. M.; Robinson, H. Phytochemistry, 1980, 19, pp. 863-868.
- [30] Lu, Z.-Z.; Xue, H.-Z.; Tu, Z.-B.; Konno, C.; Waller, D. P.; Soejarto, D. D.; Cordell, C. A.; Fong, H. H. S. J. Nat. Prod., 1987, 50, pp. 995-997.
- [31] Sanni, S. B.; Behm, H.; Garcia-Granda, S.; Beurskens, P. T.; Moers, F. G. J. Crystallogr. Spectrosc. Res., 1990, 20, pp. 483-489.

- [32] Diaz-Viciedo, R.; Hortelano, S.; Giron, N.; Masso, J. M.; Rodriguez, B.; Villar, A.; De las Heras, B. *Biochem. Biophys. Res. Commun.*, 2008, 369, pp. 761-766.
- [33] Hernandez-Terrones, M. G.; Aguilar, M. I.; Diaz, B. K.; Lotina-Hennsen, B. *Pestic. Biochem. Physiol.*, 2003, 77, pp. 12-17.
- [34] Ngamrojnavanich, N.; Tonsiengsom, S.; Lertpratchya, P.; Roengsumran, S.; Puthong, S.; Petsom, A. *Arch. Pharm. Res.*, 2003, 26, pp. 898-901.
- [35] Silva, E. A.; Takahashi, J. A.; Oliveira, A. B. *J. Braz. Chem. Soc.*, 2002, 13, 101-105.
- [36] Pyrek, J. *St. J. Nat. Prod.*, 1984, 47, pp. 822-827.
- [37] For review see: Fraga, M. M. *Phytochem. Anal.*, 1994, 5, pp. 49-56.

MOLECULAR REARRANGEMENTS OF HIGHLY FUNCTIONALIZED TERPENES. AN UNIQUE REACTIVITY OF BICYCLIC FRAMEWORK AND POLIENIC CHAIN INHIBITION UNDER SUPERACIDIC TREATMENT

Marina Grinco, Veaceslav Kulcički, Pavel F. Vlad, Alic Barba,
Elena Gorincioi, Nicon Ungur*

Institutul de Chimie al Academiei de Științe a Moldovei, 3, Academiei str., Chisinau MD-2028, Republic of Moldova
*e-mail: nicon.ungur@gmail.com, phone / fax: (+373 22) 73 97 75

Abstract. Synthesis of polyfunctional triterpene derivative [8(27),13E,17E,21E]-15-phenylsulfonyl-16-oxo-bicyclofarnesylfarnesol benzyl ether (**8**) from commercially available monoterpene geraniol and diterpene manool has been accomplished in 73% yield and its chemical transformation in superacid medium has been investigated. An unexpected rearrangement of **8** occurred, which involved methyl migration in the bicyclic fragment and total inhibition of the lateral polienic chain. A new bicyclic triterpene product [5(10),13E,17E,21E]-15-phenylsulfonyl-16-oxo-30(10→9)-abeo-bicyclofarnesylfarnesol benzyl ether (**9**), with rearranged new carbon skeleton has been obtained. Its bicyclic moiety is analogous to this of a natural triterpene neopolypodatetraene.

Keywords: triterpenes, synthesis, superacid, isomerization.

Introduction

Triterpenes is a group of terpenes with a high structural diversity, which includes natural products with more than 100 types of skeleton [1–3]. Reviews related to biological activities of triterpenes appear regularly and are focused on their anti-inflammatory [4], antitumor [5], anti-HIV [6,7] and insecticidal [8] activities, and also their use in treatment of metabolic and vascular diseases [9].

Results and discussions

The aim of the present work is development of the method for synthesis of bicyclic polyfunctional triterpenes with a new carbon skeletons and study of their conversion in superacid medium.

Synthesis of the bicyclic triterpenoids containing two structural blocks, fragment A (monoterpene - aliphatic) and fragment B (diterpene - bicyclic) has been drawn, in order to achieve the proposed goal.

Fragment A has been obtained from commercially available monoterpene – geraniol (**1**) in three steps (Scheme 1). Treatment of geraniol (**1**) with benzyl chloride in dichloromethane and sodium hydride led to the corresponding benzyl ether. Its spectral data and physico-chemical constants are in accordance with the reported ones [10]. Compound **2** has been subjected to oxidation with selenium dioxide in ethanol furnishing the α,ω -bifunctionalized derivative **3** in a modest 45% yield. Finally, the monoterpene alcohol **3** has been oxidized with pyridinium chlorochromate (PCC) into the corresponding aldehyde **4** [11] (fragment A) in a 72% yield, its overall yield is ~32%.

Synthesis of fragment B has been achieved starting from commercially available manool (**5**). It was transformed into new diterpenic phenylsulfone **6** in a two-step sequence, according to the reported method [12]. It should be mentioned that from reaction product by column chromatography also the 13Z- isomer of diterpenyl-phenylsulfone **6** was obtained in ~20% yield.

The *n*-BuLi-assisted coupling reaction of aldehyde **4** (fragment A) and diterpenylphenylsulfone **6** (fragment B) in tetrahydrofuran gave bicyclic triterpene compound **7** in a 62% yield. Compound **7** was subjected to Swern oxidation giving the [8(27),13E,17E,21E]-15-phenylsulfonyl-16-oxo-bicyclofarnesylfarnesol benzyl ether (**8**) in acceptable yield (73%). It should be mentioned that an alternative oxidation of compound **7** with PCC in dichloromethane, led to a complex mixture of compounds where the content of target compound **8** does not exceed ~30%.

The structures of coupling reaction **7** and oxidation reaction **8** products have been established on the basis of their spectral data (see Experimental part).

Since the molecule of bicyclic triterpene derivative **8** is characterized by more than one double bond that is prone to chemical transformation in acid medium, the behavior of compound **8** in superacid medium at low temperature has been further explored [13-16]. Thus, following a previous elaboration, [8(27),13E,17E,21E]-15-phenylsulfonyl-16-oxo-bicyclofarnesylfarnesol benzyl ether (**8**) has been treated with fluorosulfonic acid in 2-nitropropane at -78°C [12,17].

Table 1.

¹H (400.13 MHz) and ¹³C NMR (100.61 MHz) data of compound 9 in CDCl₃ (δ in ppm).

Position	Compound 9		
	δ ¹ H	m, J (Hz)	δ ¹³ C ^{a,b}
1	1.73, 1.98	m ^c	25.9 CH ₂
2	1.49-1.65	m ^c	20.0 CH ₂
3	1.37, 1.48	m ^c	40.0 CH ₂
4	--	--	34.6 qC
5	--	--	137.8 qC
6	1.96	m ^c	25.2 CH ₂
7	1.43	m ^c	34.2 CH ₂
8	1.60	m ^c	33.6 qC
9	--	--	40.6 qC
10	--	--	131.7 qC
11	1.34, 1.48	m ^c	27.2 CH ₂
12	1.70, 2.00	m ^c	35.9 CH ₂
13	--	--	150.8 qC
14	5.74	br. s.	119.4 qC
15	--	--	not detected
16	--	--	190.3 qC
17	--	--	132.4 qC
18	6.96	tq (7.2; 1.2)	147.0 CH
19	2.40	m	27.7 CH ₂
20	2.10	m	37.8 CH ₂
21	--	--	138.5 qC
22	5.44	tq (6.6; 1.1)	122.0 CH
23	4.00	d (6.6)	66.5CH ₂
24	1.66	s	16.5 CH ₃
25	1.80	s	12.4 CH ₃
26	1.49	s	18.4 CH ₃
27	0.86	m ^c	16.1 CH ₃
28	0.99	s	29.2 CH ₃
29	1.01	s	27.7 CH ₃
30	0.86	m ^c	21.2 CH ₃
1'	4.50	s	72.3 CH ₂
2'	--	--	138.4 qC
4', 6'	7.30	m ^c	127.8 CH
3', 7'	7.30	m ^c	128.4 CH
5'	7.30	m ^c	128.4 CH
1''	--	--	136.5 qC
2'', 6''	8.09	dm (8.0)	132.5 CH
3'', 5''	7.50	br.t. (8.0)	128.2 CH
4''	7.64	dm (7.5)	134.0 CH

^a – degree of protonation found by DEPT sequence,^b –HMBC experiments (*J* = 8 Hz),^c – signal overlapping.

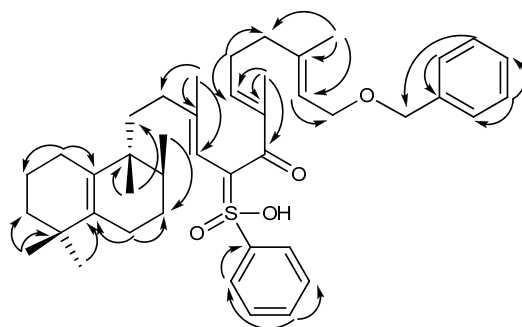
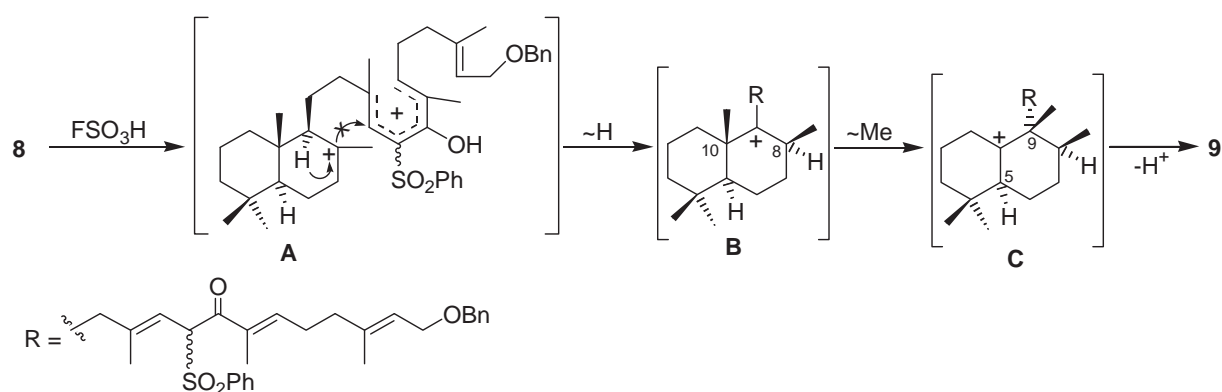


Figure 1. Selected HMBC correlations for compound 9.

The rearranged triterpene derivative **9** has been thereby obtained as a result of selective reactivity of the bicyclic part under superacidic treatment. Its plausible formation from compound **8** is depicted in Scheme 2. Due to the presence of oxygenated groups in side chain at C-16 and C-17 that can be easily protonated the bication **A**, which blocks the carbocyclisation in acid medium, is formed. In such a manner only the migration of proton from C-9 to C-8 takes place, producing the carbocation **B**. The latter is subjected to ulterior conversion into the carbocation **C**, as a result of methyl group migration from C-10 to C-9. While „quenching” the carbocation **C** the separation of proton at C-5 occurs and the final product **9** is obtained.



Scheme 2. Superacid-promoted molecular isomerization of compound 8.

It should be noted that the polyfunctional triterpene derivative **9** can be considered a congener of natural triterpenoid neopolypodatetraene (**10**), especially on considering the similarity in the bicyclic fragment (Figure 2). The latter has been isolated from a squalene hopene cyclase mutant of the prokaryotic bacterium *Alicyclobacillus acidocaldarius* F365A [18].

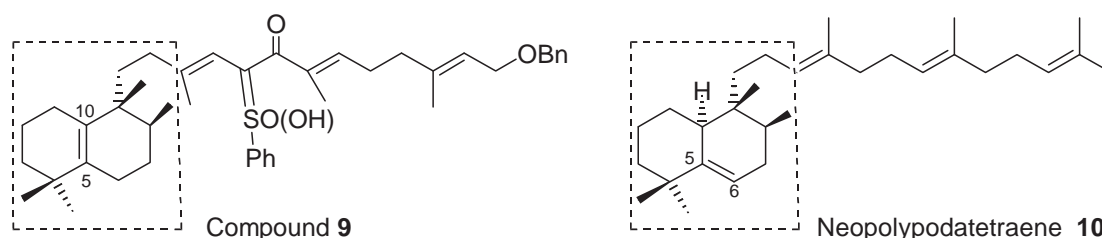


Figure 2.

Conclusions

Synthesis of polyfunctional triterpene derivative [8(27),13*E*,17*E*,21*E*]-15-phenylsulfonyl-16-oxo-bicyclopentacyclotetraene has been achieved and its chemical transformation in superacid medium has been

studied. Mentioned bicyclic triterpene product with rearranged carbon framework, which is a structural analogous of the natural triterpene neopolypodatetraene, has been obtained for the first time.

Experimental

General. Melting points (mp) were determined on a Boetius hot stage. IR Spectra were recorded on a Spectrum-100 FT-IR spectrophotometer (Perkin-Elmer), with the universal ATR sampling accessory (ν in cm^{-1}). ^1H - and ^{13}C -NMR spectra were recorded in CDCl_3 on Bruker 400 Avance III spectrometer (400.13 and 100.61 MHz); chemical shift are given in ppm and are referenced to measured in chloroform (CHCl_3) as internal standard ($\delta = 7.26$ ppm for proton and $\delta = 77.0$ for carbon). Optical rotations were measured in chloroform on a Jasco DIP 370 polarimeter, using 5 cm cell. Commercial Merck Si gel 60 (70–230 mesh ASTM) was used for flash chromatography, and Merck pre-coated SiO_2 plates were used for TLC. The chromatograms were sprayed with 0.1% solution of cerium (IV) sulfate in 2N sulfuric acid and heated at 80°C for 5 min to detect the spots. GC/MS analysis were recorded on Agilent 7890A chromatograph, equipped with quadrupole MS detector MSD 5975C and HP-5 ms capillary column (30 m/0.25 mm). Treatment of reaction mixtures in organic solvents included the extraction by Et_2O , washing of the extract with H_2O up to neutral reaction, drying over anhydrous Na_2SO_4 , and solvent removal *in vacuo*.

Geraniol benzyl ether (2). Geraniol (**1**) (12 g, 77.9 mmol) in dry THF (103 mL) was treated with 60% NaH (3.68 g), benzyl chloride (10.61 mL, 92.2 mmol) and tetrabutylammonium iodide (2.88 g, 7.79 mmol). The reaction mixture was stirred for 12 h at room temperature. Then, 10% aqueous solution of H_2SO_4 (20 mL) was added. Usual work up gave a crude reaction product (25 g), which was purified by flash chromatography using 1% ethyl acetate/light petroleum ether mixture to yield 17.52 g (92%) of the geraniol benzyl ether (**2**), as a pale yellow oil. IR liquid film (ν , cm^{-1}): 735, 1069, 1101, 1270, 1377, 1453, 1496, 1670, 1726, 2924. ^1H NMR (400 MHz, δ_{H}): 1.62 (s, 3H, H-9), 1.66 (s, 3H, H-10), 1.69 (d, $J = 0.9$ Hz, 3H, H-8), 2.06 (m, 2H, H-4), 2.12 (m, 2H, H-5), 4.04 (dd, $J = 6.8, 0.3$ Hz, 2H, H-1), 4.51 (s, 2H, H-1'), 5.12 (m, 1H, H-6), 5.42 (m, 1H, H-2), 7.34 (m, 5H, Ar-H). ^{13}C NMR (100 MHz, δ_{C}): 16.4 (q, C-10), 17.6 (q, C-9), 25.6 (q, C-8), 26.4 (t, C-5), 39.6 (t, C-4), 66.6 (t, C-1), 71.9 (t, C-1'), 138.6 (d, C-2), 124.0 (d, C-6), 127.5 (d, C-5'), 127.8 (d, C-3', 7'), 128.3 (d, C-4', 6'), 131.6 (s, C-7), 138.6 (s, C-2'), 140.3 (s, C-3). All physical properties and spectroscopic data were identical with those reported in literature [10].

8-Hydroxygeraniol benzyl ether (3). A suspension of selenium dioxide (1.45 g, 13.08 mmol) in ethanol (9 mL) was added to a solution of geranylbenzyl ether (**2**) (6.38 g, 26.15 mmol) in ethanol (89 mL). The mixture was refluxed for 3 h, cooled to 0°C, treated with NaBH_4 (500 mg, 13.08 mmol) and stirred at the same temperature for 2 h. After, the reaction was quenched with a 10% soln. of H_2SO_4 (10 mL), and the mixture was worked up as usual. The crude product (7.5 g) was submitted to flash chromatography on silica gel (200 g) with increasing gradient of ethyl acetate in light petroleum ether to give starting ether (**2**) (3.14 g, 49%) and 8-hydroxygeraniol benzyl ether (**3**) (3.05 g, 45%), as colorless viscous oil. IR liquid film (ν , cm^{-1}): 697, 736, 1067, 1453, 1639, 3429. ^1H NMR (400 MHz, δ_{H}): 1.65 (s, 3H, H-10), 1.66 (s, 3H, H-9), 2.08 (t, $J = 7.3$ Hz, 2H, H-4), 2.17 (q, $J = 7.3$ Hz, 2H, H-5), 3.97 (s, 2H, H-8), 4.02 (d, $J = 6.8$ Hz, 2H, H-1), 4.50 (s, 2H, H-1'), 5.39 (m, 2H, H-2 and H-6), 7.31 (m, 5H, Ar-H). ^{13}C NMR (100 MHz, δ_{C}): 13.6 (q, C-9), 16.4 (q, C-10), 25.8 (t, C-5), 39.1 (t, C-4), 66.5 (t, C-1), 68.9 (t, C-8), 72.1 (t, C-1'), 121.1 (d, C-2), 125.5 (d, C-6), 127.5 (d, C-5'), 127.8 (d, C-3', 7'), 128.3 (d, C-4', 6'), 135.1 (s, C-3), 139.9 (s, C-7). All physical properties and spectroscopic data were identical with those reported in literature [10].

8-Oxo-geraniol benzyl ether (4). Hydroxyether (**3**) (1.41 g, 5.42 mmol) was dissolved in dry CH_2Cl_2 (83 mL) and PCC (1.75 g, 8.13 mmol) was added. After stirring the reaction mixture at room temperature for 1.5 h, it was diluted with diethyl ether (60 mL) and passed through a short silica gel pad. The crude product (1.9 g) was subjected to flash chromatography. Elution with 4% ethyl acetate/light petroleum ether mixture gave 980 mg (70%) of unsaturated aldehyde (**4**), as a pale yellow oil. IR liquid film (ν , cm^{-1}): 697, 736, 1069, 1116, 1381, 1453, 1686, 2857, 2975. ^1H NMR (400 MHz, δ_{H}): 1.69 (s, 3H, H-10), 1.76 (d, $J = 0.8$ Hz, 3H, H-9), 2.23 (t, $J = 7.6$ Hz, 2H, H-4), 2.5 (q, $J = 7.6$ Hz, 2H, H-5), 4.06 (d, $J = 6.7$ Hz, 2H, H-1), 4.51 (s, 2H, H-1'), 5.46 (apparent tq, $J = 6.7, 1.2$ Hz, 1 H, H-2), 6.47 (td, $J = 7.6, 1.3$ Hz, 1H, H-6), 7.31 (m, 5H, Ar-H), 9.39 (s, 1H, H-8). ^{13}C NMR (100 MHz, δ_{C}): 9.0 (q, C-9), 16.2 (q, C-10), 26.9 (t, C-5), 37.6 (t, C-4), 66.3 (t, C-1), 72.0 (t, C-1'), 121.9 (d, C-2), 127.4 (d, C-5'), 127.5 (d, C-3', 7'), 128.2 (d, C-4', 6'), 138.2 (s, C-2'), 138.3 (s, C-3), 139.3 (s, C-7), 153.5 (d, C-6), 194.8 (d, C-8). All physical properties and spectroscopic data were identical with those reported in literature [11].

Synthesis of 8(17),13E-bicyclogeranylgeranylphenylsulfone (6). A solution of phosphorus tribromide (1.54 g, 5.69 mmol) in dry ether (5.0 mL) was added dropwise to a stirred solution of manool (**5**) (1.20 g, 4.14 mmol) in dry ether (10 mL) with cooling on an ice bath. The mixture was stirred for 2 h at room temperature and treated with saturated NaHCO_3 solution. The ether layer was separated, washed with brine, dried, and concentrated *in vacuo*. The resulting

bromide (1.25 g, 86%) was added to a solution of the sodium salt of benzenesulfonic acid (0.90 g, 5.45 mmol) in dry DMF (10 mL). The mixture was stirred at room temperature under argon in the dark for 3 h, treated with NaCl solution, and extracted with ether. The extract was worked up as usual to afford a liquid product that was chromatographed on silica gel (42 g) with gradient elution by petroleum ether: AcOEt to elute 13*E*-bicyclogeranylgeranylphenylsulfone (**6**) (1.09 g, overall for two steps ~74%), as colorless crystals, m.p. 87-88°C (from hexane), $[\alpha]_D^{25} +32.2^\circ$ (*c* 1.45, CHCl₃). IR liquid film (ν , cm⁻¹): 730, 1149, 1306, 1447, 1587, 1642, 2927. ¹H NMR (400 MHz, δ_H): 0.65 (*s*, 3H, H-20), 0.79 (*s*, 3H, H-19), 0.86 (*s*, 3H, H-18), 1.29 (*s*, 3H, H-16), 3.80 (*d*, *J* = 8 Hz, 2H, H-15), 4.42 (*d*, *J* = 1.2 Hz, 1H, H_b-17), 4.80 (*d*, *J* = 1.4 Hz, 1H, H_a-17), 5.14 (*td*, *J* = 8.0, 1.3 Hz, 1H, H-14), 7.68 (*m*, 5H, Ph-H). ¹³C NMR (100 MHz, δ_C): 14.5 (*q*, C-20), 16.2 (*q*, C-16), 19.4 (*t*, C-2), 21.7 (*q*, C-19), 21.8 (*t*, C-11), 24.4 (*t*, C-6), 33.6 (*s*, C-4), 33.6 (*q*, C-18), 38.3 (*t*, C-7), 38.6 (*t*, C-12), 39.1 (*t*, C-1), 39.7 (*s*, C-10), 42.1 (*t*, C-3), 55.5 (*d*, C-5), 56.1 (*t*, C-15), 56.3 (*d*, C-9), 106.2 (*t*, C-17), 110.0 (*d*, C-14), 128.6 (*d*, C-3'', 5''), 128.9 (*d*, C-2'', 6''), 133.4 (*d*, C-4''), 138.8 (*s*, C-1'') 147.2 (*s*, C-13), 148.5 (*s*, C-8). Found (%): C, 75.42; H, 9.31. C₂₆H₃₈SO₂. Calculated (%): C, 75.31; H, 9.24.

[8(27),13E,17E,21E]-15-phenylsulfonyl-16-hydroxy-bicyclofarnesylfarnesol benzyl ether (7). Compound **6** (529 mg, 1.28 mmol, 1.2 eq.) was co-evaporated with benzene, dried under high vacuum, and then dissolved in anhydrous THF (4.6 mL) and cooled to -78 °C. Then *n*-BuLi (1.7 M, 0.75 mL, 1.28 mmol, 1.2 equiv) was added drop-wise to the 8(17),13*E*-bicyclogeranylgeranylphenylsulfone (**6**) solution over 2 min. under argon atmosphere. The resulting bright yellow solution was stirred at -78°C for 30 min and gradually warmed to -40°C over 1 h and then cooled to -78°C. Aldehyde **4** (279 mg, 1.07 mmol, 1 equiv) was dried under high vacuum, dissolved in THF (4.6 mL), cooled to -78 °C, and added drop-wise to the sulfone anion solution using a syringe. After 30 min of stirring at -78°C, the reaction mixture was gradually heated to -40°C and sat. aq. NH₄Cl (4 mL) was added followed by usual workup. The residue (900 mg) was purified by silica gel flash column chromatography (10% ethyl acetate/light petroleum ether mixture) affording compound **7** (472 mg, 66%), as a clear yellow oil. IR liquid film (ν , cm⁻¹): 730, 1144, 1230, 1446, 2191, 2290, 2947. ¹H NMR (400 MHz, δ_H): 0.64 (*s*, 3H, H-30), 0.79 (*s*, 3H, H-29), 0.86 (*s*, 3H, H-28), 1.11 (*s*, 3H, H-26), 1.49 (*s*, 3H, H-25), 1.61 (*s*, 3H, H-24), 3.95 (*m*, 1H, H-15), 4.00 (*d*, *J* = 6.7 Hz, 2H, H-23), 4.37 (*d*, *J* = 0.8 Hz, 1H, H_b-27), 4.49 (*s*, 2H, H-1'), 4.61 (*d*, *J* = 9.7 Hz, 1H, H-16), 4.67 (*m*, 1H, H-14), 4.80 (*d*, *J* = 0.9 Hz, 1H, H_a-27), 5.37 (*t*, *J* = 6.7 Hz, 1H, H-22), 5.42 (*t*, *J* = 6.8 Hz, 1H, H-18), 7.31 (*m*, 5H, Ar-H), 7.68 (*m*, 5H, Ph-H). ¹³C NMR (100 MHz, δ_C): 10.6 (*q*, C-25), 14.5 (*q*, C-30), 16.1 (*q*, C-26), 16.5 (*q*, C-24), 19.4 (*t*, C-2), 21.7 (*q*, C-29), 24.4 (*t*, C-6), 26.0 (*t*, C-11), 29.7 (*t*, C-19), 33.3 (*s*, C-4), 33.6 (*q*, C-28), 38.3 (*t*, C-7), 38.8 (*t*, C-12), 38.9 (*t*, C-20), 39.2 (*t*, C-1), 39.8(*s*, C-10), 42.2 (*t*, C-3), 55.6 (*d*, C-5), 56.5 (*d*, C-9), 66.6 (*t*, C-23), 68.6 (*d*, C-15), 72.1 (*t*, C-1'), 76.5 (*d*, C-16), 106.2 (*t*, C-27), 114.0 (*d*, C-14), 121.3 (*d*, C-22), 127.5 (*d*, C-5'), 127. 8 (*d*, C-3', 7'), 128.3 (*d*, C-4', 6'), 128.8 (*d*, C-3'', 5''), 129.4 (*d*, C-2'', 6''), 130.2 (*d*, C-18), 133.4 (*s*, C-17), 133.8 (*d*, C- 4''), 137.7 (*s*, C-1''), 138.6 (*s*, C-2'), 139.6 (*s*, C-21), 145.3 (*d*, C-13), 148.5 (*s*, C-8). Found (%): C, 76.53; H, 8.89. C₄₃H₆₀SO₄. Calculated (%): C, 76.74; H, 8.99.

[8(27),13E,17E,21E]-15-phenylsulfonyl-16-oxo-bicyclofarnesylfarnesol benzyl ether (8). A solution of DMSO (0.085 mL, 1.21 mmol) in CH₂Cl₂ (1.8 mL) was added dropwise to a stirred solution of oxalyl chloride (0.07 mL, 0.61 mmol) in CH₂Cl₂ (1.8 mL) cooled to -60 °C. After 5 min of stirring at this temperature, a solution of compound (**7**) (185 mg, 0.275 mmol) in CH₂Cl₂ (1.8 mL) was added dropwise. After 30 min of stirring (-60°C) triethylamine (0.5 mL, 3.03 mmol) was added to the reaction mixture, and after another 15 min the cooling bath was removed and water (3 mL) was added at room temperature. After separation of the phases, the aqueous phase was extracted with CH₂Cl₂ (3×10 mL) and the combined organic phase was subsequently washed with a 20% H₂SO₄, a sat. NaHCO₃ solution, brine to neutral pH. Drying with Na₂SO₄ and subsequent evaporation of the solvent gave a crude reaction product, which was submitted to flash chromatography (8% ethyl acetate/light petroleum ether) to give polar ketone **8** (134 mg, 0.2 mmol, 73%), as a pale yellow oil. IR liquid film (ν , cm⁻¹): 745, 1144, 1309, 1394, 1449, 1665, 1791, 2289, 2986, 3365. ¹H NMR (400 MHz, δ_H): 0.82 (*s*, 3H, H-29), 0.87 (*s*, 3H, H-28), 0.92 (*s*, 3H, H-30), 1.65 (*s*, 3H, H-26), 1.68 (*s*, 3H, H-24), 1.82 (*s*, 3H, H-25), 4.04 (*d*, *J* = 6.6 Hz, 2H, H-23), 4.42 (*d*, *J* = 0.9 Hz, 1H, H_b-27), 4.51 (*s*, 2H, H-1'), 4.82 (*d*, *J* = 1.0 Hz, 1H, H_a-27), 5.15 (*d*, *J* = 3.0 Hz, 1H, H-14), 5.46 (*t*, *J* = 6.6 Hz, 1H, H-22), 5.63 (*d*, *J* = 3.0 Hz, 1H, H-15), 6.69 (*m*, 1H, H-18), 7.31 (*m*, 5H, Ar-H), 7.65 (*m*, 5H, Ph-H). ¹³C NMR (100 MHz, δ_C): 11.8 (*q*, C-25), 16.4 (*q*, C-24), 17.1 (*q*, C-26), 26.3 (*t*, C-11), 19.3 (*t*, C-2), 20.1 (*q*, C-30), 21.7 (*q*, C-29), 24.4 (*t*, C-6), 27.6 (*t*, C-19), 33.25 (*s*, C-4), 33.28 (*q*, C-28), 37.9 (*t*, C-20), 38.3 (*t*, C-7), 39.0 (*t*, C-1), 40.39 (*t*, C-12), 40.41 (*s*, C-10), 41.8 (*t*, C-3), 51.9 (*d*, C-5), 56.3 (*d*, C-9), 66.5 (*t*, C-23), 68.7 (*d*, C-15), 72.3 (*t*, C-1'), 106.2 (*t*, C-27), 113.5 (*d*, C-14), 122.2 (*d*, C-22), 127.5 (*d*, C-5'), 127.8 (*d*, C-3', 7'), 128.3 (*d*, C-4', 6'), 128.5 (*d*, C-3'', 5''), 130.0 (*d*, C-2'', 6''), 133.7 (*d*, C- 4''), 137.4 (*s*, C-1''), 137.8 (*s*, C-17), 138.4 (*s*, C-2'), 138.6 (*s*, C-21), 145.0 (*d*, C-18), 147.1 (*s*, C-13), 148.5 (*s*, C-8), 192.2 (*s*, C-16). Found (%): C, 76.83; H, 8.82. C₄₃H₅₈SO₄. Calculated (%): C, 76.97; H, 8.71.

[5(10),13E,17E,21E]-15-phenylsulfonyl-16-oxo-30(10→9)-abeo-bicyclofarnesylfarnesol benzyl ether (9). Compound **8** (40 mg, 0.06 mmol) was dissolved in 2-nitropropane (0.7 mL) and a solution of FSO₃H (0.017 mL, 0.3 mmol, 5 equiv.) in 2-nitropropane (0.2 mL) was added under argon to the resulting solution at -78°C. After 20 min of stirring,

the reaction mixture was quenched with a solution of triethylamine (0.5 mL) in light petroleum ether (0.5 mL), then reaction mixture was warmed to room temperature, diluted with brine (10 mL). After usual work-up the crude reaction product (42 mg), was submitted to flash chromatography (1% ethyl acetate/benzene) to give compound **9** (25 mg, 62%). IR liquid film (ν , cm^{-1}): 740, 1145, 1312, 1385, 1451, 1668, 1793, 2286, 2993, 3362. ^1H NMR (see: Table 1). ^{13}C NMR (see: Table 1). Found (%): C, 77.12; H, 8.91. $\text{C}_{43}\text{H}_{58}\text{SO}_4$. Calculated (%): C, 76.97; H, 8.71.

References

- [1] Hill, R. A.; Connolly, J. D. *Nat. Prod. Rep.*, 2013, 30 (7), pp. 1028-1065, and previous reviews.
- [2] Domingo, V.; Arteaga, J. F.; del Moral, J. F. Q.; Barrero, A. F. *Nat. Prod. Rep.*, 2009, 26 (1), pp. 115-134.
- [3] Xu, R.; Fazio, G. C.; Matsuda, S. P. *Phytochemistry*, 2004, 65 (3), pp. 261-291.
- [4] Sporn, M. B.; Liby, K. T.; Yore, M. M.; Fu, L.; Lopchuk, J. M.; Gribble, G. W. *J. Nat. Prod.*, 2011, 74, pp. 537-545.
- [5] Bishayee, A.; Ahmed, S.; Brankov, N. Perloff, M. *Front. Biosci.*, 2011, 16, pp. 980-996.
- [6] Cassels, B. K.; Asencio, M. *Phytochem. Rev.*, 2011, 10, pp. 545-564.
- [7] Kuo, R.-Y.; Qian, K.; Morris-Natschke, S. L.; Lee, K.-H. *Nat. Prod. Rep.*, 2009, 26 (10), pp. 1321-1344.
- [8] Gonzalez-Coloma, A.; Lopez-Balboa, C.; Santana, O.; Reina, M. and Fraga, B. M.; *Phytochem. Rev.*, 2011, 10, pp. 245-260.
- [9] Sheng, H.; Sun, H. *Nat. Prod. Rep.*, 2011, 28, pp. 543-593.
- [10] Altman, L. J.; Ash, L.; Stuart Marson, S. *Synthesis*, 1974; (2), pp. 129-131.
- [11] Masaki, Y.; Hashimoto, K.; Kaji, K. *Tetrahedron Lett.*, 1978, 19 (46), pp. 4539-4542.
- [12] Kulcički, V.; Ungur, N.; Vlad, P. F. *Tetrahedron*, 1998, 54 (39), pp. 11925-11934.
- [13] Ungur, N.; Nguen, V. T.; Popa, N. P.; Vlad, P. F. *Chem. Nat. Comp.*, 1993, 28 (6), pp. 561-568.
- [14] Korchagina, D. V.; Gavriljuk, O. A.; Barkhash, V. A.; Vlad, P. F.; Ungur, N. D.; Popa, N. P. *Zh. Org. Khim.*, 1993, 29 (2), pp. 323-325.
- [15] Ungur, N. ; Popa, N. P.; Kulcitki, V. N.; Vlad, P. F. *Chem. Nat. Comp.*, 1993, 29 (5), pp. 618-621.
- [16] Ungur, N.; Popa, N. P.; Vlad, P. F. *Chem. Nat. Comp.*, 1993, 29 (5), pp. 613-617.
- [17] Kulcički, V.; Grinco, M.; Barba, A.; Ungur, N.; Vlad, P. F. *Chem. Nat. Comp.* 2007, 43 (3), pp. 268-273.
- [18] Sato, T; Hoshino, T. *Biosci., Biotechnol., Biochem.*, 2001, 65 (10), pp. 2233-2242.

STARCH SULFURIC ACID: AN ALTERNATIVE, ECO-FRIENDLY CATALYST FOR BIGINELLI REACTION

Ramin Rezaei^{a*}, Sara Malek^a, Mohammad Reza Sheikhi^a, Mohammad Kazem Mohammadi^b

^aDepartment of Chemistry, Firoozabad Branch, Islamic Azad University, P.O. Box 74715-117 Firoozabad, Iran

^bDepartment of Chemistry, Ahvaz Branch, Islamic Azad University, Ahvaz, Iran

*e-mail: rezaieramin@yahoo.com

Abstract. The one-pot multicomponent synthesis of 3,4-dihydropyrimidinone derivatives using starch sulfuric acid as an environmentally friendly biopolymer-based solid acid catalyst from aldehydes, β -keto esters and urea/thiourea without solvent is described. Compared with classical Biginelli reaction conditions, this new method has the advantage of minimizing the cost operational hazards and environmental pollution, good yields, shorter reaction times and simple work-up.

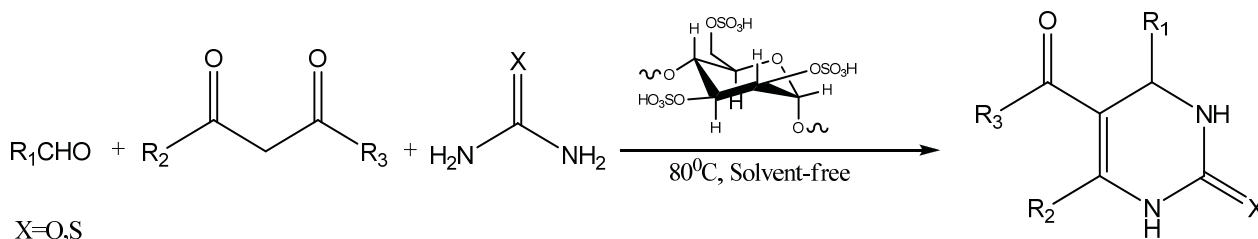
Keywords: Biginelli reaction, dihydropyrimidinones, starch sulfuric acid, solvent-free, biodegradable catalyst.

Introduction

Dihydropyrimidinones are attractive organic compounds which show important biological activities such as antiviral, antitumor, antibacterial and anti-inflammatory actions [1-3]. The more convenient procedure for the preparation of dihydropyrimidinones first reported by P. Biginelli in 1893, consists of the one-pot condensation of β -dicarbonyl compounds with aldehydes and urea or thiourea under strongly acidic conditions [4]. One major disadvantage of this method is the low yields especially in the case of aliphatic and some substituted aromatic aldehydes. To circumvent this problem, a variety of new catalysts has been introduced in the literature. In recent years, many protocols involving the use of Lewis and Bronsted acids such as graphite supported lanthanum chloride, [5] alumina supported MoO_3 [6], antimony(III) chloride [7], copper(II) tetrafluoroborate [8], bismuth nitrate [9], iron(III) trifluoroacetate and trifluoromethanesulfonate [10], yttrium(III) nitrate hexahydrate [11], TaBr_5 [12], Trichloroisocyanuric acid (TCCA) [13], PSSA [14], chloroacetic acid [15], *p*-TsOH [16], HCl [17], acetic acid [18], silica sulfuric acid [19], concentrated H_2SO_4 [20], H_3BO_3 [21], HBF_4 [22], chiral phosphoric acid [23], $\text{H}_3\text{PW}_{12}\text{O}_{40}$ [24], $\text{H}_3\text{PMo}_{12}\text{O}_{40}$ [25], $\text{Al}_2\text{O}_3/\text{MeSO}_3\text{H}$ [26], HClO_4 doped silica [27], bentonite/PS- SO_3H nanocomposite [28], sulfated tungstate [29], imidazol-1-yl-acetic acid [30], zeolite-supported HPA [31] and a number of other catalysts [32-38] are reported. However, at a practical level, these often require relatively harsh reaction conditions such as high reaction temperatures, expensive or highly acidic catalysts, and prolonged reaction times. In most of the cases stoichiometric amounts of catalyst are required in order to achieve good yields. In addition, most of the reactions require tedious work-up procedures and column purification, which ultimately results in diminished yields. Therefore, in spite of a large number of methods reported for this transformation, there is still need to develop a more efficient, simple, milder protocol using conservational catalyst.

In recent years, the direction of science and technology has been shifting more towards eco-friendly, natural product resources and reusable catalysts. Thus, natural biopolymers are attractive candidates in the search for such solid support catalysts [39]. Starch as a one of the most common and easy to recover biopolymer become in the scope of many research [40, 41].

We now report an efficient catalyzed method for the synthesis of dihydropyrimidinones via the three-component reaction of β -dicarbonyl compounds with aldehydes and urea or thiourea under mild conditions (Scheme 1). To the best of our knowledge, the use of starch sulfuric acid (SSA) as a catalyst for the synthesis of dihydropyrimidinones previously has not been reported.



Scheme 1.

Experimental

All chemicals and analytical grade solvents were purchased from Merck or Fluka chemical company. Melting points were determined in open glass capillaries on Mettler 9100 melting point apparatus. Infrared (IR) spectra were recorded using a 4300 Shimadzu FT-IR spectrometer. ^1H NMR and ^{13}C NMR spectra were recorded on a Bruker 250MHz spectrometer. Mass spectra were recorded on a Shimadzu QP 1100 BX mass spectrometer. All products were known compounds and identified by comparing their physical data to their authentic samples.

General procedure for the Preparation of starch sulfuric acid

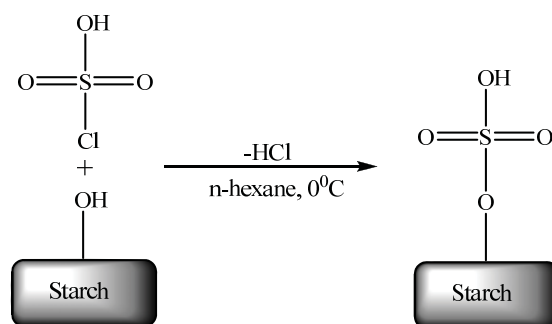
To a magnetically stirred mixture of 5.0 g of starch in 20 mL of n-hexane, 1.0 g of chlorosulfonic acid (9 mmol) was added drop wise at 0°C during 2 h. HCl gas was removed from the reaction vessel immediately. After the addition was complete, the mixture was stirred for 2 h. Then the mixture was filtered and washed with 30 mL of acetonitrile and dried at room temperature to afford 5.25 g of starch sulfuric acid as a white powder. Sulfur content of the samples by conventional elemental analysis, was 0.55 mmol/g for starch sulfuric acid. The number of H^+ sites on the starch- SO_3H was determined by acid–base titration was 0.50 meq/g. This value corresponds to about 90% of the sulfur content, indicating that most of the sulfur species on the sample are in the form of the sulfonic acid groups.

General procedure for the synthesis of dihydropyrimidinones

SSA (0.05 g) was added to a mixture of aldehyde (1 mmol), β -dicarbonyl compound (1 mmol) and urea or thiourea (1.5 mmol). The neat reaction mixture was heated with stirring for appropriate time at 80°C (progress of the reaction was monitored by TLC). At the end of reaction, SSA washed and filtered off with water and ethanol to remove urea (or thiourea) from the surface of the catalyst. Then, the catalyst dried and was maintained for new runs. The filtrate was concentrated and the crude product was recrystallized from ethanol to afford the pure product. Products were identified by comparison with melting points of the authentic compounds. The isolated catalyst was dried at 70°C overnight and was reused in the next runs without further purification. The catalyst could be reused at least three times without an appreciable decrease of the yield and reaction rate.

Results and discussion

SSA is readily prepared by the dropwise addition of chlorosulfonic acid to mixture of starch in n-hexane at 0°C . It is important to note that, this reaction is easy and clean without any work-up procedure due to HCl gas is evolved from the reaction vessel immediately. This white homogeneous, nonhygroscopic solid acid is stable under reaction conditions (Scheme 2).



Scheme 2.

We are interested in studying Biginelli reaction with the aim to develop an operationally simple method for the synthesis of some DHPMs. We started our study of the one-pot three-component Biginelli condensation using SSA as the catalyst (Scheme 1), by examining the conditions for the reaction using benzaldehyde, ethylacetoacetate and urea to afford the corresponding DHPM product. In order to optimize the reaction conditions we conducted this reaction in different solvents (Table 1). By using water and ethanol as solvent, the catalyst led to the good conversion but in longer reaction times. The best results were obtained under solvent-free conditions yielding Biginelli products in excellent conversion in shorter reaction times (entry 7, Table 1). No product was formed in the absence of the catalyst (entry 5, Table 1) whereas in the presence of starch sulfuric acid (0.05 g), under the same conditions yield increased to 60% (entry 6, Table 1). The yield of dihydropyrimidinone increased with increasing the amounts of the catalyst from 0.05 to 0.1 g. The use of 0.15 g of SSA permitted the reaction time to be decreased to 5 min, the yield unexpectedly decreased to 75% (entry 8, Table 1). A possible explanation for the low product yield is that the starting material or the product may have been destroyed during the reaction when an excess amount (0.15 g) of SSA was used in the exothermic reaction and

that 0.1 g SSA was sufficient to catalyze the reaction effectively. The reaction temperature was also optimized, below 80 °C the reaction proceeded slow giving a relatively low yield and no improvement was observed above 80 °C (entries 9-10, Table 1). All further studies were carried out under solvent-free conditions with 0.1g catalyst at 80 °C. Varying the amount of reactants, the best result was obtained when the molar ratio of benzaldehyde, ethyl acetoacetate and urea was 1.0:1.0:1.2.

Table 1.

Effect of solvents on Biginelli reaction of benzaldehyde (1 mmol), ethyl acetoacetate (1 mmol), urea (1.2 mmol), over starch sulfuric acid.

Entry	Solvent	T(°C)	Catalyst (g)	Time (min)	Yield (%)
1	Acetonitrile	Reflux	0.1	150	80
2	Ethanol	Reflux	0.1	45	85
3	THF	Reflux	0.1	120	50
4	Water	Reflux	0.1	30	85
5	Solvent-free	80	-	120	0
6	Solvent-free	80	0.05	120	60
7	Solvent-free	80	0.1	8	90
8	Solvent-free	80	0.15	5	75
9	Solvent-free	r.t	0.1	180	35
10	Solvent-free	60	0.1	30	50

The structural variations in the aldehydes had no significant effect on the yield and with aldehydes bearing sensitive functional groups like Cl, NO₂, and OCH₃ the reaction proceeded smoothly to afford the corresponding products in excellent yields (entries 2-4 Table 2). SSA also worked well even with an acid-sensitive aldehyde such as furfural without leading to the formation of any side products (entry 7, Table 2). The reaction of other 1,3-dicarbonyl compounds such as acetylacetone was also run with benzaldehyde and urea in the presence of SSA under solvent-free conditions and the corresponding dihydropyrimidinone was obtained in high yields (entry 8 Table 2). Thiourea has been also used with success to provide the corresponding dihydropyrimidin-2-(1H)-thiones in high yields (entries 9–11, Table 2). It is well known that for Biginelli reaction, aromatic aldehyde works very well, but aliphatic aldehyde works hard, however it is noteworthy that catalyzed the reaction with aliphatic aldehyde. Reaction was very slow and practically did not give any product at 80 °C.

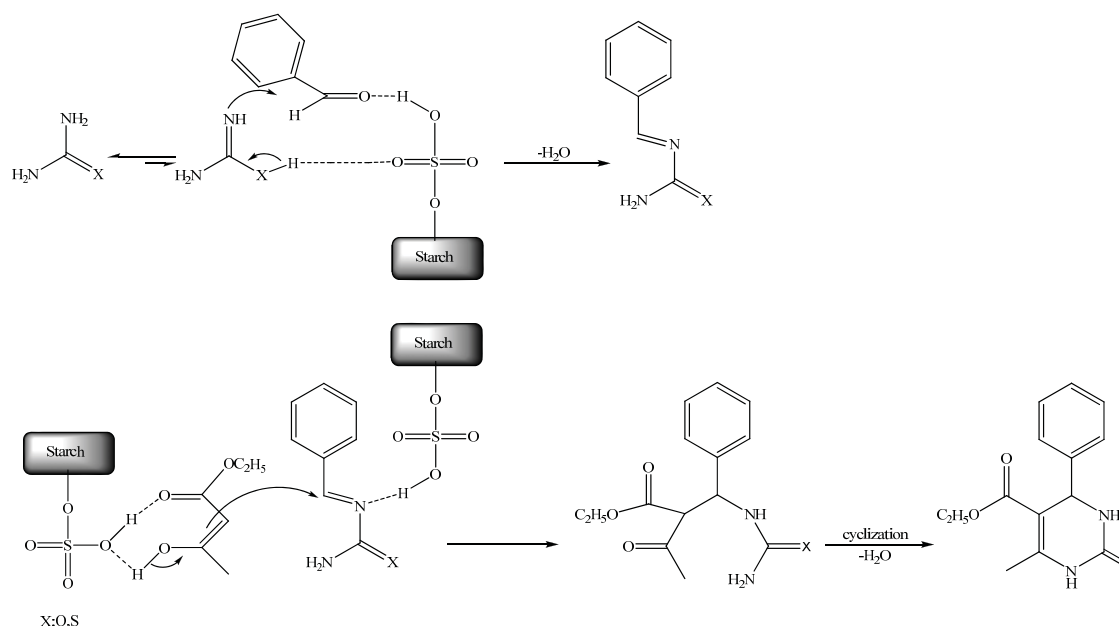
Table 2.

Synthesis of 3,4-dihydropyrimidin-2 (1H)-ones, catalyzed by starch sulfuric acid.

Entry	R ₁	R ₂	R ₃	X	Yield (%)	Time (min)	M.p. (°C)	
							Found	Reported
1	C ₆ H ₅	CH ₃	OC ₂ H ₅	O	85	43	192-194	198-200[15]
2	4-ClC ₆ H ₄	CH ₃	OC ₂ H ₅	O	82	35	208-210	211-213[15]
3	4-NO ₂ C ₆ H ₄	CH ₃	OC ₂ H ₅	O	90	42	200-202	205-207[32]
4	4-CH ₃ OC ₆ H ₄	CH ₃	OC ₂ H ₅	O	80	55	194-196	201-203[18]
5	4-CH ₃ C ₆ H ₄	CH ₃	OC ₂ H ₅	O	87	52	210-212	212-214[25]
6	Ph CH=CH	CH ₃	OC ₂ H ₅	O	77	62	226-228	232-235[19]
7	2-Furyl	CH ₃	OC ₂ H ₅	O	90	70	195-197	201-203[36]
8	C ₆ H ₅	CH ₃	CH ₃	O	86	46	228-230	233-236[37]
9	C ₆ H ₅	CH ₃	OC ₂ H ₅	S	84	48	204-206	208-210[5]
10	4-ClC ₆ H ₄	CH ₃	OC ₂ H ₅	S	92	40	214-216	208-210[38]
11	4-CH ₃ OC ₆ H ₄	CH ₃	OC ₂ H ₅	S	80	49	143-145	150-152[5]

The mechanism of the Biginelli reaction established by Kappe proposed that the key step in this cyclocondensation process should involve the formation of N-acyliminium ion intermediate. The suggested mechanism for the Biginelli reaction catalyzed by SSA under solvent-free conditions is outlined in Scheme 3.

A comparative study was performed for the use of SSA with some of the reported catalysts for the Biginelli reaction (Table 3). In most methods, the reaction was performed in solvent such as acetic acid, dioxane and toluene. Thus, SSA promoted the reactions more effectively than the other catalysts and should be considered as one of the best choice for selecting an economically convenient, user friendly catalyst.



Scheme 3.

Table 3.

Biginelli reaction with benzaldehyde, ethylacetoacetate and urea with different catalysts.

Entry	Catalyst	Condition	Time	Yield (%)	References
1	TaBr ₅	Solvent free/100 °C	40 min	97	[12]
2	Trichloroisocynuric acid (TCCA)	Ethanol/ Reflux	12 h	94	[13]
3	Montmorillonite KSF	Solvent free/100 °C	48 h	77	[17]
4	BF ₃ .OEt ₂ /Cu(OAc) ₂	Acetic acid/65 °C	18 h	71	[18]
5	Silica-sulfuric acid	Ethanol/Reflux/	6 h	91	[19]
6	H ₃ PMo ₁₂ O ₄₀	Acetic acid/Reflux	5 h	90	[25]
7	Bentonite/PS-SO ₃ H nanocomposite	Solvent-free/100 °C	30 min	89	[28]
8	Sulfated tungstate	Solvent-free/80 °C	60 min	92	[29]
9	Imidazol-1-yl-acetic acid.	Solvent-free/100 °C	35 min	90	[30]
10	Starch sulfuric acid(SSA)	Solvent free/100 °C	10 min	90	This work

In conclusion, we have shown an efficient SSA catalyzed one-pot synthesis of 3,4-dihydropyrimidin-2-(1H)-ones and thione analogs by multicomponent Biginelli reactions under solvent-free conditions, using commercially available substrates. The attractive features of this protocol are its green-ness with respect to solvent-free reaction, recyclability of catalyst, mild reaction conditions, short reaction times and high yield.

The spectral data

5-(Ethoxycarbonyl)-6-methyl-4-phenyl-3,4-dihydropyrimidin-2(1H)-one (Table 2, entry 1): IR (KBr): 3240, 1725, 1635 cm⁻¹. ¹H NMR (DMSO-d₆): δ = 9.20 (s, 1H, NH), 7.75 (s, 1H, NH), 7.10–7.28 (m, 5H, arom CH), 5.14 (s, 1H, CH), 3.97 (q, J = 7.5 Hz, 2H, OCH₂), 2.25 (s, 3H, CH₃), 1.09 (t, J = 7.5 Hz, 3H, OCH₂CH₃). ¹³C-NMR (DMSO-d₆) δ: 14.11, 17.94, 54.91, 60.05, 100.95, 112.85, 113.05, 125.15, 125.81, 129.05, 131.20, 150.16, 155.47, 163.81.ESI-MS 261 (M+H).

5-(Ethoxycarbonyl)-6-methyl-4-(4-chlorophenyl)-3,4-dihydropyrimidin-2(1H)-one (Table 2, entry 2): IR (KBr): 3240, 1723, 1643 cm⁻¹. ¹H NMR (DMSO-d₆): δ = 9.26 (s, 1, NH), 7.79 (s, 1H, NH), 7.40–7.30 (m, 4H, arom CH), 5.14 (s, 1H,

CH), 3.99 (q, $J = 7.5$ Hz, 2H, OCH_2), 2.25 (s, 3H, CH_3), 1.09 (t, $J = 7.5$ Hz, 3H, OCH_2CH_3). $^{13}\text{C-NMR}$ (DMSO-d_6) δ : 14.18, 18.62, 55.72, 60.21, 101.55, 118.17, 130.32, 142.29, 152.31, 153.39, 159.17, 165.83.ESI-MS 295 (M+H).

5-(Ethoxycarbonyl)-6-methyl-4-(4-nitrophenyl)-3,4-dihydropyrimidin-2(1H)-one (Table 2, entry 3): IR (KBr): 3239, 1724, 1645, cm^{-1} . $^1\text{H NMR}$ (DMSO-d_6): $\delta = 9.27$ (s, 1H, **NH**), 8.20 (d, $J = 9.15$ Hz, 2H, arom **CH**), 7.91 (s, 1H, **NH**), 7.50 (d, $J = 9.18$ Hz, 2H, arom **CH**), 5.18 (d, $J = 2.25$ Hz, 1H, **CH**), 3.79 (q, $J = 7.50$ Hz, 2H, OCH_2), 2.25 (s, 3H, OCH_2CH_3), 1.10 (t, $J = 7.50$ Hz, 3H, CH_3). $^{13}\text{C-NMR}$ (DMSO-d_6) δ : 14.22, 18.71, 55.81, 60.15, 101.60, 118.15, 130.37, 138.34, 152.26, 153.41, 159.15, 165.85.ESI-MS 306 (M+H).

5-(Ethoxycarbonyl)-4-(4-methoxyphenyl)-6-methyl-3,4-dihydropyrimidine-2(1H)-one (Table 2, entry 4): IR (KBr): 3241, 1718, 1636 cm^{-1} . $^1\text{H NMR}$ (DMSO-d_6): $\delta = 9.15$ (s, 1H, **NH**), 7.76 (s, 1H, **NH**), 7.15 (d, $J = 8.65$ Hz, 2H, arom **CH**), 6.92 (d, $J = 8.65$ Hz, 2H, arom **CH**), 5.12 (s, 1H, **CH**), 3.96 (q, $J = 7.50$ Hz, 2H, OCH_2), 3.76 (s, 3H, $\text{C}_6\text{H}_4\text{-OCH}_3$), 2.24 (s, 3H, CH_3), 1.10 (t, $J = 7.50$ Hz, 3H, CH_3). $^{13}\text{C-NMR}$ (DMSO-d_6) δ : 14.32, 18.80, 55.23, 55.40, 60.17, 101.68, 114.06, 127.97, 136.22, 146.16, 153.59, 159.30, 165.87.ESI-MS 291 (M+H).

5-(Ethoxycarbonyl)-6-methyl-4-(4-methylphenyl)-3,4-dihydropyrimidin-2(1H)-one (Table 2, entry 5): IR (KBr): 3242, 1715, 1633 cm^{-1} . $^1\text{H NMR}$ (DMSO-d_6): $\delta = 9.16$ (s, 1H, **NH**), 7.80 (s, 1H, **NH**), 7.16–7.12 (m, 4H, arom **CH**), 5.09 (s, 1H, **CH**), 3.96 (q, $J = 7.50$ Hz, 2H, OCH_2CH_3), 2.27 (s, 3H, $\text{C}_6\text{H}_4\text{-CH}_3$), 2.21 (s, 3H, CH_3), 1.08 (t, $J = 7.50$ Hz, 3H, OCH_2CH_3). $^{13}\text{C-NMR}$ (DMSO-d_6) δ : 14.25, 17.62, 53.20, 61.75, 106.48, 115.16, 126.87, 136.52, 147.38, 150.25, 158.35, 167.80.ESI-MS 275 (M+H).

5-(Ethoxycarbonyl)-6-methyl-4-styryl-3,4-dihydropyrimidin-2(1H)-one (Table 2, entry 6): IR (KBr): 3246, 1704, 1650 cm^{-1} . $^1\text{H NMR}$ (DMSO-d_6): $\delta = 9.12$ (s, 1H, **NH**), 7.79 (s, 1H, **NH**), 7.42–7.25 (m, 5H, arom **CH**), 6.33 (d, $J = 15.90$ Hz, 1H, HC=CH), 6.20 (d, $J = 15.80$ Hz, 1H, CH=CH), 4.74 (d, $J = 4.80$ Hz, 1H, **CH**), 4.09 (q, $J = 7.50$ Hz, 2H, OCH_2), 2.20 (s, 3H, CH_3), 1.10 (t, $J = 7.50$ Hz, 3H, OCH_2CH_3). $^{13}\text{C-NMR}$ (DMSO-d_6) δ : 14.21, 17.31, 51.84, 59.45, 98.54, 127.34, 128.54, 129.54, 130.59, 131.24, 135.24, 145.34, 153.62, 165.23.ESI-MS 287 (M+H).

5-(Ethoxycarbonyl)-4-(2-furyl)-6-methyl-3,4-dihydropyrimidin-2(1H)-one (Table 2, entry 7): IR (KBr): 3239, 1705, 1644 cm^{-1} . $^1\text{H NMR}$: $\delta = 9.22$ (s, 1H, **NH**), 7.74 (s, 1H, **NH**), 7.53 (d, $J = 6.0$ Hz, 1H, furyl **CH**), 6.30–6.08 (d, $J = 3.0$ Hz, 2H, furyl-**CH**), 5.20 (s, 1H, **CH**), 4.02 (q, $J = 7.50$ Hz, 2H, CH_2CH_3), 2.22 (s, 3H, CH_3), 1.12 (t, $J = 7.50$ Hz, 3H, OCH_2CH_3). $^{13}\text{C-NMR}$ (DMSO-d_6) δ : 14.15, 17.55, 54.33, 61.44, 106.45, 106.72, 110.36, 142.25, 147.38, 150.28, 152.55, 167.62.ESI-MS 251 (M+H).

5-Aceto-6-methyl-4-phenyl-3,4-dihydropyrimidin-2(1H)-one (Table 2, entry 8): IR (KBr): 3241, 1715, 1643 cm^{-1} . $^1\text{H NMR}$: $\delta = 9.20$ (s, 1H, **NH**), 7.76 (s, 1H, **NH**), 7.35–7.25 (m, 5H, arom **CH**), 5.25 (s, 1H, **CH**), 2.24 (s, 3H, CH_3CO), 2.07 (s, 3H, CH_3). $^{13}\text{C-NMR}$ (DMSO-d_6) δ : 18.65, 52.32, 54.70, 108.47, 113.36, 122.41, 131.17, 130.51, 154.11, 160.20, 164.42.ESI-MS 247 (M+H).

5-(Ethoxycarbonyl)-6-methyl-4-phenyl-3,4-dihydropyrimidin-2(1H)-thione (Table 2, entry 9): IR (KBr): 3258, 1671, 1576 cm^{-1} . $^1\text{H NMR}$: $\delta = 10.33$ (s, 1H, **NH**), 9.64 (s, 1H, **NH**), 7.35–7.19 (m, 5H, C_6H_5), 5.16 (d, $J = 3.50$ Hz, 1H, **CH**), 4.05 (q, $J = 7.20$ Hz, 2H, OCH_2CH_3), 2.28 (s, 3H, CH_3), 1.09 (t, $J = 7.20$ Hz, 3H, OCH_2CH_3). $^{13}\text{C-NMR}$ (DMSO-d_6) δ : 14.23, 17.91, 54.85, 60.15, 100.90, 112.84, 115.12, 125.15, 126.85, 129.64, 131.45, 150.27, 162.63, 180.25.ESI-MS 277 (M+H).

4-(4-Chlorophenyl)-5-ethoxycarbonyl-6-methyl-3,4-dihydropyrimidin-2(1H)-thione (Table 2, entry 10): IR (KBr): 3255, 1657, 1560 cm^{-1} . $^1\text{H NMR}$: $\delta = 10.36$ (s, 1H, **NH**), 9.65 (s, 1H, **NH**), 7.43–7.19 (m, 4H, C_6H_4), 5.16 (s, 1H, **CH**), 4.00 (q, $J = 6.50$ Hz, 2H, OCH_2CH_3), 2.25 (s, 3H, CH_3), 1.08 (t, $J = 6.50$ Hz, 3H, OCH_2CH_3). $^{13}\text{C-NMR}$ (DMSO-d_6) δ : 14.22, 18.35, 58.37, 61.73, 104.25, 126.42, 128.44, 132.72, 141.48, 160.37, 167.25, 174.18.ESI-MS 311 (M+H).

5-Ethoxycarbonyl-4-(4-methoxyphenyl)-6-methyl-3,4-dihydropyrimidin-2(1H)-thione (Table 2, entry 11): IR (KBr): 3250, 1651, 1598, 1561 cm^{-1} . $^1\text{H NMR}$: $\delta = 10.29$ (s, 1H, **NH**), 9.59 (s, 1H, **NH**), 7.14–6.87 (m, 4H, C_6H_4), 5.10 (s, 1H, **CH**), 3.95 (q, $J = 7.25$ Hz, 2H, OCH_2CH_3), 3.71 (s, 3H, OCH_3), 2.27 (s, 3H, CH_3), 1.09 (t, $J = 7.25$ Hz, 3H, OCH_2CH_3). $^{13}\text{C-NMR}$ (DMSO-d_6) δ : 14.32, 18.05, 55.24, 55.49, 60.45, 101.84, 114.32, 127.74, 137.25, 147.15, 159.45, 165.62, 182.48.ESI-MS 307 (M+H).

References

- [1] Kappe, C.O. Acc. Chem. Res. 2000, 33, 879.
- [2] Kappe, C.O. Tetrahedron. 1993, 49, 6937.
- [3] Kappe, C.O. Eur. J. Med. Chem. 2000, 35, 1043.
- [4] Biginelli, P. Gazz. Chim. Ital. 1983, 23, 360.
- [5] Khabazzadeh, H.; Saidi, K.; Sheibani, H. Bioorg. Med. Chem. Lett. 2008, 18, 278.
- [6] Jain, S.L.; Prasad, V.V.D.N.; Sain, B. Catal. Commun. 2008, 9, 499.
- [7] Cepanec, I.; Litvić, M.; Filipan- Litvić, M.; Grünigold, I. Tetrahedron. 2007, 63, 11822.
- [8] Kamal, A.; Krishnaji, T.; Azhar, M.A. Catal. Commun. 2007, 8, 1929.
- [9] Banik, B.K.; Reddy, A.T.; Datta, A.; Mukhopadhyay, C. Tetrahedron Lett, 2007, 48, 7392.

- [10] Adibi, H.; Samimi, H.A.; Beygzadeh, M. *Catal. Commun.* 2007, 8, 2119.
- [11] Nandurkar, N.S.; Bhanushali, M.J.; Bhor, M.D.; Bhanage, B.M. *J. Mol. Catal. A: Chem.* 2007, 14, 271.
- [12] Ahmed, N.; Lier, J.E. *Tetrahedron Lett.* 2007, 48, 5407.
- [13] Bigdeli, M.A.; Jafari, S.; Mahdavinia, G.H.; Hazarkhani, H. *Catal. Commun.* 2007, 8, 1641.
- [14] Polshettiwar, V.; Varma, R.S. *Tetrahedron Lett.* 2007, 48, 7343.
- [15] Yu, Y.; Liu, D.; Liu, C.; Luo, G. *Bioorg. Med. Chem. Lett.* 2007, 17, 3508.
- [16] Jin, T.; Zhang, S.; Li, T. *Synth. Commun.* 2002, 32, 1847.
- [17] Bigi, F.; Carloni, S.; Frullanti, B.; Maggi, R.; Sartori, G. *Tetrahedron Lett.* 1999, 40, 3465.
- [18] Hu, E.H.; Sidler, D.R.; Dolling, U.-H. *J. Org. Chem.* 1998, 63, 3453.
- [19] Salehi, P.; Dabiri, M.; Zolfigol, M.A.; Bodaghi Fard, M.A. *Tetrahedron Lett.* 2003, 44, 2889.
- [20] Hassani, Z.; Islami, M.R.; Kalantari, M. *Bioorg. Med. Chem. Lett.* 2006, 16, 4479.
- [21] Ismaili, L.; Nadaradjane, A.; Nicod, L.; Guyon, C.; Xicluna, A.; Robert, J.F.; Refouvelet, B. *Eur. J. Med. Chem.* 2007, 1.
- [22] Chen, W.-Y.; Qin, S.; Jin, J.R. *Catal. Commun.* 2007, 8, 123.
- [23] Chen, X.-H.; Xu, X.-Y.; Liu, H.; Cun, L.-F.; Gong, L.-Z. *J. Am. Chem. Soc.* 2006, 128, 14802.
- [24] Heravi, M.M.; Derikvand, F.; Bamoharram, F.F. *J. Mol. Catal. A: Chem.* 2005, 242, 173.
- [25] Heravi, M.M.; Bakhtiari, K.; Bamoharram, F.F. *Catal. Commun.* 2006, 7, 373.
- [26] Sharghi, H.; Jokar, M. *Synth. Commun.* 2009, 50, 958.
- [27] Narahari, S.R.; Reguri, B.R.; Gudaparthi, O.; Mukkanti, K. *Tetrahedron Lett.* 2012, 53, 1543.
- [28] Kalbasi, R.J.; Massah, A.R.; Daneshvarnejad, B. *Appl. Clay. Sci.* 2012, 55, 1.
- [29] Salim, S.D.; Akamanchi, K.G. *Catal. Commun.* 2011, 12, 1153.
- [30] Kargar, M.; Hekmatshoar, R.; Mostashari, A.; Hashemi, Z. *Catal. Commun.* 2011, 15, 123.
- [31] Moosavifar, M. *C. R. Chimie.* 2012, 15, 444.
- [32] Shaabani, A.; Bazgir, A.; Teimuri, F. *Tetrahedron Lett.* 2003, 44, 857.
- [33] Shirini, F.; Marjani, K.; Taherpour Nahzomi, H. *Arkivoc.* 2007, 51.
- [34] Bigi, F.; Carloni, S.; Frullanti, B.; Maggi, R.; Sartori, G. *Tetrahedron Lett.* 1999, 40, 3465.
- [35] Yadav, J.S.; Reddy, B.V.S.; Srinivas, R.; Venogopal, C.; Ramalingam, T. *Synthesis.* 2001, 1341.
- [36] Lee, K.Y.; Ko, L.Y. *Bull. Korean Chem. Soc.* 2004, 25, 1929.
- [37] Fu, N.F.; Yuan, Y.F.; Cao, Z.; Wang, Z.W.; Wang, J.T.; Peppe, C. *Tetrahedron.* 2002, 58, 4801.
- [38] Xue, S.; Shen, Y.C.; Li, Y.L.; Shen, X.M.; Guo, Q.X. *Chin. J. Chem.* 2002, 20, 385.
- [39] Clark, J.H.; Macquarrie, D.J. *Green Chemistry and Technology*, Blackwell, Abingdon, 2002.
- [40] Tomasik, P. *Chemical and Functional Properties of Food Saccharides*; CRC Press; 2004.
- [41] Morris; D.L. *Science.* 1948, 107, 254.

TASK-SPECIFIC IONIC LIQUIDS FOR EXTRACTIVE DESULPHURIZATION OF DIESEL FUEL

Fliur Macaev*, Eugenia Stîngaci

Institute of Chemistry of the Academy of Sciences of Moldova, 3, Academiei str., Chisinau MD-2028, Republic of Moldova
*e-mail: fmacaev@cc.acad.md; phone / fax (+373 22) 73 97 54

Abstract. Task-specific ionic liquids based on imidazolium cation containing carbonitrile, carboxyl, and alkyl chains have been employed in an attempt to design new functionalized liquids for solvent extraction of sulphur compounds from diesel fuel.

Keywords: task-specific ionic liquids, extractive desulphurization, diesel fuel.

Introduction

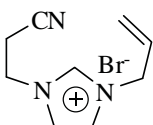
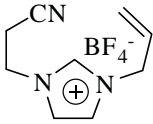
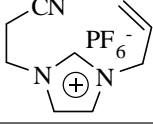
Many concepts and technologies have been developed during the last 20 years to desulphurize the least reactive sulphur species from the diesel feed in order to effectively reach the near zero sulphur content at attainable costs [1]. Functionalized ionic liquids are relatively cheap, easy to synthesize, have no measurable vapor pressure and can be competitive with conventional solvents and adopted in many industrial applications [2]. Hence, there is considerable interest in using them in place of volatile organic solvents for new production technology of ultra-low sulphur petroleum fractions. It is known that the presence of sulphur in heavy fuel oils leads to emission of SO_x which endangers public health [1]. It is worth noting that environmental regulations focus attention on reduction of emissions from the transport sector with the purpose of improving air quality [3]. Moreover, according to the European Union regulation, gasoline and diesel fuels should not exceed 10 ppm of total sulphur content starting from 2010 [4]. A current desulphurizing technology has included adsorptive desulphurization, hydrodesulphurization, oxidative desulphurization and extractive desulphurization. The last one is preferred over other separation methods for its advantages in less costly and easier disposal, since it incurs no chemical consumption or byproduct formation unlike other chemical methods [1]. Ionic liquids as selective extraction agents of different compounds were discussed earlier due to their novelty and theoretical interest [2, 5-27]. This prompted us to find new compounds having a carbonitrile, carboxyl and alkyl functional groups attached to an imidazolium cation. These compounds can be considered task-specific ionic liquids and can be useful for the removal of sulphur-containing compounds from the diesel fuel. In order to obtain new extractors, a number of ionic liquids were prepared from 1*H*-imidazole and studied for application in desulphurization of diesel fuel.

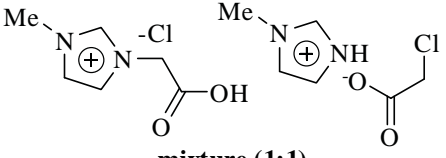
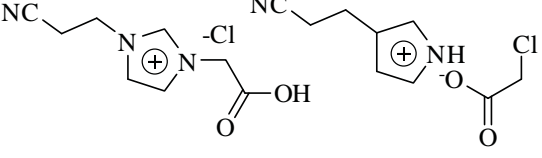
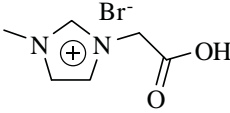
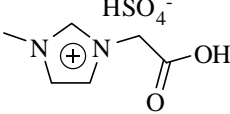
Results and discussion

Previously, various types of ionic liquids were employed in the extractive desulphurization of diesel fuel because of their properties, such as immiscibility with fuels, high affinity to sulphur-containing substances, low volatility and high thermal stability [5-27]. Task-specific ionic liquids **1-8** used in this study were reported by us previously [28-31].

Table 1.

Degree of diesel desulphurization in dependence on the ionic liquid used.

No. Compound	Structure	Ref.	Degree of desulphurization (%)
1		28	65
2		28	68
3		28	69

4	 mixture (1:1)	29	88
5	 mixture (1:1)	29	87
6		30	54
7		30	78
8	$[\text{Fe}_3\text{O}(\text{H}_3\text{C}-\text{C}_3\text{H}_3\text{N}_2-\text{COO})_6(\text{H}_2\text{O})_3](\text{FeCl}_4)_7$	31	100

As shown in the table 1, the imidazolium-based molten salts **1-8** have functional groups like carbonitrile, carboxyl, and alkyl group, along with different anions (Cl^- , Br^- , HSO_4^- , FeCl_4^-). Firstly, the extraction ability of allyl- and carbonitrile- substituted ionic liquids **1-3** was evaluated for removal of sulphur species from the model diesel fuel. It was found that efficiency of extractive desulphurization of substances **1-3** was up to 65-69%. The effect of the chain substituent on imidazolium ring was also investigated. Desulphurization with task-specific ionic liquids **4** and **5** clearly exhibited much higher extraction ability than ionic liquids **1-3**. For a comparison, performances of the specific ionic liquids with protonated and coordinated carboxyl group were tested for extractive desulphurization. However, the extraction ability of ionic liquid **6** was lower than that of the corresponding mixture **4**. The reason for a higher extraction ability of **4** is not clear. The highest extractive desulphurization was obtained with task-specific ionic liquid **7** that exists as liquid at room temperature like mixtures **5** and **6**. Desulphurization in the presence of metal containing ionic liquid **8** with FeCl_4^- anions and $\{\text{Fe}^{\text{III}}\text{O}\}$ cationic core clearly demonstrated that all the sulphur substances were completely extracted from the diesel fuel.

We believe that extractive desulphurization of diesel fuel is based on the fact that sulphur-containing compounds are more soluble in task-specific ionic liquids than in hydrocarbons. It is worth noting that such approach can be realized under ambient conditions.

Conclusions

The reported data represent a straightforward procedure for the efficient and facile extractive desulphurization of the diesel fuel with task-specific ionic liquids. The procedure has remarkable practical utility because of its simplicity and the applied functionalized ionic liquids are relatively cheap and easy to synthesize. The studies on the extractive desulphurization of underground water with application of task-specific ionic liquids are underway in our laboratory.

Experimental methods

Task-specific ionic liquids **1-8** were prepared using the methods [28-31]. Desulphurization experiments were conducted in 15 mL tubes. Task-specific ionic liquids were added into the model diesel fuel containing 0.06% of sulphur species. The weight ration of specific ionic liquid/model diesel fuel was set at 1:4. After mixing with 1200 rotation per minute for 6 hours, diesel fuel was removed by filtration (in case **1-3** and **6**) or decantation (in case **4, 5, 7** and **8**). Determination of sulphur content by lamp method was realized according to the GOST 19121-73 [32]. 1 mL of diesel fuel was diluted with 3 mL of n-heptane and incinerated in a burner-lamp connected to absorber (filled with 10 mL of Na_2CO_3 water solution) at reduced pressure (90 mm of the mercury column). Afterwards, the lamp was washed with 1 mL of n-heptane and it was fully incinerated in duplicate. Water solution of Na_2CO_3 from the absorber, containing

sulphur oxides, is then coloured with methylene orange and is titrated with HCl solution until the colour changes into the pink. The mass fraction of the sulphur is then determined according to the following equation:

$$X = \frac{(V - V_1) \cdot K \cdot 0.0008 \cdot 100}{m}$$

where, V - volume, mL of 0.05 N solution of HCl, used for titration of the control probe; V_1 - volume, mL of 0.05 N solution of HCl, used for titration of the probe after incineration and absorption; K -correction factor to the titre of 0.05 N solution of HCl; 0.0008- weight of sulphur, equivalent to 1 mL of 0.05 N solution of HCl, g; m - weight of the probe, g. The result of the determination is expressed as the arithmetical mean of 2 parallel experiments.

Acknowledgments

We thank the bilateral BMBF project (01DK13029) for financial support and Dr. Denis Prodius for helpful discussions.

References

- [1] Abinaya, K.; Sivalingam, A.; Kannadasan, T. IJSR 2013, 2, pp. 172-175.
- [2] Macaev, F.; Green chemistry protocols: specific ionic liquids as recyclable reagents, catalysts, solvents and extractors. In Environmental Security Assessment and Management of Obsolete Pesticides in Southeast Europe, Eds. L.Simeonov, F. Macaev and B. Simeonova, Springer. 2013, 475 p.
- [3] (a)Wasserscheid, P.; Keim, W. Angew. Chem. 2000, 112, 3926-3945; (b) European Directive for emissions of light duty vehicles (70/220/CE amended by 99/69/EC as Euro3 and 2002/80/EC as Euro4), European Directive for emissions of heavy duty vehicles (88/77/CE amended by 1999/96/CE as Euro4 and Euro5).
- [4] Directive of the European Parliament and of the Council, Brussels COM (11.05.2001) 241 final (BS EN 590-2004/DIN EN 590-2004) Automotive fuels, Diesel, Requirements and test methods; and 2003/17/EC OJ L 76, 22.3.2003, p.10.
- [5] Nirmal Ravi, V.; Anantharaj, R.; Tama, B. Chem. Eng. J. 2011, 166, pp. 30-39.
- [6] Zhao, D.; Wang, Y.; Duan, E. Molecules 2009, 14, pp. 4351-4357.
- [7] Xuemei, C.; Yufeng, H.; Jiguang, L.; Qianqing, L.; Yansheng, L.; Xianming, Z.; Xiaoming, P.; Wenjia, Y. Chin. J. Chem. Eng. 2008, 16, pp. 881-884.
- [8] Mochizuki, Y.; Sugawara, K. Energ. Fuel. 2008, 22, pp. 3303-3307.
- [9] Alonso, L.; Arce, A.; Francisco, M.; Soto, A. Fluid Phase Equilib. 2008, 270, pp. 97-102.
- [10] Nie, Y.; Li, C.; Meng, H.; Wang, Z. Fuel Process. Technol. 2008, 89, pp. 978-983.
- [11] Xuemei, C.; Yufeng, H.; Jiguang, H.; Qianqing, L.; Yansheng, L.; Xianming, Z.; Xiaoming, P.; Wenjia, Y. Chin. J. Chem. Eng., 2008, 16, pp. 881-884.
- [12] Ko, N.H.; Lee, J.S.; Huh, E.H.; Lee, H.; Jung, K.D., Kim, H.S.; Cheong, M. Energ. Fuel. 2008, 22, pp. 1687-1690.
- [13] Alonso, L.; Arce, A.; Francisco, M.; Soto, A. J. Chem. Eng. Data. 2008, 53, pp. 1750-1755.
- [14] Alonso, L.; Arce, A.; Francisco, M.; Soto, A. Fluid Phase Equilib. 2008, 263, pp. 176-181.
- [15] Wang, J. L.; Zhao, D. S.; Zhou, E. P.; Dong, Z. J. Fuel Chem. Technol. 2007, 35(3), pp. 293-296.
- [16] Alonso, L.; Arce, A.; Francisco, M.; Soto, A. J. Chem. Eng. Data. 2007, 52, pp. 2409-2412.
- [17] Nie, Y.; Li, C.; Wang, Z. H. Ind. Chem. Res. 2007, 46, pp. 5108-5112.
- [18] Rang, H.; Kann, J.; Oja, V. Oil Shale, 2006, 23, 2, pp. 164-176.
- [19] Nie, Y.; Li, C.; Sun, A.; Meng, H.; Wang, Z. Energ. Fuel. 2006, 20, pp. 2083-2087.
- [20] Feng, J.; Li, C. X.; Meng, H.; Wang, Z. H. Petrochem. Technol. 2006, 35, pp. 272-275.
- [21] Zhang, S.; Zhang, Q.; Zhang, Z. C. Ind. Eng. Chem. Res. 2004, 43, pp. 614-622.
- [22] Eber, J.; Wasserscheid, P.; Jess, A. Green Chem. 2004, 6, pp. 316-322.
- [23] Huang, C.; Chen, B.; Zhang, J.; Liu, Z.; Li, Y. Energ. Fuel. 2004, 18, pp. 1862-1864.
- [24] Bösman, A.; Datsevich, L.; Jess, A.; Lauter, A.; Schmitz, C.; Wasserscheid, P. Chem. Commun. 2001, 23, pp. 2494-2495.
- [25] Wasserscheid, P.; Jess, A.; Bösman, A.; Datsevich, L.; Lauter, A.; Schmitz, C. Pat. DE 101 55 281 A1, 2003.
- [26] Zhang, S.; Zhang, Q. Green Chem., 2002, 4, pp. 376-379.
- [27] Sheldon, R. Chem. Commun. 2001, 23, pp. 2399-2407.
- [28] Munteanu, V.; Stingaci, E.; Barba, A.; Pogrebnoi, S.; Macaev, F. Chem. J. Moldova, 2007, 2, pp. 119-122.

- [29] Macaev, F.; Styngach, E.; Shargarovskii, V.; Bets, L.; Vlad, L.; Barba, A. *Russ. J. Org. Chem.* 2010, 46 (4), pp. 610-611.
- [30] Sargorovschi, V.; Sucman, N.; Iudin, T.; Stingaci, E.; Macaev, F. *Chem. J. Moldova*, 2010, 5 (1), pp. 109-117.
- [31] Prodius, D.; Macaev, F.; Stingaci, E.; Pogrebnoi, V.; Mereacre, V.; Novitchi, G.; Kostakis, G. E.; Anson, C. E.; Powell, A. K. *Chem. Commun.* 2013, 49, pp. 1915-1917.
- [32] GOST 19121-73 Petroleum Products Determination of sulphur content by lamp method.



Victor Isac (1943 - 1995)

HAPPINESS OF EVOCATION

Victor Isac would have reached the 70 years

Victor Isac was a teacher by vocation, scientist and man of culture, who served with honor and honesty education and our national school by writing some prestigious books with didactical or monographic character, through excruciating teacher activity, bringing a good name to the country and leaving behind him an unforgettable memory. In his short-life (July 8, 1943 - October 3 1995) he succeeded to publish more than 220 scientific and scientific-didactic papers, including 14 monographs, textbooks, and studies. Alongside the noble toil of teacher and researcher he has assumed the function of Dean, leading the Faculty of Chemistry at the State University of Moldova from 1981 until the last moment of his life. It seems that God loved too much his soul, so that he was snatched from us so early.

Born in the village Drepcauti, district Edinet, he graduated with honors the Faculty of Chemistry (1969) and obtained his doctorate (1972) at the State University of Moldova with the Ph.D thesis „The decomposition of hydrogen peroxide catalyzed by trivalent iron complexes and divalent manganese with triethylenetetramine and histidine “(1973). His work has been highly appreciated by academician Anthony Ablov in his opinion as the first official reviewer on the thesis defense. The second thesis “The coordination compounds of manganese and iron in redox catalysis” (1990) has brought the scientific title of Doctor Habilitatus in chemistry. Since 1992 he holds the title of university professor.

Victor Isac was a consecrated researcher who pulled deep furrows on the field of physical chemistry. The coordinative systems with catalyses, peroxides and oxides proprieties studied by him come today the ambient safeguarding threatened by a too excessive pollution. I worked with this distinguished scientist, publishing in collaboration with him 36 scientific papers and I have to confess that this communion was for me, and I hope for him, too, a necessity and a real delight.

The works achieved by this hardworking researcher refer to some issues of stringent actuality such as the activation of molecular oxygen and hydrogen peroxide by the coordination compounds of iron and manganese (the complex of trivalent iron with triethylenetetramine, for example, often is rightfully nicknamed “inorganic catalase”), establishment the legalities that govern these processes, the elucidation of reactions mechanisms and designating the ways of using the eventual results.

In the molecular biology epoch of glory, the modeling of the living specific processes through coordinative systems containing iron or manganese ion, a helatofor (polyamine, amino acid, etc.), an organic substrate occurs as handsome as it is and troublesome, because it contains the entire spectrum of investigations: from fundamental research through advanced research, including technological transfer, to implementation in practice.

In terms of fundamental science Professor Victor Isac had argued and developed new concepts on the likelihood of initiation phase in homogeneous catalysis and the route of process for the catalytic oxidation of colorings and other organic substrates, he introduced new concepts regarding the nature of the reaction in available reactant volume, unleashed by the active catalytic center and is responsible itself for the catalytic act. Practically, he elaborated new kinetic methods of analysis (domain nicknamed and as catalimetric) of the micro quantities of manganese and iron

which satisfy the requirements of precision, simplicity and rapidity, as well as one procedure for catalytic purification of solutions with large quantities of hydrogen peroxide.

The achievements of Professor Victor Isac were highly appreciated by granting in 1998 (post-mortem), side by side with Professor Alexei Sacio, whose disciple is, and with academician Gheorghe Duca, of State Prize of Republic of Moldova in Science, Technology and the Production for the cycle of papers "The fundamental and applied aspects of the homogeneous catalysis processes."

It would be a pity not to evoke in these pages the moral being and human dimension of this unforgettable friend and colleague. He was tall fitly framed together in an athletic figure, he had a safe and calm step, but his blue eyes, vivid and bright, had emanating gentleness, wisdom and inner beauty. Elegant in motion, delicate - more specifically, genteel - in appreciations, endowed by nature with the faculty of the mind to understand easily, quickly and in depth all that had been happening around, whatever may have been the subject of discussion, he knew how to reach the proposed in all circumstances. He manifested a great courage, but, also, a maximum objectivity and self-control in all his actions, leaving aside the personal interest, emotions, and feelings. His inexhaustible workforce, destined by God with the boundless love for those nearby - colleagues, PhD students, students, pupils - it was a man of total passion, spread all over nobility, tenderness, honesty and dignity. To these is added his communicability, who had generated solid friendships, reliable and beautiful relations and which had continued until the last moments of his life. The Department of Chemistry will still feel great and irreparable empty left by his untimely disappearance.

That certain such was to be the image of the Victor Isac comes to confirm the following testimony. It was in 1967. Faculty of Chemistry starts the distribution of graduates. Lieutenant-colonel at department of personnel of Academy of Sciences and the author of these rows - then deputy director for scientific work at the Institute of Chemistry - was to fill vacancies for research and doctoral studies with young specialists. The first among graduates appeared before the Commission Victor Isac and immediately announced that he will remain at the Department of Physical Chemistry. Military-"cadrovic" flinch and whisper my ear: Here, it's "frame" no the joke! It seems that he was spellbound of a the vigorous figure of graduate while the faculty leadership had saw in Victor Isac the embodiment of a brilliant intelligence, a moderate temperament and sublime character dominated by the modesty, magnanimity and virtue. And all were right.

During my time as a President of Commission for license exams and theses of High School I was given to meet with teachers that view in person of the student an intruder, to be held "in the bridle" always persecuting him. This antagonism in teacher-student relationship seems too obsolete and hazardously from the belief that teachers themselves have to draw benefits from the scientific contact with their students. This antagonism in teacher-student relationship seems too obsolete and hazardously from the belief that teachers themselves have to draw benefits from the scientific contact with their learners, treating them as if they were adults. In this context professor Victor Isac was to be the kind of parent for students, who always put his shoulder to facilitate the way to a younger colleague called to carry forward the torch of research in chemistry, i.e. to achieve what the teacher was unable to do. Without fail, perhaps without knowing, Victor Isac has followed exhortation and counsel from the First Catholic Epistle of Apostle St. Peter: "Feed the herd of God, which is among you, taking the oversight *thereof*, not by constraint, but willingly; not for filthy lucre, but of a ready mind".

Victor Isac was always to make considerable efforts for good academic training and have great fulfillments. Through his lectures in physical chemistry, writing textbooks and compendiums for discipline, engagement of students in research, he succeeded in promoting the much coveted university triad of: 1) the transmission of knowledge, 2) development of development of the free flight for convergent and divergent thinking, 3) the formation of some personalities, future professionals, at large scale. Thus succeeds to give brightness discipline that served with honor and devotion. Maybe, it can therefore has scored the so quickly to vouchsafe of all scientific and educational titles to Doctor Habilitatus in Chemistry and University Professor and enter into the first rows of the cohort of teachers of the highest quality.

Victor Isac came the sublime understanding that the intellectual potential of the nation is in decline and that only the valence and lucidity of the young generation resides our future. The scientific advice even from birth of this "CHIMCONT" was appointed as a Dean of the Faculty of Chemistry Victor Isac. And it was in the auspicious hour. It soon appeared a set of textbooks signed by Svetlana Kudritki, Boris Pasencin, Galina Dragalina, Nadejda Velisco Peter Chetrus, Victor Isac, in which authors took everything they found most useful from the worldwide practice and added to it their own experience acquired in teaching at all levels from us. In this context, a special mention deserves the elaboration by Victor Isac together with professors from Romania, experienced specialists of some university textbooks such as: "Physical Chemistry: Chemical kinetics and catalysis" (Chisinau, Science, 1994, 639 pages), authors Victor Isac and Natalia Hurduc; "Physical Chemistry: Practical Applications" (Chisinau: Science, 1995, 759 pages), authors Victor Isac, Ana Onu, Cornelia Tudoreanu and George Nemțoi, "Physical Chemistry. Electrochemistry" (Chisinau: Science, 1997, 479 pages), authors George Nemțoi and Victor Isac.

With the participation of Professor Victor Isac four scientific-didactic conferences were organized in which chemistry teachers from middle schools, high schools, colleges and institutions of higher education from Romanian and

universal space participated. At the last Conference held in the spring of 1998 for the participants it was hard to imagine that Victor Isac is no more. To cover somehow this gap were ad-hoc printed and distributed among participants the few materials about life and activity of more regretted professor and scholar.

It always found among students chairing the Chemistry Olympiads in the country and activating in the structure of the selection boards abroad Olympiads. Professor Alexander Cecal from University of Iasi (he, also, Dean of the Faculty of Chemistry) once had confessed that Victor Isac was more waited and appreciated at International Olympiads and that when he was to go into the shadows the absence of this great teacher was felt in full.

The notorious scholar conscious that only in love and harmony can be done the great things; Victor Isac always loved with passion his colleagues and with a fine and bouncy calligraphy – proof of a given alloy from nobility and intellect – used to give autographs to others. Here's what he had written on the title page of the book "The coordination compounds of manganese in catalysis"(Chisinau: Science, 1990, 322 pages), elaborated in collaboration with his magistrate Alexei Saciov "The highly esteemed Prof. Dr. Dumitru Batir with much respect and wishes of good health and new achievements". And so he wishes to everyone health, exactly what he had not.

Dumitru BATÎR,
Doctor Habilitatus in chemistry,
university professor
State Prize Laureate